Department of Medicine, Hematology

CENTRO DE INVESTIGACIÓN DEL CÁNCER – IBMCC

VNiVERSiDAD D SALAMANCA

CAMPUS OF INTERNATIONAL EXCELLENCE

DOCTORAL DISSERTATION

Molecular analysis of rare cytogenetic abnormalities in chronic lymphocytic leukemia: from genomic alterations to metabolic reprogramming

With the approval of the University of Salamanca, Department of Medicine, this thesis will be defended on 14th June 2023 in the Lecture Hall, Centro de Investigación del Cáncer - IBMCC, Salamanca.

Supervisors:

Prof. Dr. Jesús M. Hernández Rivas

Dra. Ana E. Rodríguez Vicente

Claudia Pérez Carretero

2023

Esta tesis doctoral corresponde a la Modalidad de Compendio de Artículos, dos de los cuales han sido publicados en revistas internacionales, una de ellas de primer decil y otra de primer cuartil, y dos de ellos son manuscritos en preparación.

ARTÍCULO 1

Título: Chronic lymphocytic leukemia patients with chromosome 6q deletion as the sole cytogenetic abnormality display a high frequency of *RPS15* mutations and have a dismal prognosis.

Autores: Claudia Pérez Carretero[1,2], Teresa González[1,2], Miguel Quijada Álamo[1,2], Gian Matteo Rigolin[3], Adrian Dubuc[4], Ángela Villaverde Ramiro[1,2,] Alberto Rodríguez[1,2], Juan Nicolás Rodríguez[5], Araceli Rubio[6], Julio Dávila[7], Mª Jesús Vidal[8], Isabel González Gascón y Marín[9], José Ángel Hernández Rivas[9], Rocío Benito[1,2], Matt Davids[10], Jeremy Abrasom[11], Antonio Cuneo[3], Paola Dal Cin[4], Ana-Eugenia Rodríguez-Vicente[1,2] Jesús-María Hernández-Rivas[1,2]

Afiliaciones de los autores: [1]University of Salamanca, IBSAL, I_{BM}CC, CSIC, Cancer Research Center, Salamanca, Spain. [2]Department of Hematology, University Hospital of Salamanca, Salamanca, Spain. [3]Hematology Section, St. Anna University Hospital, Ferrara, Italy- [4]Department of Pathology, Brigham and Women's Hospital, Boston, MA, USA. [5]Department of Hematology. Hospital Juan Ramon Jimenez, Huelva, Spain. [6]Department of Hematology, Hospital Miguel Servet, Zaragoza, Spain. [7]Department of Hematology, Hospital Nuestra Señora de Sonsoles, Ávila, Spain. [8]Department of Hematology, Hospital Universitario, León, Spain. [9]Department of Hematology, Hospital Universitario Infanta Leonor. Universidad Complutense, Madrid, Spain. [10]Dana Farber Cancer Institute, Boston, MA, USA. [11]Massachusetts General Hospital, Boston, MA, USA.

Estado del artículo: Manuscrito en preparación.

ARTÍCULO 2

Título: Chronic lymphocytic leukemia patients with *IGH* translocations are characterized by a distinct genetic landscape with prognostic implications.

Autores: Claudia Pérez-Carretero[1,2], María Hernández-Sánchez[1,2,3], Teresa González[1,2], Miguel Quijada-Álamo[1,2], Marta Martín-Izquierdo[1,2], Jesús-María Hernández-Sánchez[1,2], María-Jesús Vidal[4], Alfonso García de Coca[5], Carlos Aguilar[6], Manuel Vargas-Pabón[7], Sara Alonso[8], Magdalena Sierra[9], Araceli Rubio-Martínez[10], Julio Dávila[11], José R. Díaz-Valdés[12], José-

Antonio Queizán[12], José-Ángel Hernández-Rivas[13], Rocío Benito[1,2], Ana E. Rodríguez-Vicente[1,2] and Jesús-María Hernández-Rivas[1,2]

Afiliaciones de los autores: [1]Universidad de Salamanca, IBSAL, Centro de Investigación del Cáncer, IBMCC-CSIC, Salamanca, Spain. [2]Servicio de Hematología, Hospital Universitario de Salamanca, Salamanca, Spain. [3]Department of Medical Oncology, Dana Farber Cancer Institute, Boston, Massachusetts, USA. [4]Servicio de Hematología, Hospital Universitario, León, Spain. [5]Servicio de Hematología, Hospital Clínico, Valladolid, Spain. [6]Servicio de Hematología, Complejo Hospitalario de Soria, Soria, Spain. [7]Servicio de Hematología, Hospital Jarrio, Asturias, Spain. [8]Servicio de Hematología, Hospital Universitario Central de Asturias, Oviedo, Spain. [9]Servicio de Hematología, Hospital Virgen de la Concha, Zamora, Spain. [10]Servicio de Hematología, Hospital Miguel Servet, Zaragoza, Spain. [11]Servicio de Hematología, Hospital Nuestra Señora de Sonsoles, Ávila, Spain. [12]Servicio de Hematología, Hospital General de Segovia, Segovia, Spain. [13]Servicio de Hematología. Hospital Universitario Infanta Leonor. Universidad Complutense. Madrid, Spain.

Estado del artículo: publicado en la revista internacional **International Journal of Cancer. 2020** Nov 15;147(10):2780-2792. doi: 10.1002/ijc.33235.

ARTÍCULO 3

Título: *TRAF3* alterations are frequent in del-3'IGH chronic lymphocytic leukemia patients and define a specific subgroup with adverse clinical features.

Autores: Claudia Pérez-Carretero[1,2], María Hernández-Sánchez[1,2,3], Teresa González[1,2], Miguel Quijada-Álamo[1,2], Marta Martín-Izquierdo[1,2], Sandra Santos-Mínguez[1,2], Cristina Miguel-García[1,2], María-Jesús Vidal[4], Alfonso García-De-Coca[5], Josefina Galende[6], Emilia Pardal[7], Carlos Aguilar[8], Manuel Vargas-Pabón[9], Julio Dávila[10], Isabel Gascón-Y-Marín[11], José-Ángel Hernández-Rivas[11], Rocío Benito[1,2], Jesús-María Hernández-Rivas[1,2] and Ana-Eugenia Rodríguez-Vicente[1,2]

Afiliaciones de los autores: [1]Universidad de Salamanca, IBSAL, Centro de Investigación del Cáncer (IBMCC-CSIC), Salamanca, Spain. [2]Servicio de Hematología, Hospital Universitario de Salamanca, Salamanca, Spain. [3]Departamento de Bioquímica y Biología Molecular, Facultad de Farmacia. Universidad Complutense de Madrid, Madrid, Spain (Present affiliation). [4]Servicio de Hematología, Hospital Universitario, León, Spain. [5]Servicio de Hematología, Hospital Clínico, Valladolid, Spain.[6]Servicio de Hematología, Hospital El Bierzo, Ponferrada, Spain [7]Servicio de Hematología, Hospital Virgen del Puerto, Plasencia, Spain [8]Servicio de

Hematología, Complejo Hospitalario de Soria, Soria, Spain. [9]Servicio de Hematología, Hospital Jarrio, Asturias, Spain. [10]Servicio de Hematología, Hospital Nuestra Señora de Sonsoles, Ávila, Spain. [11]Servicio de Hematología. Hospital Universitario Infanta Leonor. Universidad Complutense. Madrid, Spain.

Estado del artículo: publicado en la revista internacional **American Journal of Hematology. 2022** Jul;97(7):903-914. doi: 10.1002/ajh.26578.

ARTÍCULO 4

Título: *TRAF3* alterations enhance metabolic plasticity through metabolic reprogramming in chronic lymphocytic leukemia.

Autores: Claudia Pérez Carretero[1,2], Miguel Quijada Álamo[1,2], Mariana Tannoury[3], Léa Dehgane[3], Alberto Rodríguez Sánchez[1,2], David J. Sanz[1,2], Teresa González[1,2], Rocío Benito[1,2], Élise Chapiro[4], Florence Nguyen[4], Ana E. Rodriguez Vicente[1,2], Santos A. Susin[3], Jesús María Hernández Rivas[1,2]

Afiliaciones de los autores: [1]University of Salamanca, IBSAL, IBMCC, CSIC, Cancer Research Center, Salamanca, Spain, [2]Department of Hematology, University Hospital of Salamanca, Salamanca, Spain, [3]Drug Resistance in Hematological Malignancies, Centre de Recherche des Cordeliers, UMRS 1138, INSERM, Sorbonne Université, Université Paris Cité, F-75006 Paris, France, [4]Drug Resistance in Hematological Malignancies, Centre de Recherche des Cordeliers, UMRS 1138, INSERM, Sorbonne Université, Université Paris Cité, F-75006 Paris, France; Groupe Hospitalier Pitié-Salpêtrière, Assistance Publique-Hôpitaux de Paris, F-75013 Paris, France.

Estado del artículo: Manuscrito en preparación.

D. **Jesús María Hernández Rivas**, Doctor en Medicina, Catedrático del Departamento de Medicina de la Universidad de Salamanca, Médico Adjunto del Servicio de Hematología del Hospital Clínico Universitario de Salamanca e Investigador del Centro de Investigación del Cáncer de Salamanca e Instituto de Investigación Biomédica de Salamanca,

D.ª **Ana Eugenia Rodríguez Vicente**, Doctora en Biociencias por la Universidad de Salamanca e Investigadora del Centro de Investigación del Cáncer e Instituto de Investigación Biomédica de Salamanca,

CERTIFICAN

Que Dª Claudia Pérez Carretero, graduada en Biotecnología por la Universidad de Salamanca, ha realizado bajo nuestra dirección el trabajo de Tesis Doctoral titulado "*Molecular analysis of rare cytogenetic abnormalities in chronic lymphocytic leukemia: from genomic alterations to metabolic reprogramming*", y que éste reúne, a nuestro juicio, las condiciones de originalidad y calidad científica requeridas para su presentación y defensa ante el tribunal correspondiente para optar al grado de Doctor, con mención "Doctor Internacional", por la Universidad de Salamanca.

La tesis doctoral ha sido escrita en inglés y, de acuerdo con la normativa de la Universidad de Salamanca para la obtención del título de Doctor, el doctorando presenta un resumen significativo en castellano de la misma.

Y para que así conste a los efectos oportunos, firmamos el presente certificado en Salamanca a de de 2023.

Fdo:

Prof. Dr. Jesús M. Hernández Rivas Dra. Ana E. Rodríguez Vicente

This thesis was performed being Claudia Pérez Carretero supported by "Ayuda predoctoral en Oncologia de la Asociación Española Contra el Cáncer"(2019), "Contrato predoctoral FI19/00191 del Instituto de Salud Carlos III/Fondo Social Europeo" (2020-2022), and by "Beca de Investigación de la Fundación Española de Hematología y Hemoterapia (FEHH) 2022" (March 2023-February 2024).

Acknowledgements:

- Fondo de Investigaciones Sanitarias (FIS) PI15/01471, PI18/01500 and PI21/00983 Instituto de Salud Carlos III (ISCIII), European Regional Development Fund (ERDF) "Una manera de hacer Europa".
- Consejería de Educación, Junta de Castilla y Léon (SA271P18 & SA118P20).
- Proyectos de Investigación del SACYL, Spain. GRS 1944/B/19
- "Fundación Memoria Don Samuel Solórzano Barruso" (FS/33-2020).
- Red Temática de Investigación Cooperativa en Cáncer (RTICC) (RD12/0036/0069)
- Centro de Investigación Biomédica en Red de Cáncer (CIBERONC CB16/12/00233)
- SYNtherapy "Synthetic Lethality for Personalized Therapy-based Stratification In Acute Leukemia" (ERAPERMED2018-275); ISCIII (AC18/00093), co-funded by ERDF/ESF, "Investing in your future".
- Nemhesys. NGS Establishment in Multidisciplinary Healthcare Education SYStem. Project Ref.: 612639-EPP-1-2019-1-ES-EPPKA2-KA
- Fundación Española de Hematología y Hemoterapia (FEHH)

Table of contents

LIST OF ABBREVIATIONS

ACLY	ATP-citrate lyase
ACSS2	Acetyl-CoA synthetase
AID	Activation-induced cytidine deaminase
AKT	V-Akt murine thymoma viral oncogene homolog 1
ALL	Acute lymphoblastic leukemia
allo-TPH	Allogeneic stem cell transplantation
amp	Amplification
APOBEC	Apolipoprotein B MRNA Editing Enzyme
APRIL	A proliferation inducing ligand (TNFSF13)
ARID1A	AT-rich interaction domain 1A
ASXL1	Additional sex combs like 1, transcriptional regulator 1
ATM	Ataxia telangiectasia mutated
ATP	Adenosine triphosphate
BAFF	B-cell activating factor (TNFSF13B)
BAFF-R	B-cell activating factor receptor
BAK	B-cell CLL/lymhoma-2 antagonist/killer 1
BAX	B-cell CLL/lymhoma-2 associated X protein
BAZ2A	Bromodomain adjacent to zinc finger domain 2A
BCL11A	B cell CLL/lymphoma 11A
BCL2	B-cell CLL/lymhoma-2
BCL3	B-cell CLL/lymphoma 3
BCL6	B-cell CLL/lymphoma 6
BCLXL	B-cell CLL/lymphoma-extra large
BCOR	B-cell CLL/lymphoma 6 corepressor
BCR	B cell receptor
BH3	B-cell CLL/lymphoma 2 homology domain 3
BIM	B-cell CLL/lymhoma-2-like protein 11
BIRC2	Baculoviral inhibitor of apoptosis (IAP) repeat containing 2
BIRC3	Baculoviral inhibitor of apoptosis (IAP) repeat containing 3
BPTES	Bis-2- (5-phenylacetamido -1,3,4-thiadiazol-2-yl) ethyl sulfide
BRAF	V-Raf murine sarcoma viral oncogene homolog B
BTG1	B-cell translocation gene 1
BTK	Bruton's tyrosine kinase
C968	Compound 968
CARD11	Caspase recruitment domain family member 11
CAR-T	Chimeric antigen receptor T
CC	Conventional cytogenetics
CCND1	Cyclin D1
CCND2	Cyclin D2
CCR7	C-C motif chemokine receptor 7
CD10	Cluster of differentiation 10
CD19	Cluster of differentiation 19
CD20	Cluster of differentiation 20
CD200	Cluster of differentiation 200
CD23	Cluster of differentiation 23

CD31	Cluster of differentiation 31
CD38	Cluster of differentiation 38
CD40	Cluster of differentiation 40
CD40L	Cluster of differentiation 40 ligand
CD43	Cluster of differentiation 43
CD49d	Cluster of differentiation 49 family member D
CD5	Cluster of differentiation 5
CD79b	B-cell antigen receptor complex-associated protein beta chain
CD81	Cluster of differentiation 81
CDKN2A/B	Cyclin dependent kinase inhibitor 2A/2B
CDR3	Complementary determining region 3
CGH	Comparative genome hybridization
CHC	Cyano-4-hydroxycinnamate
CHD2	Chromodomain helicase DNA binding protein 2
CHK2	Checkpoint kinase 2
CK	Complex karyotype
CK1ε	Casein kinase 1 isoform epsilon
CLL	Chronic lymphocytic leukemia
CLL-IPI	International prognostic index of CLL
CNA	Copy number alteration
CNV	Copy number variation
CoA	Coenzime A
CPT1	Carnitine palmitoyl transferases 1
CPT2	Carnitine palmitoyl transferases 2
CREBBP	Cyclic AMP-responsive element-binding protein (CREB)-binding protein
CRISPR	Clustered regularly interspaced short palindromic repeats
CT	Computerized tomography
C-terminal	Carboxyl-terminal
CXCL12	C-X-C motif chemokine ligand 12
CXCL13	C-X-C motif chemokine ligand 13
CXCR4	C-X-C motif chemokine receptor 4
CXCR5	C-X-C motif chemokine receptor 5
DDR	DNA damage response
DDX3X	DEAD-box helicase 3 X-linked
del	Deletion
DLBCL	Diffuse large B-cell lymphoma
DLEU2	Deleted in lymphocytic leukemia 2
DLEU7	Deleted in lymphocytic leukemia 7
DNA	Deoxyribonucleic acid
DON	6-Diazo-5-oxo-L-norleucine
DSB	Double-strand break
ECAR	Extracellular acidification rate
EGR2	Early growth response 2
ERIC	European research initiative on CLL
ERK	Extracellular signal-regulated kinase
ESI	Electrospray ionization
ETC	Electron transport chain
EWSR1	Ewing sarcoma RNA binding protein 1

FAD	Flavin adenine dinucleotide
FAT1	Focal adhesion targeting atypical cadherin 1
FBXW7	F-Box and WD repeat domain containing 7
FCR	Fludarabine + cyclophosphamide + rituximab
FDA	Food & drug administration
FISH	Fluorescence *in situ* hybridization
FL	Follicular lymphoma
FUBP1	Far upstream element binding protein 1
GLS1	Glutaminase 1
GLUT1	Glucose transporter 1
GLUT4	Glucose transporter 4
GPNA	L-γ-glutamyl-p-nitroanilide
HIF	Hypoxia-inducible factor
HILIC	Hydrophilic interaction liquid chromatography
HIST1H1B	Histone cluster 1 H1 family member B
HIST1H1E	Histone cluster 1 H1 family member E
HR	Homologous recombination
IG	Immunoglobulin
IGH	Immunoglobulin heavy chain
IGHV	Immunoglobulin heavy chain variable region
IGHV-M	Immunoglobulin heavy chain variable region mutated
IGHV-UM	Immunoglobulin heavy chain variable region unmutated
IGLL5	Immunoglobulin lambda-like polypeptide 5
IgM	Immunoglobulin M
IKZF3	IKAROS family zinc finger 3
IL-2	Interleukin 2
Indel	Insertion/deletion
IRAK1	Interleukin 1 receptor associated kinase 1
IRAK2	Interleukin 1 receptor associated kinase 2
IRF4	Interferon regulatory factor 4
iwCLL	International workshop on CLL
KLHL6	Kelch like family member 6
KRAS	V-Ki-Ras2 Kirsten rat sarcoma 2 viral oncogene homolog
LC-MS	Liquid chromatography-mass spectrometry
LDH-A	Lactate dehydrogenase A
LPL	Lipoprotein lipase
MAP2K1	Mitogen-activated protein kinase, kinase 1
MAPK	Mitogen-activated protein kinase
Mb	Megabase
MBL	Monoclonal B-cell lymphocytosis
MCL1	Myeloid cell leukemia 1
MDR	Minimal deleted region
MED12	Mediator complex subunit 12
MGA	MYC-associated factor (MAX) gene-associated protein
miR-155	microRNA 155
miR-15a/16-1	microRNA 15a/16-1
miR-34a	microRNA 34a

miRNA	microRNA
MM	Multiple myeloma
MPC	Mitochondrial pyruvate carrier
MRD	Minimal residual disease
MS	Matutes score
MTC1	Monocarboxylate transporter 1
mTOR	Mammalian target of rapamycin
MYC	V-Myc avian myelocytomatosis viral oncogene homolog
MYD88	Myeloid differentiation primary response 88
NAD	Nicotinamide adenine dinucleotide
NF-kB	Nuclear factor of kappa B
NFKB2	Nuclear factor of kappa B subunit 2
NFKBIE	Inhibitor of nuclear factor kappa B epsilon gene
NGS	Next-generation sequencing
NHEJ	Non-homologous end joining
NHL	non-Hodgkin lymphoma
NIK	Nuclear factor of kappa B inducing kinase
NLC	Nurse-like cell
NOTCH1	Notch receptor 1
NOXA	Phorbol-12-myristate-13-acetate-induced protein 1
NRAS	Neuroblastoma RAS viral (V-Ras) oncogene homolog
NXF1	Nuclear RNA export factor 1
OCR	Oxygen consumption rate
OGM	Optical genome mapping
ORR	Overal response rate
OS	Overall survival
OXPHOS	Oxidative phosphorylation
PAM	Protospacer adjacent motif
PAX5	Paired box 5
PBMC	Peripheral blood mononuclear cell
PC1	Mitochondrial protein complex 1
PCR	Polymerase chain reaction
PDH	Pyruvate dehydrogenase
PDK1	Pyruvate dehydrogenase 1
PI3K	Phosphatidylinositol-4,5-bisphosphate 3-kinase
PI3Kγ	Phosphatidylinositol-4,5-bisphosphate 3-kinase catalytic subunit gamma isoform
PI3Kδ	Phosphatidylinositol-4,5-bisphosphate 3-kinase catalytic subunit delta isoform
PKM2	Pyruvate kinase M2
PLCG2	Phospholipase C gamma 2
POT1	Protection of telomeres 1
PRKAB2	Protein kinase AMP-activated non-catalytic subunit beta 2
PTEN	Phosphatase and tensin homolog
PTPN11	Protein tyrosine phosphatase non-receptor type 11
PUMA	P53 up-regulated modulator of apoptosis
Q-TOF	Quadrupole-time of flight
RB1	Retinoblastoma-associated protein 1
REL	V-Rel avian reticuloendotheliosis viral oncogene homolog

RelA	V-Rel avian reticuloendotheliosis viral oncogene homolog A
RelB	V-Rel avian reticuloendotheliosis viral oncogene homolog B
RING	Really intersting new gene
RNA	Ribonucleic acid
ROR1	Receptor tyrosine kinase like orphan receptor 1
ROS	Reactive oxygen species
RPS15	Ribosomal protein S15
RS	Richter's syndrome
RT	Retention time
RTK	Receptor tyrosine kinase
SAMHD1	SAM and HD domain containing deoxynucleoside triphosphate triphosphohydrolase 1
sCD23	soluble CD23
SETD2	SET domain containing 2, histone lysine methyltransferase
SF3B1	Splicing factor 3b subunit 1
sgRNA	Single-guide RNA
SHM	Somatic hypermutation
sIgM	soluble sIgM
SLC1A4	Solute Carrier Family 1 Member 4
SLC1A5	Solute Carrier Family 1 Member 5
SLC44A2	Solute Carrier Family 44 Member 2
SLL	Small lymphocytic lymphoma
SNHG5	Small Nucleolar RNA Host Gene 5
SNP	Single-nucleotide polymorphism
SNV	Single-nucleotide variant
SPEN	Spen family transcriptional repressor
SSB	Single-strand break
SYK	Spleen associated tyrosine kinase
SYNCRIP	Synaptotagmin Binding Cytoplasmic RNA Interacting Protein
t	Translocation
TCA	tricarboxylic acid
TCL1	T-cell leukemia/lymphoma 1
TK	Thymidine kinase
TLR2	Toll-like receptor 2
TLR6	Toll-like receptor 6
TME	Tumor microenvironment
TNF	Tumor necrosis factor
TNFAIP3	Tumor necrosis factor α induced protein 3
TP53	Tumor protein P53
TRAF2	Tumor necrosis factor receptor associated factor 2
TRAF3	Tumor necrosis factor receptor associated factor 3
TFT	Time to first treatment
U1	U1 small nuclear RNA
UTR	Untranslated region
VAF	Variant allele frequency
VCAM1	Vascular cell adhesion molecule 1
WES	Whole-exome sequencing
WGS	Whole-genome sequencing

WHO	World Health Organization
WNT5A	Wingless-type MMTV integration site family, member 5A
WT	Wild-type
XPO1	Exportin 1
ZAP70	Zeta chain of T-cell receptor associated protein kinase 70
ZMYM3	Zinc finger MYM-type containing 3
ZNF292	Zinc finger protein 292
α4β1	Alpha 4 beta 1 integrin (VLA-4)
β_2M	Beta-2 microglobulin
2-DG	2-deoxy-D-glucose

LIST OF TABLES AND FIGURES

INTRODUCTION

RESULTS: CHAPTER 1

RESULTS: CHAPTER 2

INTRODUCTION

1. CHRONIC LYMPHOCYTIC LEUKEMIA: DISEASE OVERVIEW

Chronic lymphocytic leukemia (CLL) is a hematological disease characterized by the clonal expansion and accumulation of small, mature and neoplastic B cells in the blood, bone marrow and other lymphoid tissues[1-3]. CLL is the most common leukemia in western countries, accounting for nearly 30% of all leukemias, with an incidence of 4.7 cases per 100000 inhabitants[4]. Males are more frequently affected than females, in a male-to-female ratio of 1.7:1, and the median age at diagnosis is 70-72[5]. Early-stage CLL diagnosis in younger patients seems to increase in the last years due to more frequent blood testing. Although CLL is a sporadic disease, there is clear evidence of inherited predisposition. Relatives of CLL patients show an increased risk of developing the disease, as well as other types of non-Hodgkin lymphomas[6-8].

1.1 Diagnosis

The first consensus criteria for CLL diagnosis were established in the 1990s[9], and they have undergone multiple revisions over the last few decades[10]. According to the 2018 International Workshop on CLL (iwCLL) guidelines, CLL diagnosis is mainly based on laboratory features, namely blood count, morphology and immunophenotyping[11]. Most CLL patients present an indolent disease, while a minority of cases can have B symptoms, defined as persistent fever, night sweats, weight loss or fatigue, and in some cases, they also have palpable lymphadenopathy, splenomegaly and/or hepatomegaly[5].

CLL diagnosis requires the presence of more than $5x10^9$/L B-lymphocytes in peripheral blood persisting for longer than 3 months, and the immunophenotype needs to be assessed by flow cytometry to confirm the clonality of the B cells[5]. The **CLL immunophenotype** is characterized by the co-expression of the T-cell antigen CD5, and B-cell antigens CD19, CD20 and CD23. In addition, CLL B cells often show lower CD20 and CD79B expression than normal B cells, and either kappa or lambda immunoglobulin light chains expression in each clone[12, 13]. To refine the diagnosis of CLL, the expression or other markers can be assessed, such

as CD43, CD81, CD200, CD10, or ROR1[14]. Based on the antigenic profile, **Matutes' score (MS) system** was designed to ensure CLL diagnosis. A score of 0 or 1 is assigned according to the presence of a strong expression of CD5 and CD23, and a low or absent expression of CD79b/CD22, sIgM and FMC7. CLL cases have a score of 4 or 5, while a score of less than 3 corresponds to non-CLL cases[12, 13]. Regarding morphology, CLL cells are small, mature lymphocytes with a narrow border of cytoplasm, a dense nucleus without discernible nucleoli and partially aggregated chromatin[9, 15]. Rarely, CLL cells can have an atypical morphology, with cleaved nuclei and/or lymphoplasmacytoid features, and an atypical immunophenotype (MS<4). This entity is referred to as **atypical CLL**[16-18].

CLL development may be preceded by **monoclonal B-cell lymphocytosis (MBL)**, an asymptomatic precursor state characterized by the presence of fewer than $5x10^9$/L B-lymphocytes and the absence of lymphadenopathy or organomegaly (as defined by physical examination or CT scans), cytopenias, or disease-related symptoms[19]. According to the number of B-lymphocytes in peripheral blood, MBL can be classified into low-count MBL and high-count MBL ($< 0.5 \times 10^9$/L and $\geq 0.5 \times 10^9$/L, respectively)[20-22]. MBL progresses to overt CLL at a rate of 1-2% per year[19].

According to the World Health Organization (WHO) classification of hematopoietic neoplasias, there is a clinical variant of CLL named **small lymphocytic lymphoma** (**SLL**)[23]. SLL is defined by the accumulation of B cells in the lymph nodes and the absence of peripheral clonal lymphocytes and cytopenias. Although SLL is considered the same histological entity as CLL, its diagnosis should be confirmed by a lymph node biopsy[11, 23].

During the natural clinical course of CLL, the development of an aggressive B-cell lymphoma occurs in 0.05%-0.5% of cases per year. This histological transformation is known as **Richter's syndrome (RS),** and it is associated with a dismal prognosis[24, 25]. A lymph biopsy is required to determine Richter transformation. Histologically, most RS cases (95%) transform to diffuse large B cell lymphoma (DLBCL), and less frequently to Hodgkin lymphoma (5%)[24, 26-28]. In most cases (80%), RS clonally evolves from the CLL clone, showing a more aggressive

disease than RS clonally CLL-unrelated[26, 29]. The latter transformation derives from other B cell precursors and should be considered as a second independent malignancy in the same patient, with an outcome more similar to *de novo* DLBCL[24, 29].

1.2 Prognostic markers and risk scoring systems

CLL displays a remarkably **clinical heterogeneity**, ranging from an asymptomatic disease that does not require treatment, to a rapid disease progression characterized by an urgent need for therapy, refractoriness to treatment, and short overall survival (OS)[2, 10]. Due to this variable clinical course, several efforts have been made to identify prognostic markers that help clinicians to predict the clinical outcome of patients, and predictive biomarkers able to predict treatment response in the targeted therapy era[30, 31].

1.2.1 Rai and Binet staging systems

For more than 4 decades, two **clinical staging systems** developed by Rai *et al* and Binet *et al.* have been used to classify patients into different risk subgroups, based on physical examination and blood counts[5, 32, 33]. Rai stage system classifies patients into 5 categories, more recently grouped into low (0-I), intermediate (II) and high risk (III-IV) subgroups[32, 34]. This stratification is defined by the presence of lymphocytosis, anemia and/or thrombocytopenia, as well as the number of enlarged lymph nodes, and palpable splenomegaly and hepatomegaly[32]. The Binet stage system classifies patients into three categories (A, B and C), considering the aforementioned parameters, in addition to hemoglobin levels and platelet count[33]. Other parameters such as the lymphocyte doubling time and bone marrow infiltration were subsequently implemented as easily measurable prognostic markers[35, 36].

Due to their simplicity and low-cost requirements, these staging systems remain the first approach for patients' risk stratification. Nevertheless, their inability to predict disease progression in early-stage patients (Binet A or Rai 0) is a significant limitation nowadays. In order to complete these prognostication systems, a plethora of **new prognostic markers** have been described in the last decades[37].

1.2.2 Serum and immunophenotypic markers

More robust prognostic markers have been identified thanks to the development of newer techniques such as immunoenzymatic assays, flow cytometry, cytogenetics and molecular biology.[4] High levels of serum markers measured by immunoenzymatic assays, including β-2 microglobuline (B_2M), timidine kinase (TK) or soluble CD23 have been related to higher burden disease and poor outcome[38-40]. Additionally, immunophenotypic markers such as CD38, ZAP70 and CD49d have been validated as prognostic indicators[41-43]. The expression of these markers (≥30% of positive cells for CD38 and CD49d, and ≥20% of positive cells for ZAP70) has been associated with the unmutated status of the variable heavy chain of immunoglobulins (IGHV) and poor outcome[43-45].

1.2.3 Mutational status of the immunoglobulin heavy chain variable (IGHV) region

CLL can be classified into two main subsets according to the mutational status of the immunoglobulin heavy chain variable (IGHV) region: mutated or unmutated[41, 46-48]. The acquisition of mutations in the IGHV region (somatic hypermutation-SHM) occurs during normal B cell development in the germinal centers of lymph nodes after exposure to a T cell-dependent antigen[49].

CLL cells with **IGHV-unmutated (IGHV-UM)** status originate from a B cell that has not undergone differentiation in the germinal centers, while **IGHV-mutated (IGHV-M)** cells come from a post-germinal B cell that does undergo SHM, similar to the immune response of normal B cells to an antigen (**Figure 1**)[46, 50]. IGHV-M CLL subtype accounts for 60% of CLL cases and is defined when there is less than 98% of homology with the germline nucleotide sequence. It is associated with a favorable outcome and low-risk genetic alterations[11, 41, 48]. Conversely, IGHV-UM subtype shows more than 98% of homology with the germline sequence, and associates with poor prognosis, high-risk genetic lesions and a higher propensity to undergo clonal evolution[29, 41, 48, 50, 51].

In CLL the B-cell receptor immunoglobulin (BCR IG) repertoire is biased, and there are subsets of cases with closely homologous or "steryotyped" complementarity-determining region 3 (CDR3) sequences[52]. The most common

BCR IG stereotyped subsets in CLL are #1, #2, #8 and #4, showing different clinical and biological features[53-56]. A recent study identified subset #2 as an independent risk factor of prognosis, however, IGHV stereotypes are not routinely assessed in clinical practice[57].

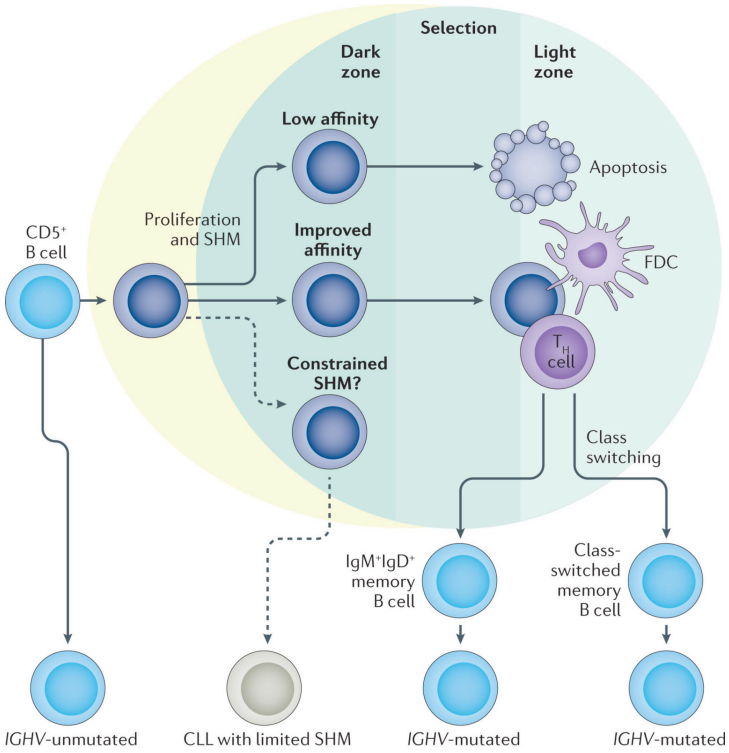

Figure 1. Cellular origin of IGHV-M and IGHV-UM CLL cells. Schematic representation of normal B cells that undergo somatic hypermutation in the germinal centers (dark zone), express the fittest B cells receptor (light zone), and may subsequently experience immunoglobulin class-switch recombination. CLL cells with IGHV-UM originate from CD5+ B cell prior to undergo SHM, and most CLL cells with IGHV-M originate from CD5+ B cells that have passed through the germinal center, and some of them have also experienced class-switch recombination *(adapted from Kipps et al. 2017)*[3].

1.2.4 Genetic biomarkers

Large-scale CLL genomic studies have revealed the presence of numerous genetic alterations, reflecting a great genetic heterogeneity that underlies the clinical heterogeneity observed in CLL[3, 50, 58]. A more extensive description of the genetic alterations and their functional role in CLL pathogenesis will be addressed in *section 2*. In this section, I will focus on the prognostic implications of some of the most recurrent alterations reported in CLL.

Approximately, 80% of CLL patients present at least one cytogenetic alteration[58]. Given the low mitotic rate of CLL cells that hindered conventional cytogenetics (CC), the implementation of fluorescence in situ hybridization (FISH) improved the assessment of the most recurrent CLL **chromosomal abnormalities**: 13q deletion (del(13q), in ~50% of cases at diagnosis), 11q deletion (del(11q), 10-18%), trisomy 12 (+12, 12-20%) and 17p deletion (del(17p), 5-8%)[59, 60]. Since the 2000s, FISH analysis has been considered the gold standard for cytogenetic risk stratification, and the classic four-probe CLL FISH panel is usually performed in clinical routine[51]. Five prognostic categories were first defined by Döhner *et al*, and were further validated in several studies (**Figure 2**)[59, 61-63].

The presence of del(13q) is associated with a favorable prognosis, even better than the absence of cytogenetic abnormalities (normal karyotype)[59]. Trisomy 12 has been related to an intermediate outcome, although its prognostic relevance remains controversial[59]. Patients with del(11q) and del(17p) show an adverse clinical course, associated with rapid disease progression, short OS, and poor response to treatment, especially to chemotherapy regimens[59, 64]. In the targeted therapy era, del(11q) prognosis has significantly improved, as patients with this abnormality show better responses to BTK inhibitors[65]. Del(11q) and del(17p) encompass tumor suppressor genes that can be mutated in the remaining allele: *ATM* and *TP53*, respectively. *ATM* and *TP53* mutations contribute to dismal prognosis and are enriched in patients with resistance to DNA-damaging chemotherapy-based regimens[66-72]. In addition to its prognostic value, **del(17p)/*TP53* mutation** assessment is crucial for treatment decisions, especially in the context of novel targeted therapies. Therefore, recent studies recommend the implementation of *TP53* screening in clinical routine before each therapy and at relapse[73-75]. More recently, CC has recovered its prognostic relevance since it has been demonstrated that complex karyotype (≥3 chromosomal abnormalities) is associated with an adverse outcome[76].

In the last decade, the expansion of next-generation sequencing (NGS) techniques has led to the identification of several genetic alterations (somatic mutations, copy number variations, non-coding alterations or epigenetic modifications), many of them with potential implications in prognosis[77-82].

Mutations in *NOTCH1, SF3B1*, and *BIRC3* have been associated with unfavorable outcome and IGHV-UM [77, 80, 83-87], while *MYD88* mutations correlate with a better prognosis and low-risk markers (IGHV-M and del(13q))[88-90]. However, the low incidence of these alterations and the technical limitations impair their implementation in routine practice.

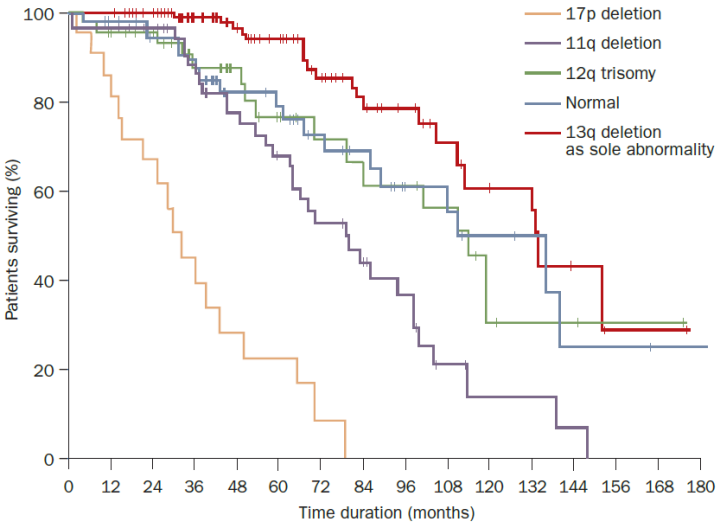

Figure 2. Patients risk stratification by Döhner hierarchical model. Impact of cytogenetic alterations (del(17p), del(11q), +12 and del(13q) as the sole abnormality) on overall survival among CLL patients *(taken from Cramer et al. 2011, adapted from Döhner et al. 2000)*[51, 59].

As previously mentioned, the search for new prognostic markers has significantly increased in the last few years to develop more robust prognostic models. After Rai and Binet staging systems establishment[32, 33], other prognostic scores have implemented new parameters considering also genetic features[91-95]. The most expanded prognostic score is the **International Prognostic Index for CLL (CLL-IPI)**[94]. CLL-IPI combined five risk factors: age (>65 years), clinical stage (Binet B–C or Rai I–IV), serum β-2 microglobulin concentration (>3.5 mg/L), IGHV mutational status (unmutated) and *TP53* status (del(17p) and/or *TP53* mutation). Using a weighted grading of these factors, this prognostic model stratifies patients in four risk subgroups with significantly different OS[94]. Other prognostic models also considered genetic mutations and complex karyotype to refine prognosis[96-98]. Nevertheless, most of the proposed prognostic models so far were designed considering chemotherapeutic regimens. For that reason, new prognostic models

as well as new indicators are needed for the assessment of prognosis in the targeted therapy era.

1.3 CLL treatments

CLL is a clinically heterogeneous disease and not all patients require therapy at the time of diagnosis[5]. Patients should be under surveillance without treatment initiation unless there is evidence of active or symptomatic disease. An "active" disease needs to be well documented and met at least one of the iwCLL guidelines criteria, based on biological and clinical parameters[11].

The assessment of the response should be performed by physical examination and blood count evaluation at least 2 months after completion of therapy, or after maximal response achievement in continued therapies (defined as the absence of improvements for at least 2 months)[4, 11]. According to the iwCLL guidelines, there are five categories of treatment response: complete remission, partial remission, progressive disease, stable disease and refractory disease. Nowadays, the evaluation of minimal residual disease (MRD; <1 CLL cell per 10000 leukocytes) by flow cytometry, PCR or high-throughput techniques is significantly increasing, especially to determine treatment response in clinical trials[99-101]. However, MRD assessment is not always performed in routine practice.

In case of treatment initiation, many options are available for CLL patients, highlighting chemoimmunotherapy and novel targeted therapies.

1.3.1 Chemoimmunotherapy

Chemotherapy has been considered the first option for initial CLL treatment for more than 50 years. Cytostatic agents used in CLL included alkylating agents (chlorambucil, bendamustine and cyclophosphamide) and purine analogs (fludarabine and pentatostin)[102]. Chlorambucil monotherapy was the "gold standard" of chemotherapy regimens, until the spreading of fludarabine-base regimens and the combination of these agents with **immunotherapy** (especially anti-CD20s: rituximab, obinutuzumab or ofatumumab). Some of the most prevalent **chemoimmunotherapeutic approaches** were chlorambucil plus obinutuzumab,

and the triple combination FCR (fludarabine, cyclophosphamide and rituximab), with higher response rates and longer progression-free survival[103-105].

1.3.2 Novel targeted therapies

In the last few years, new advances in molecular biology and the identification of druggable biological pathways in CLL have prompted the development of novel targeted therapies. Moreover, due to the improvements in terms of overall response rates (ORRs) and lower toxicity, these new approaches are gradually displacing chemoimmunotherapeutic regimens [106, 107].

BCR inhibitors

B-cell receptor (BCR) signaling plays an important role in CLL pathogenesis[108]. Antigen binding to the receptor activates a network of upstream kinases, including Bruton tyrosine kinase (BTK), spleen tyrosine kinase (SYK), or phosphatidylinositol-3-kinase (PI3K). Subsequently, BTK and PI3K phosphorylation results in downstream activation of secondary molecular pathways such as MAPK-ERK, PI3K-AKT-MTOR and/or NF-kB signaling, dysregulating target gene expression, and promoting B cell proliferation, migration and survival[108-110]. In CLL, continuous BCR stimulation is required to maintain B cell survival, which makes it a potent druggable target[111]. BCR inhibitors are classified as BTK and PI3K inhibitors (**Figure 3**).

The most widely used first-in-class **BTK inhibitor** for CLL treatment is **ibrutinib**[112]**.** Ibrutinib is an orally active and small molecule that irreversibly binds to the cysteine 481 residue (C481) of BTK, inhibiting the phosphorylation of PLCG2 and downstream signaling[113]. Additionally, this drug also disrupts the interactions of the B cell with the tumor microenvironment[114]. Ibrutinib is approved for frontline treatment, as well as in patients at relapse, especially in those with del(17p) and/or IGHV-UM[115-118]. **Acalabrutinib** is a second-generation more selective covalent BTK inhibitor that also targets C481 residue. It was approved by the FDA for first-line treatment and after relapse, with fewer adverse effects[119, 120]. Other second-generation BTK inhibitors also targeting C481 residue are under investigation, such as zanubrutinib and tirabrutinib[121, 122]. In the last years, third-generation **noncovalent BTK inhibitors** including pirtobrutinib (LOXO-305), ARQ-351,

fenebrutinib, and vecabrutinib have been developed[123, 124]. These drugs inhibit BCR signaling without binding to C481, maintaining their potency in patients harboring mutations in this residue. Phase 1-2 clinical trials have already demonstrated a high efficacy of pirtobrutinib in ibrutinib-refractory CLL patients[124].

PI3K inhibitors represent an alternative option for BCR inhibition, indicated in relapse settings. **Idelalisib** is an inhibitor of the PI3Kδ isoform, which reduces B cell proliferation and survival by blocking BCR and chemokine-receptor-mediated signaling[125]. Idelalisib was approved by the FDA for refractory CLL patients, preferably used in combination with rituximab[126, 127]. **Dual PI3K inhibitors** such as duvelisib (PI3Kδ/γ) and umbralisib (PI3Kδ/CK1ε) are currently under evaluation, especially to assess their efficacy and safety in combination with other inhibitors (anti-CD20, acalabrutinib or venetoclax)[128-130]. Although umbralisib showed a better safety profile than other PI3K inhibitors, the presence of adverse events still limits their use as an alternative to BTK inhibitors[127, 130].

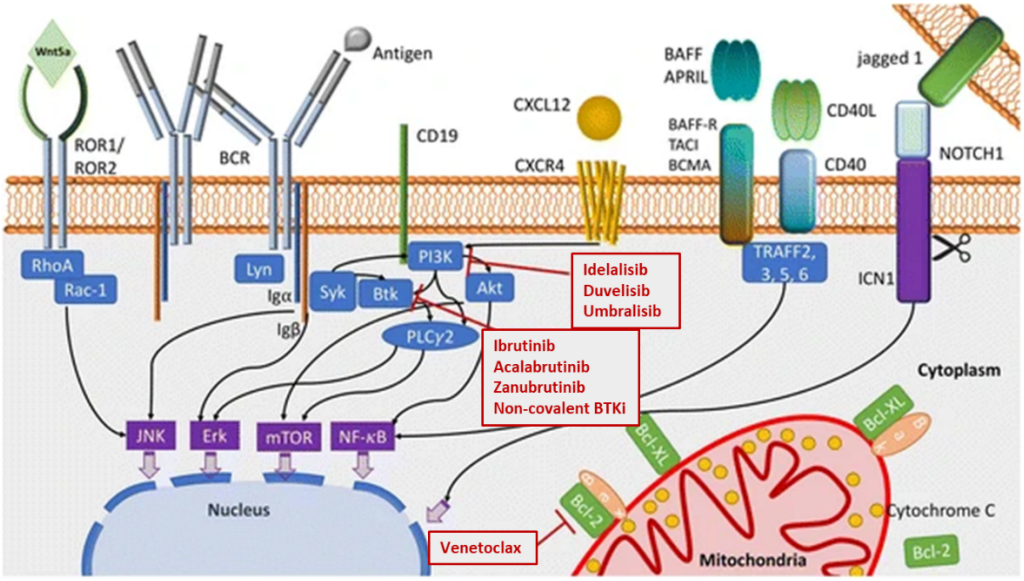

Figure 3. **Targeted therapies in CLL**. Schematic representation of molecular pathways and targets of BTK inhibitors (ibrutinib, acalabrutinib, zanubrutinib and non-covalent BTK inhibitors), PI3K inhibitors (idelalisib, duvelisib and umbralisib) and BCL2 inhibitor (venetoclax) in the CLL cell *(adapted from Ferrer et al. 2018)*[131].

BCL2 inhibitors

BCL2-family, consisting of pro-apoptotic (BAX, BAK) and anti-apoptotic proteins (BCL2, BCLXL, MCL1), are crucial regulators of the apoptotic process.

BCL2 sequesters the pro-apoptotic proteins BAX and BAK and prevents them from oligomerization, inhibiting the permeabilization of the mitochondrial membrane. BH3-only members (i.e. BIM, NOXA, PUMA) can bind to BCL2, releasing BAX and BAK and promoting oligomerization and apoptosis[132]. **Venetoclax** is a small BH3-mimetic molecule that binds to BCL2, activating pro-apoptotic proteins and restoring the apoptotic process[133, 134] (**Figure 3**). Venetoclax was previously indicated for refractory CLL patients[135, 136], and results of CLL14 phase 3 trial showed that the combination of venetoclax plus obinutuzumab also improved progression-survival in untreated patients[137, 138].

Despite the improvements in survival, some CLL patients are refractory to novel therapies and different mechanisms of resistance have been identified, as described in section 2: *clonal evolution and targeted therapies evasion mechanisms*.

Besides chemoimmunotherapy and targeted therapies, there are other options for CLL management. Allogeneic stem cell transplantation (allo-TPH) is a curative approach, indicated for high-risk and refractory patients to BCR inhibitors[139, 140]. However, with the development of novel agents, the benefits and indications for this approach are a matter of debate[141]. Chimeric antigenic receptor T (CAR-T) cell therapy, another promising alternative for CLL treatment, is currently under investigation, as initial ORRs were not as good as those observed in other hematological diseases[142-144].

Since CLL therapy has experienced a significant shift from chemotherapy to novel agents, and new genetic prognostic markers have emerged, the **treatment algorithm** has also changed in the last few years[112]. **Figure 4** shows the algorithm for first-line treatment and refractory CLL patients. The wide variety of treatment options and the new algorithm based on biological features (*TP53* and *IGHV* status) are contributing to developing a highly efficient and more individualized CLL therapy. However, despite these advances, CLL still remains an incurable disease and many patients relapse to current therapies, which brings to light the necessity of searching for new combinations of treatments and novel CLL targets.

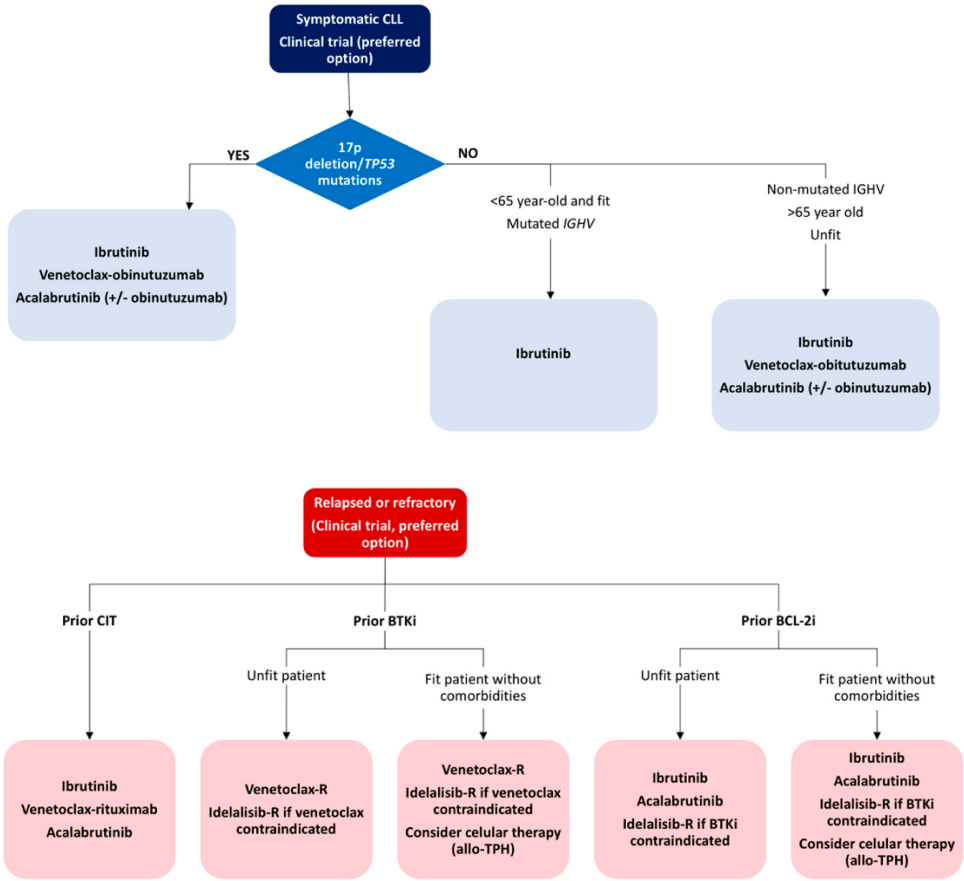

Figure 4. Treatment algorithm for treatment naïve and refractory CLL patients. CIT: chemoimmunotherapy; BTKi: BTK inhibitor; BCL2i: BCL2 inhibitor; R: rituximab; Allo-TPH: allogeneic stem cell transplantation *(taken from Pérez-Carretero et al. 2021)*[31].

2. CLL PATHOGENESIS

CLL represents an ideal model to explore cancer growth and evolution, as it undergoes variable clinical courses conditioned by a wide variety of molecular alterations. In addition, CLL cells are continuously circulating in peripheral blood, facilitating the obtention of high-purity tumor samples for high-throughput studies. CLL pathogenesis involves multilayered changes, ranging from specific genetic alterations to variations in the interaction with the microenvironment, which confer a phenotypic advantage to the B cell that may also be influenced by external selective pressures, such as CLL treatments. All these events converge in disrupted or constitutive activated biological pathways that determine clonal dynamics, disease progression, and ultimately, resistances or vulnerabilities to CLL therapy.

2.1. CLL genetic alterations

Characterization of the CLL genome has revealed its great genetic heterogeneity, with a small number of highly recurrent alterations, and multiple rare genetic events with potential roles in CLL pathogenesis. Hence, there is a lack of a common genetic alteration within this disease. The variable clinical course of CLL patients reflects its genetic heterogeneity, and several studies have demonstrated that the presence of certain genetic alterations correlates with distinct clinical implications. Genetic CLL lesions include chromosomal abnormalities, somatic mutations, non-coding genetic alterations and epigenetic modifications.

2.1.1. Chromosomal abnormalities

Chromosomal abnormalities are the hallmark of CLL and were initially detected by CC in the 1980s[58, 145, 146]. However, the low mitotic rate of CLL cells hampered the identification of these alterations, which were detected in only 40-50% of patients[60]. FISH allows the identification of chromosomal abnormalities irrespective of the B cell mitotic activity, demonstrating that approximately 80% of CLL patients had at least one cytogenetic alteration[59]. The most recurrent chromosomal abnormalities detected by FISH are 13q deletion (del(13q)), 11q deletion (del(11q)), trisomy 12 and 17p deletion

(del(17p)). Other recurrent alterations that are not routinely assessed by FISH are 6q deletion and 14q rearrangements, as well as deletions involving the *IGH* gene[59, 147]. Newer cytogenetic techniques with higher resolution, such as comparative genomic hybridization (CGH) arrays, optical genome mapping (OGM) or next-generation sequencing (NGS), provided a more comprehensive analysis of the CLL genetic landscape, identifying less frequent chromosome gains and losses[58, 148, 149]. Moreover, thanks to the implementation of novel cell stimulation protocols, CC has recovered its relevance in the last years, especially for the assessment of translocations and complex karyotype[147, 150, 151].

2.1.1.1. Recurrent chromosomal abnormalities in CLL

The most recurrent chromosomal abnormalities in CLL are routinely assessed in the clinic by using the 4-probe FISH panel. The main features of these alterations are described below.

13q deletion. Deletion of 13q14 region is the most frequent chromosomal abnormality in CLL, present in more than 50% of cases, being monoallelic in 80% of them[59, 61, 63, 152]. It appears at the early stages of the disease and associates with good prognosis and IGHV-M[62, 153]. The size of the del(13q) varies among patients, although the minimal deleted region (MDR) encompasses long non-coding RNAs (***DLEU2, DLEU7***), and the microRNA cluster **MIR15A–MIR16-1**[154-156]. The microRNA cluster has been suggested to have a role in apoptosis and cell cycle, by modulating Cyclin D2 and BCL2 expression[156, 157]. A higher proportion of cells with del(13q) and an increased size of the deletion has been related to a more aggressive disease, and in 20% of del(13q) patients, the deletion extended to the tumor suppressor RB1, contributing to a worse outcome within this subgroup[158-163]. By contrast, it has not been confirmed that biallelic del(13q) associates with a poorer outcome[153, 164, 165].

11q deletion. Deletion of 11q22-23 region can be found in 12-20% of CLL patients at diagnosis, and is associated with adverse outcome, lymphadenopathies, and IGHV-UM[59, 61, 166-168]. As reported by our group, the number of cells with this alteration influences clinical outcome[169]. The size of this deletion is large (>20 Mb) and variable among patients[170]. Del(11q) encompasses the ***ATM* gene**, a tumor suppressor gene with a relevant role in DNA damage response (DDR) and cell cycle arrest[171, 172]. One-

third of del(11q) patients harbor mutations in the remaining allele, resulting in a biallelic alteration of this gene.[173] Due to the DDR deficiency, del(11q) patients with *ATM* mutations accumulate a high number of genomic alterations, which can be related to a worse prognosis and chemorefractoriness[66, 67, 174]. Del(11q) may also encompass the ***BIRC3* gene**, a negative regulator of the non-canonical NF-kB signaling. *BIRC3* mutations in the remaining allele have also been described, and recent studies have demonstrated their important role in CLL progression, as well as their impact in prognosis[175-177]. The haploinsufficiency of other genes encompassed in del(11q) may have a role in del(11q) pathogenesis, however, limited studies have investigated these molecular mechanisms and their implications.

Trisomy 12. Trisomy 12 appears with a frequency of 10-20% in CLL[59, 61, 62]. This alteration has been correlated with an intermediate prognosis, suggesting that genes located in chromosome 12 may have a role in CLL pathogenesis[59, 178]. This entity is characterized by an atypical morphology and immunophenotype, with high expression of CD38 and CD49d[179, 180]. Trisomy 12 has been extensively associated with ***NOTCH1* mutations**, which negatively refine the clinical outcome of patients harboring this cytogenetic alteration[96, 180-183]. Moreover, a high frequency of mutations in genes involved in **MAPK signaling** has been reported within this subgroup[184, 185], and whole genome and exome studies suggested patterns of co-occurrence with other genetic alterations, such as *BIRC3* mutations[78, 86]. In terms of cytogenetic alterations, trisomy 12 frequently co-occurs with trisomy 18 and 19, 14q deletions and 14q translocations involving the *IGH* gene[178, 186-192]. Nevertheless, these alterations only occur in the ~30% of cases with trisomy 12, revealing the great heterogeneity of this entity and that further pathogenic mechanisms underlying this alteration remain to be elucidated.

17p deletion. Deletions of 17p13 region are found in 5-10% of patients at diagnosis, but the frequency increases up to 40% in patients at relapse[59, 61, 193]. Del(17p) is the highest risk cytogenetic alteration, associated with a marked poor outcome and refractoriness to chemotherapeutic regimens, even when it is present in a low number of cells[64, 194]. This alteration is more commonly found in the IGHV-UM subgroup and has been related to Richter's transformation[25, 29, 195, 196]. Del(17p) encompasses the **tumor suppressor gene *TP53***, and 80% of patients with this deletion harbor mutations in the remaining allele, being the main mechanism underlying the

pathogenesis of CLLs with this alteration[72, 197]. *TP53* plays an important role in cell cycle arrest, DDR and apoptosis. Hence, *TP53* inactivation is determinant for chemotherapy response, as it hampers the apoptosis induction of DNA-damaged cells[64, 70, 198-200]. Del(17p) and *TP53* inactivation promote the accumulation of alterations and genomic instability, which seems to underlie Richter´s transformation and contributes to a dismal prognosis and resistance to therapy [148, 171, 193, 195, 196, 201].

2.1.1.2. Rare chromosomal abnormalities in CLL

In addition to the four most recurrent cytogenetic alterations, CC, FISH, CGH arrays and NGS studies have identified a large number of less frequent copy number alterations (CNAs), including trisomy 18 and trisomy 19, deletions or losses of 3p, 6q, 6p, 8p, 9p, 10q, 14q, 18p, and 20p, and gains of 2p, 8q, 17q, 20q[79, 148, 171, 172, 202-205]. These alterations may encompass CLL driver genes such as *XPO1* in amp(2p)[203], *MYC* in amp(8q)[204], or *TRAF3* in del(14q)[205]. Besides chromosomal gains and losses, chromosomal translocations have also been identified in CLL[147, 202, 206, 207]. Although they are not a hallmark of this disease, a low but not insignificant percentage of CLL patients present 14q rearrangements that frequently involve the IGH gene[208-210].

6q deletion. Del(6q) is a rare CLL alteration detected in 3-7% of patients by CC and FISH, generally as a second cytogenetic abnormality or in the context of complex karyotype[171, 211-214]. The presence of del(6q) has been associated with an intermediate and inferior outcome; however, its independent prognostic impact is still controversial, due to its co-occurrence with complex karyotype and lack of studies in large cohorts[211, 214-217]. The size of the del(6q) is very heterogeneous and an MDR has not been identified[171]. Nevertheless, 6q21-24 is the most commonly deleted region among different studies[171, 213-216, 218]. Biologically, del(6q) has been associated with a low expression of *FOXO3*, a candidate tumor suppressor gene that is encompassed in 6q21[218]. *FOXO3* is involved in the PI3K-AKT pathway, and its phosphorylation modulates the transcription of pro-apoptotic factors[219]. *TNFAIP3* gene, a negative regulator of NF-kB signaling located in 6q23, has also been suggested as a tumor suppressor gene involved in del(6q) pathogenesis[214]. However, the role of these candidate genes and the molecular mechanisms underlying this cytogenetic alteration have not been well established in CLL. Besides, the 6q FISH-probe is not widely used

in clinical routine, which limits the identification and further investigations of this alteration.

14q rearrangements and deletions involving the *IGH* gene. Chromosome 14q32 rearrangements/translocations were first reported at a frequency of ~5% in CLL patients[59, 220]. However, with the emergence of high-throughput cytogenetic techniques and large-scale genomic studies, the frequency of 14q translocations increased up to 10-15%.[221-223] 14q32 rearrangements involve the **immunoglobulin heavy chain (*IGH*) gene**, which can be translocated with multiple partners such as *BCL2, BCL3, BCL6, BCL11A* or *MYC*, being the most common the t(14;18) or *IGH::BCL2* fusion (**Figure 5**)[59, 188, 208, 210, 224-228]. The ***IGH* translocation** is associated with intermediate-adverse outcome, although it has been suggested that the prognosis is dependent on the translocated partner[206-209, 229, 230]. Some studies have shown that patients with *IGH::BCL2* fusions have a better outcome than those with other *IGH* translocations in terms of time to first treatment (TFT) [224, 227, 231]. The main pathomechanism of *IGH* translocations relies on the overexpression of the *IGH* partner, (e.g.: t(14;18)) leads to the overexpression of *BCL2*, an outer mitochondrial membrane protein that inhibits the apoptotic process in B cells)[210, 232]. Moreover, *IGH* translocations associate with trisomy 12 and *NOTCH1* mutations[178]. Nevertheless, IGH-translocated patients constitute a heterogeneous subgroup, and further investigations regarding the pathogenesis and molecular consequences as well as the clinical impact of the translocations are needed.

In addition to the translocations, *IGH* gene can also be involved in 14q deletions (del(14q)) within CLL patients. Del(14q) appears in approximately 2-5% of patients, and it has been associated with an intermediate or adverse clinical outcome, similar to del(11q) prognosis[148, 189, 191, 233]. The size of the deletion ranges from 14q24 to 14q32, being the most frequent breakpoint the IGH locus (~50% of del(14q))[189, 191, 233]. In the majority of ***IGH* deletions**, only part of the gene is deleted, concretely, the 3'-flanking site[234]. Del(14q) has been correlated with the presence of trisomy 12, *NOTCH1* mutations and IGHV-UM[191, 233]. This deletion may encompass tumor suppressor genes with a key role in its pathogenesis such as ***TRAF3***[205]. *TRAF3* is a negative regulator of the non-canonical NF-kB signaling, which can be inactivated by the 14q deletion and mutations in CLL and other B-cell malignancies[205, 235-237]. Furthermore, this gene is implicated in multiple functions such as inflammation or immune response, and more

recently, metabolism [238, 239]. Other tumor suppressor genes may be targeted by del(14q) and further molecular characterization would be of great interest. Nowadays, the assessment of *IGH* alterations (translocations and deletions) can be easily performed by FISH, but this probe is not included in the classic CLL FISH panel, hampering the study of these cytogenetic alterations.

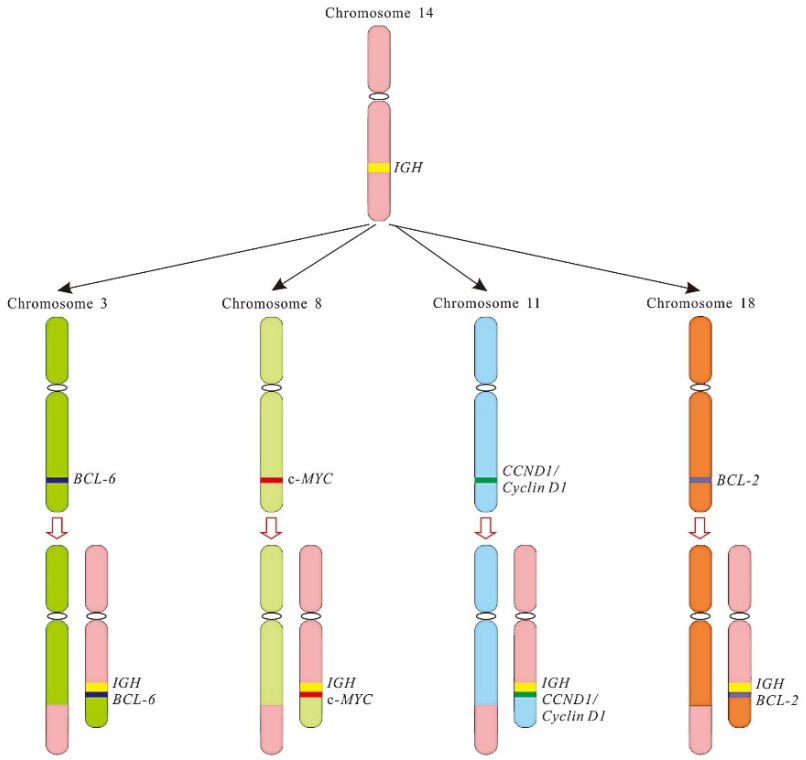

Figure 5. Chromosomal translocations involving *IGH* and multiple translocated-partners (*BCL6, c-MYC, CCND1* and *BCL2*) in B-cell neoplasms *(adapted from Zheng et al. 2013)*[240].

2.1.1.3. Complex karyotype

Complex karyotype (CK) is defined as the presence of 3 or more cytogenetic abnormalities, and it is found in 10-15% of patients at diagnosis, and in up to 30% of patients at relapse[60, 147, 151, 202, 241]. Traditionally, CK has been assessed by CC, nevertheless, CGH arrays and novel approaches such as optical genome mapping (OGM) provide additional and valuable structural information at higher resolution, becoming promising cytogenomic techniques for whole genome screening[148, 149].

CK has been associated with poor prognosis and high-risk markers such as **del(17p)/*TP53*, del(11q)/*ATM* alterations** and IGHV-UM status[76, 147, 241-243]. In recent years, the clinical outcome of patients with CK has been demonstrated to be heterogeneous, and dependent on the type and number of chromosomal

alterations[147, 244]. Concretely, the presence of 5 or more cytogenetic abnormalities was identified as a risk factor independent of clinical stage or IGHV status[151]. Moreover, the presence of certain genetic alterations also contributed to refining their prognosis. For instance, CK patients with *ATM, TP53* alterations or translocations have a worse outcome, while patients with trisomy 12 and additional trisomy 18 or 19 in the context of CK had a better clinical course[192, 243-246]. A recent study has also identified that the presence of **chromothripsis** refines prognosis within patients showing CK[247]. In addition, CK has been associated with refractoriness to chemoimmunotherapy, and with a poor response to novel agents[98, 246, 248-250]. Molecular mechanisms responsible for the worse outcome of CK patients could be related to a defective DDR, as many of these patients harbor *ATM* and *TP53* alterations but considering the high heterogeneity and genomic instability of this group, additional biological mechanisms can be affected[251].

2.1.2. Somatic mutations

Whole-genome and whole-exome sequencing studies (WGS, WES) have provided a more comprehensive characterization of the mutational landscape of CLL, with available data from more than 1000 patients[77-79, 88, 252-255]. Considering the mutational burden of ~1 mutation/Mb previously reported in CLL and the **large number of putative CLL drivers that mutates at low frequencies**, at least 1000 CLL samples would need to be analyzed to confidently identify >90% of drivers mutated in 2% of patients[256]. Indeed, previous WES and WGS studies including ~500 samples identified approximately 50 putative driver genes, whereas in a recent multi-omic study of ~1000 CLLs, the number of candidate drivers increased up to 82[81]. In addition, large-scale genomic studies developed new algorithms for the detection of recurrent CNAs and shed light on the origin processes of somatic mutations. The main mutation signatures or mechanisms responsible for mutation generation in CLL are the aging-related signature, the APOBEC signature, the canonical activation-induced cytidine deaminase (c-AID) and the non-canonical AID (nc-AID) signatures[257]. AID is involved in SHM, and the aberrant activity of this enzyme has been demonstrated to be responsible for the generation of certain mutations[258]. New signatures were also found recently, such as SBS18, which could be related to the damage induced by reactive oxygen species (ROS)[81].

The average of single nucleotide variants (SNVs) or somatic insertion and deletions (Indels) in CLL ranges from 15.3 to 26.9 per patient. A **small number of genes are mutated in 5-20% of patients, such as *SF3B1, NOTCH1, ATM*, *TP53 or BIRC3***, while the vast majority of CLL drivers mutate at lower frequencies **(Figure 6)** [77, 78, 80, 83, 252, 255]. The biological and clinical implications of the most recurrently mutated genes have been further investigated in the last few years.

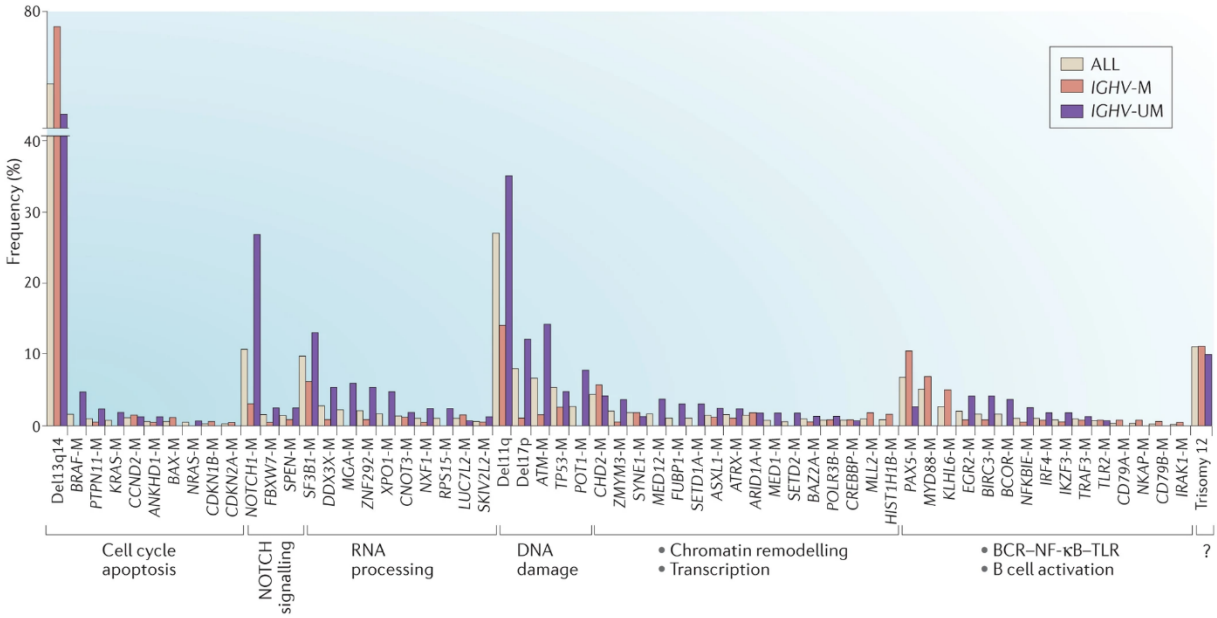

Figure 6. The genetic landscape of CLL. Frequencies of recurrent mutated genes and chromosomal abnormalities within IGHV-M (pink bars) and IGHV-UM (purple bars) CLL subsets, grouped into molecular pathways *(taken from Fabbri et al. 2016)*[50].

The mutational frequencies of CLL drivers vary among studies[255], probably due to the variable limits of detection for each NGS approach, the different bioinformatic algorithms applied, and the characteristics of the CLL cohort. Some gene mutations are associated with certain biological and clinical CLL subgroups: *NOTCH1* mutations appear in 25-30% of patients with trisomy 12[178, 181, 190, 259], while *ATM* and *BIRC3* mutations affect 30% and 10% of del(11q) patients, respectively, and *SF3B1* mutations also associate with the latter cytogenetic alteration[66, 82, 173, 175, 176]. As previously commented, up to 80% of del(17p) patients harbor *TP53* mutations in the remaining allele[72, 199]. Moreover, the frequency of mutation of the aforementioned genes increases at relapse or when there is a need for treatment[70, 177, 193, 259-262]. *TP53* and *NOTCH1* mutations are also remarkably high in Richter´s syndrome[29, 84, 195]. Thus, the mutational

frequency depends to a great extent on the biological and clinical characteristics of the study cohort.

In terms of biological consequences, ***SF3B1*** encodes for a key component in the spliceosome machinery and mutations in this gene are located in hotspot regions, affecting the HEAT domains. The most recurrent missense variant results in the amino acid substitution K700E, which disrupts the interaction between RNA and *SF3B1*[263, 264] ***NOTCH1*** most recurrent mutation is a frameshift deletion in exon 34 that affects the C-terminal PEST domain, required for proteasomal degradation. In addition, 3'-UTR mutations that disrupt the PEST domain have been described. In both cases, mutations contribute to the stabilization of NOTCH1 and the constitutive activation of Notch signaling[77, 83, 259]. In ***ATM***, somatic SNVs, indels and splice-site mutations result in a dysfunctional or truncated protein and have been identified along the gene, with no hotspot regions[67, 174, 175]. ***TP53*** mutations are missense, frameshift, non-sense and splice-site substitutions that can lead to a gain-of-function or *TP53* inactivation[71, 265]. As already mentioned, *ATM* and *TP53* mutations contribute to a defective DDR and cell cycle control[66, 68, 72, 266]. Most ***BIRC3*** mutations are frameshift substitutions affecting the C-terminal RING domain, which results in defective E3 ubiquitin-ligase activity and in constitutive activation of the non-canonical NF-kB pathway[177, 260, 267].

Several studies have demonstrated a **negative clinical impact** of *SF3B1, NOTCH1, ATM, BIRC3* and *TP53* mutations on CLL outcome, all of them associated with IGHV-UM[80, 86, 87, 96, 200]. *NOTCH1, SF3B1* and *ATM* mutations are associated with a shorter TFT and their impact on OS is still controversial[67, 85-87, 182, 268]. *BIRC3* mutations refine the negative outcome of del(11q) and IGHV-UM patients, contributing to a worse prognosis[86, 176]. It is noteworthy to highlight that *TP53* clonal and subclonal mutations are a high-risk prognostic factor associated with shorter OS, but also a predictive marker of response[72, 75, 197, 199, 265]. *TP53, SF3B1* and *BIRC3* mutations have been correlated with chemorefractoriness, while *NOTCH1* mutations associate with a poorer response to anti-CD20 treatments.[78, 197, 200, 260, 261, 269, 270]

Besides the most recurrent genes, the **frequencies of the remaining mutated drivers form a long and decreasing tail**. NGS studies identified previous unrecognized genes such as *XPO1, POT1, MED12, CHD2, MYD88, EGR2, SETD2, BRAF,*

RPS15 or NFKBIE, among many others[77, 78, 81, 254]. Despite the large number of putative CLL drivers, they can be grouped into several **molecular pathways**, revealing the different mechanisms that can underly CLL pathogenesis (*see section: Molecular pathways altered in CLL*)[3, 50, 271].

Subsequent studies have also tried to characterize the prognostic impact of some of the rarely mutated genes. Mutations in ***NFKBIE, RPS15, EGR2* and *POT1*** have been associated with IGHV-UM and shorter OS or TFT, as well as the mutations in genes involved in the **MAPK** signaling pathway[86, 184, 185, 246, 254, 272, 273]. Furthermore, results from a recent study of ERIC (European research initiative on CLL) pointed out that mutations in *XPO1* together with *SF3B1* mutations, were able to negatively refine the TFT of IGHV-UM patients, while *NFKBIE* and *NOTCH1* mutations were significantly associated with shorter TFT in the IGHV-M subgroup[87]. Furthermore, *RPS15* as well as *TP53, NOTCH1, BIRC3,* and *ATM*, are more frequently mutated in high-risk subgroups and at relapse[193, 254]. Conversely, other gene mutations such as those of *MYD88* are associated with IGHV-M, del(13q) and a better prognosis[89, 274]. Despite all these findings, further harmonization efforts are needed to achieve a consensus regarding the prognostic significance of mutations in CLL.

2.1.3. Non-coding and epigenetic alterations

Apart from mutations in the coding regions, large-scale genomic studies also identified recurrent **non-coding mutations**[77, 78, 257, 275]. As mentioned, mutations in 3'UTR of *NOTCH1* are a recurrent event in 1-4% of CLL patients, with similar biological and clinical implications to *NOTCH1* coding mutations[77, 85, 276]. Non-coding mutations in the *PAX5* enhancer region have been described, located in chromosome 9p13 and resulting in a decreased expression of the gene[277]. A recent study reported non-coding mutations in *ATM* and *TCL1*, and in other CLL drivers such as *IKZF3, SAMHD1, PAX5* and *BIRC3*, significantly associated with IGHV-UM[277]. Furthermore, the presence of non-coding mutations in CLL drivers co-occurs with the concomitant mutations in the coding regions, suggesting a functional role in the pathogenesis of the disease[77, 200, 278].

Additionally, **miRNAs expression** has been shown to be altered in CLL. Two of the main dysregulated miRNAs are miR-15a/16-1, located within the 13q deletion MDR and with a functional role in modulating BCL2 expression by targeting the UTR

region of the gene[154, 157]. Other miRNAs such as miR-34a in del(17p) or miR-155 had an impact on DNA damage response and cell cycle, and BCR signaling, respectively[279-282]. Moreover, a negative clinical impact of these alterations has been suggested in different studies[279, 281, 282].

In addition to the genetic alterations, CLL cells also display a wide variety of **epigenetic modifications**[283]. Epigenomics comprises the study of DNA methylation, chromatin accessibility, post-translational modifications, and three-dimensional (3D) genomic structure. Regarding DNA methylation, chromatin marks and histone modifications, CLL undergoes a distinct global reconfiguration when compared to normal B cells[284]. Indeed, a substantial intra-tumoral heterogeneity has also been reported. Besides, CLL cells gradually accumulate hypomethylation in heterochromatin with low-CpG content and hypermethylation in high-CpG content regions, after subsequent rounds of mitosis[285]. According to this, specific epigenetic fingerprints have been correlated with the cellular origin and the evolutionary history of the B cell[286]. Based on methylation patterns, 3 different CLL subgroups have been proposed: naïve B cell-like CLL and memory B cell-like CLL, which mainly correspond to IGHV-UM and IGHV-M, respectively, and a new intermediate subtype with a distinct epigenetic imprint[287]. Moreover, each subgroup associates with different clinical and genetic features[288].

Several efforts have been made to find a link between genetic and epigenetic features. Despite the global epigenomic changes observed in CLL, only 1-4% of patients harbored mutations in genes involved in chromatin remodeling or modification[283]. Thus far, those changes cannot be just attributed to alterations at the DNA level. Nevertheless, distinct epigenetic patterns have been found in patients with *MYD88* mutations and trisomy 12, suggesting a role of these alterations in epigenetics[289]. Epigenetic imprints have also been explored in the context of CLL therapy, and their analysis could be useful to track the response to treatments such as ibrutinib[290]. However, due to the complexity of CLL epigenetic configuration, further investigations are needed to better understand its biological and clinical implications.

2.2. Molecular pathways altered in CLL

Despite the great number of genetic alterations reported in CLL, most of them converge in a specific set of constitutively activated or disrupted molecular pathways. Moreover, these pathways are interconnected, and many genes may be involved in multiple molecular mechanisms. These include BCR-TLR-NF-kB signaling, Notch signaling, DNA damage response, cell cycle regulation, chromatin remodeling and RNA/ribosomal processing (**Figure 6**).

Antigen binding stimulates **BCR signaling** in normal B cells, activating a downstream cascade. In CLL, different mechanisms contribute to the constitutive activation of this pathway[109], such as gain-of-function mutations in genes that encode for downstream **MAP-ERK kinases** (*BRAF, KRAS, NRAS, MAP2K1, PTPN11*)[184, 185]. In addition, other mutations indirectly deregulate BCR signaling (*EGR2, BCOR, KLHL6, CARD11, IKZF3, IGLL5, PAX5*), and **Toll-like receptor (TLR) and inflammatory pathways** (*MYD88, IRF4, TRAF3, TLR2/6, IRAK1/2/4*)[77, 78, 89, 110, 238]. Mutations and CNAs have also been reported in **NF-kB** signaling, which is downstream of BCR and TLR and consists of two main pathways: the canonical and the non-canonical or alternative signaling[291]**.** Alterations have been described in both of them, promoting signaling activation (canonical: *NFKBIE*, *TNFAIP3*/del6q23, *REL*/amp2p16; non-canonical: *BIRC3, TRAF3, TRAF2*, *NFKB2*/del10q24)[77, 78, 177, 205, 267, 272, 292].

Notch signaling is frequently dysregulated in CLL by mutations in 3'-UTR and coding regions of *NOTCH1*[77, 253]. Positive and negative regulators of this pathway can be also altered by gene mutations (*FBXW7, MED12, SPEN, CREBBP*). All of them result in Notch signaling activation and promote the translocation of NOTCH to the nucleus, modulating the expression of NF-kB factors, *TP53* or *MYC*[182, 276] Moreover, Notch signaling can be activated in CLL independently of somatic mutations[293]. In parallel, **MYC regulation** is mediated by multiple genes, and some of them have been found to be mutated in CLL (*FUBP1, MGA, PTPN11, FBXW7*)[78]. All these altered pathways converge in a B cell activation responsible for an enhanced proliferation, differentiation and survival[108].

As mentioned before, some of the most recurrently altered genes in CLL by mutations and/or deletions (*ATM*/del(11q) and *TP53*/del(17p)) are involved in **DNA**

damage response (DDR) and cell cycle regulation[66, 70, 173, 266, 294]. The disruption of these genes results in a defective response to DNA lesions such as DNA double-strand breaks (DSBs) or single-strand breaks (SSB), which hinders the activation of checkpoints for cell cycle arrest and favors genomic instability[295]. Besides *ATM* and *TP53*, a large number of genes are involved in DDR signaling, and some of them mutate in CLL (*POT1, CCND2, SAMHD1 PTPN11, CHK2, CDKN2A/B*)[77, 78, 172]. Moreover, *TP53* disruption and other alterations such as *BCL2* overexpression dysregulate **the apoptotic process**, which enhances CLL cells survival and may affect treatment response[70, 77, 156, 157].

Additionally, mutations in genes involved in **chromatin remodeling** have been reported in CLL (*CHD2, ZMYM3, ARID1A, ASXL1, SETD2, HIST1H1B, HIST1H1E, BAZ2A*), and a high number of gene alterations related to **RNA export and metabolism** (*SF3B1, XPO1, RPS15, FUBP1, DDX3X, NXF1, U1, ZNF292, RPSA, EWSR1*) have been identified in the last WES and WGS studies[77, 78, 81, 296]. It should be noted that, although some of them have been further examined by functional studies[263, 297-300], the specific biological function of most of them in CLL pathogenesis remains to be determined.

2.3. CLL microenvironment

The interactions between CLL and tumor microenvironment (TME) cells are crucial for CLL proliferation and survival. Concretely, CLL cells depend on growth and survival signals received from different types of TME cells, including bone marrow stromal cells, monocyte-derived nurse-like cells (NLCs) and T cells, among others. These CLL-TME interactions occur in the proliferation centers, located in lymph nodes and bone marrow, and involve a wide range of survival factors, chemokines, cytokines, adhesion molecules and their respective receptors.

Bone marrow stromal cells support survival of CLL cells and protect them from apoptosis. Interactions with the **stromal cells** can be promoted by CXCL12 secretion, which is recognized by CLL cells through the corresponding receptor (CXCR4). Adhesion can also be favored by the binding of α4β1 integrin on CLL cells and VCAM1 on stromal cells, subsequently activating downstream signaling cascades (AKT, NF-kB, etc.)[301, 302].

NLCs stimulate CLL cells chemotaxis through CXCL12/CXCL13 secretion (recognized by CXCR4 and CXCR5, respectively)[303]. NLCs express TNF ligands APRIL and BAFF, which binds to the corresponding receptors BCMA, TACI and BAFF-R on CLL cells[304]. Moreover, CD31 (expressed by NLCs) interacts with the CD38 CLL receptor[305]. NLCs also secrete WNT5A, a ligand of CLL receptors ROR1 and ROR2[306]. In parallel, BCR stimulation in CLL cells induces the secretion of CCL3/CCL4, chemokines detected by NLC and **T cells**[307]. CLL cells also interact with CD40L-expressing T cells through the CD40 receptor, triggering NF-kB activation[308].

In addition to these interactions, CLL cells may receive other pro-survival signals from the aforementioned and other cell types (dendritic, endothelial cells, etc), activating signaling cascades that promote the production of signals that in turn stimulate TME cells[110]. Thus, the crosstalk between CLL and TME constitutes a potent mechanism underlying CLL pathogenesis, which may contribute to clonal evolution and may interfere with CLL therapy.

2.4. Clonal evolution and targeted therapies evasion mechanisms

Clonal evolution is the process through which CLL cells acquire a phenotypic advantage that allows them to develop and expand over time. CLL is characterized by a great intertumoral heterogeneity underlying the variable clinical outcome of patients, and by an intratumoral heterogeneity with different subclones that may show distinct genetic patterns[78, 88, 309-311]. Growth dynamics strongly rely on the clonal genetic composition, but also on tumor-microenvironment interactions, epigenetic and transcriptional changes[312]. All in all, clonal evolution based on the acquisition of certain alterations will determine CLL progression, therapy response and refractoriness[313].

A recent study has identified at least two different growth patterns that could explain the intertumoral heterogeneity within CLL: **logistic growth and exponential unbound growth**[312]. In patients exhibiting logistic growth, the subclonal composition remains stable, while patients with exponential CLL growth show shorter time to treatment and IGHV-UM, together with a greater number of

CLL driver mutations and more profound shifts in subclonal proportions during the course of the disease[312].

Regarding the intra-tumoral heterogeneity of CLL, WES and WGS studies have identified founder clones, which often harbor alterations in genomic drivers consistently clonal, such as *MYD88* mutation, del(13q) or trisomy 12[78, 88]. On the other hand, subclonal alterations may emerge during the disease, being present in a small fraction of cells (subclone), and may confer a clonal advantage that drives progression, such as *ATM, TP53, BIRC3* or *SF3B1* mutations[78, 88, 314]. Genetic alterations are often accompanied by transcriptomic and epigenetic changes[285, 315]. Clonal evolution of the competing subclones will be determined by the growth acceleration rates that confer each alteration or the co-occurrence of different alterations within the same subclone[312]. Moreover, these different growth rates may result in different patterns of clonal evolution: **linear and branching evolution.** In linear evolution, there is a founder clone that sequentially acquires additional alterations, which allow the latter subclone to outcompete, while in branching evolution, multiple subclones with different alterations co-evolve and compete for dominance, with mutations in the same driver (convergent evolution) or in different drivers (divergent evolution)[311, 316, 317].

A determinant factor for clonal evolution is **CLL therapy**. CLL treatments reduce the subclonal populations more sensitive to the selective pressure, in favor of the more resistant clones [313, 317]. As different treatments exert different selective pressures, the alterations that confer resistance are also variable depending on the type of treatment. Furthermore, a higher clonal diversity could increase the probability of evading the treatment selective pressure[88, 309, 310, 312]. For instance, CLL subclones with *TP53* alterations are frequently selected after chemotherapeutic regimens, while different evasion mechanisms have been identified in response to targeted therapies[103, 104, 134, 197, 317-319].

The most common **mechanisms of resistance** to novel agents are alterations in the binding site of the target (**Figure 7**). **Mutations in *BTK* and in *PLCG2*** genes confer resistance to the BTK inhibitor **ibrutinib** (**Figure 7A**) [320-322]. *BTK*-C481S mutation in the binding site is the most predominant, inhibiting the

drug binding to the target[323]. A recent study has reported other *BTK* mutations at relapse (V416L, A428D, M437R, T474I, and L528W), which also confer resistance to novel non-covalent BTK inhibitors[324]. Gain-of-function *PLCG2* mutations (R665W, S707Y and L845F) activate BCR signaling independent of BTK inhibition [322, 325]. Thus far, *BTK* and *PLCG2* mutations are subclonal, rarely co-existing within the same clone and with different growth rates that may be conditioned by the acquisition of additional alterations[326]. Besides, other mechanisms of resistance to ibrutinib have been described, such as del(8p). This region encompasses a TNF-family extrinsic apoptotic receptor (TRAIL), whose loss may contribute to apoptotic resistance.[320]

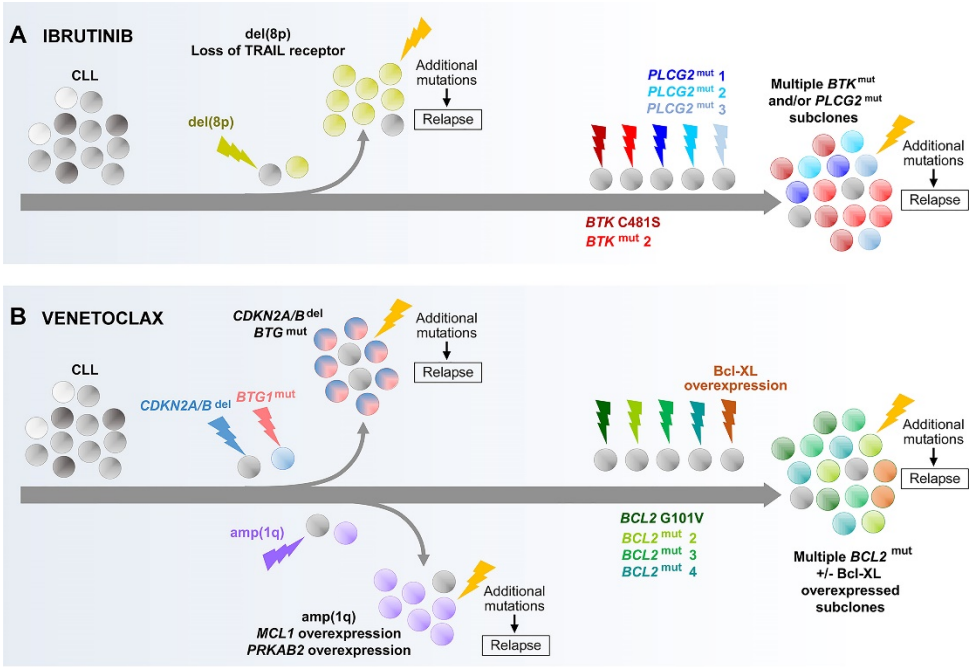

Figure 7. Molecular alterations driving the development of resistance to A) ibrutinib and B) venetoclax. Evolutionary paths undertaken by CLL cell through point *BTK*, *PLCG2* and *BCL2* mutations and the co-evolution of multiple subclones with different genetic alterations *(adapted from Kwok et al. 2022)*[313].

Regarding **venetoclax**, ***BCL2*-G101V mutation** is the most common resistance mechanism, resulting in a diminished binding affinity of this drug to *BCL2* [327] (**Figure 7B**). *BCL2* mutations have also been identified as subclonal events, and multiple mutations can be found within the same patient (convergent evolution)[328, 329]. Nevertheless, there is still a significant number of refractory patients without *BCL2* mutations, which suggests the presence of other

mechanisms of resistance. Among them, the upregulation of anti-apoptotic factors such as *MCL1* or *BCLXL*, the downregulation of the pro-apoptotic effector BAX, as well as *CDKN2A/B* and *BTG1* mutations could be driving venetoclax resistance[319, 330, 331]. Amp(1q) has also been reported as a recurrent alteration in a subset of venetoclax-resistant patients. This region contains *MCL1* and *PRKAB2* genes. *PRKAB2* overexpression enhances oxidative phosphorylation, conferring a metabolic advantage to CLL cells[331]. Recent studies have also reported **metabolic dysregulation** and NF-kB activation after venetoclax treatment, revealing that multiple mechanisms may be involved in the emergence of resistance to this drug[330, 332].

Nevertheless, it is still undetermined whether these alterations emerge during treatment or are already present before treatment initiation. Thus, to better understand the clonal dynamics and evolutionary process underlying the mechanisms of resistance, it would be of great interest to perform further multiomic, longitudinal and single-cell studies in large CLL cohorts.

3. METABOLISM: A NEW HALLMARK OF CANCER

Metabolic reprogramming is considered one of the hallmarks of cancer and consists of different metabolic alterations that sustain new biomass generation and tumor development, especially under restricted conditions. Multi-layer adaptations promote enhanced metabolic flexibility and plasticity of tumor cells, including dysregulation of nutrient uptake, alterations of intracellular metabolic pathways, and metabolite-induced changes in cancer and TME cell gene expression. Metabolic changes are mediated by the activation of oncogenic pathways, which may be directly or indirectly dependent on genetic mutations.

3.1. Cancer-associated metabolic changes

Nutrient uptake is essential for cell growth and proliferation[333]. The main sources of energy in proliferating cells are **glucose and glutamine**[333, 334]. These nutrients undergo different intracellular processes for ATP production and macromolecule biosynthesis, being oxidative phosphorylation (OXPHOS) the dominant pathway for ATP production in aerobic conditions. The reducing power of the carbon skeletons derived from glucose or glutamine oxidation is captured by NAD+/FAD+ to generate NADH/FADH, which transfers electrons to the electron transport chain (ETC) for ATP generation, in the mitochondrial membrane. This process depends on the presence of O_2[334].

Since the last century, solid tumor cells are known to metabolize **glucose** in a distinct manner than normal cells for **ATP production**, increasing its consumption through the glycolytic pathway, which is called the "**Warburg effect**" or aerobic glycolysis[335] (**Figure 8A**). In this process, the excess of pyruvate is converted to lactate, instead of being used as a fuel of the tricarboxylic acid (TCA) cycle, even with sufficient oxygen availability to completely oxidate glucose. More recently, it has been reported that enhanced glycolysis also facilitates the **synthesis of biomolecules** from different intermediates in tumor cells[333] (**Figure 8B**).

An increased **demand for glutamine** has been demonstrated as the second major metabolic mechanism for cancer proliferation[336, 337]. Glutamine can be a carbon

source for the TCA cycle after being converted to α-ketoglutarate in a series of metabolic reactions. Additionally, glutamine can be used as a **nitrogen source** for amino acids and nucleotide synthesis and maintains **redox homeostasis** by synthesizing glutathione, an antioxidant that regulates reactive oxygen species (ROS) levels[336]. Whereas high ROS levels may result in cell death, controlled ROS accumulation promotes tumorigenesis by inhibiting tumor suppressors such as PTEN and activating MAP kinases and hypoxia-inducible factors (HIF-1α)[338].

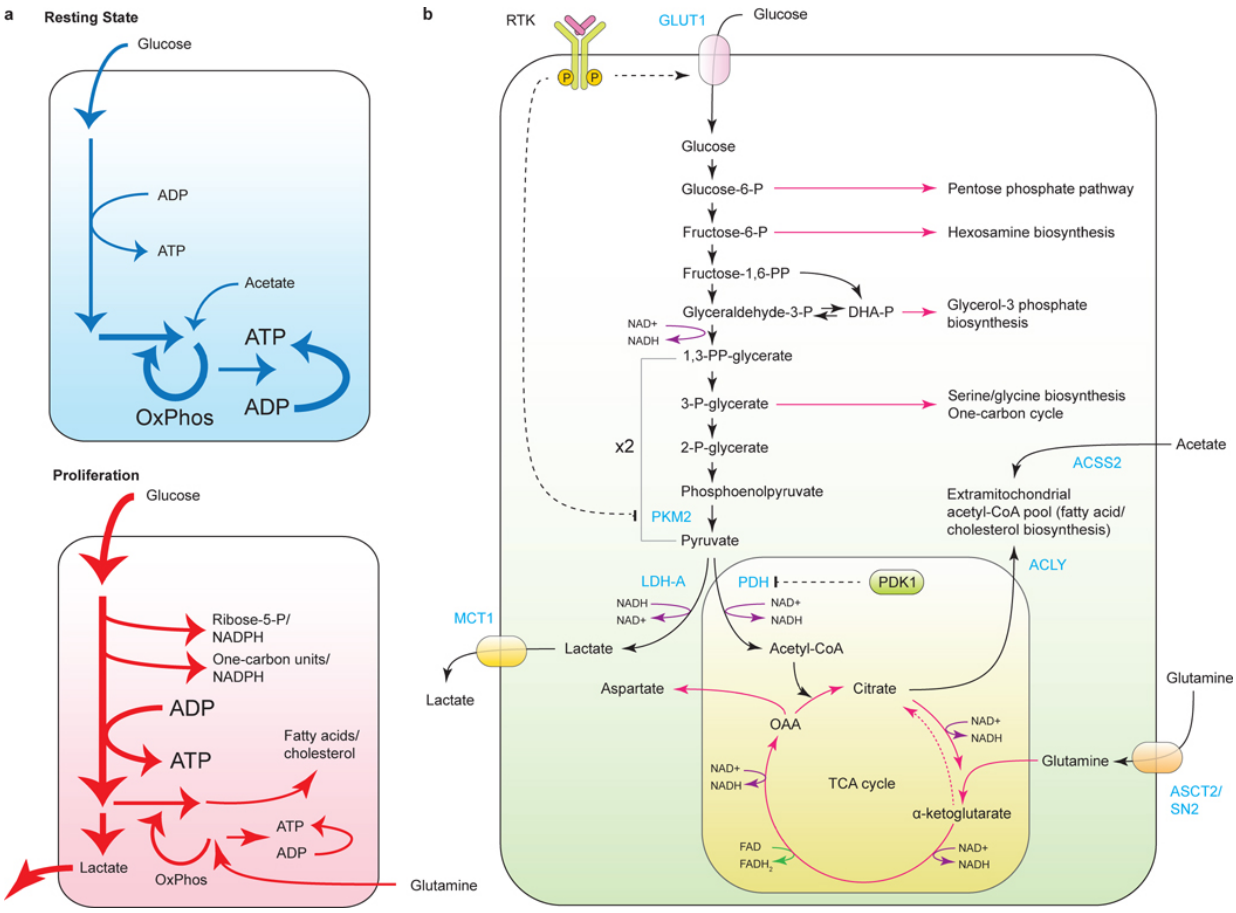

Figure 8. Schematic representation of glycolysis and tricarboxylic acid (TCA) cycle in cellular metabolism for intermediates biosynthesis and NADH production. A) Representation of the preferential use of oxidative phosphorylation OXPHOS in resting cells comparing to the increased glycolytic metabolism in cancer or proliferating cells. B) Representation of the central carbon metabolism through the glycolytic pathway in the cytoplasm and oxidative reactions in TCA cycle in the mitochondria. RTK, receptor tyrosine kinase; GLUT1, glucose transporter 1; PKM2, pyruvate kinase M2; ACSS2, acetyl-CoA synthetase 2; LDH-A, lactate dehydrogenase A; PDH, pyruvate dehydrogenase; PDK1, pyruvate dehydrogenase kinase 1; ACLY, ATP-citrate lyase; MCT1, monocarboxylate transporter 1; ASCT2/SN2/SLC1A5, glutamine transporter *(taken from Pavlova et al., 2016)*[333].

Under the nutrient or oxygen deprivation often occurring in the TME, tumor cells can **modify their metabolic specificities** and redirect their metabolism to alternative metabolic pathways and self-catabolic autophagy processes[339]. Pyruvate is the main fuel of the TCA cycle in normal conditions (**Figure 8**). However, during glucose deprivation, pyruvate levels derived from glycolysis decrease, and tumor cells may redirect glutamine metabolism to restore TCA cycle activity[340]. Several studies have mimicked glucose deprivation by inhibiting the mitochondrial pyruvate carrier (MPC), demonstrating the importance of glutamine metabolism under nutrient-restricted conditions[341]. Conversely, glutamine deprivation may be compensated by an increased metabolism of other amino acids, such as asparagine or alanine, to maintain TCA cycle function[333, 342]. Additionally, **fatty acids** play an important role in tumor development under metabolic stress conditions, as certain cancer types associate with a profound increase in lipid biosynthesis and appear to prefer fatty acid oxidation as a source of energy for maintaining cell proliferation and survival[343] (**Figure 8B**).

Metabolites are not only the intermediates of metabolic reactions or recipients of aberrant growth signals but also, they are able to directly **drive changes in cell gene expression and TME**[333, 344]. Acetyl-CoA serves as an enzymatic substrate in histone acetylation, and its availability mediates the deposition of acetyl marks that regulates the accessibility of chromatin for transcription factors assembly[345]. Increased glucose uptake and activation of MAPK-AKT signaling significantly promote histone acetylation and the activation of gene expression[333]. Other metabolites such as S-adenosylmethionine or α-ketoglutarate also work as cofactors or substrates of enzymatic reactions, affecting histone methylation and diverse posttranslational modifications[333, 334]. Moreover, tumor cells may reprogram TME cells by secreting growth factors or **metabolites that alter the cellular microenvironment**. For instance, the high metabolism of glucose and glutamine results in extracellular lactate accumulation, which has been demonstrated to attenuate the immune response of T cells, monocytes and macrophages, and promote HIF-1α stabilization and NF-kB and PI3K signaling activation in endothelial cells[346].

A wide variety of **oncogenic alterations** underly metabolic reprogramming, promoting transcriptional dysregulation of key metabolic genes such as enzymes or transporters. PI3K/AKT signaling induces glucose uptake by activating the expression

of glucose transporter GLUT1 and the first glycolytic enzyme hexokinase [334]. KRAS activation also upregulates GLUT1, and modulates the expression of key enzymes of glutamine metabolism[347]. Additionally, GLUT transporters expression is regulated by *TP53*, and inactivation of this gene may favor glucose uptake and glycolysis[348]. *MYC* overexpression has multiple metabolic effects, inducing the expression of enzymes involved in aerobic glycolysis (lactate dehydrogenase (*LDHA*): catalyzes the conversion of pyruvate to lactate) and glutaminolysis (glutaminase (*GLS1*): converts glutamine to glutamate), or glutamine transporters such as *SLC1A5/ASCT2*[349]. Activation of mTOR signaling mediates autophagy and biosynthesis of macromolecules such as proteins or fatty acids, by the integration of different signals[350]. Interestingly, glutamine appears to be a sensitive regulator of mTOR pathway[351]. Nonetheless, despite all these findings, many questions regarding the implications and causes of metabolic reprogramming remain to be determined.

3.2. Targeting cancer metabolism

The field of cancer metabolism has become a topic of a renewed interest in the last few years. Although most studies focused on glucose and glutamine metabolism, a wider range of metabolites and alternative metabolic pathways may be used by tumor cells to achieve an enhanced proliferation and adaptation capacity to nutrient scarcity conditions. Furthermore, understanding the cancer metabolomic landscape may encourage the **identification of metabolic vulnerabilities and new targets for cancer treatment.**

A broad spectrum of metabolic inhibitors is currently used for research and some of them have been proposed as potential strategies for cancer therapy, alone or in combination with chemotherapy, radiotherapy, or novel agents[352-355]. **Table 1** shows the different type of available drugs targeting metabolism, which can either inhibit metabolic enzymes and transporters or work as analogs of metabolites at different steps of metabolic reactions. However, the clinical implementation of metabolic inhibitors is limited by their high toxicity rates.[356] For instance, the development of promising OXPHOS inhibitors which target mitochondrial protein complex 1 (PC1) such as IACS-010 has been discontinued after phase I trials due to neurotoxicity[357]. Nevertheless, other drugs such as CB-839, a glutamine metabolism inhibitor, are under investigation

in multiple clinical trials with high efficacy and tolerable toxicity (NCT02071862, NCT02771626, NCT02861300), being a promising strategy especially in combination with other agents [358].

Table 1. Summary of preclinical inhibitors or clinical therapeutic drugs and their mechanisms of action in cancer cell metabolism.

Metabolic target	Type of inhibitor	Drug	Mechanism of action	References
Glucose metabolism	Glucose analogue	2-deoxy-D-glucose	Inhibits hexokinase activity	353
	Glucose transporter inhibitor	Ritonavir	Inhibits glucose transporter GLUT4	352
Pyruvate metabolism	Pyruvate transporter inhibitors	CHC	Inhibit MPC (pyruvate import to the mitochondria)	
		UK-5099		359
		Thiazolidinediones		360
	LDHA inhibitor	Oxamate	Inhibits pyruvate conversion to lactate	354
Glutamine metabolism	Glutamine analogue	DON	Inhibits glutamine metabolism (low selectivity)	
		JHU083	Pro-drug of DON	361
	GLS inhibitors	BPTES	Inhibit glutaminolysis (conversion of glutamine to glutamate)	362
		Compound 968		363
		CB-839		358
	Glutamine transporter inhibitors	GPNA	Inhibits glutamine transporters SLC1A5/SLC7A5	364
		Sulfasalazine	Inhibits cysteine-glutamine transporter SLC7A11	365
		V-9302	Inhibits glutamine transporter SLC1A5	366
Fatty acids metabolism	Fatty acid transporter inhibitors	Etomoxir	Inhibit CPT1 (fatty acids import to the mitochondria)	367
		ST1326		368
	LPL inhibitor	Orlistat	Inhibits lipid synthesis/lipolysis	369
OXPHOS	PC1 inhibitors	Metformin	Inhibit protein complex I in the mitochondrial electron transport chain	352
		IACS- 010759		357
		ASP4132		370
		IM156		371

CHC, alpha-cyano-4-hydroxycinnamate; MPC, mitochondrial pyruvate carrier; LDHA, lactate dehydrogenase; DON, 6-Diazo-5-oxo-L-norleucine; BPTES, Bis-2- (5-phenylacetamido -1,3,4-thiadiazol-2-yl) ethyl sulfide; GLS, glutaminase; GPNA, L-γ-glutamyl-p-nitroanilide; CPT, carnitine palmitoyl transferase; LPL, lipoprotein lipase; PC1, protein complex I.

3.3. Metabolic changes in hematological malignancies: CLL

Though metabolism of solid tumors has been extensively investigated for decades, few studies have explored the metabolic changes that occur in hematological neoplasms [333]. Hematological cells are reported to show metabolic dysregulation too, although the metabolic processes seem to differ to some extent from those of solid tumors and are not well characterized yet. Several hematological cancers such as acute myeloid leukemia, B-cell lymphomas or multiple myeloma have an aberrant increase of glycolysis and OXHPOS for enhanced proliferation and survival[333]. Moreover, recent studies have demonstrated that fatty acid oxidation and biosynthesis are key processes in their metabolism [333, 334, 372].

In CLL, the cellular metabolism remains largely unknown. Warburg effect is not the predominant process in CLL cells, although it can be stimulated upon Notch-c-Myc activation[373]. In contrast, a significantly **increased OXPHOS** has been described in CLL when compared to normal B cells[372, 374]. Some studies identified an aberrant expression of the lipoprotein lipase (LPL) in IGHV-UM CLL, which metabolizes triacylglycerol into fatty acids, and an upregulation of the carnitine palmitoyl transferases CPT1 and CPT2, suggesting a **preference for fatty acid metabolism** as a source of energy for cell survival[372, 375]. Regarding other metabolic pathways, recurrent cytogenetic alterations such as 11q deletion have been related to an **altered glutamine metabolism**, which has been identified as a target of ibrutinib treatment [376]. **TME** plays an important role in CLL proliferation centers and affects CLL OXPHOS[377]. In addition, stromal cells metabolize cystine into cysteine, which is secreted to the extracellular medium and incorporated into CLL cells for glutathione synthesis, enhancing cell survival[378]. A recent study demonstrated that CD40 and BCR stimulation by TME engaged glucose and glutamine metabolism, as well as TCA cycle activity and OXPHOS in CLL[379].

Additionally, some studies have suggested that certain **CLL therapies may induce metabolic alterations**. Venetoclax-resistance can be accompanied by increased OXPHOS, and several metabolic changes may take place in the CLL lymph node after venetoclax or ibrutinib treatment[331, 380]. Furthermore, novel strategies based on the combination of venetoclax or ibrutinib with metabolic inhibitors have been proposed as an alternative therapy to manage CLL and overcome drug resistance[367, 379].

As shown in previous sections, CLL exhibits multiple **genetic alterations**, and some of them may have an impact on metabolism, such as *TP53* deficiency, del(11q) or MYC dysregulation[349, 372, 376, 381, 382]. Furthermore, some of the newly identified CLL drivers are likely to induce metabolic changes by affecting different oncogenic pathways[81]. Nonetheless, despite the recent advances, CLL metabolism is still poorly understood. Thus, the investigation of the metabolic alterations as well as their clinical and biological implications would be of great interest, improving the knowledge of CLL pathogenesis and enabling the identification of novel therapeutic vulnerabilities.

4. CYTOGENOMIC AND HIGH-THROUGHPUT TECHNIQUES FOR THE STUDY OF CLL

4.1. Cytogenomic techniques

The introduction of **conventional cytogenetics (CC)** in the late 1970s has been one of the most important innovations in cytogenetics, allowing the identification of chromosomal abnormalities by an overview of the genomic architecture of condensed chromosomes (karyotype)[58]. This technique is based on chromosomal banding staining of cells in metaphase. CLL cells have a low mitotic rate and mitogens for cell division induction are required, being the most commonly used nowadays the CpG-oligonucleotide and IL-2[150]. Despite CLL cell stimulation, the difficulty of achieving suitable metaphases and the low resolution (10Mb) still limited the implementation of this technique for the routinely analysis of CLL genetic alterations. Nevertheless, according to ERIC recommendations, CC still remains the gold standard methodology, as it is capable of providing an overview of the clonal landscape and intraclonal hierarchy, and identifies structural and numerical aberrations and hence, the presence of complex karyotype, which has been demonstrated to show a relevant clinical significance in the last years[11, 98, 243, 383].

In the late 1990s, **fluorescence *in situ* hybridization (FISH)** allowed to identify CLL cytogenetic abnormalities not only in metaphase but also in interphase nuclei, overcoming the main CC limitation and with a higher resolution (100Kb) and sensitivity (alterations detected down to 5% of cells)[59]. FISH probes are complementary to a specific region of the genome, labeled with a fluorescent reporter. Different types of probes can be used for the assessment of structural and numeric alterations of a gene or chromosomal region (locus-specific probe), chromosomal rearrangements (break-apart probe: one of the rearranged genes is unknown; dual-fusion probe: both genes are known) or chromosomal gain or losses (centromeric probes).

FISH studies demonstrated that chromosomal abnormalities were more frequent than previously reported in CLL[59]. Nowadays, FISH analyses enable patients classification into different risk subgroups according to the presence of cytogenetic alterations (del(13q), del(11q), del(17) and +12) by the assessment of the classical 4-probe CLL panel[59]. In addition to the clinical applications, the high sensitivity, specificity and rapid turnover of FISH make this technique a useful tool for different research applications such as gene mapping, the study of 3D chromosome organization in interphase nuclei or the identification of translocation breakpoints.[384]

In addition to these techniques, higher-resolution methodologies such as genomic arrays, optical genome mapping (OGM) and next-generation sequencing (NGS) allow not only the assessment of numerical and structural genomic variations, but also the identification of copy number alterations (CNAs) of specific genes involved in the genomic alterations[81, 148, 149, 385]. Hence, they are becoming useful tools for achieving a more comprehensive genome characterization of CLL patients.

4.2. Next-generation sequencing

Next-generation sequencing (NGS) approaches have revolutionized the comprehension of the genomic landscape of CLL [255]. Whole-genome and whole-exome sequencing (WGS, WES) studies provided valuable genetic information from coding and non-coding regions, revealing novel candidate CLL drivers and recurrent CNAs[77, 78, 81]. In parallel, next-generation RNA sequencing (RNAseq) has also contributed to CLL molecular characterization, identifying transcriptionally dysregulated pathways in this disease[77, 78, 81]. Despite the panoramic genetic view provided by these studies, high costs and time-consuming bioinformatic analyses and interpretation of the results hinder the implementation of these approaches in daily routine.

Targeted NGS approaches allow for the evaluation of the mutational status and/or CNAs of chosen genes or regions of interest in a more cost-effective manner and with a great depth of coverage that increase technical sensitivity[386]. Indeed, several CLL studies have used custom-designed gene panels for the identification

of mutations, with lower limits of detection than WES or WGS studies[387]. Two main forms of targeted NGS have been described: amplicon or capture-based approaches. **Amplicon-based enrichment** is the most widely used in CLL studies and utilizes designed primers to amplify the regions of interest[388]. By contrast, in **capture-based approaches,** the regions of interest are enriched by the hybridization of sequences attached to biotinylated probes[388]. Amplicon-based enrichment is a cheaper option and requires less amount of starting material, whereas hybrid-capture presents other advantages, such as less production of PCR duplicates and higher specificity in regions of repeated sequences, difficult to amplify[388]. In sum, captured-based targeted NGS is more accurate and provides a more uniform target selection, making the amplicon-based approach more desirable on small scale and under cost or sample availability constraints. Detailed procedures regarding library preparation, data analyses and variant interpretation of capture-based NGS are described in the methods section and supplementary appendixes of *Chapters 2 and 3*. It should be noted that, despite the advantages of targeted NGS approaches for research and their utility to detect clonal and subclonal mutations, MRD or Ig rearrangements in CLL[99, 311, 389, 390], standardization of protocols and pipeline bioinformatic analyses is still needed in order to implement this technology in clinical practice.

4.3. Genome-editing CRISPR/Cas9 technology

In vitro and *in vivo* models that mimic the genetic alterations observed in patients have been traditionally used to study the individually functional or biological implications of the large number of alterations described in cancer. Regarding *in vitro* settings, limited CLL lines with different genetic alterations are currently available, highlighting MEC1 cell line harboring del(17p), HG3 with del(13q) and PGA1 cell line with trisomy 12 and del(13q)[391].

Notably, these models have experienced a huge development in the last few years, mainly due to the implementation of the **Clustered Regularly Interspaced Short Palindromic Repeats (CRISPR)/Cas9 system (Figure 9).** This technology makes it possible to reproduce loss-of-function mutations, which results in a complete gene inactivation, and also to introduce specific DNA substitutions

or a short DNA sequence in the genome, resulting in a gain-of-function phenotype[392] (**Figure 9**). In addition to the rapid and precise engineering of these alterations, CRISPR/Cas9 system versatility offers almost unlimited options for genome editing, from triggering chromosomal deletions to targeting multiple genes in large-scale genome screens[294, 393].

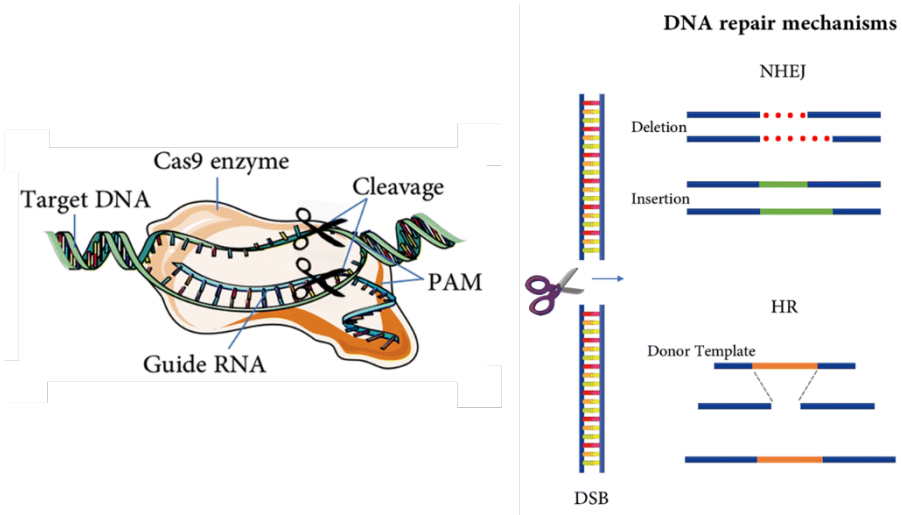

Figure 9. CRISPR/Cas9-genome editing system. The nuclease Cas9 cleavage in the recognition site protospacer adjacent motif (PAM) sequence, adjacent to the region of interest, by complementary binding of a single-guide RNA molecule (sgRNA). Cas9 induces a double-strand break (DSB) within nucleotides 17-18 of the target sequence, which can be repaired by non-homologous end joining (NHEJ) repair mechanism of the cell, inducing indels that result in loss-of-function mutations, or homologous recombination (HR) repair, which in the presence of a donor template introduce precise DNA modifications (*adapted from Montaño et al. 2018)*[394].

In CLL, several studies have mimicked CLL driver mutations such as *NOTCH1, TP53, FBXW7, RPS15, ATM* or *BIRC3* in *in vitro* and *in vivo* models by applying CRISPR/Cas9-editing technology, to delve into their biological functions[266, 267, 294, 300, 395-397]. Thus, this approach has significantly expanded the possibilities for the study of CLL pathogenesis by modeling cancer biology in cellular and animal models, being an extremely useful tool to discover novel functions of the edited targets, and to identify new therapeutic vulnerabilities and resistances.

4.4. Extracellular flux analysis

Increased glycolysis and OXPHOS are the main metabolic processes used by cancer cells for ATP production, which allows them to develop and maintain a

proliferating phenotype[333]. The extracellular flux analysis by applying Seahorse Real-Time Cell Metabolic methodology has been pivotal to characterize cancer metabolism, as it measures OXPHOS and glycolysis by monitoring the cellular **oxygen consumption rate (OCR) and extracellular acidification rate (ECAR)**[398, 399]. OCR corresponds to the aerobic component and ECAR to the glycolytic one, as the latter is an indicator of lactate production[398].

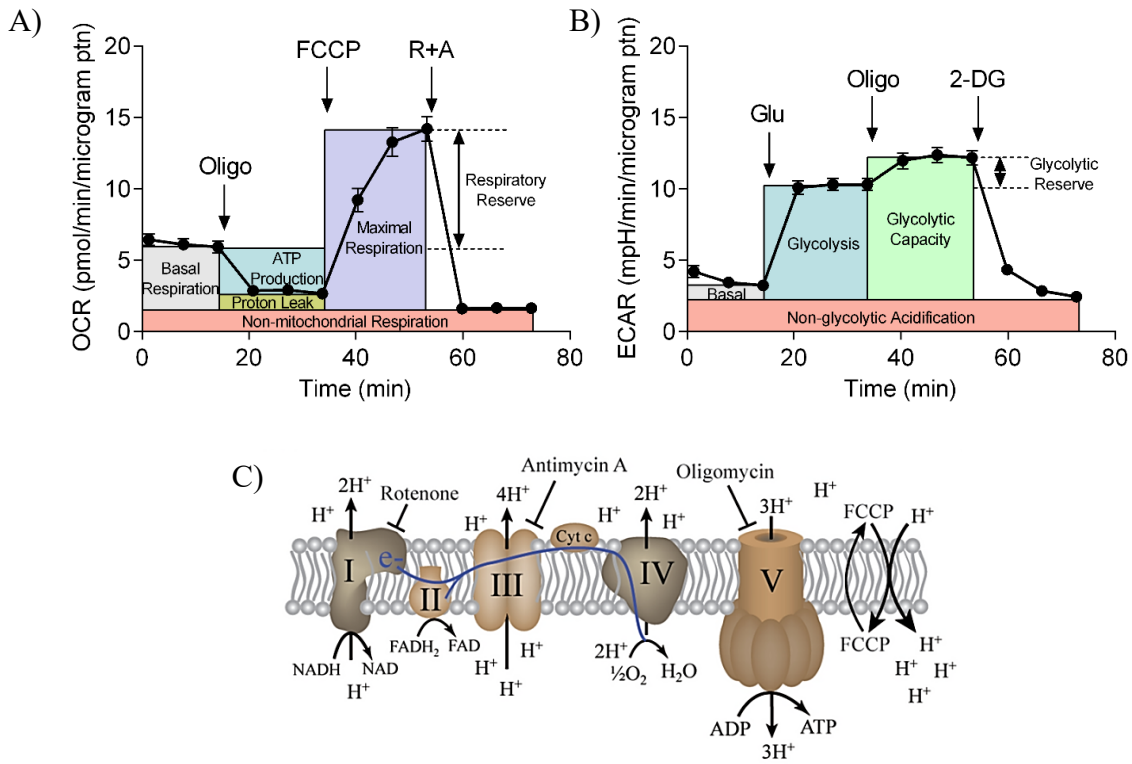

Figure 10. Extracellular flux analysis using Seahorse technology. A) Representation of OCR measurement expressed by µg per protein in mito stress test. Indices of basal respiration, ATP production, proton leak, maximal respiration, respiratory reserve and non-mitochondrial respiration, are assessed by a sequential application of FCCP and the OXPHOS inhibitors oligomycin and the combination of rotenone and antimycin (R+A). B) ECAR measurement expressed by µg per protein in gluco stress test carried out by a sequential application of glucose (glu), oligomycin and 2-deoxyglucose (2-DG) to assess glycolysis, glycolytic capacity and glycolytic reserve. C) Inhibition of protein complexes in the electron transport chain (ETC) in the mitochondrial membrane by rotenone (Complex I), antimycin A (Complex III) and oligomycin (Complex V), which block electron transportation at different points during extracellular flux analysis. FCCP dissipates H+ gradient mimicking ATP synthase (Complex V) maximal activity. (*adapted from Yang et al. 2017 and Underwood et al 2020)*[399, 400].

The respiratory and glycolytic activity can be determined by measuring the time course of OCR and ECAR upon dissecting different components of the electron

transport chain (ETC) with metabolic inhibitors or substrates (**Figure 10**)[398]. Two stress tests have been developed: the **mitochondrial stress test** (Mito stress test) and the **glycolytic stress test** (Gluco stress test), which measure mitochondrial respiration and glycolysis respectively, through different indices (**Figure 10**)[399]. In addition to OCR and ECAR measurement, seahorse technology assesses the activity of components of the ETC and the associated supercomplexes, using different metabolic substrates or inhibitors in permeabilized cells [398, 399](**Figure 10**).

This approach has been extensively applied for metabolic characterization of different types of cancer[401, 402]. In CLL, contemporary studies to this thesis have identified metabolic changes in the lymph node and treatment-associated metabolic alterations by using the seahorse technique[331, 379, 403]. Moreover, OCR and ECAR measurement in response to CLL drugs or metabolic inhibitors could provide valuable information to depict CLL metabolic specificities for mitochondrial respiration, and to identify new metabolic vulnerabilities.

4.5. Metabolomic liquid chromatography coupled to mass spectrometry

Multiple approaches have been developed to study metabolism in cancer cells[404-406]. Liquid chromatography coupled to mass spectrometry (LC-MS) constitutes a powerful technology for metabolite profiling of biological samples[404]. This approach can assess the presence and abundance of hydrophilic metabolites, which account for most metabolites involved in cancer metabolism. Metabolite extraction methods have been optimized for each biological sample (culture media, cells, tissue, urine or serum)[404].

Liquid chromatography (LC) enables the separation of hydrophilic metabolites, which permits quantitative and qualitative metabolite detection by **mass spectrometry (MS) (Figure 11).** Two main types of LC can be used: hydrophilic interaction liquid chromatography and ion-pairing reagent application[404]. Once the metabolites have been eluted and ionized, they can be distinguished by a targeted analysis (triple-quadrupole) or by a high-resolution MS non-targeted analysis (Q-TOF or Q-orbitrap (exactive)), based on the molecular mass of the metabolite to charge ratio (m/z). Finally, the relation between the

retention time (RT) from chromatographic separation and metabolite MS specificity determines the metabolite identity[404] **(Figure 11).** It is important to highlight that this technique exclusively uncovers the analysis of hydrophilic metabolites, and there is a lack of analytic platforms that provides coverage for the whole spectrum of metabolites. Concretely, in hematological malignancies, lipids are essential macromolecules for cellular architecture and metabolism and tumor development, and their study needs to be addressed through specific MS-based lipidomics techniques[407, 408].

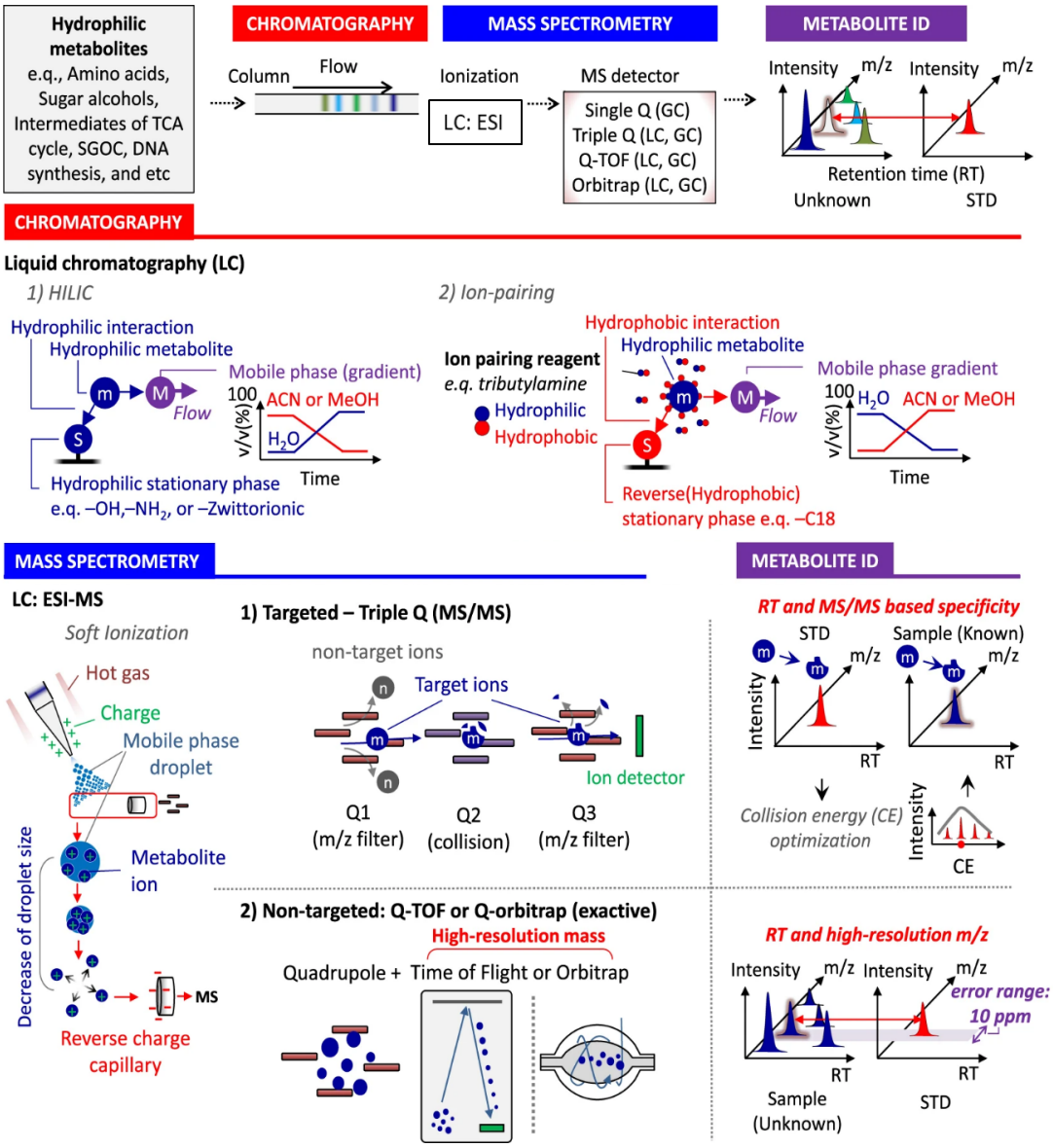

Figure 11. Schematic representation of chromatography coupled to mass spectrometry (LC-MS) methodology for metabolite profiling. Liquid chromatography (LC): during hydrophilic interaction liquid chromatography (HILIC), water-soluble metabolites interact with the hydrophilic stationary phase, whereas ion-pairing reagent application (with both hydrophilic and hydrophobic

residues in the same molecule) is based on the interaction of metabolites with the hydrophobic stationary phase. Consecutively, metabolites are eluted from the column through a mobile phase gradient. Mass spectrometry (MS): electrospray ionization (ESI) is applied for ionizing metabolites in the liquid mobile phase and metabolites are charged by the high voltage of the probe to enter the MS compartment. Metabolite ID: metabolites can be distinguished by a targeted analysis (triple-quadrupole) or by a high-resolution MS non-targeted analysis (Q-TOF or Q-orbitrap (exactive)), according to the molecular mass of the metabolite to charge ratio (m/z). Metabolite identity will be determined by the relation between the retention time (RT) from chromatographic separation and metabolite MS specificity. TCA: tricarboxylic acid, SGOC: serine, glycine, and one carbon, Q-TOF: quadrupole-time of flight, CAN: acetonitrile; MeOH: methanol (*adapted from Kang et al. 2018)*[404].

All in all, LC-MS-based approaches have been crucial for relevant advances in the comprehension of cancer metabolism[405, 406]. Several metabolomic studies have been performed in CLL, and they have revealed new roles of TME in metabolic reprogramming, as well as metabolic preferences of CLL cells and potential biomarkers for CLL treatment indication[377, 379, 409]. However, many questions about CLL metabolism are still unresolved, and further multi-omics studies by integrating genomic and metabolomic approaches could help to elucidate whether and how the wide range of CLL drivers may be underlying metabolic changes in the CLL cell.

HYPOTHESIS

Chronic lymphocytic leukemia (CLL) displays a heterogeneous clinical and biological behavior. In the last decade, the explosion of high-throughput molecular techniques has significantly improved the comprehension of the pathogenesis of the disease, offering new perspectives that may finally translate into the assessment of new prognostic biomarkers and novel therapeutic strategies for a better management of patients.

Chromosomal abnormalities are a hallmark of CLL and each cytogenetic alteration associates with a different outcome, which enables to stratify patients in risk subgroups. For the last decades, the most recurrent cytogenetic alterations have been routinely assessed by the classical 4-probe CLL FISH panel. With regard to the less frequent chromosomal abnormalities that are not included in the standard FISH analysis, 6q21 deletion, 14q32 deletions or 14q32 translocations have been suggested to impact prognosis, although there is still some controversy among studies. Furthermore, the prevalence of these alterations is probably underestimated, which makes it difficult to establish their real incidence and hence, their prognostic significance.

The widespread next-generation sequencing (NGS) techniques have allowed the identification of a plethora of genetic alterations, including mutations and copy number alterations (CNAs), in a large number of CLL drivers, demonstrating a lack of a disease-specific genetic aberration. Several efforts have been made to obtain a comprehensive characterization of the molecular landscape of CLL, by integrating chromosomal and mutational information. These approaches have revealed that certain genetic mutations have a clinical impact, which may contribute to better refine CLL prognosis, especially within the cytogenetic-risk stratification model. Although the vast majority are coding mutations, some studies demonstrated that non-coding mutations may also affect the pathobiology and clinic of the disease, such as the 3'UTR *NOTCH1* mutations. It should be noted that just a few genetic mutations have been investigated as potential prognostic markers, and the clinical impact of several alterations remains to be determined.

Additionally, NGS approaches permitted to further investigate CLL pathogenesis, identifying patterns of co-occurrence between chromosomal

alterations and somatic mutations that may drive CLL progression. A common pathogenic mechanism related to these concurrent events is the biallelic inactivation of genes encompassed within the altered chromosome by the presence of mutations in the remaining allele, such as *ATM* in del(11q) or *TP53* in del(17p). Regarding 6q and 14q deletions and translocations, inactivation of certain suppressor genes by haploinsufficiency has been suggested, but it has not been further confirmed. *TRAF3*, a tumor suppressor located in 14q32, appears to be inactivated by a double-hit alteration (deletion and mutation) in other B-cell malignancies such as multiple myeloma (MM) or Non-Hodgkin lymphoma (NHL). However, despite the identification of 14q deletions in CLL, the incidence and association of *TRAF3* mutations with this alteration, as well as its biological role, are mostly unknown, probably due to their low incidence and limited evaluation at both biological and clinical levels.

In the last few years, to overcome the sample availability constraints and the difficulty of manipulating CLL cells *ex vivo*, CRISPR/Cas9-edited *in vitro* and *in vivo* models have become a useful tool for evaluating the biological implications of CLL alterations. Moreover, recent advances in the study of cellular metabolism in cancer have demonstrated that hematological malignancies may alter their metabolic specificities to sustain a proliferating phenotype, and concretely, metabolic alterations have been identified in CLL, mainly after therapy refractoriness. Nevertheless, despite these advances, whether and how metabolic changes may be influenced by the wide range of CLL drivers or how they could affect CLL pathogenesis and disease progression is largely unexplored. Thus, the study of metabolism could contribute to improve the knowledge of CLL molecular pathomechanisms and to identify new therapeutic vulnerabilities and resistances.

Altogether, I believe it is essential a further expansion of the molecular characterization of CLL, considering rare chromosomal abnormalities, CNAs, as well as coding and non-coding mutations, and also to assess unexploited biological implications of candidate CLL drivers in the disease. Taken this into consideration, the integration of genome-editing, genomic and metabolomic approaches would be of great utility to address these questions and to better understand the role of rare genetic alterations in CLL pathogenesis, progression, and therapy response.

AIMS

GENERAL AIM

To characterize the prognostic impact and the molecular profile of CLL patients with rare cytogenetic alterations involving chromosome regions 6q and 14q32, as well as to evaluate the clinical and biological implications of the candidate CLL gene drivers more frequently altered within these subgroups through the combination of high-throughput sequencing, genome-editing and metabolic approaches.

SPECIFIC AIMS

1. To evaluate the prognostic significance and clinical implications of 6q deletion, del(6q), 14q32/*IGH* translocations (IGH*R*) and 14q32/*IGH* deletions in CLL outcome.
2. To characterize the mutational profile of CLL patients carrying del(6q), focusing on those with del(6q) as the sole abnormality, and its implication in refining CLL patients' prognosis.
3. To analyze the mutational pattern of CLL patients with IGH*R* and to evaluate the prognostic impact of the mutations identified within this subgroup.
4. To determine the molecular characteristics of CLL patients showing IGH deletion, and the incidence and clinical significance of biallelic *TRAF3* inactivation in this subgroup of patients.
5. To elucidate the biological consequences of biallelic *TRAF3* inactivation in NF-κB signaling and cellular metabolism through CRISPR/Cas9-edited cellular models that mimic *TRAF3* mutations observed in CLL patients.
6. To assess the impact of *TRAF3* inactivation on treatment response to CLL drugs and novel combinations of metabolic inhibitors in cellular models and primary CLL cells.

RESULTS

This section includes the experimental work performed on this thesis, including Material and Methods, Results and Discussion. This section has been divided into four chapters:

Chapter 1. Claudia Pérez Carretero, Teresa González, Miguel Quijada Álamo, Gian Matteo Rigolin, Adrian Dubuc, Ángela Villaverde Ramiro, Alberto Rodríguez, Juan Nicolás Rodríguez, Araceli Rubio, Julio Dávila, Mª Jesús Vidal, Isabel González Gascón y Marín, José Ángel Hernández Rivas, Rocío Benito, Matt Davids, Jeremy Abrasom, Antonio Cuneo, Paola Dal Cin, Ana-Eugenia Rodríguez Vicente and Jesús-María Hernández-Rivas. **Chronic lymphocytic leukemia patients with chromosome 6q deletion as the sole cytogenetic abnormality display a high frequency of *RPS15* mutations and have a dismal prognosis.** *Manuscript in preparation.*

Chapter 2. Claudia Pérez Carretero, María Hernández Sánchez, Teresa González, Miguel Quijada Álamo, Marta Martín Izquierdo, Jesús María Hernández Sánchez, María Jesús Vidal, Alfonso García de Coca, Carlos Aguilar, Manuel Vargas Pabón, Sara Alonso, Magdalena Sierra, Araceli Rubio Martínez, Julio Dávila, José R. Díaz Valdés, José Antonio Queizán, José Ángel Hernández Rivas, Rocío Benito[2], Ana E. Rodríguez Vicente and Jesús María Hernández Rivas. **Chronic lymphocytic leukemia patients with *IGH* translocations are characterized by a distinct genetic landscape with prognostic implications.** *International Journal of Cancer.* 2020 Nov 15;147(10):2780-2792. doi: 10.1002/ijc.33235.

Chapter 3. Claudia Pérez Carretero, María Hernández Sánchez, Teresa González, Miguel Quijada Álamo, Marta Martín Izquierdo, Sandra Santos Mínguez, Cristina Miguel García, María Jesús Vidal, Alfonso García De Coca, Josefina Galende, Emilia Pardal, Carlos Aguilar, Manuel Vargas Pabón, Julio Dávila, Isabel Gascón Y Marín, José Ángel Hernández Rivas, Rocío Benito, Jesús María Hernández Rivas and Ana Eugenia Rodríguez Vicente. ***TRAF3* alterations are frequent in del-3'IGH chronic lymphocytic leukemia patients and define a specific subgroup with adverse clinical features.** *American Journal of Hematology.* 2022 Jul;97(7):903-914. doi: 10.1002/ajh.26578.

Chapter 4. Claudia Pérez Carretero, Miguel Quijada Álamo, Mariana Tannoury, Léa Dehgane, Alberto Rodríguez Sánchez, David J. Sanz, Teresa González, Rocío Benito, Élise Chapiro, Florence Nguyen, Ana E. Rodriguez Vicente, Santos A. Susin and Jesús María Hernández Rivas. ***TRAF3* alterations enhance metabolic plasticity through metabolic reprogramming in chronic lymphocytic leukemia.** *Manuscript in preparation*.

All of them have been developed to accomplish the general aim of this work and give the title to this doctoral dissertation: "**Molecular analysis of rare cytogenetic abnormalities in chronic lymphocytic leukemia: from genomic alterations to metabolic reprogramming**".

A General Discussion, with additional data and which comprises all research, is addressed in a separate section of this thesis.

In addition, the supplementary material corresponding to each of the chapters indicated above is collected at the end of the thesis.

CHAPTER 1

Chronic lymphocytic leukemia patients with chromosome 6q deletion as the sole cytogenetic abnormality display a high frequency of *RPS15* mutations and have a dismal prognosis

Claudia Pérez Carretero[1,2], Teresa González[1,2], Miguel Quijada Álamo[1,2], Gian Matteo Rigolin[3], Adrian Dubuc[4], Ángela Villaverde Ramiro[1,2,] Alberto Rodríguez[1,2], Juan Nicolás Rodríguez[5], Araceli Rubio[6], Julio Dávila[7], Mª Jesús Vidal[8], Isabel González Gascón y Marín[9], José Ángel Hernández Rivas[9], Rocío Benito[1,2], Matt Davids[10], Jeremy Abrasom[11], Antonio Cuneo[3], Paola Dal Cin[4], Ana-Eugenia Rodríguez-Vicente[1,2] Jesús-María Hernández-Rivas[1,2]

1. University of Salamanca, IBSAL, IBMCC, CSIC, Cancer Research Center, Salamanca, Spain.
2. Department of Hematology, University Hospital of Salamanca, Salamanca, Spain.
3. Hematology Section, St. Anna University Hospital, Ferrara, Italy
4. Department of Pathology, Brigham and Women's Hospital, Boston, MA, USA
5. Department of Hematology. Hospital Juan Ramon Jimenez, Huelva, Spain
6. Department of Hematology, Hospital Miguel Servet, Zaragoza, Spain
7. Department of Hematology, Hospital Nuestra Señora de Sonsoles, Ávila, Spain
8. Department of Hematology, Hospital Universitario, León, Spain.
9. Department of Hematology, Hospital Universitario Infanta Leonor. Universidad Complutense, Madrid, Spain.
10. Dana Farber Cancer Institute, Boston, MA, USA
11. Massachusetts General Hospital, Boston, MA, USA.

Manuscript in preparation

Chronic Lymphocytic Leukemia patients with chromosome 6q deletion as the sole cytogenetic abnormality display a high frequency of *RPS15* mutations and have a dismal prognosis

Claudia Pérez Carretero[1,2], Teresa González[1,2], Miguel Quijada Álamo[1,2], Gian Matteo Rigolin[3], Adrian Dubuc[4], Ángela Villaverde Ramiro[1,2,] Alberto Rodríguez[1,2], Juan Nicolás Rodríguez[5], Araceli Rubio[6], Julio Dávila[7], Mª Jesús Vidal[8], Isabel González Gascón y Marín[9], José Ángel Hernández Rivas[9], Rocío Benito[1,2], Matt Davids[10], Jeremy Abrasom[11], Antonio Cuneo[3], Paola Dal Cin[4], Ana-Eugenia Rodríguez-Vicente*[1,2], Jesús-María Hernández-Rivas[1,2]

1. University of Salamanca, IBSAL, IBMCC, CSIC, Cancer Research Center, Salamanca, Spain.
2. Department of Hematology, University Hospital of Salamanca, Salamanca, Spain.
3. Hematology Section, St. Anna University Hospital, Ferrara, Italy
4. Department of Pathology, Brigham and Women's Hospital, Boston, MA, USA
5. Department of Hematology. Hospital Juan Ramon Jimenez, Huelva, Spain
6. Department of Hematology, Hospital Miguel Servet, Zaragoza, Spain
7. Department of Hematology, Hospital Nuestra Señora de Sonsoles, Ávila, Spain
8. Department of Hematology, Hospital Universitario, León, Spain.
9. Department of Hematology, Hospital Universitario Infanta Leonor. Universidad Complutense, Madrid, Spain.
10. Dana Farber Cancer Institute, Boston, MA, USA
11. Massachusetts General Hospital, Boston, MA, USA.

AERV and JMHR shared senior authorship

ABSTRACT

Objectives: Deletion of the short arm of chromosome 6, del(6q), is a rare cytogenetic alteration that appears in ~5% of patients with chronic lymphocytic leukemia (CLL). Although del(6q) has been traditionally related to an intermediate outcome, the molecular mechanisms underlying pathogenesis and its impact in prognosis are still not well characterized. For that, we aimed to assess for the first time the mutational profile of del(6q) CLL patients and evaluate the clinical implications of this alteration.

Patients and Methods: Patients' samples and clinical data were collected from 3 different institutions in a multicenter study. A targeted next-generation sequencing (NGS) approach using a custom-designed panel of 54 CLL-related genes was applied for the mutational analysis of 39 patients with del(6q). Within this cohort, 15 patients showed del(6q) as the sole cytogenetic abnormality.

Results: CLL patients with del(6q) as the sole abnormality had shorter time to first treatment (TFT) (median 0 months *vs.* 36 months, p=0.0013) and a distinct mutational profile, with a significantly high mutational frequency of *RPS15* (40%), associated with a shorter TFT (5 *vs.* 13 months, p=0.027). Furthermore, our results revealed that *TP53* mutations were more frequent in CLLs carrying del(6q) in addition to other cytogenetic alterations (38%), showing more genomic instability and shorter overall survival (median 31 months *vs.* median not reached, p=0.046).

Conclusion: Mutational and clinical analyses showed that CLL patients displaying del(6q) as the only cytogenetic abnormality had a distinct mutational profile with a high frequency of *RPS15* mutations that may be driving pathogenesis and the adverse outcome.

1 INTRODUCTION

Chronic lymphocytic leukemia is a clinically heterogeneous disease, with survival times ranging from months to decades, reflecting a great biological diversity (1). FISH-

*Correspondence: anerv@hotmail.com.

based classification has been used to identify chromosomal abnormalities commonly associated with CLL, including del(17)(p13), del(13)(q14), del(11)(q22), and trisomy 12 (2). Other less-common cytogenetic aberrations have also been noted, including del(6q)in 3–7% of cases (2-4) mostly as a secondary chromosome anomaly or in the context of complex karyotypes (5).

The prognostic significance of del(6q) remains controversial, likely due to its uncommon occurrence compared to the four others more routinely-noted FISH defects. Several studies have suggested an association of del(6q) with inferior outcomes, allocating these CLL cases in an intermediate-risk category (6, 7), although other studies have shown no difference in outcomes (4, 8). Cytogenetic analysis recurrently detected del(6q) in other B cell malignancies and solid tumors (9-13). The recurrence of a 6q deletion in cancer strongly suggests that this region contains unidentified tumor-suppressor gene(s) and therefore it deserves further investigation for its role in the malignant process (5, 14, 15).

Next-generation sequencing (NGS) studies have provided a better knowledge of the genetic complexity and heterogeneity of CLL, and new insights into the molecular landscape

Table 1. Karyotype and FISH information of 39 chronic lymphocytic leukemia patients with del(6q). % Indicates the proportion of cells that were positive for the FISH probe (cut-off for clonal abnormality: 6q->9%, 11q-, +12, 13q- and 17p->10%).

ID	Karyotype	6q- by FISH (% of cells)	11q- by FISH (% of cells)	+12 by FISH (% of cells)	13q- by FISH (% of cells)	17p- by FISH (% of cells)
P1	46,XX,del(6q)[6]/46,XX,sl,del(11q)[4]/46,XX[7]	0	88	0	0	2
P2	47,XX,t(2;7)(p12;p21),+5,+del(6)(q21),del(9)(q21),add(11)(q24,)[2]/46,XX [18]	0	0	0	0	0
P3	47,XY,+21[4]/46,XY,del(6)(q22q25)[2]/46,XY[7]	0	0	0	0	0
P4	46,XX,del(6)(q21),add(7)(p21),del(11)(q13),del(13)(q14q21)[2]/46,XX [18]	9	61	0	82	0
P5	46,XX,der(6)t(6;13)(q21;q14),+del(6)(q21),+8,-13,-15,-17,+mar [15]	0	0	0	80	87
P6	46,XX,del(6)(q21)[2]/46,XX[18]	90	0	0	0	0
P7	82-90,XXXX,del(6)(q21),add(11)(q21)x2[10]/46,XX[5]	0	21	45	0	0
P8	46,XY,del(6)(q21q26)[2]/46,XY,sl,del(13)(q14),add(11)(q24),add(14)(q32)[7]/46,XY[6]	0	0	0	90	0
P9	46,XX,del(6)(q16q26),add(10)(q26)[7]/46,XX[13]	0	0	0	0	0
P10	46,XX,del(6)(q16q26)[10]/46,XX[10]	0	0	0	0	0
P11	46,XX,del(6)(q21)[2]/46,XX[9]	11	0	0	0	0
P12	47,XY,+12[8]/47,sl,del(6)(q21)[2]/46,XY[6]	0	0	0	0	0
P13	46,XY,del(6)(q21),add(9)(p13),add(17)(q13)[15]/46,XY[13]	0	0	0	7	68
P14	46,XY,del(6)(q21)[10]	0	0	0	0	0
P15	46,XY,del(11)(q21)[4]/46,XY,del(6)(q21)[2]	0	40	0	0	15
P16	46,XX,del(6)(q16q26)[10]/46,XX[10]	0	0	0	0	0
P17	47,XY,+12[2]/47,XY,sl,dup(1)(q24q42),del(6)(q22q26),del(11)(q13q24)[7]	0	0	69	0	17
P21	46,XY,del(6)(q21)[4]/46,XY[12]	0	0	0	0	0
P22	46,XY,del(6)(q23)[6]/46,XY[14]	0	0	0	0	0
P23	46,XY,del(6)(q21)[6]/46,XY[14]	0	0	0	0	0
P24	44,XY,-5,del(6)(q11),-8,der(10)t(10;?21)(q22;?q21),del(11)(q11),del(13)(q14), del(14)(q24),+der(14)t(5;14)(q21;q32),add(17)(p11),-21[13]/46,XY[5]	0	0	0	72.5	96
P25	46,XX,del(13)(q22q31[5]/46,sl,del(6)(q22)[2]/46XX[20]	0	0	0	0	0
P26	47,XY,add(1)(p36),der(2)t(2;?)(p23;?),del(3)(p21),del(6)(q23),+12,del(13)(q12q14), del(14)(q24),der(17)t(17;?)(q25;?)[16]/46,XY[4]	0	0	68	23	0
P27	46,XX,del(6)(q21),del(11)(q13),del(13)(q14q22)[11]/46,XX[9]	0	86.5	0	86	0
P28	46,XX,del(13)(q14q22),del(17)(p12) [6]/46,sl,XX,del(6)(q21)[6]/46,XX[8]	0	0	0	27	27
P29	46,XY,del(6)(q21),del(13)(q12q14)[3]/46,XY,sl,add(10)(q26)[4]/46,XY[13]	0	0	0	30	0
P18	46,XX,del(6)(q13q25)[13]/46,XY[7]	0	0	0	0	0
P19	46,XY,del(6)(q21q25)[3]/46,sl,del(9)(p22p24)[11]/46,XY[6]	0	0	0	15	0
P20	46,XX,del(6)(q13q21)[12]/46,XX[8]	0	0	0	0	0
P30	46,XY,del(6)(q21q25)[13]/46,XY[7]	0	0	0	0	0
P31	46,XY,del(6)(q13q21)[2]/46,sl,del(11)(q13q23)[7]/46,sd1,del(11)(q21q23)[5]/ 45,XY,dup(2)(p13p25),der(17)t(17;19)(p13;p12),-19[cp4]/46,XY[2]	0	20.5	0	0	16
P32	45,XX,add(5)(q31),der(6;17)(q10;q10)[12]/46,XX[8]	0	0	0	0	84
P33	46,XY,del(6)(q21q25)[5]/46,sl,t(3;17)(p21;q25),del(19)(p13)[2]/46,XY[13]	0	0	0	0	0
P34	46,XX,del(6)(q15q25)[12]/46,XX[3]	0	0	0	0	0
P35	46,XY,del(6)(q13q27)[14]/46,XY[6]	0	0	0	0	0
P36	46,XY,del(6)(q13q15)[8]/46,XY[6]	0	0	0	0	0
P37	45,XY,del(6)(q23),-18[20]	0	0	0	0	0
P38	46,XY, del(6)(q2?1q2?4), add(14)(q32)[3]/44,X,-Y,i(6)(p10),-17[1]/45,X,-Y[6]/46,XY[10]	0	0	0	0	0
P39	46,XX,del(6)(q21q26)[19]/46,XX[1]	0	0	0	0	0

of CLL have been achieved.(16-18). In addition to the well-documented *TP53* aberrations, recurrent somatic mutations have been discovered within genes involved in key cellular processes (e.g., NOTCH signaling, RNA splicing, nuclear factor κB signaling). Such mutations tend to be enriched in high-risk CLL patients and have been associated with inferior outcome and even chemo-refractory disease (19-22).

However, del(6q) CLL patients remain poorly characterized at the molecular level, partly due to the low incidence of cases, inclusion of both previously untreated and treated CLL patients, the co-occurrence with other cytogenetic alterations, and lack of adequate accounting of other confounding factors. In our study, we comprehensively characterize for the first time the genetic landscape of CLL with del(6q) identified by karyotyping, since we believe that a mutational screening by NGS could allow for a refinement of our capability to predict overall survival (OS) and time to first treatment (TFT) in these patients, as well as provide novel insights into del(6q) CLL pathobiology.

2 PATIENTS AND METHODS

2.1 Patients

Patients' samples and clinical data were collected from 3 different institutions: Brigham and Women's Hospital (MA, USA), Hospital of Ferrara (Italy) and University Hospital of Salamanca (Spain) in the time-frame between 1997 and 2018, diagnosed according to the International Workshop on CLL (iwCLL) criteria (23). The study was based on 39 CLL patients carrying del(6q) and 315 as the control group. Patients included in the control group were representative of the disease in terms of clinical and biological characteristics and CLL-IPI scores, as shown in a previous study (24).

The study was approved by the local ethical committees. Written informed consent was obtained from all participants before they entered the study.

2.2 Conventional cytogenetics and fluorescence in situ hybridization (FISH)

Conventional cytogenetics were performed to assess the presence of 6q deletion (del(6q)) in a total of 39 samples, 28 of them analyzed before therapy. Median time from diagnosis to karyotyping was 2 years (range: 0-11). Interphase FISH was performed on peripheral blood or bone marrow samples using the 4-probe CLL panel (ATM, CEP12, D13S319, and TP53, Vysis, Abbott Laboratories, IL, USA), and the 6q21 probe (CytoTest) was used to validate the presence of the deletion when it appeared in <2 metaphases. The methods used for FISH analysis have been described elsewhere (25). Signal screening was carried out in at least 200 cells with well-delineated fluorescent spots.

2.3 Next-generation sequencing (NGS)

Mutational analysis by next generation sequencing (NGS) was performed in the same sample as the karyotype and the FISH. Genomic DNA was extracted from mononucleated cells isolated from peripheral blood. The Agilent SureSelectQXT Target Enrichment system for Illumina Multiplexed Sequencing (Agilent Technologies, Santa Clara, CA, USA) was used to produce custom-designed libraries of exonic regions from 54 CLL-related candidate driver genes. Paired-end sequencing (151-bp reads) was run on the Illumina NextSeq instrument (Illumina, San Diego,CA, USA). Data analysis was performed using a previously validated in-house pipeline (26-28)(**Supplementary Methods**).

2.4 Statistical analysis

Statistical analyses were performed using IBM SPSS v23.0 for Windows (IBM Corp., Armonk, NY, USA) and R v4.0.2. Mann–Whitney U test was used for assessing statistical associations considering continuous variables, while the chi-square and Fisher's exact tests were used to determine associations between categorical variables and patterns of mutual co-occurrence or exclusivity. Overall survival (OS) and time to first treatment (TFT) were calculated from the date FISH test was performed to the date of death, first treatment, or last follow-up (considering disease-unrelated deaths as competing events). Statistically significant variables related to OS and TFT were estimated by the Kaplan–Meier method, using the log-rank test to compare the curves of each group. Results were considered statistically significant for values of $p<0.05$.

3 RESULTS

3.1 Cytogenetic characteristics of del(6q) patients

Thirty-nine patients had a 6q deletion (del(6q)-CLLs) identified by karyotyping. Within this subgroup, 15 out of 39 del(6q)-CLLs (38%) had del(6q) as the sole abnormality (6q- only). In the remaining 24, del(6q) co-occurred with other cytogenetic alterations (6q-/+others) assessed by karyotyping and/or FISH, being the most common the presence of 13q deletion (13q-) in 23% of cases (9/39), 17p deletion (17p-) in 20.5% (8/39), 11q deletion (11q-) in 18% (7/39) and trisomy 12 (+12) in 7.7% (3/39). Notably, 15 of them showed complex karyotype (≥3 abnormalities) (**Table 1**). In 16 out of 24 6q-/+others cases, del(6q) was a primary cytogenetic aberration, being present in the major clone with abnormal karyotype.

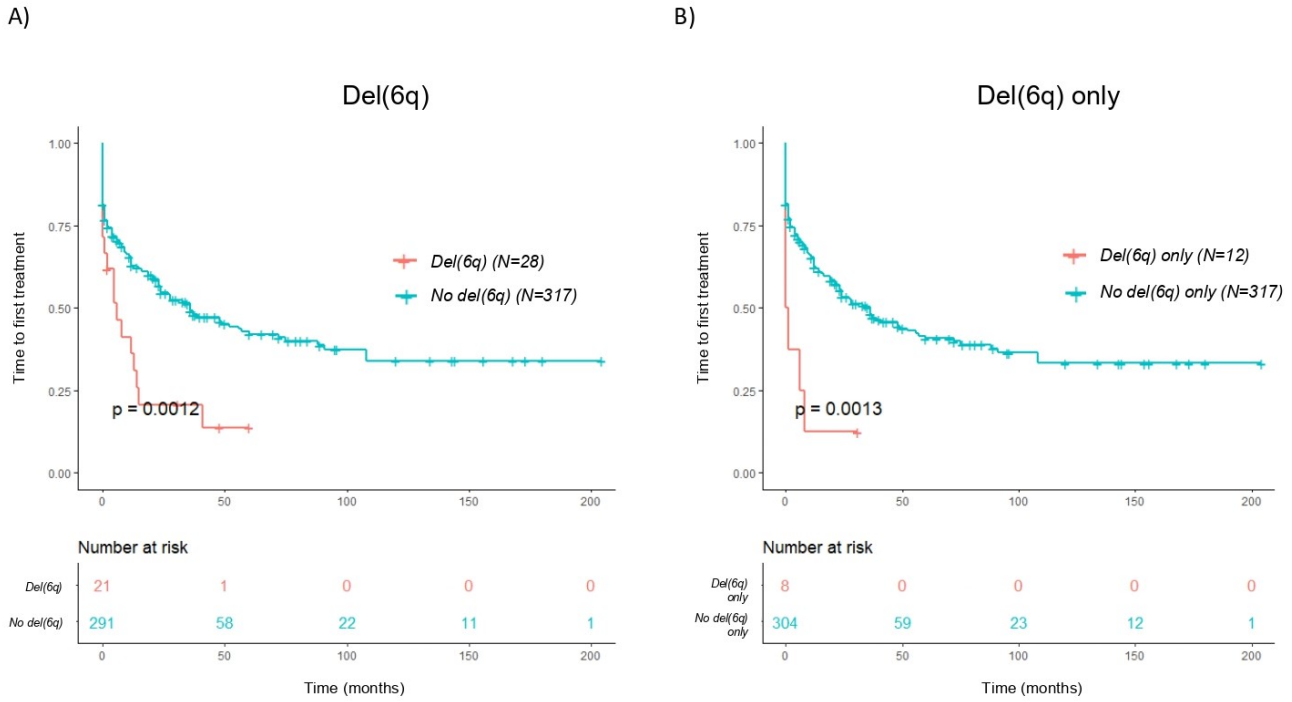

Figure 1. Clinical impact of del(6q) on CLL. Kaplan Meier analyses of time to first treatment according to A) the presence of 6q deletion (del(6q)) and B) the presence of del(6q) as the sole abnormality (del(6q) only).

3.2 Del(6q) patients show an intermediate-adverse clinical outcome

The whole series of 39 patients with del(6q) showed more adverse risk markers including unmutated *IGHV* (75.8% *vs* 45.7%, *p*=0.003), CD38 positivity (51.7% *vs* 28.3%, *p*=0.017), and ZAP70 positivity (63.3% *vs* 15.9%, *p*>0.001) (**Suppl. Table S1**). The median follow-up of del(6q) patients was 6.1 years. Del(6q) was detected at or near diagnosis in 24/39 cases (cut-off: 2 years from diagnosis), while 15/39 showed the deletion later in the disease course. A total of 11 patients received treatment before sampling date, and 82% were treated during follow-up. The presence of del(6q) was associated with shorter time to first treatment (TFT) when compared to the control group (N=317) (median: 6 *vs* 36 months, *p*=0.0012) (**Figure 1A**), independently of the presence of additional cytogenetic abnormalities. In addition, the TFT from the karyotyping date of patients with del(6q) as the sole abnormality was shorter than in the control group (0 *vs* 36, *p*=0.0013) (**Figure 1B**). However, no statistically significant differences were noted in overall survival (64 *vs* 144, *p*=0.319) (data not shown).

3.3 Patients with del(6q) as the sole abnormality display a distinct mutational pattern

According to the mutational analyses, 92% of del(6q) CLLs exhibited at least one mutation in one of the 54 genes analyzed, and the most frequently mutated genes were *TP53* (28%), *RPS15* (26%), *NFKBIE* (15%) and *ATM* (15%) (**Figure 2A**). Interestingly, in patients with del(6q) as a primary event (n=31), the most recurrent mutated genes were *RPS15* (25.8%), *TP53* (25.8%) and *NOTCH1* (19.3%).

Notably, the mutational landscape varies depending on the presence of additional cytogenetic alterations (**Figure 2B**). Patients with del(6q) as the sole abnormality (6q- only), exhibited higher mutational frequencies in *RPS15* (6/15, 40%), *XPO1* and *ATM* (3/15, 20% each). Regarding *RPS15*, most mutations were missense and located in hotspot codons in exon 4 (**Suppl. Figure S1A)**. *RPS15*-mutated patients presented other genetic mutations such as *NOTCH1, NFKBIE, TP53, ATM* and *XPO1* (**Figure 2A**), although the analysis of patterns of co-occurrence showed that certain combinations of gene mutations are significantly rare events within this cohort, highlighting the presence of simultaneous *RPS15* and *TP53* mutations (p<0.001) (**Suppl. Figure S1B)**.

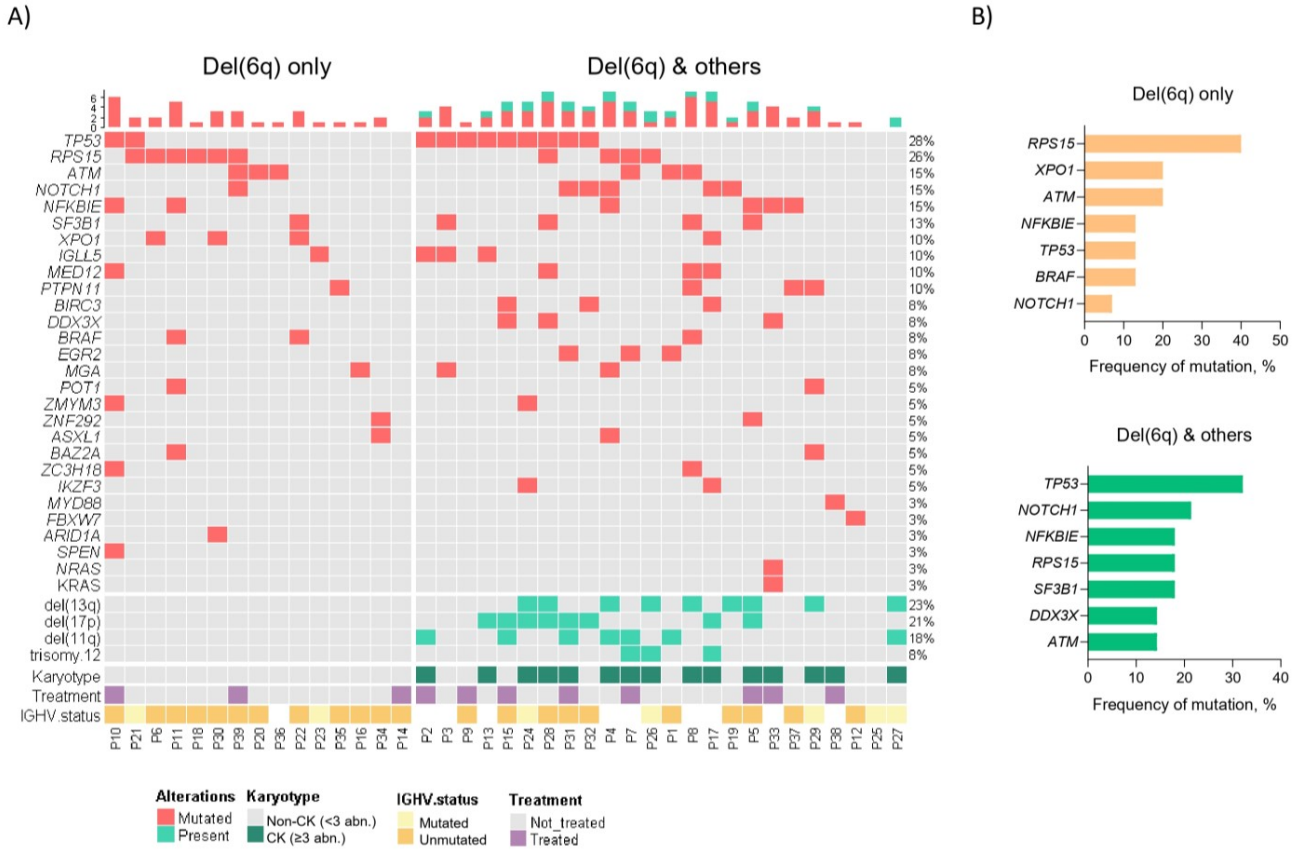

Figure 2. Mutational landscape of CLLs with del(6q). (A) Waterfall plot of genetic landscape of 39 patients grouped according to the presence of del(6q) as the sole abnormality (del(6q) only) or combination with other cytogenetic alterations (del(6q) other). Mutations are shown in red and FISH alterations in green. Karyotype, treatment and IGHV status information are shown below the mutational heatmap. CK: complex karyotype. B) Mutational frequencies of del(6q) CLLs according to the presence of del(6q) as the sole abnormality or in combination with other cytogenetic alterations.

In patients with del(6q) and additional cytogenetic alterations (6q-/+others), the most frequently mutated gene was *TP53* (9/24, 38%), followed by *NOTCH1 (*5/24, 21%) and *NFKBIE* (4/24, 17%)(**Figure 2B**). Within this subgroup, *TP53*-mutated 6q-/+others patients also showed mutations in other genes: *BIRC3, NOTCH1, RPS15* and *DDX3X* (2/11 each) and, as expected, 5/11 exhibited del(17p) and complex karyotype (**Figure 2A**). Interestingly, *TP53* and *ATM* mutations were mutually exclusive events in this study (p<0.001) (**Suppl. Figure S1B)**.

3.4 The presence of *RPS15* and *TP53* mutations could be associated with a dismal prognosis in CLL patients displaying del(6q)

Given the high incidence of *RPS15* and *TP53* mutations within this cohort, we next assessed their clinical impact. Strikingly, only *RPS15* mutations contributed to a worse outcome in del(6q) subgroup in terms of TFT (5 *vs.* 13 months, *p*=0.027) (**Figure 3A**) (**Suppl. Figure S2**). Conversely, the presence of *TP53* mutations was associated with a significant shorter OS in this subgroup of patients (31 months *vs.* median not reached, *p*=0.046) (**Figure 3B**), while RPS15 mutations did not impact OS (p=0.12) (**Suppl. Figure S3**).

It is noteworthy to mention that while most *RPS15* mutations (8/10) were detected in untreated patients, and located in different codons, two of them were detected at relapse in 2 patients in the same codon (S139, NM_001018), after anti-CD20 (P7) and chemotherapeutic (P39) regimens. In-

terestingly, the patient treated with anti-CD20 (P7) exhibited the del(6q) as the sole cytogenetic abnormality, and both of them (P7, P39) were refractory to ibrutinib (**Suppl. Figure S4**).

4 DISCUSSION

Detection of genetic changes has remarkably improved the risk stratification of CLL. Nevertheless, the prognostic significance and molecular underpinnings of 6q deletion in CLL remain unclear. Despite its low incidence, we evaluate a large cohort of del(6q) CLL patients, combining cytogenetic and mutational analysis.

Previous studies suggested that del(6q) is acquired late in the disease, as a secondary abnormality(5). However, our work showed that this alteration may occur as the first and only cytogenetic alteration (**Table 1**). Besides, our results demonstrated a strong association between del(6q) and bad prognosis markers, as well as a short time to first treatment, which is consistent with previously reported data (**Suppl. Table S1** and **Figure 1**)(4, 6). Although some works attributed the adverse outcome of del(6q) CLLs to concomitant high-risk alterations (5, 7), here we proved that 6q deletion as the single cytogenetic abnormality contributed to a worse prognosis, showing that the intermediate-adverse outcome is not just due to genomic instability or the accumulation of different genetic alterations (4, 7, 8).

The major finding of our study was the presence of a significant association between del(6q) and genetic mutations, with a distinct mutational profile depending on whether the del(6q) appears as the sole abnormality or in combination with other cytogenetic alterations (**Figure 2**). Surprisingly, the most frequently mutated gene in del(6q) only CLL patients was *RPS15 (*40%). In treatment-naïve CLL patients,

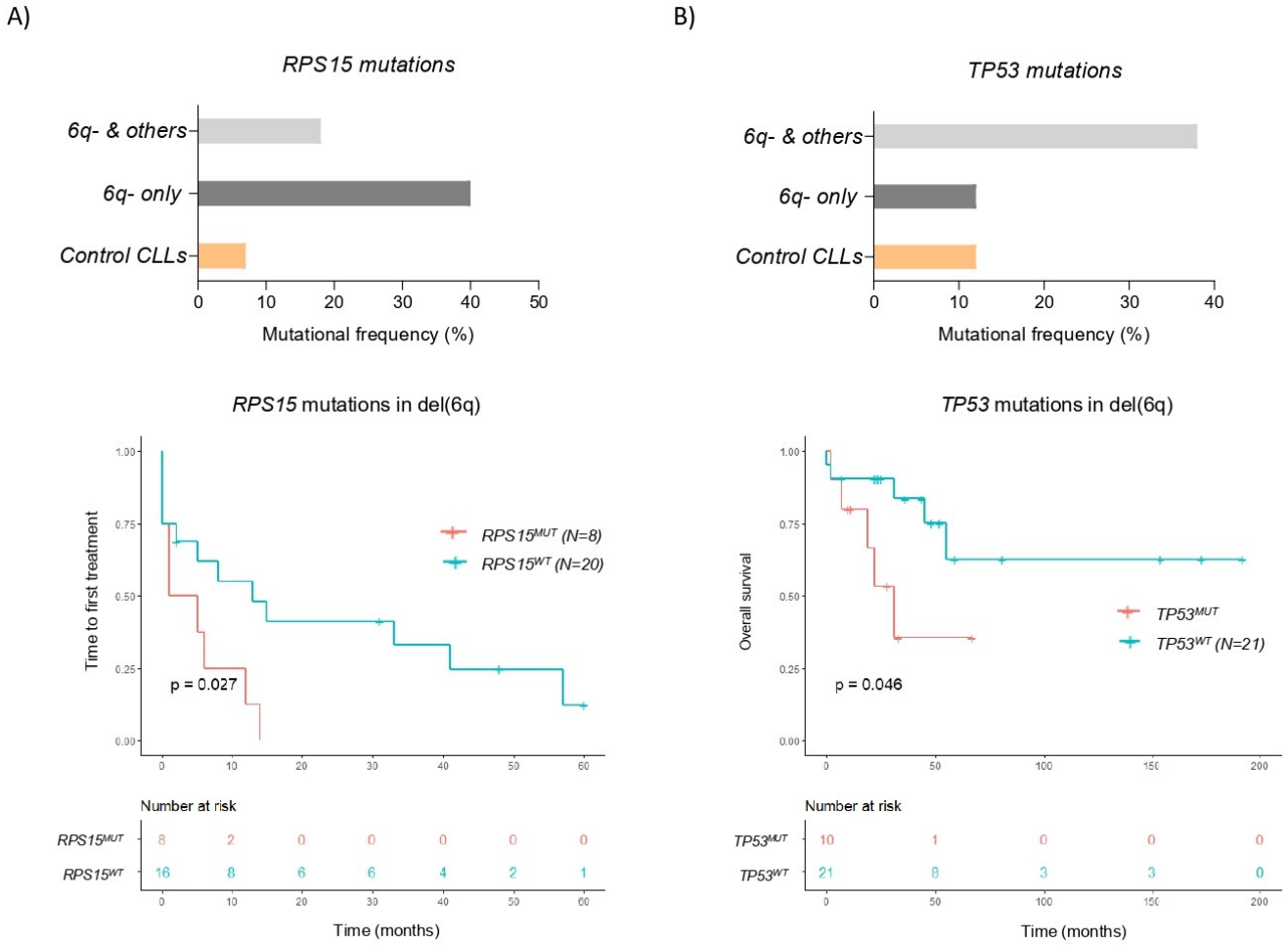

Figure 3. Figure 3. Clinical impact of mutations on del(6q) patients. A) Incidence of *RPS15* mutations in del(6q)-CLL and clinical impact on time to first treatment. B) Incidence of *TP53* mutations in del(6q)-CLL and clinical impact on overall survival.

RPS15 mutations are infrequent (~4%), but enriched at relapse or in high-risk subgroups such as del17p (~20%) (29-31), which would be in line with the fact that these mutations contributed to a worse outcome in del(6q) CLL patients (**Figure 3**). Although most *RPS15* mutations were detected before treatment initiation in our cohort, two patients showed these alterations at relapse, and moreover, those patients were refractory to the subsequent ibrutinib administration. These findings may indicate that del(6q) together with *RPS15* mutations are clonally selected after treatment and may have a predictive significance for following therapies, revealing a significant impact on the pathogenesis and outcome of CLL.

On the other hand, del(6q) CLL patients with additional cytogenetic aberrations had *TP53* as the most frequently mutated gene. Despite the previously reported association between *RPS15* and *TP53* mutations (29, 30), they are not significantly concurrent events within this subgroup (**Suppl. Figure S1B)**. *RPS15* was more recurrently mutated in combination with del(6q) only, while *TP53* mutations appeared together with del(6)q more commonly in the context of complex karyotype and with other alterations such as del(17p), suggesting a higher genomic instability that might be responsible for the poor outcome observed in this subgroup. Altogether, these results could indicate the presence of different driving forces of tumor development within del(6q) CLL patients. To further confirm the pathogenic impact and clonality of these alterations, it would be necessary to perform further functional analysis in *in vitro* or *in vivo* models harboring these concurrent alterations and validate these results in larger del(6q) CLL cohorts by applying single-cell sequencing approaches at different time points during the disease course.

5 CONCLUSIONS

In summary, our work demonstrates the genetic complexity of patients carrying 6q deletion and their association with mutations previously related to relapse (*RPS15* and *TP53*), highlighting the presence of higher mutational frequencies of *RPS15* in patients with del(6q) as the sole abnormality. Moreover, the co-occurrence of these genetic alterations with 6q deletion contributed to a worse clinical outcome and disease progression, demonstrating the importance of assessing their mutational status and considering all of them in the CLL genetic context to improve treatment decision-making.

CONFLICT OF INTEREST

The authors declare no competing financial interests.

AUTHOR CONTRIBUTIONS

CPC designed research, performed sample selection, carried out NGS and statistical analyses and drafted the manuscript. TG performed sample selection and FISH analyses. AVR performed data analysis and interpretated the results. MQA and AR performed NGS studies and data analysis and critically reviewed the manuscript. JNR, AR, JD, MJV, LG and IGGM provided patients' clinical data. JAHR, AD, MD, JA, GMR, AC and PDC provided patients' samples and clinical data and critically reviewed the manuscript. RB designed sequencing studies and contributed to data analysis. AERV performed data analysis and together with JMHR conceived the study, designed and supervised the research, and critically reviewed and approved the final version of the manuscript. All authors discussed the results and revised the manuscript. results.

FUNDING

This work was supported by grants from Instituto de Salud Carlos III (ISCIII) &FEDER (PI21/00983) (co-funded by the European Union), Consejería de Educación-Junta de Castilla y León (SA118P20), Gerencia Regional de Salud-SACYL (GRS2140/A/20, GRS2385/A/21), Fundación Mutua Madrileña (FMM, AP176752021), Red Temática de Investigación Cooperativa en Cáncer (RTICC) (RD12/0036/0069) and Centro de Investigación Biomédica en Red de Cáncer (CIBERONC CB16/12/00233).

CPC is supported by a research grant from FEHH ("Fundación Española de Hematología y Hemoterapia"; Beca de Investigación FEHH 2022). AR is fully supported by an "Ayuda predoctoral de la Junta de Castilla y León" by the Fondo Social Europeo Plus (FSE+) (JCYL- EDU/1868/2022 PhD scholarship).

ACKNOWLEDGMENTS

We are grateful to I. Rodríguez, S. González, M.Á. Ramos, A. Martín, A. Díaz, A. Simón, M. del Pozo, V. Gutiérrez and S. Pujante from the Centro de Investigación del Cáncer, Salamanca, for their technical assistance.

REFERENCES

1. Rodriguez-Vicente AE, Diaz MG, Hernandez-Rivas JM. Chronic lymphocytic leukemia: a clinical and molecular heterogenous disease. Cancer Genet. 2013;206(3):49-62.
2. Dohner H, Stilgenbauer S, Benner A, Leupolt E, Krober A, Bullinger L, et al. Genomic aberrations and survival in chronic lymphocytic leukemia. N Engl J Med. 2000;343(26):1910-6.
3. Stilgenbauer S, Bullinger L, Benner A, Wildenberger K, Bentz M, Dohner K, et al. Incidence and clinical significance of 6q deletions in B cell chronic lymphocytic leukemia. Leukemia. 1999;13(9):1331-4.
4. Wang DM, Miao KR, Fan L, Qiu HR, Fang C, Zhu DX, et al. Intermediate prognosis of 6q deletion in chronic lymphocytic leukemia. Leuk Lymphoma. 2011;52(2):230-7.
5. Finn WG, Kay NE, Kroft SH, Church S, Peterson LC. Secondary abnormalities of chromosome 6q in B-cell chronic lymphocytic leukemia:

a sequential study of karyotypic instability in 51 patients. Am J Hematol. 1998;59(3):223-9.
6. Cuneo A, Rigolin GM, Bigoni R, De Angeli C, Veronese A, Cavazzini F, et al. Chronic lymphocytic leukemia with 6q- shows distinct hematological features and intermediate prognosis. Leukemia. 2004;18(3):476-83.
7. Audil HY, Hampel PJ, Van Dyke DL, Achenbach SJ, Rabe KG, Smoley SA, et al. The prognostic significance of del6q23 in chronic lymphocytic leukemia. Am J Hematol. 2021;96(6):E203-E6.
8. Jarosova M, Hruba M, Oltova A, Plevova K, Kruzova L, Kriegova E, et al. Chromosome 6q deletion correlates with poor prognosis and low relative expression of FOXO3 in chronic lymphocytic leukemia patients. Am J Hematol. 2017;92(10):E604-E7.
9. Merup M, Moreno TC, Heyman M, Ronnberg K, Grander D, Detlofsson R, et al. 6q deletions in acute lymphoblastic leukemia and non-Hodgkin's lymphomas. Blood. 1998;91(9):3397-400.
10. Thelander EF, Ichimura K, Corcoran M, Barbany G, Nordgren A, Heyman M, et al. Characterization of 6q deletions in mature B cell lymphomas and childhood acute lymphoblastic leukemia. Leuk Lymphoma. 2008;49(3):477-87.
11. Walker GJ, Palmer JM, Walters MK, Hayward NK. A genetic model of melanoma tumorigenesis based on allelic losses. Genes Chromosomes Cancer. 1995;12(2):134-41.
12. Noviello C, Courjal F, Theillet C. Loss of heterozygosity on the long arm of chromosome 6 in breast cancer: possibly four regions of deletion. Clin Cancer Res. 1996;2(9):1601-6.
13. Hyytinen ER, Saadut R, Chen C, Paull L, Koivisto PA, Vessella RL, et al. Defining the region(s) of deletion at 6q16-q22 in human prostate cancer. Genes Chromosomes Cancer. 2002;34(3):306-12.
14. Amiel A, Mulchanov I, Elis A, Gaber E, Manor Y, Fejgin M, et al. Deletion of 6q27 in chronic lymphocytic leukemia and multiple myeloma detected by fluorescence in situ hybridization. Cancer Genet Cytogenet. 1999;112(1):53-6.
15. Juliusson G, Merup M. Cytogenetics in chronic lymphocytic leukemia. Semin Oncol. 1998;25(1):19-26.
16. Landau DA, Tausch E, Taylor-Weiner AN, Stewart C, Reiter JG, Bahlo J, et al. Mutations driving CLL and their evolution in progression and relapse. Nature. 2015;526(7574):525-30.
17. Puente XS, Bea S, Valdes-Mas R, Villamor N, Gutierrez-Abril J, Martin-Subero JI, et al. Non-coding recurrent mutations in chronic lymphocytic leukaemia. Nature. 2015;526(7574):519-24.
18. Knisbacher BA, Lin Z, Hahn CK, Nadeu F, Duran-Ferrer M, Stevenson KE, et al. Molecular map of chronic lymphocytic leukemia and its impact on outcome. Nat Genet. 2022;54(11):1664-74.
19. Mansouri L, Sutton LA, Ljungstrom V, Bondza S, Arngarden L, Bhoi S, et al. Functional loss of IkappaBepsilon leads to NF-kappaB deregulation in aggressive chronic lymphocytic leukemia. J Exp Med. 2015;212(6):833-43.
20. Messina M, Del Giudice I, Khiabanian H, Rossi D, Chiaretti S, Rasi S, et al. Genetic lesions associated with chronic lymphocytic leukemia chemo-refractoriness. Blood. 2014;123(15):2378-88.
21. Rossi D, Fangazio M, Rasi S, Vaisitti T, Monti S, Cresta S, et al. Disruption of BIRC3 associates with fludarabine chemorefractoriness in TP53 wild-type chronic lymphocytic leukemia. Blood. 2012;119(12):2854-62.
22. Mansouri L, Thorvaldsdottir B, Sutton LA, Karakatsoulis G, Meggendorfer M, Parker H, et al. Different prognostic impact of recurrent gene mutations in chronic lymphocytic leukemia depending on IGHV gene somatic hypermutation status: a study by ERIC in HARMONY. Leukemia. 2022.
23. Hallek M, Cheson BD, Catovsky D, Caligaris-Cappio F, Dighiero G, Dohner H, et al. iwCLL guidelines for diagnosis, indications for treatment, response assessment, and supportive management of CLL. Blood. 2018;131(25):2745-60.
24. Pérez-Carretero C, Hernández-Sánchez M, González T, Quijada-Álamo M, Martín-Izquierdo M, Santos-Mínguez S, et al. TRAF3 alterations are frequent in del-3'IGH chronic lymphocytic leukemia patients and define a specific subgroup with adverse clinical features. Am J Hematol. 2022;97(7):903-14.
25. González MB, Hernández JM, García JL, Lumbreras E, Castellanos M, Fernández-Calvo J, et al. The value of fluorescence in situ hybridization for the detection of 11q in multiple myeloma. Haematologica. 2004;89(10):1213-8.
26. Quijada-Álamo M, Hernández-Sánchez M, Alonso-Pérez V, Rodríguez-Vicente AE, García-Tuñón I, Martín-Izquierdo M, et al. CRISPR/Cas9-generated models uncover therapeutic vulnerabilities of del(11q) CLL cells to dual BCR and PARP inhibition. Leukemia. 2020.
27. Quijada-Álamo M, Pérez-Carretero C, Hernández-Sánchez M, Rodríguez-Vicente AE, Herrero AB, Hernández-Sánchez JM, et al. Dissecting the role of TP53 alterations in del(11q) chronic lymphocytic leukemia. Clin Transl Med. 2021;11(2):e304.
28. Hernández-Sánchez M, Rodríguez-Vicente AE, González-Gascón Y Marín I, Quijada-Álamo M, Hernández-Sánchez JM, Martín-Izquierdo M, et al. DNA damage response-related alterations define the genetic background of patients with chronic lymphocytic leukemia and chromosomal gains. Exp Hematol. 2019.
29. Ljungström V, Cortese D, Young E, Pandzic T, Mansouri L, Plevova K, et al. Whole-exome sequencing in relapsing chronic lymphocytic leukemia: clinical impact of recurrent RPS15 mutations. Blood. 2016;127(8):1007-16.
30. Yu L, Kim HT, Kasar S, Benien P, Du W, Hoang K, et al. Survival of Del17p CLL Depends on Genomic Complexity and Somatic Mutation. Clin Cancer Res. 2017;23(3):735-45.
31. Machnicki MM, Górniak P, Pępek M, Szymczyk A, Iskierka-Jażdżewska E, Steckiewicz P, et al. Predictive significance of selected gene mutations in relapsed and refractory chronic lymphocytic leukemia patients treated with ibrutinib. European Journal of Haematology. 2021;106(3):320-6.

CHAPTER 2

Chronic lymphocytic leukemia patients with *IGH* translocations are characterized by a distinct genetic landscape with prognostic implications

Claudia Pérez-Carretero[1,2], María Hernández-Sánchez[1,2,3], Teresa González[1,2], Miguel Quijada-Álamo[1,2], Marta Martín-Izquierdo[1,2], Jesús-María Hernández-Sánchez[1,2], María-Jesús Vidal[4], Alfonso García de Coca[5], Carlos Aguilar[6], Manuel Vargas-Pabón[7], Sara Alonso[8], Magdalena Sierra[9], Araceli Rubio-Martínez[10], Julio Dávila[11], José R. Díaz-Valdés[12], José-Antonio Queizán[12], José-Ángel Hernández-Rivas[13], Rocío Benito[1,2], Ana E. Rodríguez-Vicente[1,2] and Jesús-María Hernández-Rivas[1,2]

1. Universidad de Salamanca, IBSAL, Centro de Investigación del Cáncer, IBMCC-CSIC, Salamanca, Spain.
2. Servicio de Hematología, Hospital Universitario de Salamanca, Salamanca, Spain.
3. Department of Medical Oncology, Dana Farber Cancer Institute, Boston, Massachusetts, USA.
4. Servicio de Hematología, Hospital Universitario, León, Spain.
5. Servicio de Hematología, Hospital Clínico, Valladolid, Spain.
6. Servicio de Hematología, Complejo Hospitalario de Soria, Soria, Spain.
7. Servicio de Hematología, Hospital Jarrio, Asturias, Spain.
8. Servicio de Hematología, Hospital Universitario Central de Asturias, Oviedo, Spain.
9. Servicio de Hematología, Hospital Virgen de la Concha, Zamora, Spain.
10. Servicio de Hematología, Hospital Miguel Servet, Zaragoza, Spain.
11. Servicio de Hematología, Hospital Nuestra Señora de Sonsoles, Ávila, Spain.
12. Servicio de Hematología, Hospital General de Segovia, Segovia, Spain.
13. Servicio de Hematología. Hospital Universitario Infanta Leonor. Universidad Complutense. Madrid, Spain.

International Journal of Cancer. 2020 Nov 15;147(10):2780-2792. doi: 10.1002/ijc.33235

Received: 16 January 2020 | Revised: 19 June 2020 | Accepted: 7 July 2020
DOI: 10.1002/ijc.33235

CANCER GENETICS AND EPIGENETICS

IJC
International Journal of Cancer

Chronic lymphocytic leukemia patients with *IGH* translocations are characterized by a distinct genetic landscape with prognostic implications

Claudia Pérez-Carretero[1,2] | María Hernández-Sánchez[1,2,3] | Teresa González[1,2] | Miguel Quijada-Álamo[1,2] | Marta Martín-Izquierdo[1,2] | Jesús-María Hernández-Sánchez[1,2] | María-Jesús Vidal[4] | Alfonso García de Coca[5] | Carlos Aguilar[6] | Manuel Vargas-Pabón[7] | Sara Alonso[8] | Magdalena Sierra[9] | Araceli Rubio-Martínez[10] | Julio Dávila[11] | José R. Díaz-Valdés[12] | José-Antonio Queizán[12] | José-Ángel Hernández-Rivas[13] | Rocío Benito[1,2] | Ana E. Rodríguez-Vicente[1,2] | Jesús-María Hernández-Rivas[1,2]

[1]Universidad de Salamanca, IBSAL, Centro de Investigación del Cáncer, IBMCC-CSIC, Salamanca, Spain
[2]Servicio de Hematología, Hospital Universitario de Salamanca, Salamanca, Spain
[3]Department of Medical Oncology, Dana Farber Cancer Institute, Boston, Massachusetts
[4]Servicio de Hematología, Hospital Universitario, León, Spain
[5]Servicio de Hematología, Hospital Clínico, Valladolid, Spain
[6]Servicio de Hematología, Complejo Hospitalario de Soria, Soria, Spain
[7]Servicio de Hematología, Hospital Jarrio, Asturias, Spain
[8]Servicio de Hematología, Hospital Universitario Central de Asturias, Oviedo, Spain
[9]Servicio de Hematología, Hospital Virgen de la Concha, Zamora, Spain
[10]Servicio de Hematología, Hospital Miguel Servet, Zaragoza, Spain
[11]Servicio de Hematología, Hospital Nuestra Señora de Sonsoles, Ávila, Spain
[12]Servicio de Hematología, Hospital General de Segovia, Segovia, Spain
[13]Servicio de Hematología, Hospital Universitario Infanta Leonor, Universidad Complutense, Madrid, Spain

Correspondence
Ana E. Rodríguez-Vicente, PhD, IBSAL, IBMCC-Centro de Investigación del Cáncer (USAL-CSIC), Campus Miguel de Unamuno, 37007 Salamanca, Spain.
Email: anaerv@hotmail.com

Funding information
Instituto de Salud Carlos III, Grant/Award Numbers: PI15/01471, PI18/01500; Instituto de Salud Carlos III/Fondo Social Europeo 'El Fondo Social Europeo invierte en tu futuro', Grant/Award Numbers: CD19/00222, FI19/00191; European Regional Development Fund; Spanish Fondo de Investigaciones Sanitarias;

Abstract

Chromosome 14q32 rearrangements/translocations involving the immunoglobulin heavy chain (*IGH*) are rarely detected in chronic lymphocytic leukemia (CLL). The prognostic significance of the *IGH* translocation is controversial and its mutational profile remains unknown. Here, we present for the first time a comprehensive next-generation sequencing (NGS) analysis of 46 CLL patients with *IGH* rearrangement (IGH*R*-CLLs) and we demonstrate that IGH*R*-CLLs have a distinct mutational profile with recurrent mutations in *NOTCH1*, *IGLL5*, *POT1*, *BCL2*, *FBXW7*, *ZMYM3*, *MGA*, *BRAF* and *HIST1H1E* genes. Interestingly, *BCL2* and *FBXW7* mutations were significantly associated with this subgroup and almost half of *BCL2*, *IGLL5* and *HISTH1E*

Abbreviations: CLL, chronic lymphocytic leukemia; COSMIC, Catalogue of Somatic Mutations in Cancer; DLBCL, diffuse large B-cell lymphoma; FISH, fluorescence in situ hybridization; FL, follicular lymphoma; ICGC, International Cancer Genome Consortium; IGH, immunoglobulin heavy chain; IGHR-CLLs, CLL patients with IGH rearrangements; IGHV, immunoglobulin heavy-chain variable; NGS, next-generation sequencing; NHL, non-Hodgkin lymphoma; OS, overall survival; TFT, time to first treatment; VAF, variant allele frequency.

Ana E. Rodríguez-Vicente and Jesús-María Hernández-Rivas contributed equally to this study.

Ayuda Predoctoral de la Junta de Castilla y León, Grant/Award Number: JCYL-EDU/529/2017; Centro de Investigación Biomédica en Red de Cáncer, Grant/Award Number: CB16/12/00233; Red Temática de Investigación Cooperativa en Cáncer, Grant/Award Number: RD12/0036/0069; Fundación Memoria Don Samuel Solórzano Barruso; Fundación Científica Asociación Española Contra el Cáncer; Fundación Española de Hematología y Hemoterapia/Janssen; Proyectos de Investigación del SACYL, Grant/Award Numbers: GRS1653/A17, 1847/A/18; Consejería de Educación, Junta de Castilla y León, Grant/Award Number: SA271P18

mutations reported were previously identified in non-Hodgkin lymphomas. Notably, *IGH/BCL2* rearrangements were associated with a lower mutation frequency and carried *BCL2* and *IGLL5* mutations, while the other IGH*R*-CLLs had mutations in genes related to poor prognosis (*NOTCH1*, *SF3B1* and *TP53*) and shorter time to first treatment (TFT). Moreover, IGH*R*-CLLs patients showed a shorter TFT than CLL patients carrying 13q−, normal fluorescence in situ hybridization (FISH) and +12 CLL, being this prognosis particularly poor when *NOTCH1*, *SF3B1*, *TP53*, *BIRC3* and *BRAF* were also mutated. The presence of these mutations not only was an independent risk factor within IGH*R*-CLLs, but also refined the prognosis of low-risk cytogenetic patients (13q−/normal FISH). Hence, our study demonstrates that IGH*R*-CLLs have a distinct mutational profile from the majority of CLLs and highlights the relevance of incorporating NGS and the status of *IGH* by FISH analysis to refine the risk-stratification CLL model.

KEYWORDS

chromosomal translocations, chronic lymphocytic leukemia, clinical molecular genetics, cytogenetics, high-throughput sequencing, prognostic biomarkers

1 | INTRODUCTION

Chronic lymphocytic leukemia (CLL) is a disease that displays extreme clinical heterogeneity, clearly reflecting the marked biological diversity, which has led to the identification of a plethora of prognostic markers.[1-4] Chromosomal abnormalities are the hallmark of the disease and their correlation to the clinical course has contributed to patients risk stratification since the 2000s.[5] In the last years, CLL molecular and cellular biology has been enriched by seminal insights that have led to a better understanding of CLL pathogenesis[2] and, consequently, to the identification of molecular markers whose evaluation is well-established in clinical routine, such as the immunoglobulin heavy-chain variable (*IGHV*) mutational status or *TP53* gene abnormalities. The integration of these markers together with the new relevant genetic alterations reported in next-generation sequencing (NGS) studies, specifically those of *NOTCH1*, *SF3B1* and *BIRC3* genes, could be used to refine Döhner hierarchical cytogenetic model.[2,6-12]

Although more than 80% of CLL patients carry cytogenetic alterations, chromosome 14q32 rearrangements/translocations involving the immunoglobulin heavy chain (*IGH*) gene was considered a rare aberration affecting fewer than 4% of CLL patients.[5,13] Nevertheless, with the emergence of new molecular approaches and large-scale genomic studies in CLL, a higher incidence of *IGH* rearrangements has been reported in the recent years (5%-15%).[14-16] This cytogenetic abnormality contributes to CLL pathogenesis by deregulating the *IGH*-partner genes[17,18] and their prognostic significance remains controversial. Previous studies have shown that patients carrying 14q32 rearrangements (IGH*R*-CLLs) have an intermediate-adverse outcome,[19-21] particularly when compared to favorable and intermediate-risk cytogenetics.[22,23] However, some studies have reported that patients carrying 14q32 rearrangements with *BCL2* have a better clinical course.[24,25]

What's New?

The prognostic significance of the immunoglobulin heavy chain (IGH) translocation in chronic lymphocytic leukemia (CLL) is controversial and its mutational profile remains unknown. Here, the authors assessed for the first time the genetic landscape of CLL patients with IGH rearrangements by targeted next-generation sequencing, characterising recurrently-mutated genes with prognostic implications and demonstrating that these entities exhibit an intermediate mutational profile between CLL and non-Hodgkin lymphoma. Moreover, the findings showed that the incorporation of next-generation sequencing and the IGH-probe in the CLL-fluorescence in situ hybridisation panel used in clinical routine could be useful, especially for elucidating prognosis in normal FISH cases.

CLL patients with *IGH* rearrangements remain poorly characterized at the molecular level, partly due to the low incidence of cases, the IGH*R* cooccurrence with other cytogenetic alterations, and the difficulty of distinguishing between IGH*R*-CLLs and forms of non-Hodgkin lymphoma (NHL).[26] Furthermore, the *IGH* probe is not included in the classic four-probe CLL FISH panel for the 13q14, 12p11.1-q11, 11q22 and 17p13 regions used in routine clinical practice,[26] which is partially responsible for this subgroup passing unnoticed. In our study, we characterize the genetic landscape of CLL patients with 14q32/*IGH* translocations for the first time, demonstrating that IGH*R*-CLLs have a distinct mutational profile from other

classic cytogenetic groups of CLLs, dependent on whether *BCL2* is involved or not in the *IGH* rearrangement, and as well as the presence of certain mutations. Taken together, our results improve our understanding of the molecular underpinnings of this cytogenetic CLL subgroup, allowing us to refine the prognosis of IGH*R*-CLL patients.

2 | METHODS

2.1 | Patients

The study was based on 862 CLL patients, diagnosed according to the International Workshop on CLL criteria.[27,28] All of them were screened for *IGH* translocation and positive cases for IGH rearrangement were individually reviewed to rule out the possibility that they represented a different lymphoproliferative disorder (see Supplementary Methods). Samples and clinical data were collected from 16 Spanish institutions.

Mutational analysis was performed in 233 untreated CLL patients: 46 with 14q32/*IGH* rearrangements and 187 as the control group. Patients in the control group were selected according to sample and clinical data availability and absence of treatment and were representative of the disease in terms of demographic and clinical characteristics (Supplementary Table S1). Patients risk classification criteria is described in Supplementary Methods and a diagram of the patients included in the different outcome analyses is shown in Supplementary Figure S1.

In the IGH*R*-CLL group, the median time between diagnosis and *IGH* rearrangement detection was 1 month (range: 0-117 months), and the median follow-up was 57 months (range: 1-157 months). Within IGH*R*-CLLs, 31/46 (67.4%) received treatment after FISH test, with a median time to first treatment (TFT) of 19 months (range: 7-30). Most of them (93.5%) received conventional chemoimmunotherapy and two patients were treated with ibrutinib.

The study was approved by the local ethical committee (*Comité Ético de Investigación Clínica*, *Hospital Universitario de Salamanca*). Written informed consent was obtained from all participants before they entered the study.

2.2 | Fluorescence in situ hybridization (FISH)

Interphase FISH was performed on peripheral blood or bone marrow samples using the following commercially probes: ATM, CEP12, D13S319 and TP53 (Vysis, Abbott Laboratories, IL). Dual color break-apart FISH probes were performed for *IGH*/*BCL2* and *IGH*/*BCL6* translocations. The methods used for FISH analysis have been described elsewhere.[29] Signal screening was carried out in at least 200 cells with well-delineated fluorescent spots. In all cases, a score of ≥10% was considered positive, based on the cutoff value used by our laboratory.

2.3 | Next-generation sequencing

NGS studies were performed in 233 cases and in the same sample as the FISH test. Genomic DNA was isolated from peripheral blood or bone marrow by magnetically activated cell sorting CD19+ B-lymphocytes. B-cell purity was greater than 98% by flow cytometry, as previously described in our group.[30] The Agilent SureSelect^{QXT} Target Enrichment system for Illumina Multiplexed Sequencing (Agilent Technologies, Santa Clara, CA) was used to produce libraries of exonic regions from 54 genes CLL-related as well as from *BCL2*, *IGLL5* and *NOTCH1* UTR regions (Supplementary Methods). Genes included in the custom-designed panel[31,32] are involved in CLL pathogenesis and the UTR regions were considered due to the previous identification of *IGLL5*, *BCL2* and *NOTCH1* UTRs somatic mutations in CLL[8,33,34] (Supplementary Table S2). Paired-end sequencing (151-bp reads) was run on the Illumina NextSeq instrument (Illumina, San Diego, CA).

2.4 | Data analysis

Raw data quality control was performed with FastQC (v0.11.8) and Picard tools (v2.2.4) to collect sequencing metrics. Demultiplexed files (FASTQ) were aligned to the reference genome (GRCh37/hg19 genome), read duplicates were marked with SAMTools (v1.3.1) and postalignment was performed with Genome Analysis Toolkit (v3.5). Coverage for each region was assessed using BEDTools (v.2.26.0). A minimum quality score of Q30 was required for ensuring high-quality sequencing results. Finally, somatic variant calling, and annotation were performed using an in-house pipeline, based on VarScan (v2.4) and ANNOVAR (v.2017Jul16), respectively.

Median coverage of target regions was 600 reads/base, with at least 100X in 97% of them. To validate variants detected with variant allele frequency (VAF) <5% using the custom panel, samples were conducted to resequencing using different amplicon-based approaches (Illumina Nextera XT/454 Roche[30]) with read depth above 1000X, allowing to report variants down to 2% (Supplementary Methods).

Data were then filtered according to the severity of the consequence, considering variants that lead to an amino acid change in the protein sequence (missense, nonsense, frameshift) and those in the splice site and UTRs. To discard single nucleotide polymorphisms (SNPs), minor allelic frequencies (MAFs) were consulted in several databases (dbSNP, 1000 genomes, Exome Aggregation Consortium and our in-house database) and only variants with a MAF of <0.01 were selected for further analysis. In addition, variants with a VAF between 40% and 60% or greater than 90% were manually reviewed prioritizing variants described in in silico tools (Polymorphism Phenotyping v2 [PolyPhen-2], Sorting Intolerant From Tolerant [SIFT] and ClinVar) as deleterious, damaging, pathogenic or likely pathogenic.

Aligned reads were manually reviewed with the Integrative Genomics Viewer to confirm and interpret variant calls and reduce the risk of false positives. Variants described in the Catalogue of Somatic Mutations in Cancer database (COSMIC82 database) or mutations in driver genes previously described in seminal papers were rescued for the analysis (CLL and NHL).[7,8,33,35-37] Manually screening in VarSome and International Cancer Genome Consortium (ICGC) Databases was performed for assessing the functional impact of mutations.

2.5 | Statistical analysis

Statistical analyses were performed using IBM SPSS v23.0 for Windows (IBM Corp., Armonk, NY) and SDM-PSI v6.21 software for the false discovery rate (FDR) correction in multiple comparisons. Continuous variables were analyzed with the Mann-Whitney *U* test, while the chi-square and Fisher's exact tests were used to assess associations between categorical variables. Overall survival (OS) and TFT were calculated from the date FISH test was performed to the date of death, first treatment or last follow-up (considering disease-unrelated deaths as competing events). Statistically significant variables related to OS and TFT were estimated by the Kaplan-Meier method, using the log-rank test to compare the curves of each group. Univariate and multivariate analyses of the OS and TFT employed the Cox regression method. Results were considered statistically significant for values of $P < .05$. FDR was used to correct *P*-values for multiple hypotheses testing when appropriate, by applying the Benjamini and Hochberg method.[38] Adjusted *P*-values (*Q*-values) were considered significant when $Q < .1$.

3 | RESULTS

3.1 | CLL patients with *IGH* translocations have a distinct mutational profile with high mutation frequencies in *NOTCH1*, *BCL2*, *FBXW7*, *ZMYM3* and *MGA*

NGS analysis of the 233 CLL patients revealed that 75% of cases had at least one mutation in any of the 54 genes included in the targeted-NGS approach, and the median frequency of mutations per patient was 2 (range: 0-7). The most frequently mutated genes were *NOTCH1* (19.3%), *IGLL5* (15%), *SF3B1* (10.7%), *TP53* (10%), *ATM* (9%), *POT1* (8.5%), *RPS15* (6.9%), *CHD2* (6%), *NFKBIE* (5.1%), *BIRC3* (5.1%) and *XPO1* (4.3%).

Regarding the 46 IGH*R*-CLLs, we identified a total of 109 mutations located in 35 genes. The median frequency of mutations per patient was 2 (range: 0-6), and 82% of patients (38/46) harbored at least one mutation. Moreover, 61% of patients (28/46) presented more than one mutated gene. The most frequently mutated genes in this cohort were *NOTCH1* (30.4%), *IGLL5* (17.4%), *SF3B1* (13%), *POT1* (13%), *TP53*, *BCL2*, *FBXW7*, *ZMYM3* and *MGA* (8.7% each) followed by *BRAF*, *EGR2* and *RPS15* (6.5% each) (Figure 1A; Supplementary Table S3). Other genes such as *ATM* (4.3%) or *CHD2* and *MYD88* (2.2% each) were mutated at low frequencies.

The comparison between the mutational profiles of IGH*R*s-CLLs and the control group showed higher mutation frequencies in *NOTCH1*, *BCL2*, *FBXW7*, *ZMYM3* and *MGA* within IGH*R*-CLLs, especially those of *BCL2* and *FBXW7* ($Q = .048$, $Q = .06$, respectively) (Figure 1A; Supplementary Table S3).

Furthermore, 61% of IGH*R*-CLLs (28/46) carried additional FISH alterations (Figure 1B). Their mutational profile was analyzed with respect to the presence of IGH*R* together with 13q, 11q, 17p deletion or trisomy 12, and only *TP53* mutations were significantly associated with 17p or 11q deletion in IGH*R*-CLLs ($Q = .048$). We observed that the mutational profile of patients with IGH*R* as a sole aberration (18/46) was similar to that of the entire IGH*R*-CLL cohort: *NOTCH1* (33.3%), *IGLL5* (27.8%), *SF3B1* (16.7%), *BCL2*, *ZMYM3*, *MGA* and *FUBP1* (11.1% each) followed by *FBXW7* and *BRAF* (5.6% each). All mutation frequencies are shown in Supplementary Table S4.

Interestingly, we reported a higher incidence of *IGLL5*, *BCL2* and *HIST1H1E* mutations in this subgroup compared to the described in previous large-scale CLL studies[7,8] (Figure 1B). IGH*R*-CLL patients showed *IGLL5* mutations targeting the signal peptide domain (4/10) and the 5′UTR region (3/10), *BCL2* mutations affecting the 5′UTR region (2/6) and the exon 2 (4/6), and *HIST1H1E* mutations located in the exon 1 (Figure 2). According to the ICGC Database, most of the coding mutations in *IGLL5* (6/7), *BCL2* (3/4) and *HIST1H1E* (1/2) identified in our study had functional impact in the gene function (Table 1). In addition, 6 out of 17 mutations detected in the aforementioned three genes were previously described in NHL (as reported in the COSMIC and ICGC database and whole-exome and whole-genome data from NHL patients[35-37,39,40]).

Moreover, five of the mutations reported in *IGLL5* and *BCL2* were located in the 5′UTR of the gene. Specifically, the novel *BCL2* recurrent mutation identified in the 5′UTR region (genomic position chr18:60985900) was exclusively found in IGH*R*-CLLs when compared to the control group ($P = .048$) (Supplementary Figure S2).

Detailed lists of the mutations detected in the IGH*R*-CLLs and the control group are shown in Supplementary Tables S5-S7.

3.2 | CLL patients with *IGH/BCL2* exhibit a lower mutation frequency and a different mutational profile than patients with other *IGH* translocations

We next sought to assess whether the mutational landscape changes depend on the *IGH* translocation partner, for example, *BCL2* and *BCL6*. In our study, 13/46 patients (28%) carried *IGH/BCL2* translocation (Figure 1B) and 2/46 (4.3%) harbored an *IGH/BCL6* rearrangement (ID 8 and 20). Due to the small number of *BCL6* rearrangements, we performed further analysis comparing *IGH/BCL2* vs the rest of IGH*R* cases.

In the IGH*R* patients, fewer CLLs with *IGH/BCL2* translocation had mutations in at least one gene compared to the subgroup with other *IGH* translocations (7/13, 54% vs 31/33, 94%; $P = .001$). The median mutation frequency per patient was significantly lower in the group with *IGH/BCL2* compared to that without it (1 vs 2, $P = .030$).

The most frequently mutated genes in the *IGH/BCL2* group were *BCL2* (23%), *IGLL5* (23%), *HIST1H1E* (15%) and *NOTCH1* (15%), whereas for all other IGH*R*-CLLs, the most frequently mutated genes were *NOTCH1* (36%), *SF3B1* (18%), *POT1* (18%), *TP53* (12%), and *FBXW7* (12%) (Supplementary Figure S3A). It is worth mentioning that neither *TP53* nor *SF3B1* mutations, widely associated with poor prognosis, were detected in CLL patients with an *IGH/BCL2* translocation, reflecting a different mutational profile

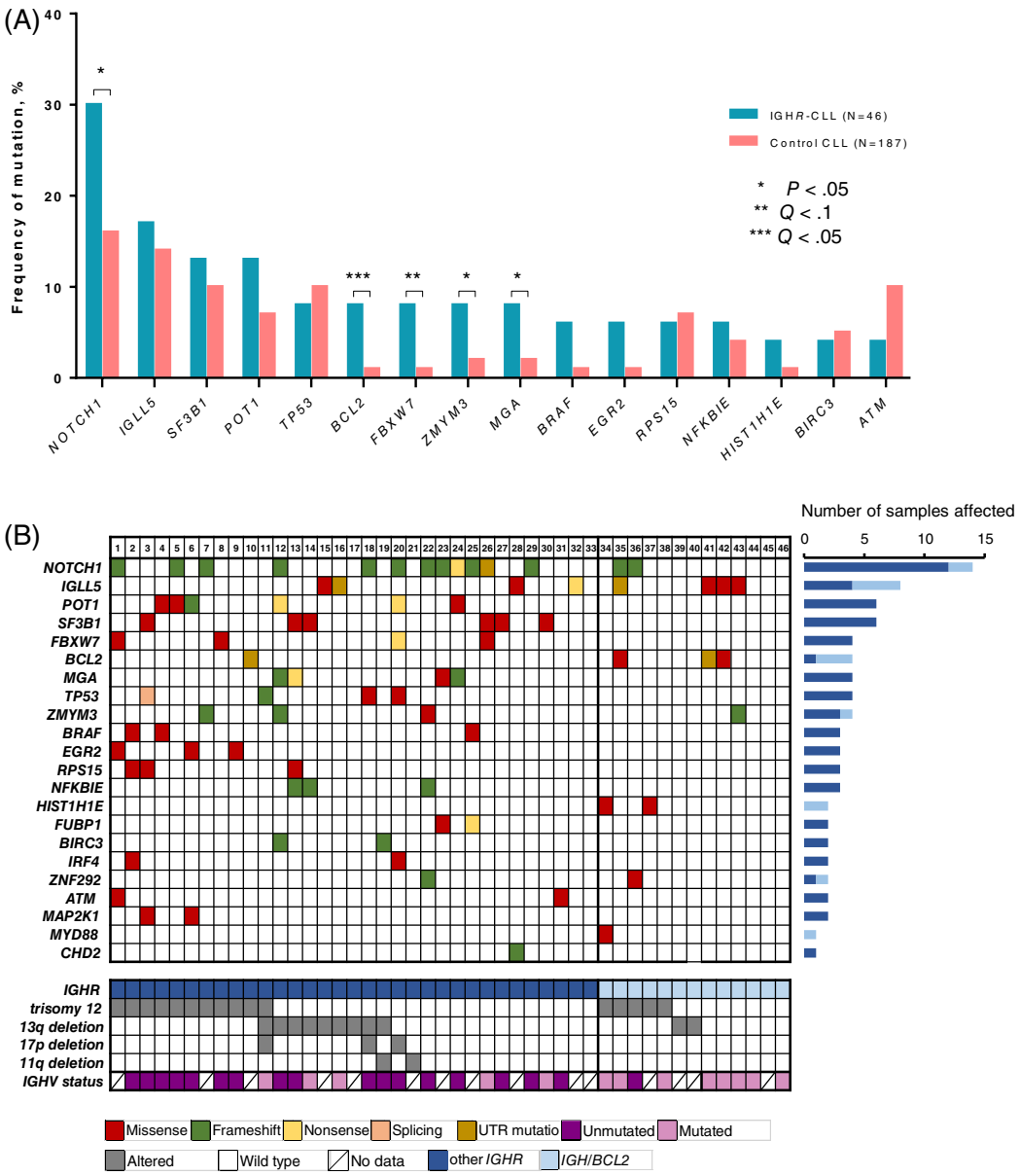

FIGURE 1 Mutational profile of CLL patients with *IGH* rearrangements. A, Mutational frequencies and associations in the CLL cohort according to the presence of *IGH* rearrangements. Significant p/q-values are annotated with asterisks (N = 233). B, Each column represents a patient; each row corresponds to a genomic alteration. Patients are clustered according to the IGHR (*IGH/BCL2* translocation is indicated in light blue; other *IGH* translocations are shown in dark blue). Missense, frameshift, nonsense, splicing and UTR mutations are reported in red, green, yellow, pink and brown, respectively. The presence of a cytogenetic alteration is shown in gray and the *IGHV* unmutated status is represented in purple (N = 46) [Color figure can be viewed at wileyonlinelibrary.com]

from all other IGH*R*-CLLs. The mutational analysis of nine *IGH/BCL2* cases previously reported in a WES/WGS study of CLL[8] also showed the presence of mutations in *BCL2*, and *NOTCH1*, and the absence of poor-prognosis genes such as *TP53* or *SF3B1* (Supplementary Figure S3B). However, no statistically significant associations were detected in our analysis, probably due to the small number of cases (Supplementary Table S8).

In *IGH/BCL2* cases that also harbored *BCL2* mutations, we observed that 60% to 87% of the cells carried the rearrangement, while *BCL2* mutations VAFs range from 11% to 40%, suggesting that somatic mutations occurred later in time than the rearrangement (Table 1).

3.3 | Patients carrying *IGH* translocations exhibit an intermediate-adverse outcome

We also analyzed the clinical and biological characteristics of IGH*R*-CLLs within the entire cohort (N = 862) (Table 2). Patients carrying this cytogenetic alteration showed a higher incidence of poor

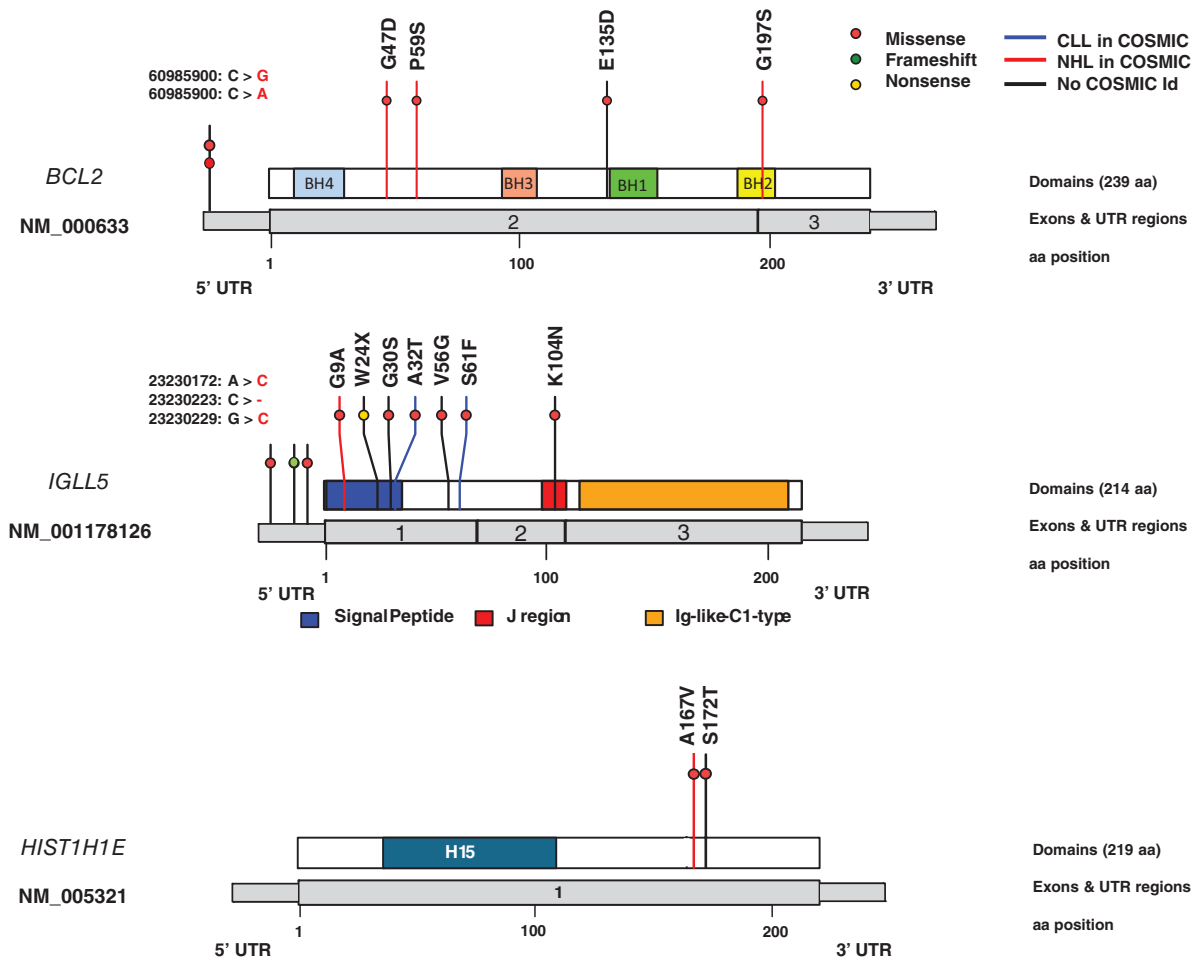

FIGURE 2 Schematic representation of *BCL2*, *IGLL5* and *HIST1H1E* mutations. Positions of coding mutations are indicated according to the aminoacid change at the protein level; positions of UTR mutations are indicated according to the nucleotide change in the DNA sequence (GRCh37/hg19 genome); with respect to the UTR regions, only *BCL2* and *IGLL5* 5′UTR regions were covered in the sequencing analysis (see Supplementary Table S2). Number of cases are denoted by circles in each mutation line and the color of the circles indicates the mutation subtype (missense, frameshift and nonsense). Mutations identified in the COSMIC database in non-Hodgkin lymphomas (NHL) are represented with red lines; mutations reported in the COSMIC database in CLL are indicated with blue lines; all other mutations are shown in black. Aa, aminoacid [Color figure can be viewed at wileyonlinelibrary.com]

prognosis markers such as Binet stage B or C (Q = .039), high β2-microglobulin (Q = .0007) and lactate dehydrogenase levels (Q = .054), unmutated *IGHV*) (Q = .054) and need for treatment (Q = .007). In addition, two IGH*R*-CLLs developed Richter syndrome during follow-up (patient IDs: 18 and 35). Regarding the presence of additional cytogenetic alterations, 34.8% of IGH*R*-CLL patients (16/46) carried trisomy 12, showing significant co-occurrence of the two events (trisomy 12 and IGH*R*) (Q = .0007). By contrast, the presence of the 13q deletion in IGH*R*-CLLs was significantly less frequent than in CLLs without *IGH* rearrangements (Q = .0014) (Table 2).

Within IGH*R*-CLLs, 31/46 (67.4%) received treatment after FISH test, with a median TFT of 19 months (95% confidence interval [CI]: 7-30 months). Patients with an *IGH* translocation showed shorter TFT than the 13q− and normal FISH subgroups (median: 19 vs 120 and 184 months; P < .0001, P < .0001), and longer TFT than the 11q− and 17p− subgroups (19 vs 5, 6 months; P = .042, P = .31). The median TFT of the +12 subgroup was slightly higher than that of IGH*R*-CLLs (28 vs 19 months; P = .37). In terms of OS, we observed similar trends (Supplementary Figure S4A). Differences in outcome among the cytogenetic subgroups were consistent with the prevalence of unfavorable clinical and biological features in IGH*R*-CLLs, suggesting that this subgroup exhibits an intermediate-adverse prognosis. In addition, the clinical comparison between IGHR-CLLs and control CLLs selected for the mutational analysis (N = 233) showed quite similar results to the presented in this section, also demonstrating that control group was representative of the entire cohort (Supplementary Table S1; Supplementary Figure S4B).

In our entire cohort (N = 862), 31% of patients showed no alterations using 13q14/D13S319, 12p11.1-q11/CEP12, 11q22/ATM, 17p13/P53 probes. However, it is worth mentioning that 6.7% of patients who would be classified as normal FISH in our cohort using the four-probe CLL FISH panel customarily used in routine clinical

TABLE 1 *IGLL5*, *BCL2* and *HISTH1E* mutations identified in IGHR-CLLs (N = 46)

ID Patient	*IGH/BCL2* translocation (% of cells)	Gene	DNA[a]/cDNA change: AA change	VAF, %	Function	ID COSMIC[b]	Previously described	SIFT/polyPhen-2 pathogenicity prediction	Reported as somatic in VarSome	Functional impact[b] ICGC
10	No	BCL2	C60985900G	12.74	5′UTR	—	—	—	Yes	—
41	Yes (85)	BCL2	C60985900A	33.87	5′UTR	—	—	—	Yes	—
41	Yes (85)	BCL2	c.G405T:p.E135D	30.15	Exonic	—	—	T/P	Yes	Unknown
42	Yes (60)	BCL2	c.G140A:p.G47D	11.39	Exonic	COSM220809	DLBCL[35]	T/P	Yes	Yes
35	Yes (87)	BCL2	c.G589A:p.G197S	40.1[c]	Exonic	COSM5947452	DLBCL/FL[36]	-/B	Yes	Yes
35	Yes (87)	BCL2	c.C175T:p.P59S	37.82[c]	Exonic	COSM4170930	DLBCL/FL[36]	T/B	Yes	Yes
28	No	IGLL5	c.G26C:p.G9A	51.09	Exonic	COSM5713869	DLBCL	T/B	Yes	—
15	No	IGLL5	c.G312T:p.K104N	9.42	Exonic	—	—	D/P	Yes	Yes
32	No	IGLL5	c.G72A:p.W24X	42.86	Exonic	—	—	—	—	Yes
16	No	IGLL5	C23230223-	26.12	5′UTR	—	CLL[33]	—	—	—
16	No	IGLL5	G23230229C	26.51	5′UTR	—	—	—	Yes	—
41	Yes (85)	IGLL5	c.G88A:p.G30S	33.93	Exonic	—	—	D/P	Yes	Yes
35	Yes (87)	IGLL5	c.T167G:p.V56G	19.88	Exonic	—	CLL[8]	T/B	Yes	Yes
35	Yes (87)	IGLL5	c.C182T:p.S61F	19.88	Exonic	COSM3357314	CLL[8]/DLBCL	T/B	Yes	Yes
35	Yes (87)	IGLL5	A23230172C	17.58	5′UTR	—	CLL[8]	—	—	—
43	Yes (41)	IGLL5	c.G94A:p.A32T	43.48	Exonic	COSM5949859	CLL	D/B	Yes	Yes
34	Yes (77)	HIST1H1E	c.G515C:p.S172T	42.33	Exonic	—	—	D/D	—	—
37	Yes (98)	HIST1H1E	c.C500T:p.A167V	41.74	Exonic	COSM1292261	FL[39]/CLL[7]	T/B	Yes	Yes

Notes: Unknown: reported in ICGC database with unknown functional impact in the gene. "—" indicates the variant has not been previously reported in the databases or seminal papers.

Abbreviations: AA, aminoacid; B, benign; CLL, chronic lymphocytic leukemia; D, damaging; DLBCL, diffuse large B-cell lymphoma; FL, follicular lymphoma; P, pathogenic; T, tolerable; VAF, variant allele frequency.

[a]Positions of UTR mutations are indicated according to the nucleotide change in the DNA sequence (GRCh37/hg19 genome) (reference transcripts: see Supporting Table S5).

[b]Haematopoietic and lymphoid tissue.

[c]Confirmed as somatic in the matched CD19-cell fraction.

practice, actually carried an *IGH* rearrangement. The presence of this cytogenetic alteration had a negative effect on the TFT within this group of patients: CLL patients with IGH*R* as the sole FISH abnormality had a significantly shorter TFT than those without any FISH aberration (23 vs 120 month, *P* = .01) (Figure 3A).

The presence of the *IGH/BCL2* translocation was associated with mutated *IGHV* (*P* = .001), and patients with this alteration showed a longer TFT than those with another IGH*R* (56 vs 4 months, *P* = .05). By contrast, the presence of *IGH/BCL2* rearrangement was not associated to any additional cytogenetic alteration (13q−, *Q* = .822; +12, *Q* = .822; 11q−/17p−, *Q* = .822) and there was no significant difference in terms of OS between patients with *IGH/BCL2* and patients with other *IGH* rearrangements (*P* = .433) (Supplementary Figure S5).

3.4 | Genetic mutations refine the prognosis of IGH*R* and low-risk cytogenetic CLL patients

IGH*R*-CLL untreated patients with at least one mutated gene showed a shorter TFT than IGH*R*-CLLs without gene mutations (10 months vs median TFT not reached, *P* = .026) (Figure 3B). These differences were more significant among recurrent gene mutations previously associated with worse prognosis (*NOTCH1*, *SF3B1*, *TP53*, *BIRC3* and *BRAF*) (2 vs 88 months, *P* < .0001) (Figure 3C). Specifically, TFT was shorter in IGH*R* patients with *TP53* mutations (0 vs 23 months, *P* < .0001) as well as with *BRAF* mutations (2 vs 23 months, *P* = .042) (Supplementary Figure S6). In contrast, the presence of *IGLL5* or *BCL2* mutations showed a better impact in terms of TFT, as IGH*R*-CLL patients with mutated *IGLL5* or *BCL2* showed a longer TFT than those without mutations in any of these genes (median TFT not reached vs 9 months, *P* = .001) (Figure 3D).

In the univariate analysis, other variables associated with a shorter TFT were Binet's stage B/C (*P* = .001), splenomegaly (*P* = .025), unmutated *IGHV* status (*P* = .013), *TP53* disruption/mutation (*P* = .003) and the absence of *IGLL5/BCL2* mutations (*P* = .008). Only the presence of mutations in *NOTCH1*, *SF3B1*, *TP53*, *BIRC3* and *BRAF* was significantly related to a shorter TFT within IGH*R*-CLL patients in the multivariate analysis (HR = 0.255, 95% CI = 0.07-0.9, *P* = .030) (Table 3).

Since the presence of mutations in these five genes has a prognostic impact within IGH*R*-CLL patients as well as in the control group (median TFT not reached vs 12 months, *P* < .0001) (Supplementary Figure S7), we propose an integrated mutational and cytogenetic model to account for our observations in the studied cohort (187 control and 46 IGHR-CLLs). Low-risk patients in our control series (13q−/normal FISH, N = 134) segregated into two groups according to the

TABLE 2 Clinical and biological characteristics of CLL patients depending on the presence of *IGH* rearrangements (N = 862)

Characteristic	*IGH*-translocation (N = 46)	no *IGH*-translocation (N = 816)	*P*	*Q*
Median age at diagnosis, years (range)	69 (43-89)	66 (25-97)	.112[b]	.542
Gender male, %	63	63.8	.698[c]	.814
Median time from diagnosis to FISH, months (range)	1 (0-117)	1 (0-253)	.568[b]	.808
Binet B or C, %	38.6	22.2	**.014**[c]	**.039**
Median WBC[a] count, $\cdot 10^9$/L (range)	17.6 (2.3-196)	17.8 (2.4-964)	.721[b]	.841
Median lymphocytes count, $\cdot 10^9$/L (range)	11.6 (0.6-186)	12.2 (0.8-960)	.874[b]	.874
Median platelet count, $\cdot 10^9$/L (range)	172 (55-295)	187 (2-587)	.456[b]	.808
Median hemoglobin level, g/dL (range)	14.1 (6.6-16.5)	14.2 (4.4-18.9)	.577[b]	.808
High β2-microglobulin level, %	67.4	36.3	**<.0001**[c]	**.0007**
High lactate dehydrogenase level, %	27.3	15.7	**.027**[c]	**.054**
Hepatomegaly, %	7.1	6.9	.824[c]	.852
Splenomegaly, %	15.9	16.8	.852[c]	.852
B symptoms, %	11.1	7.9	.595[c]	.757
Richter transformation	4.3	1.7	.148[c]	.259
IGHV-unmutated, %	60.6	44.9	**.025**[c]	**.054**
13q deletion, %	26.1	43.1	**.0003**[c]	**.0014**
trisomy 12, %	34.8	14.5	**<.0001**[c]	**.0007**
11q deletion, %	4.3	10.9	.426[c]	.596
17p deletion, %	6.5	4.3	.334[c]	.520
Need for treatment, %	67.4	44.0	**.002**[c]	**.007**
Median follow-up, months (range)	57 (1-157)	133 (106-159)	.155[b]	.543

Note: Significant values are shown in bold.
[a]White blood cells.
[b]Mann-Whitney *U* test.
[c]χ^2 test.

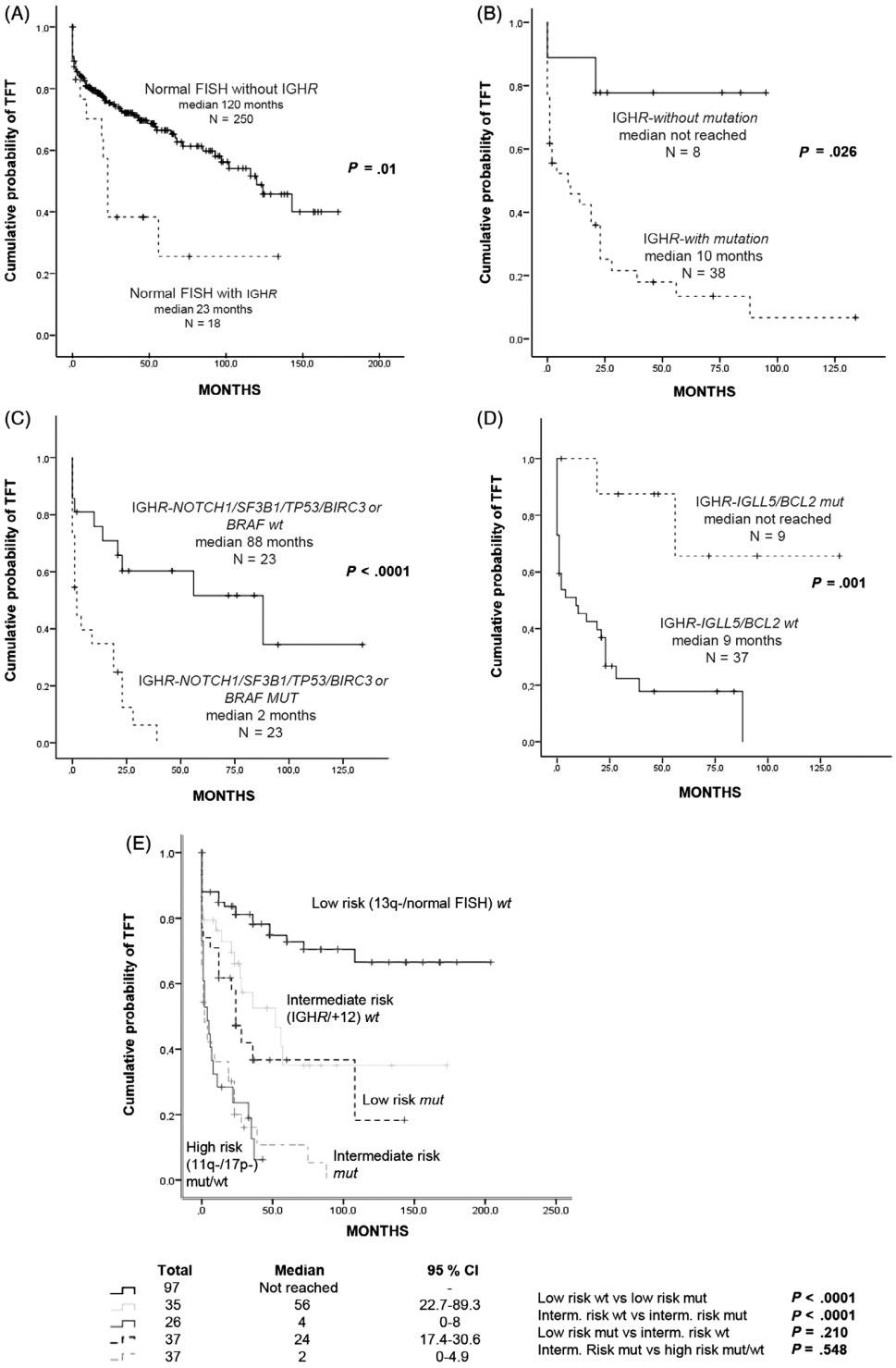

FIGURE 3 Clinical impact of IGH*R* and genetic mutations in CLL patients. A, Kaplan-Meier analysis of TFT according to the presence of *IGH* translocation in CLLs with normal FISH (N = 268). Kaplan-Meier analysis of TFT in IGHR-CLL patients with (B) any mutation, (C) *NOTCH1*, *SF3B1*, *TP53*, *BIRC3* or *BRAF* mutations and (D) *IGLL5/BCL2* mutations (N = 46). E, Kaplan-Meier analysis of TFT in the three risk stratifications subgroups according to the presence of mutations in *NOTCH1*, *SF3B1*, *BIRC3*, *TP53* and *BRAF* genes. In low-risk patients, the presence of mutations in some of these five genes is significantly associated with shorter TFT (median not reached vs 24 months, $P < .0001$) as well as in the intermediate-risk subgroup (56 vs 2 months, $P < .0001$)

presence of mutations in *NOTCH1*, *SF3B1*, *TP53*, *BIRC3* and *BRAF* (median TFT not reached vs 24 months, $P < .0001$) (Figure 3E). These mutations also contributed to a worse outcome in intermediate-risk patients (IGH*R* /+12, N = 72) (56 vs 2 months, $P < .0001$). However, the small number of cases with these mutations was insufficient to demonstrate a statistically significant difference in clinical impact in the high-risk cytogenetics subgroup (11q−/17p−, N = 27) (4 vs 0 months, $P = .580$). The median TFT of those intermediate-risk patients with mutations was similar to that of patients with high-risk cytogenetic alterations (2 vs 5 months; $P = .548$), and the TFT of low-risk patients with mutations was not significantly different from that of intermediate-risk patients without mutations in any of the five genes (24 vs 56, $P = .210$). Therefore, by including *NOTCH1*, *SF3B1*, *TP53*, *BIRC3* and *BRAF* mutations in the cytogenetic model,

TABLE 3 Univariate and multivariate analysis for time to first treatment (TFT) in IGH*R*-CLL patients (N = 46)

	Univariate				Multivariate			
		95% CI				95% CI		
	HR	Lower	Upper	*P*	HR	Lower	Upper	*P*
Male gender	0.675	0.33	1.37	.276				
Binet B/C	0.257	0.12	0.56	**.001**	0.558	0.22	1.43	.221
CD38 positivity	0.810	0.36	1.82	.614				
IGHV-unmutated	0.325	0.13	0.79	**.013**	0.566	0.20	1.64	.29
LDH high	0.726	0.32	1.66	.448				
β2M high	0.558	0.25	1.27	.163				
Hepatomegaly	0.340	0.10	1.16	.085				
Splenomegaly	0.368	0.15	0.88	**.025**	0.403	0.14	1.19	.099
B symptoms	0.483	0.18	1.27	.141				
11q deletion	0.421	0.09	1.82	.246				
IGH/BCL2 translocation absence	0.443	0.18	1.09	.076				
IGLL5/BCL2 mutations absence	0.139	0.03	0.60	**.008**	0.821	0.14	4.76	.828
TP53 disruption/mutation	0.143	0.04	0.51	**.003**	0.304	0.07	1.28	.105
BRAF mutations	0.325	0.09	1.13	.076				
NOTCH1/SF3B1/TP53/BIRC3/BRAF mutations	0.204	0.08	0.47	**.0002**	0.255	0.07	0.88	**.030**
Presence of mutation	0.238	0.05	10.0	.051				

Note: Significant values are shown in bold.
Abbreviations: β2M, β2-microglobulin level; LDH, lactate dehydrogenase level.

approximately 27.6% (37/134) of low-risk patients were reclassified into an intermediate-risk subgroup, and 51% (35/72) of intermediate-risk patients were reclassified into a high-risk subgroup (Figure 3E).

4 | DISCUSSION

The identification of novel recurrent mutations in CLL has provided a more comprehensive perspective on the genomic landscape and the biological mechanisms underlying the clinical heterogeneity of the disease.[2-4,7,8] Previous studies have shown that CLLs carrying *IGH* rearrangement could have a worse outcome than low-risk cytogenetic CLL patients.[22,23] However, their clinical course and molecular characteristics are not well defined.[19-24] Here, we adopted a targeted NGS approach to assess for the first time the mutational profile of 46 IGH*R*-CLL patients.

Overall, the mutational analysis revealed that IGH*R*-CLL patients had a high incidence of mutations, not only in well-known CLL drivers such as *NOTCH1*, *SF3B1*, *POT1*, *TP53* and *FBXW7*—previously described in unselected large CLL cohorts—but also in less commonly mutated genes such as *BCL2*, *FBXW7*, *ZMYM3* and *MGA*,[7,8,33] being *BCL2* and *FBXW7* significantly associated with the *IGH* translocation (Figure 1A). Although we observed the cooccurrence between IGH*R* and trisomy 12 previously described, we demonstrated that IGH*R*-CLLs mutational profile did not depend on the presence of additional cytogenetic aberrations: CLLs with only IGH*R* also exhibited a high mutation frequency in genes well-known associated with trisomy 12 such as *NOTCH1*,[8] as well as in the majority of recurrently mutated genes in the entire IGH*R*-CLL cohort (Figure 1B).

Strikingly, several IGH*R*-CLLs showed mutations in *IGLL5*, *BCL2* and *HIST1H1E*, mainly those with *IGH/BCL2* translocations (Supplementary Figure S3A). Although these gene mutations have been detected at low frequencies in other CLL cohorts,[7,8] they have been extensively reported in other hematological malignances such as diffuse large B-cell lymphoma (DLBCL) and follicular lymphoma (FL)[35-37,39-44] (Table 1). Considering that our series of IGH*R*-CLL patients is well characterized at the immunophenotypic and clinical levels, the presence of mutations previously described in lymphomas suggests that patients with *IGH* translocation are a cytogenetic subgroup with a mutational profile distinct from the other CLLs and, probably, with different genetic mechanisms underlying their disease pathogenesis. Here, we demonstrated that IGH*R*-CLLs had an intermediate genetic landscape between those of CLL and NHL, and we suggest that the mutational analysis of patients with *IGH* translocations such as *IGH/BCL2* could help distinguish between CLL and NHL cases.

In this work, we have reported mutations in coding and non-coding regions of *BCL2* and *IGLL5* and, specifically, we identified a novel recurrent 5′UTR mutation in *BCL2*. Although this mutation has not been previously described, proximal mutations have been detected in other CLL and NHL studies.[8,34,44] Moreover, the vast majority of *BCL2* mutations reported in Puente et al were detected in cases harboring *IGH/BCL2* translocations,[8] which is consistent with our results (Supplementary Figure S3). Regarding *IGLL5*, a previous

study identified 5′UTR and coding mutations in low-risk *IGHV*-mutated CLLs as well as in the presence of rearrangements.[33] These statements are consistent with our results, as most of patients harboring mutations in both genes exhibited mutated *IGHV* and were associated with longer TFT (Figure 3D). In addition, data compiled in the ICGC repository suggested a functional impact of the *BCL2* and *IGLL5* coding mutations in the gene function. However, the functional impact of UTR somatic mutations has not been well-established yet. Puente et al demonstrated the negative impact of the 3′UTR mutation in *NOTCH1*[8] and recent findings from the Pan-Cancer Analysis of Whole Genomes Consortium identified novel driver candidates, including mutations in UTR regions, with a potential role in CLL pathogenesis.[45] Nevertheless, further investigation is needed in order to determine the importance of *BCL2* and *IGLL5* non-coding mutations in CLL.

The clinical impact of *IGH* translocations is currently under discussion.[19-25] The median TFT was shorter in IGH*R*-CLLs than that of patients with low-risk cytogenetic alterations, but similar to that of patients with trisomy 12 (Supplementary Figure S4A), indicating that *IGH* translocations could be associated with an intermediate-adverse outcome. Indeed, 6.7% of CLL patients who would be considered "normal FISH" using the customary four-probe CLL FISH panel in our study, carried the *IGH* translocation and also had a worse prognosis than CLLs lacking IGH*R* (Figure 3A), thus highlighting the value of including the *IGH* probe in the CLL FISH panel to improve patient outcome prediction.[25]

Previous studies have shown that patients with an *IGH/BCL2* translocation had a favorable clinical course, similar to that of patients with low-risk chromosomal alterations, whereas patients with other *IGH* rearrangements had a similar prognosis to the high-risk subgroups.[24,25] In our study, patients with *IGH/BCL2* not only were associated with *IGHV*-M and longer TFT (Supplementary Figure S5A), but also exhibited lower mutation rate compared to other *IGH* translocations that may contribute to understand why these entities have a better prognosis than the rest of IGH*R*. Regarding the mutational profile of *IGH/BCL2* translocations, a previous large-scale CLL study showed mutations in *BCL2*, *IGLL5* and *NOTCH1* within nine *IGH/BCL2* cases, which strongly supports our findings (Supplementary Figure S3B). On the other hand, IGH*R*-CLLs without *IGH/BCL2* rearrangement presented higher mutation frequencies in genes related to bad prognosis, such as *NOTCH1*, *SF3B1*, *TP53*, *BRAF* and *RPS15* (Figure 1B; Supplementary Figure S3A). The high frequency of these mutations may reflect a genomic instability in IGH*R*-CLLs without *IGH/BCL2*, which could be also influenced by the role of the translocated partner in the rearrangement. Furthermore, two IGH*R*-CLLs developed Richter transformation to DLBCL. One of them harbored *IGH/BCL2* rearrangement together with trisomy 12 and *NOTCH1*, and the other patient had an IGH*R* with unknown partner, *NOTCH1* and *TP53* mutations. These observations are in line with previous findings regarding the molecular pathways frequently altered at transformation.[46,47] Altogether, these molecular characteristics could be the underlying mechanisms of the IGH*R*-CLLs poorer outcome.[25]

In our cohort, patients harboring *NOTCH1*, *SF3B1*, *TP53*, *BIRC3* or *BRAF* mutations experienced an adverse clinical course (Figure 3C), which is consistent with previous studies.[6-8,11,48] Within IGH*R*-CLLs, the presence of these mutations contributed to shorter TFT being identified as an independent adverse prognostic factor (Table 3). Specifically, IGH*R*-CLL patients harboring *BRAF* mutations exhibited an adverse outcome (Supplementary Figure S6A), which corroborates previous results showing that patients carrying these mutations display an aggressive disease.[49,50]

Therefore, the present study proposes an integrated mutational and cytogenetic model for CLL prediction that includes IGH*R* and *BRAF* mutational status as novel components with respect to previous prognostic models.[9,10] The presence of mutations in any of the aforementioned five genes caused a significant shift to a more aggressive outcome in low (13q−/normal FISH) and intermediate-risk (+12/IGH*R*) CLLs, refining their prognosis and providing information that could help in therapeutic decisions. Interestingly, low-risk patients with mutations in *NOTCH1*, *SF3B1*, *TP53*, *BIRC3* or *BRAF* still had a significantly better outcome than did intermediate-risk patients with any of those mutations (Figure 3E). These results may indicate that the cooccurrence of cytogenetic abnormalities and gene mutations could have different clinical impacts, depending on the type of the genetic alterations involved.

In conclusion, our study revealed significant differences in the mutational profile and the frequencies of CLL-mutated genes in patients with *IGH* rearrangements. The distribution of genetic mutations differed within the IGH*R*-CLL subgroup: patients with *IGH/BCL2* translocation had higher frequencies of *BCL2* and *IGLL5* mutations than those without the translocation. Conversely, patients with other IGH*R* showed higher mutation frequencies of genes related to bad prognosis (*NOTCH1*, *SF3B1*, *TP53*, *BIRC3* and *BRAF*) than did those with the *IGH/BCL2*. Notably, the presence of those somatic mutations enables us to refine not only the prognosis of IGH*R*-CLLs but also the outcome of low-risk cytogenetic patients. Thus, this mutational analysis improves our understanding of the molecular heterogeneity of CLL patients and could help improve prognostic stratification of CLLs.

ACKNOWLEDGMENTS

We are grateful to S. Santos, C. Miguel, I. Rodríguez, S. González, T. Prieto, M.Á. Ramos, A. Martín, A. Díaz, A. Simón, M. del Pozo, V. Gutiérrez and S. Pujante from the Centro de Investigación del Cáncer, Salamanca, for their technical assistance. This work was supported by grants from the Spanish Fondo de Investigaciones Sanitarias, PI15/01471, PI18/01500, Instituto de Salud Carlos III (ISCIII), European Regional Development Fund (ERDF) "Una manera de hacer Europa", "Consejería de Educación, Junta de Castilla y León" (SA271P18), "Proyectos de Investigación del SACYL", Spain: GRS 1847/A/18, GRS1653/A17, "Fundación Memoria Don Samuel Solórzano Barruso", by grants (RD12/0036/0069) from Red Temática de Investigación Cooperativa en Cáncer (RTICC) and Centro de Investigación Biomédica en Red de Cáncer (CIBERONC CB16/12/00233). Claudia Pérez-Carretero was supported by an "Ayuda predoctoral en Oncología" (AECC) and is a recipient of a PFIS grant (FI19/00191) from Instituto de Salud Carlos III; María Hernández-Sánchez was supported by a grant from FEHH/Janssen ("Sociedad Española de Hematología y

Hemoterapia") and now holds a Sara Borrell post-doctoral contract (CD19/00222) from the Instituto de Salud Carlos III (ISCIII). PFIS grant and Sara Borrell post-doctoral contrat is co-founded by Fondo Social Europeo (FSE) "El Fondo Social Europeo invierte en tu futuro"; Miguel Quijada-Álamo is supported by an "Ayuda Predoctoral de la Junta de Castilla y León" (JCYL-EDU/529/2017); Jesús-María Hernández-Sánchez and Ana E. Rodríguez-Vicente are supported by research grants of FEHH ("Fundación Española de Hematología y Hemoterapia").

CONFLICT OF INTEREST

The authors declare no potential conflicts of interest.

AUTHOR CONTRIBUTIONS

Claudia Pérez-Carretero: designed research, performed the research and statistical analyses, analyzed the data and drafted the manuscript. María Hernández-Sánchez: analyzed the data and critically reviewed the manuscript, designed the custom-CLL panel and the sequencing studies. Teresa González: selected the samples and individually reviewed all IGH*R*-CLL cases by FISH and immunophenotypic studies. Miguel Quijada-Álamo: contributed to the analysis and interpretation of the results and critically reviewed the manuscript. Marta Martín-Izquierdo and Jesús-María Hernández-Sánchez: proceeded the samples and performed the next-generation sequencing studies. María-Jesús Vidal, Alfonso García de Coca, Carlos Aguilar, Manuel Vargas-Pabón, Sara Alonso, Magdalena Sierra, Araceli Rubio-Martínez, Julio Dávila, José R. Díaz-Valdés, José-Antonio Queizán and José-Ángel Hernández-Rivas: provided the patients' data. Rocío Benito: designed the custom-CLL panel and the sequencing studies. Ana E. Rodríguez-Vicente and Jesús-María Hernández-Rivas: designed research, performed research and critically reviewed and approved the final version of the manuscript.

ETHICS STATEMENT

The present study was approved by the local ethics committee (Comité Ético de Investigación Clínica, Hospital Universitario de Salamanca). Written informed consent was obtained from all participants before they entered the study.

DATA AVAILABILITY STATEMENT

The data that support the findings of this study are available from the corresponding author upon reasonable request.

ORCID

Ana E. Rodríguez-Vicente https://orcid.org/0000-0001-6516-2172

REFERENCES

1. Shanafelt TD, Geyer SM, Kay NE. Prognosis at diagnosis: integrating molecular biologic insights into clinical practice for patients with CLL. *Blood*. 2004;103(4):1202-1210.
2. Fabbri G, Dalla-Favera R. The molecular pathogenesis of chronic lymphocytic leukaemia. *Nat Rev Cancer*. 2016;16(3):145-162.
3. Rodríguez-Vicente AE, Bikos V, Hernández-Sánchez M, Malcikova J, Hernández-Rivas JM, Pospisilova S. Next-generation sequencing in chronic lymphocytic leukemia: recent findings and new horizons. *Oncotarget*. 2017;8(41):71234-71248.
4. Landau DA, Carter SL, Stojanov P, et al. Evolution and impact of subclonal mutations in chronic lymphocytic leukemia. *Cell*. 2013;152(4):714-726.
5. Döhner H, Stilgenbauer S, Benner A, et al. Genomic aberrations and survival in chronic lymphocytic leukemia. *N Engl J Med*. 2000;343(26):1910-1916.
6. Guièze R, Wu CJ. Genomic and epigenomic heterogeneity in chronic lymphocytic leukemia. *Blood*. 2015;126(4):445-453.
7. Landau DA, Tausch E, Taylor-Weiner AN, et al. Mutations driving CLL and their evolution in progression and relapse. *Nature*. 2015;526(7574):525-530.
8. Puente XS, Beà S, Valdés-Mas R, et al. Non-coding recurrent mutations in chronic lymphocytic leukaemia. *Nature*. 2015;526(7574):519-524.
9. Rossi D, Rasi S, Spina V, et al. Integrated mutational and cytogenetic analysis identifies new prognostic subgroups in chronic lymphocytic leukemia. *Blood*. 2013;121(8):1403-1412.
10. Jeromin S, Weissmann S, Haferlach C, et al. SF3B1 mutations correlated to cytogenetics and mutations in NOTCH1, FBXW7, MYD88, XPO1 and TP53 in 1160 untreated CLL patients. *Leukemia*. 2014;28(1):108-117.
11. Baliakas P, Hadzidimitriou A, Sutton LA, et al. Recurrent mutations refine prognosis in chronic lymphocytic leukemia. *Leukemia*. 2015;29(2):329-336.
12. Weissmann S, Roller A, Jeromin S, et al. Prognostic impact and landscape of NOTCH1 mutations in chronic lymphocytic leukemia (CLL): a study on 852 patients. *Leukemia*. 2013;27(12):2393-2396.
13. Nowakowski GS, Dewald GW, Hoyer JD, et al. Interphase fluorescence in situ hybridization with an IGH probe is important in the evaluation of patients with a clinical diagnosis of chronic lymphocytic leukaemia. *Br J Haematol*. 2005;130(1):36-42.
14. Nelson BP, Gupta R, Dewald GW, Paternoster SF, Rosen ST, Peterson LC. Chronic lymphocytic leukemia FISH panel: impact on diagnosis. *Am J Clin Pathol*. 2007;128(2):323-332.
15. Berkova A, Pavlistova L, Babicka L, et al. Combined molecular biological and molecular cytogenetic analysis of genomic changes in 146 patients with B-cell chronic lymphocytic leukemia. *Neoplasma*. 2008;55(5):400-408.
16. Lu G, Kong Y, Yue C. Genetic and immunophenotypic profile of IGH@ rearrangement detected by fluorescence in situ hybridization in 149 cases of B-cell chronic lymphocytic leukemia. *Cancer Genet Cytogenet*. 2010;196(1):56-63.
17. Willis TG, Dyer MJ. The role of immunoglobulin translocations in the pathogenesis of B-cell malignancies. *Blood*. 2000;96(3):808-822.
18. DE Braekeleer M, Tous C, Guéganic N, et al. Immunoglobulin gene translocations in chronic lymphocytic leukemia: a report of 35 patients and review of the literature. *Mol Clin Oncol*. 2016;4(5):682-694.
19. Mayr C, Speicher MR, Kofler DM, et al. Chromosomal translocations are associated with poor prognosis in chronic lymphocytic leukemia. *Blood*. 2006;107(2):742-751.
20. Van Den Neste E, Robin V, Francart J, et al. Chromosomal translocations independently predict treatment failure, treatment-free survival and overall survival in B-cell chronic lymphocytic leukemia patients treated with cladribine. *Leukemia*. 2007;21(8):1715-1722.
21. Jimenez-Zepeda VH, Chng WJ, Schop RF, et al. Recurrent chromosome abnormalities define nonoverlapping unique subgroups of tumors in patients with chronic lymphocytic leukemia and known karyotypic abnormalities. *Clin Lymphoma Myeloma Leuk*. 2013;13(4):467-476.
22. Gerrie AS, Bruyere H, Chan MJ, et al. Immunoglobulin heavy chain (IGH@) translocations negatively impact treatment-free survival for chronic lymphocytic leukemia patients who have an isolated deletion 13q abnormality. *Cancer Genet*. 2012;205(10):523-527.

23. Cavazzini F, Hernandez JA, Gozzetti A, et al. Chromosome 14q32 translocations involving the immunoglobulin heavy chain locus in chronic lymphocytic leukaemia identify a disease subset with poor prognosis. *Br J Haematol*. 2008;142(4):529-537.
24. Davids MS, Vartanov A, Werner L, Neuberg D, Dal Cin P, Brown JR. Controversial fluorescence in situ hybridization cytogenetic abnormalities in chronic lymphocytic leukaemia: new insights from a large cohort. *Br J Haematol*. 2015;170(5):694-703.
25. Fang H, Reichard KK, Rabe KG, et al. IGH translocations in chronic lymphocytic leukemia (CLL): clinicopathologic features and clinical outcomes. *Am J Hematol*. 2019;94(3):338–345.
26. Reddy KS. Chronic lymphocytic leukaemia profiled for prognosis using a fluorescence in situ hybridisation panel. *Br J Haematol*. 2006; 132(6):705-722.
27. Swerdlow SH, Campo E, Pileri SA, et al. The 2016 revision of the World Health Organization classification of lymphoid neoplasms. *Blood*. 2016;127(20):2375-2390.
28. Hallek M, Cheson BD, Catovsky D, et al. Guidelines for the diagnosis and treatment of chronic lymphocytic leukemia: a report from the International Workshop on Chronic Lymphocytic Leukemia updating the National Cancer Institute-Working Group 1996 guidelines. *Blood*. 2008;111(12):5446-5456.
29. González MB, Hernández JM, García JL, et al. The value of fluorescence in situ hybridization for the detection of 11q in multiple myeloma. *Haematologica*. 2004;89(10):1213-1218.
30. Quijada-Álamo M, Hernández-Sánchez M, Robledo C, et al. Next-generation sequencing and FISH studies reveal the appearance of gene mutations and chromosomal abnormalities in hematopoietic progenitors in chronic lymphocytic leukemia. *J Hematol Oncol*. 2017; 10(1):83.
31. Hernández-Sánchez M, Rodríguez-Vicente AE, González-Gascón Y Marín I, et al. DNA damage response-related alterations define the genetic background of patients with chronic lymphocytic leukemia and chromosomal gains. *Exp Hematol*. 2019;72:9-13.
32. Quijada-Álamo M, Hernández-Sánchez M, Alonso-Pérez V, et al. CRISPR/Cas9-generated models uncover therapeutic vulnerabilities of del(11q) CLL cells to dual BCR and PARP inhibition. *Leukemia*. 2020;34:1599-1612.
33. Kasar S, Kim J, Improgo R, et al. Whole-genome sequencing reveals activation-induced cytidine deaminase signatures during indolent chronic lymphocytic leukaemia evolution. *Nat Commun*. 2015;6:8866.
34. Mosquera Orgueira A, Rodríguez Antelo B, Díaz Arias J, et al. Novel mutation hotspots within non-coding regulatory regions of the chronic lymphocytic leukemia genome. *Sci Rep*. 2020;10(1):2407.
35. Morin RD, Mendez-Lago M, Mungall AJ, et al. Frequent mutation of histone-modifying genes in non-Hodgkin lymphoma. *Nature*. 2011; 476(7360):298-303.
36. Pasqualucci L, Khiabanian H, Fangazio M, et al. Genetics of follicular lymphoma transformation. *Cell Rep*. 2014;6(1):130-140.
37. de Miranda NF, Georgiou K, Chen L, et al. Exome sequencing reveals novel mutation targets in diffuse large B-cell lymphomas derived from Chinese patients. *Blood*. 2014;124(16):2544-2553.
38. Benjamini Y, Hochberg Y. Controlling the false discovery rate: a practical and powerful approach to multiple testing. *J Royal Stat Soc*. 1995;1:289-300.
39. Li H, Kaminski MS, Li Y, et al. Mutations in linker histone genes HIST1H1 B, C, D, and E; OCT2 (POU2F2); IRF8; and ARID1A underlying the pathogenesis of follicular lymphoma. *Blood*. 2014;123(10): 1487-1498.
40. Pillonel V, Juskevicius D, Ng CKY, et al. High-throughput sequencing of nodal marginal zone lymphomas identifies recurrent BRAF mutations. *Leukemia*. 2018;32(11):2412-2426.
41. Correia C, Schneider PA, Dai H, et al. BCL2 mutations are associated with increased risk of transformation and shortened survival in follicular lymphoma. *Blood*. 2015;125(4):658-667.
42. Zhang J, Grubor V, Love CL, et al. Genetic heterogeneity of diffuse large B-cell lymphoma. *Proc Natl Acad Sci USA*. 2013;110(4): 1398-1403.
43. Okosun J, Bödör C, Wang J, et al. Integrated genomic analysis identifies recurrent mutations and evolution patterns driving the initiation and progression of follicular lymphoma. *Nat Genet*. 2014;46(2): 176-181.
44. Batmanov K, Wang W, Bjørås M, Delabie J, Wang J. Integrative whole-genome sequence analysis reveals roles of regulatory mutations in BCL6 and BCL2 in follicular lymphoma. *Sci Rep*. 2017;7(1): 7040.
45. Rheinbay E, Nielsen MM, Abascal F, et al. Analyses of non-coding somatic drivers in 2,658 cancer whole genomes. *Nature*. 2020;578 (7793):102-111.
46. Fabbri G, Khiabanian H, Holmes AB, et al. Genetic lesions associated with chronic lymphocytic leukemia transformation to Richter syndrome. *J Exp Med*. 2013;210(11):2273-2288.
47. Rossi D, Gaidano G. Richter syndrome. *Adv Exp Med Biol*. 2013;792: 173-191.
48. Nadeu F, Delgado J, Royo C, et al. Clinical impact of clonal and subclonal TP53, SF3B1, BIRC3, NOTCH1, and ATM mutations in chronic lymphocytic leukemia. *Blood*. 2016;127(17):2122-2130.
49. Herling CD, Abedpour N, Weiss J, et al. Clonal dynamics towards the development of venetoclax resistance in chronic lymphocytic leukemia. *Nat Commun*. 2018;9(1):727.
50. Giménez N, Martínez-Trillos A, Montraveta A, et al. Mutations in the RAS-BRAF-MAPK-ERK pathway define a specific subgroup of patients with adverse clinical features and provide new therapeutic options in chronic lymphocytic leukemia. *Haematologica*. 2019;104 (3):576-586.

SUPPORTING INFORMATION

Additional supporting information may be found online in the Supporting Information section at the end of this article.

How to cite this article: Pérez-Carretero C, Hernández-Sánchez M, González T, et al. Chronic lymphocytic leukemia patients with *IGH* translocations are characterized by a distinct genetic landscape with prognostic implications. *Int. J. Cancer*. 2020;1–13. https://doi.org/10.1002/ijc.33235

CHAPTER 3

TRAF3 alterations are frequent in del-3'IGH chronic lymphocytic leukemia patients and define a specific subgroup with adverse clinical features

Claudia Pérez-Carretero[1,2], María Hernández-Sánchez[1,2,3], Teresa González[1,2], Miguel Quijada-Álamo[1,2], Marta Martín-Izquierdo[1,2], Sandra Santos-Mínguez[1,2], Cristina Miguel-García[1,2], María-Jesús Vidal[4], Alfonso García-De-Coca[5], Josefina Galende[6], Emilia Pardal[7], Carlos Aguilar[8], Manuel Vargas-Pabón[9], Julio Dávila[10], Isabel Gascón-Y-Marín[11], José-Ángel Hernández-Rivas[11], Rocío Benito[1,2], Jesús-María Hernández-Rivas[1,2] and Ana-Eugenia Rodríguez-Vicente[1,2]

1. Universidad de Salamanca, IBSAL, Centro de Investigación del Cáncer (IBMCC-CSIC), Salamanca, Spain.
2. Servicio de Hematología, Hospital Universitario de Salamanca, Salamanca, Spain.
3. Departamento de Bioquímica y Biología Molecular, Facultad de Farmacia. Universidad Complutense de Madrid, Madrid, Spain (Present affiliation).
4. Servicio de Hematología, Hospital Universitario, León, Spain.
5. Servicio de Hematología, Hospital Clínico, Valladolid, Spain.
6. Servicio de Hematología, Hospital El Bierzo, Ponferrada, Spain
7. Servicio de Hematología, Hospital Virgen del Puerto, Plasencia, Spain
8. Servicio de Hematología, Complejo Hospitalario de Soria, Soria, Spain.
9. Servicio de Hematología, Hospital Jarrio, Asturias, Spain.
10. Servicio de Hematología, Hospital Nuestra Señora de Sonsoles, Ávila, Spain.
11. Servicio de Hematología. Hospital Universitario Infanta Leonor. Universidad Complutense. Madrid, Spain.

American Journal of Hematology. 2022 Jul;97(7):903-914. doi: 10.1002/ajh.26578

Received: 2 February 2022 | Revised: 11 April 2022 | Accepted: 17 April 2022
DOI: 10.1002/ajh.26578

RESEARCH ARTICLE

TRAF3 alterations are frequent in del-3′IGH chronic lymphocytic leukemia patients and define a specific subgroup with adverse clinical features

Claudia Pérez-Carretero[1,2] | María Hernández-Sánchez[1,2] | Teresa González[1,2] | Miguel Quijada-Álamo[1,2] | Marta Martín-Izquierdo[1,2] | Sandra Santos-Mínguez[1,2] | Cristina Miguel-García[1,2] | María-Jesús Vidal[3] | Alfonso García-De-Coca[4] | Josefina Galende[5] | Emilia Pardal[6] | Carlos Aguilar[7] | Manuel Vargas-Pabón[8] | Julio Dávila[9] | Isabel Gascón-Y-Marín[10] | José-Ángel Hernández-Rivas[10] | Rocío Benito[1,2] | Jesús-María Hernández-Rivas[1,2] | Ana-Eugenia Rodríguez-Vicente[1,2]

[1]Universidad de Salamanca, IBSAL, IBMCC- Centro de Investigación del Cáncer (USAL-CSIC), Salamanca, Spain
[2]Servicio de Hematología, Hospital Universitario de Salamanca, Salamanca, Spain
[3]Servicio de Hematología, Hospital Universitario, León, Spain
[4]Servicio de Hematología, Hospital Clínico, Valladolid, Spain
[5]Servicio de Hematología, Hospital El Bierzo, Ponferrada, Spain
[6]Servicio de Hematología, Hospital Virgen del Puerto, Plasencia, Spain
[7]Servicio de Hematología, Complejo Hospitalario de Soria, Soria, Spain
[8]Servicio de Hematología, Hospital Jarrio, Asturias, Spain
[9]Servicio de Hematología, Hospital Nuestra Señora de Sonsoles, Ávila, Spain
[10]Servicio de Hematología, Hospital Universitario Infanta Leonor, Universidad Complutense, Madrid, Spain

Correspondence
José-Ángel Hernández-Rivas, Hematology Department, Hospital Universitario Infanta Leonor, C/Gran Vía del Este 80, Universidad Complutense, 28031 Madrid, Spain.
Email: jahr_jahr2006@yahoo.es

Ana-Eugenia Rodríguez-Vicente, IBMCC-Centro de Investigación del Cáncer (USAL-CSIC), Campus Miguel de Unamuno, 37007 Salamanca, Spain.
Email: anaerv@hotmail.com

Present address
María Hernández-Sánchez, Departamento de Bioquímica y Biología Molecular, Facultad de Farmacia, Universidad Complutense de Madrid, Madrid, Spain

Abstract

Interstitial 14q32 deletions involving IGH gene are infrequent events in chronic lymphocytic leukemia (CLL), affecting less than 5% of patients. To date, little is known about their clinical impact and molecular underpinnings, and its mutational landscape is currently unknown. In this work, a total of 871 CLLs were tested for the IGH break-apart probe, and 54 (6.2%) had a 300 kb deletion of 3′IGH (del-3′IGH CLLs), which contributed to a shorter time to first treatment (TFT). The mutational analysis by next-generation sequencing of 317 untreated CLLs (54 del-3′IGH and 263 as the control group) showed high mutational frequencies of *NOTCH1* (30%), *ATM* (20%), genes involved in the RAS signaling pathway (*BRAF*, *KRAS*, *NRAS*, and *MAP2K1*) (15%), and *TRAF3* (13%) within del-3′IGH CLLs. Notably, the incidence of *TRAF3* mutations was significantly higher in del-3′IGH CLLs than in the control group

Claudia Pérez-Carretero and María Hernández-Sánchez contributed equally to this work.
Jesús-María Hernández-Rivas and Ana-Eugenia Rodríguez-Vicente shared senior authorship.

Funding information
Universidad de Salamanca; Fundación Española de Hematología y Hemoterapia (FEHH); Centro de Investigación Biomédica en Red de Cáncer (CIBERONC), Grant/Award Number: CB16/12/00233; Red Temática de Investigación Cooperativa en Cáncer (RTICC); "Fundación Memoria Don Samuel Solórzano Barruso": FS/33–2020, Grant/Award Number: RD12/0036/0069; "Gerencia Regional de Salud, SACYL": Grant/Award Numbers: GRS2385/A/21, GRS2140/A/20; Consejería de Educación, Junta de Castilla y León, Grant/Award Number: SA118P20; European Regional Development Fund and Instituto de Salud Carlos III, Grant/Award Numbers: CD19/00222, FI19/00191; Spanish Fondo de Investigaciones Sanitarias, Grant/Award Numbers: PI21/00983, PI18/01500

($p < .001$). Copy number analysis also revealed that *TRAF3* loss was highly enriched in CLLs with 14q deletion ($p < .001$), indicating a complete biallelic inactivation of this gene through deletion and mutation. Interestingly, the presence of mutations in the aforementioned genes negatively refined the prognosis of del-3′IGH CLLs in terms of overall survival (*NOTCH1*, *ATM*, and *RAS* signaling pathway genes) and TFT (*TRAF3*). Furthermore, *TRAF3* biallelic inactivation constituted an independent risk factor for TFT in the entire CLL cohort. Altogether, our work demonstrates the distinct genetic landscape of del-3′IGH CLL with multiple molecular pathways affected, characterized by a *TRAF3* biallelic inactivation that contributes to a marked poor outcome in this subgroup of patients.

1 | INTRODUCTION

Chromosome 14q abnormalities are infrequent events in chronic lymphocytic leukemia (CLL),[1–3] in comparison to other mature B-cell neoplasms such as multiple myeloma and B-cell lymphomas.[4–6] It is noteworthy that the 14q32.33 chromosomal band, which contains IGH locus, is clinically relevant in CLL, since the mutational status of its variable chain (IGHV) represents one of the most powerful prognostic markers.[7,8] Moreover, 14q32 rearrangements involving *IGH* gene have also a prognostic impact in CLL, showing these patients an intermediate-adverse outcome and a distinct mutational profile from other classic cytogenetic subgroups.[9–14] Furthermore, the long arm of chromosome 14 has been shown to be involved not only in reciprocal rearrangements in CLL, but also in deletions.[4,5,15]

Deletions on 14q (del(14q)) are present in 2%–5% of CLL patients.[5,16] This aberration is heterogenous in size, mapping between chromosomal bands 14q24 and 14q32, and the most frequent breakpoint at the telomeric site involving the *IGH* locus (14q32.3) is observed in 45%–65% of patients with the deletion.[4,5,17] Considering the IGH-deleted region, there is also some variability, as previous studies have identified a deletion in the constant 3′ flanking site of the gene, while others also described 5′IGH deletions in the variable region.[18,19]

Regarding its prognostic significance, few studies have shown that del(14q) CLL patients present an intermediate-adverse clinical outcome.[5,17] However, due to its low incidence, its clinical impact remains controversial in CLL. In addition, this deletion has been associated with trisomy 12, as well as IGHV-unmutated (IGHV-UM) or *NOTCH1* mutations,[4,17] although, so far, detailed molecular analyses of del(14q) CLL cohorts are scarce. It has been speculated that *IGH* rearrangements were suggestive for a transcriptional activation of an oncogene by juxtaposition to the $E\mu$ enhancer of IGH, but this molecular process still remains elusive.[4,5] Alternatively, the hypothesis that del(14q) might inactivate putative tumor suppressor genes has been raised. Concretely, *TRAF3* gene, a negative regulator of the NF-κB pathway located within the deleted region (14q32.32), can be encompassed within del(14q) and it is also rarely mutated in CLL patients.[20,21]

In the present study, we evaluate a large cohort of CLL patients with del(14q), integrating for the first time their clinical and molecular genetic characteristics. We show that CLL patients with 3′IGH deletion (del-3′IGH) exhibit an intermediate-adverse prognosis, with a distinct mutational profile characterized by *TRAF3*, *NOTCH1*, *ATM*, and RAS mutations that also refine the prognosis of this subgroup. Notably, we report for the first time a high frequency of *TRAF3* biallelic alterations (deletion and mutation) with negative clinical implications in a subset of CLL patients showing a loss in 14q32. This biallelic inactivation is also an independent prognostic factor for shortening the time to first treatment (TFT), with a potential role in disease progression within CLL patients with del(14q).

2 | METHODS

2.1 | Patients

The study was based on 871 CLL patients diagnosed according to the International Workshop on CLL (iwCLL) criteria.[22] All of them were screened for *IGH* deletion, and 54 patients exhibited a deletion of 300 kb at the centromeric side of the IGH constant region (del-3′IGH). Cases with this alteration were individually reviewed to rule out any different lymphoproliferative disorder (see Supplementary Methods). Samples and clinical data were collected between August 1995 and December 2020 from 16 Spanish institutions, and all centrally analyzed in the Molecular Cytogenetics Unit of the Center for Cancer Research in Salamanca, Spain. Clinical and biological data are summarized in Table S1. Median follow-up of patients was 60 months (range: 1–340). In total, 47.5% of CLL patients were treated according to iwCLL criteria. Most patients received chemotherapy or chemoimmunotherapy regimens (95.5%), and 5% received new targeted therapies (ibrutinib, venetoclax, or idelalisib).

Mutational analysis by next-generation sequencing (NGS) was performed in 317 CLL patients: 54 del-3′IGH and 263 as a control group. All samples were analyzed before the initiation of first-line treatment. Patients in the control group were selected according to sample and clinical data availability and were representative of the

disease in terms of demographic and clinical characteristics. Clinical and biological characteristics of 317 CLLs included in NGS analyses are shown in Table S2. Cytogenetic-risk classification criteria of patients are described in Supplementary Methods. CLL-IPI and IPS-E risk scores were calculated according to the original publications, and patients were classified into low-, intermediate-, and high-risk subgroups for both scoring systems[23,24] (Table S2).

The study was approved by the local ethical committee (*Comité Ético de Investigación Clínica, Hospital Universitario de Salamanca*). Written informed consent was obtained from all participants before they entered the study.

Additional CLL patient data for an external validation CLL cohort ($n = 450$) were extracted from the International Cancer Genome Consortium (ICGC) project in which 30 CLL patients showed 14q loss.[25]

2.2 | Fluorescence in situ hybridization

Interphase fluorescence in situ hybridization (FISH) was performed on peripheral blood or bone marrow untreated samples using the following commercially available probes: ATM, CEP12, D13S319, and TP53 (Vysis, Abbott Laboratories, IL, USA). LSI IGH Dual Color Break-apart FISH probe was performed for the identification of *IGH* cytogenetic alterations. The methods used for FISH analysis have been described elsewhere.[26] Signal screening was carried out in at least 200 cells with well-delineated fluorescent spots. For the IGH probe, a score of ≥15% was considered positive, and for the rest of probes >10%, based on the cutoff value used by our laboratory. Median time from patients' diagnosis to FISH assessment was 2 months (range: 0–253).

2.3 | Next-generation sequencing

NGS studies were performed in 317 cases and in the same sample as the FISH test before the administration of any treatment, being 54 del-3′IGH and 263 non-del-3′IGH. Genomic DNA was extracted from CD19+ B-lymphocytes isolated from peripheral blood or bone marrow by magnetically activated cell sorting (MACS). B-cell purity was greater than 98% by flow cytometry, as previously described in our group.[27] The Agilent SureSelect^{QXT} Target Enrichment system for Illumina Multiplexed Sequencing (Agilent Technologies, Santa Clara, CA, USA) was used to produce custom-designed libraries of exonic regions from 54 CLL-related candidate driver genes as well as *BCL2*, *IGLL5* and *NOTCH1* UTR regions[13,28–30] (Supplementary Methods) (Table S3). Paired-end sequencing (151-bp reads) was run on the Illumina NextSeq instrument (Illumina, San Diego, CA, USA). Data analysis was performed using a previously validated in-house pipeline[13,28] (Supplementary Methods).

2.4 | Copy number variations analysis

Targeted-capture NGS data were also used to assess the deletion of *TRAF3* gene in CLL patients. The mean coverage depth of each individual target was first normalized in a set of 23 samples without deletion on 14q by FISH using the total read number of each sample. The mean coverage of all these samples was used as the reference. To detect *TRAF3* loss, the normalized coverage of targets of *TRAF3* gene from each study sample was compared with the mean coverage of the same target in the reference file generated above. Copy number variations (CNVs) were called using fixed thresholds representing the $\log_2$ ratio of mean coverage of testing to that of reference. A $\log_2$ ratio <-0.5 suggested a copy number loss/deletion of *TRAF3*. This method was based on a previously published analysis to detect deletions from targeted-capture NGS data.[31] It has been also used to determine CNVs in inherited platelet disorders[32] and, more specifically, in CLL patients using the same NGS approach.[33]

2.5 | Single-nucleotide polymorphism arrays

DNA was purified, amplified, labeled, and hybridized to the Affymetrix SNP6.0 platform (Affymetrix, Santa Clara, CA, USA) as previously described[34] for validation of *IGH* and *TRAF3* loss in CLL samples with available material.

2.6 | Statistical analysis

Statistical analyses were performed using IBM SPSS v23.0 for Windows (IBM Corp., Armonk, NY, USA) and R v4.0.2. Continuous variables were analyzed with the Mann–Whitney *U* test, while the chi-square and Fisher's exact tests were used to assess associations between categorical variables. Overall survival (OS) and time to first treatment (TFT) were calculated from the date FISH test was performed to the date of death, first treatment, or last follow-up (considering disease-unrelated deaths as competing events). Statistically significant variables related to OS and TFT were estimated by the Kaplan–Meier method, using the log-rank test to compare the curves of each group. Univariate and multivariate analyses of the OS and TFT used the Cox regression method. Results were considered statistically significant for values of $p < .05$.

3 | RESULTS

3.1 | Del-3′IGH CLL patients display an intermediate prognosis with distinct clinical features

FISH analysis, including the IGH probe, was performed in a total of 871 CLLs, revealing a deletion of 300 kb at the centromeric side of the IGH constant region in 54 patients (54/871, 6.2%). The pattern observed in the FISH analyses in these patients was a single orange signal (3′IGH), and two green signals (5′IGH), corresponding to the two alleles (Figure 1A). According to this, the alteration detected was monoallelic, and the proportion of cells expressing the 3′IGH deletion (del-3′IGH) in each sample ranged from 15% to 98%, with a median of 65%. This deletion was confirmed by single-nucleotide polymorphism (SNP) arrays in del-3′IGH cases with available material (Figure S1, Table S4).

A detailed list of the clinical and biological characteristics of patients with del-3′IGH is shown in Table S1. Median age at diagnosis was 64.5 years (range: 43–89) and the gender ratio (M:F) was 2. In addition, 51.1% of del-3′IGH cases exhibited IGHV-UM and 23.5%, a Binet stage B or C. The presence of del-3′IGH was significantly associated with splenomegaly when compared with the control group (28.5% vs. 15.9%, $p = .028$) (Table S1). In addition, a total of 35 out of 54 del-3′IGH patients received therapy during follow-up, which was significantly more frequent than those patients in the control group (64.8% vs. 46.4%, $p = .011$) (Table S1). No other significant differences were observed between both groups with respect to clinical and biological parameters.

We observed that 77.8% (42/54) of del-3′IGH cases carried additional cytogenetic alterations, being the most common the del(13q) (19/54, 35.2%), found as the sole abnormality besides the del-3′IGH, followed by trisomy 12 (12/54, 22.2%), del(11q) (6/54, 11.1%), and del(17p) (5/54, 9.3%). It is noteworthy to mention that the incidence of trisomy 12 in the del-3′IGH subgroup tended to be higher than in the control group, although it did not reach the statistical significance (22.2% vs. 15.7%, $p = .25$) (Table S1).

In univariate analyses, the presence of del-3′IGH was associated with reduced TFT (hazard ratio [HR] = 0.851, 95% confidence interval [CI] = 0.76–0.95, $p = .005$) (Figure 1B), although it was not an independent prognostic marker in multivariate analyses (data not shown). CLL patients showing del-3′IGH had a significantly shorter TFT than the non-del-3′IGH subgroup (median 45 vs. 75 months, $p = .004$), especially when compared with low-risk cytogenetics del(13q) (45 vs. 184 months, $p < .001$) or normal FISH (45 vs. 116 months, $p < .001$) (Figure 1C,D). By contrast, del-3′IGH CLL patients exhibited a similar prognosis to those with trisomy 12 (45 vs. 26 months, $p = .893$). It should be noted that del-3′IGH was detected in a subset of CLL patients categorized as normal FISH with the standard four-probe panel, showing these patients a significantly shorter TFT (5 vs. 116 months, $p < .001$) (Figure 1E). The addition of del-3′IGH to trisomy 12 also contributed to a decreased TFT close to the statistical significance (1 vs. 26 months, $p = .062$) (Figure 1F). In terms of OS, we did not observe statistically significant differences in comparison to the control group (128 months vs. median not reached, $p = .578$) (Figure S2).

3.2 | Mutations in *NOTCH1*, *ATM*, *TRAF3*, and *RAS* signaling pathway genes are enriched in del-3′IGH CLL patients

NGS analyses revealed that 81% of patients harbored at least one mutation in any of the 54 genes included in the NGS panel, and the median of mutations per patient was 2 (range: 0–7). The most recurrently mutated genes were *NOTCH1* (20%), *IGLL5* (12%), *SF3B1* (11%), *ATM* (11%), *TP53* (11%), *POT1* (8%), *RPS15* (7%), *XPO1* (5%), and *NFKBIE* (5%).

In the del-3′IGH subgroup, we identified 150 mutations located in 40 genes. Exactly 92.6% of patients (50 of 54) showed at least one mutation, with a median of 2 mutated genes per patient (range: 0–5). Most mutations (98 of 150) were clustered in 12 genes being the most frequently mutated: *NOTCH1* (29.6%), *ATM* (20.4%), RAS signaling pathway genes (*BRAF*, *KRAS*, *NRAS*, *MAP2K1*) (14.8%), and *TRAF3* (13%) (Figure 2A).

A total of 18 *NOTCH1* mutations were detected in 16 del-3′IGH CLL patients (29.6%), being the hotspot variant p.P2514fs in exon 34 the most recurrent mutation (16/18) (Table S5). Of note, there was a trend toward the enrichment of *NOTCH1* mutations in del-3′IGH CLL patients (29.6% vs. 19.6%, $p = .09$) (Figure 2A). The presence of *NOTCH1* mutations was significantly associated with del-3′IGH in comparison to the control group not involving trisomy 12 (29.6% vs. 14.8%, $p = .016$). Despite the association of *NOTCH1* mutations with trisomy 12 previously described in other cohorts, 75% (12/16) of del-3′IGH patients harboring these mutations did not show this additional cytogenetic alteration, suggesting that the enrichment of *NOTCH1* mutations in del-3′IGH CLLs is independent of the presence of additional trisomy 12 (Figure 2B).

The second most commonly mutated gene was *ATM* (20.4%). Variants identified in this case included missense substitutions (4/15), frameshift deletions/insertions (5/15), stop-gain (4/15), and splice-site mutations (2/15) (Table S5). Interestingly, mutations in this gene were significantly associated with the del-3′IGH (20.4% vs. 9.8%, $p = .037$) (Figure 2A). In terms of cytogenetic alterations, del-3′IGH CLLs with *ATM* mutations carried 13q deletion (6/11) and/or 11q deletion (4/11), but none of them showed trisomy 12 (Figure 2B).

In addition, we observed a high mutational rate in RAS signaling pathway genes in this subgroup (*BRAF*, *KRAS*, *NRAS*, *MAP2K1*) (8/54, 14.8%). This mutational frequency was higher than that observed in the control group (14.8% vs. 8.1%, $p = .13$) (Figure 2A), and similar to the one of CLLs with trisomy 12 (14.8% vs. 18.7%, $p = .61$). A total of 10 mutations were located in BRAF (5/10), *KRAS* (2/10), *NRAS* (2/10), and *MAP2K1* (1/10), mainly at hotspots (*BRAF*: G469A/R, V600E, K601E, *KRAS*: G13D, *NRAS*: Q61R/H). Moreover, these variants were present at low variant allele frequencies (VAFs) (1.85%–28%) (Table S5), and samples with these mutations displayed a higher number of mutated genes than the rest of del-3′IGH CLLs (median 4 vs. 2, $p = .001$). However, only 38% of CLL patients with RAS-related mutations had additional FISH cytogenetic alterations, and indeed, only one of them carried additional trisomy 12 (Figure 2B).

3.3 | Del-3′IGH CLLs frequently exhibit a biallelic *TRAF3* inactivation by deletion and mutation

TRAF3 showed a higher mutational frequency (7/54, 13%) within del-3′IGH CLL patients compared with the control group (1/263, 0.4%) ($p < .001$) (Figure 2A), and to previously reported large cohorts of CLL patients[21,25] (0.5%–1%). A total of 20 *TRAF3* mutations were detected in seven samples (Figure 2C). Interestingly, most *TRAF3*-mutated patients carried more than one mutation in this gene (5/7), with a median of 2 (range: 1–6) and at low VAFs (15/20 with VAF <15%) (Table S6). Regarding the type of mutations, whereas 11 out of 20 were frameshift insertion/deletion or encoded for a stop codon that led to truncated proteins, the remaining (9/20) were missense substitutions annotated as pathogenic by the bioinformatic predictors

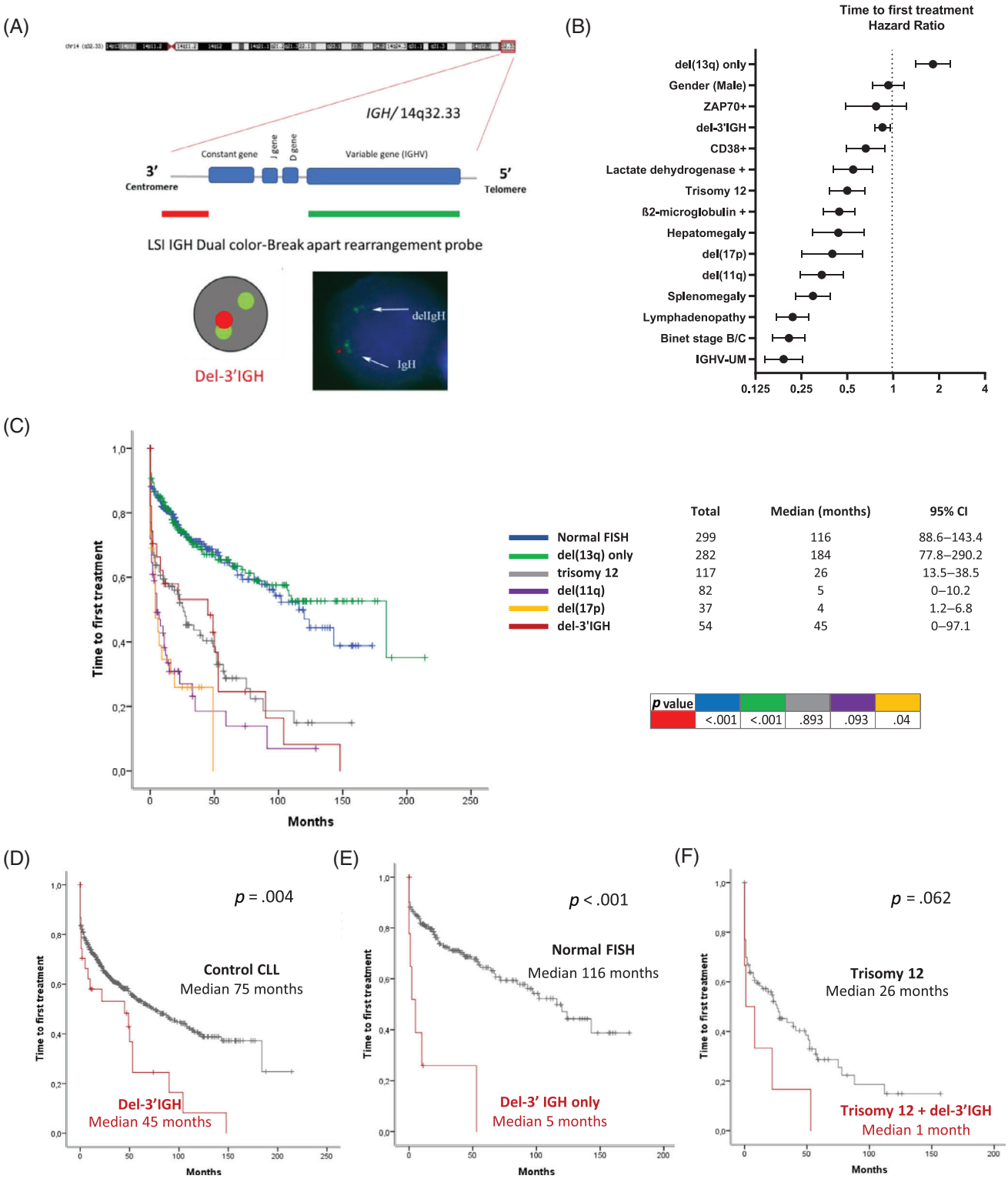

FIGURE 1 Deletion of the centromeric side of *IGH* constant region (del-3′IGH) and its clinical impact on chronic lymphocytic leukemia (CLL). (A) Schematic interphase FISH signal pattern of 3′IGH deletion (del-3′IGH) obtained with the IGH break-apart probe in CLL. (B) Hazard ratios of clinical–biological variables for time to first treatment (TFT) of CLL patients in univariate Cox regression analyses ($n = 871$). (C) TFT according to the cytogenetic alterations (del(13q), del(11q), del(17p), trisomy 12, del-3′IGH). Cytogenetic-risk classification is described in the Supplementary material. (D) TFT of del-3′IGH group versus control group in CLL. Control group represents those patients without del-3′IGH. (E) Clinical impact of del-3′IGH as the only abnormality in the context of normal FISH. (F) Clinical impact of the co-occurrence of del-3′IGH and trisomy 12 when compared with trisomy 12 as the sole abnormality. FISH, fluorescence in situ hybridization.

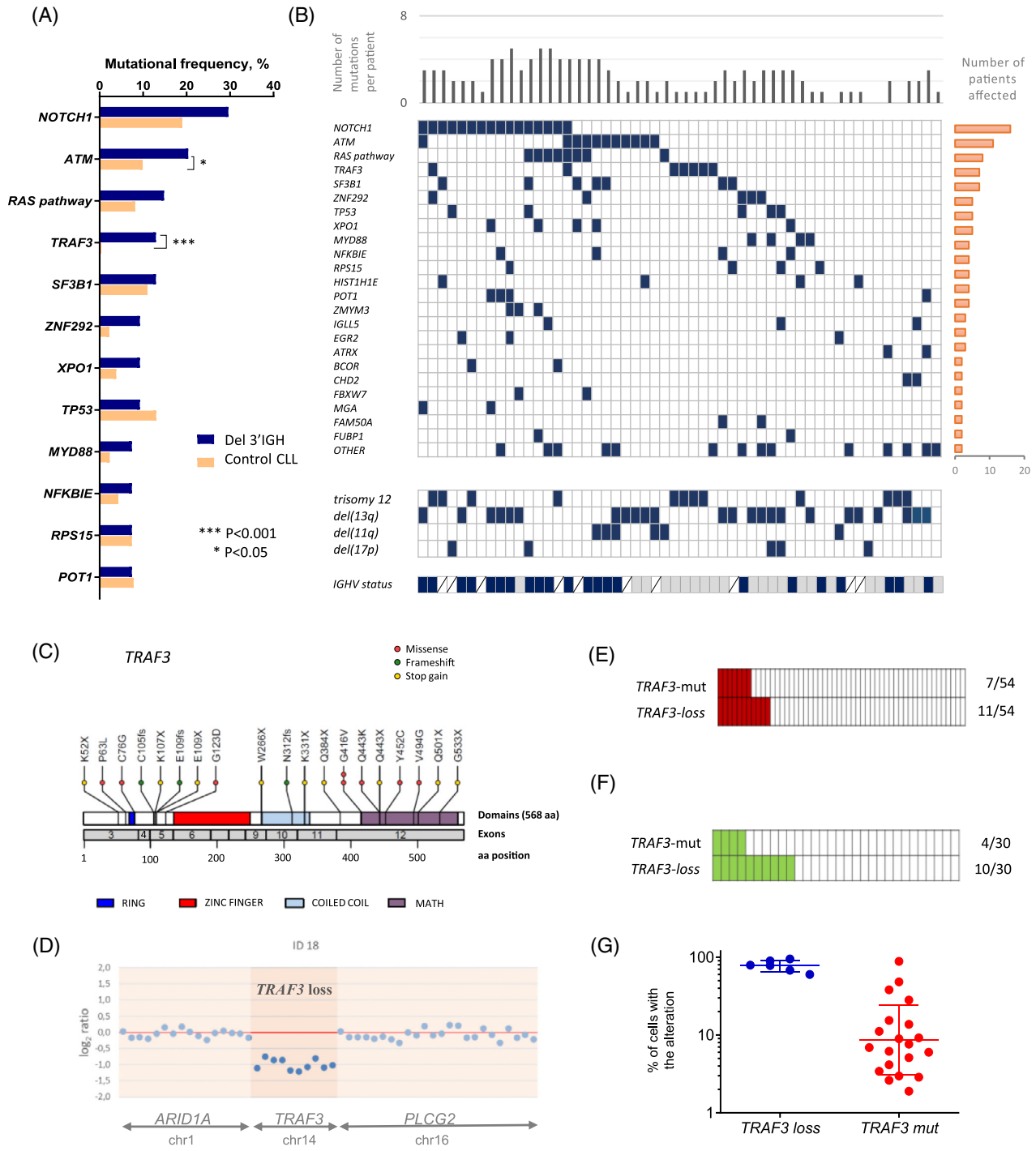

FIGURE 2 Mutational landscape of CLLs with del-3′IGH. (A) Mutational frequencies of CLL genes in del-3′IGH (blue bars) versus control group (orange bars) ($n = 317$). (B) Waterfall plot of genetic and cytogenetic landscape of 54 patients carrying del-3′IGH. Mutations and cytogenetic alterations in the heat map are shown in blue. For the IGHV status, light blue refers to mutated IGHV and dark blue to unmutated IGHV. Crossed lines represent missing data. Number of patients with each mutation are shown at the right orange chart bar and number of mutations per patient are shown in the gray chart bar above the heat map. (C) *TRAF3* mutations identified in 54 del-3′IGH CLLs. Positions of coding mutations are indicated according to the amino acid (aa) change at the protein level (Transcript: ENST00000392745/NM_145725). Number of cases are denoted by circles in each mutation line and the color of the circles indicates the mutation subtype (missense, frameshift or nonsense/stop gain). (D) Dot plot representation of *TRAF3* copy number (CN) loss in one CLL patient (all del-3′IGH cases with a *TRAF3* loss are shown in Figure S3). The *x*-axis represents the targets of chromosomes 1, 14, and 16 included in the custom NGS panel (*ARID1A*, *TRAF3*, and *PLCG2*, respectively). The y-axis shows the values of the $\log_2$ ratio. The red line indicates the reference. (E) *TRAF3* alterations by mutation and/or deletion (red bars) in our cohort of del-3′IGH CLL patients. (F) *TRAF3* alterations by deletion and/or mutation in the validation cohort[25] (green bars) (Table S8). (G) Percentage of altered cells with *TRAF3* loss (blue, % del-3′IGH cells by FISH) or *TRAF3* mutation (red, % variant allele frequency by NGS). Mean value is represented by a horizontal bar and standard deviation is represented by vertical bars. FISH, fluorescence in situ hybridization

of pathogenicity (Figure 2C, Table S5). Moreover, *TRAF3* was the only mutated gene in four cases, while three *TRAF3*-mutated patients also exhibited other genetic mutations (Figure 2B, Table S6).

TRAF3 is located in chromosome 14q32.32 region, proximal to the centromeric side of IGH locus (14q32.33). Due to this proximity, we hypothesized that del-3′IGH could comprise *TRAF3*. Indeed, the CNV analyses with NGS data in the whole cohort of 317 CLLs identified a *TRAF3* loss in 11 patients within the del-3′IGH subgroup (11/54, 20%) (Figures 2D and S3), but only 4 in the control group (4/263, 1.5%) (Table S7). Therefore, *TRAF3* loss was significantly enriched in del-3′IGH CLL patients in comparison to the control group (20 vs. 1.5%, $p < .001$). By SNP arrays, we confirmed the presence or absence of *TRAF3* deletion observed by NGS in two del-3′IGH CLL patients with available material (Figure S1, Table S4). The size of the deletion in patient A (ID 23) comprised only 14q32.33 region (*IGH* locus), with an absence of *TRAF3* loss, while deletion in patient B (ID 28) mapped from 14q24.1 to 14q32.32, including *3′IGH* locus and *TRAF3* (as we observed in CNV analysis) (Tables S4 and S7).

Integrating both mutational and CNV information, we observed that 7 of 11 patients with a *TRAF3* loss also displayed mutations in this gene (Figure 2E, Table S6). To further validate these findings, we reviewed the mutational status of 30 cases with 14q loss from an external published cohort of CLL patients with mutational and CNV information.[25] Within those patients, 14q loss comprised *TRAF3* gene in a total of 10 cases, and 4 of them harbored mutations in this gene, corroborating the presence of biallelic *TRAF3* alterations in this subset of CLL patients (Figure 2F, Table S8).

As we confirmed that *TRAF3* could be included in the 14q32.3 deletion, we next analyzed which event was earlier in time: mutation or deletion. According to our results, the deletion was present in a higher percentage of cells (mean: 70.5 ± 6.5), while mutations occurred at low VAFs (15.6 ± 4.7), indicating that *TRAF3* mutations may appear as a second or subclonal event, leading to a biallelic inactivation of this gene (Figure 2F).

3.4 | Co-occurrence of del-3′IGH and gene mutations contributes to an adverse clinical outcome in CLL patients

Given the high incidence of mutations in poor-prognosis genes, we next wondered if the combination of del-3′IGH and these alterations could have an impact in the clinic. Interestingly, only *TRAF3* mutations exhibited a significantly shorter TFT in this subgroup of patients (median TFT: 6 vs. 51 months, $p < .001$) (Figure 3A). In addition, mutations in *NOTCH1*, *ATM*, and RAS signaling pathway refined patients' outcome in terms of OS (Figure 3B–D).

Patients harboring *NOTCH1* mutations within del-3′IGH subgroup showed a shorter median OS than *NOTCH1-wt* del-3′IGH CLLs (16 months vs. median not reached, $p = .009$) (Figure 3B). Moreover, considering the whole CLL cohort ($n = 317$), we observed that median OS of cases with *NOTCH1-mut* and del-3′IGH was shorter than NOTCH1-*wt* (16 vs. 144 months, $p = .001$), with a stronger statistical significance than the comparison between *NOTCH1-mut* without the deletion and NOTCH1-*wt* cases (120 vs. 144 months, $p = .155$) (Figure S4A).

Interestingly, *ATM* mutations had a significant negative impact on del-3′IGH CLL OS (14 vs. median not reached, $p = .04$) (Figure 3C), and the presence of mutations in the RAS signaling pathway also contributed to a shorter OS in comparison to RAS-*wt* patients (12 vs. median not reached, $p = .004$) (Figure 3D). As we observed in *NOTCH1*-mutated cases with concurrent del-3′IGH, those patients with mutations in *ATM* or in RAS signaling pathway genes that also carried del-3′IGH had a significantly reduced OS than non-del-3′IGH CLLs harboring these mutations, when compared with cases without these alterations (*ATM*: 14 months vs. median not reached, $p = .006$; 92 months vs. median not reached, $p = .99$) (RAS-related genes: 12 months vs. median not reached, $p = .001$; 41 months vs. median not reached, $p = .001$) (Figure S4B,C). Hence, these results demonstrate that concurrent del-3′IGH and mutations in the aforementioned genes could contribute to a worse outcome in CLL patients.

3.5 | *TRAF3* biallelic inactivation drives progression in del-3′IGH patients and constitutes an independent prognostic marker of TFT

Considering that *TRAF3* has an exceptional high frequency of mutation and that it is the only gene with an impact on TFT within this subgroup, we were prompted to delve into the clinical implications of *TRAF3* alterations (deletion and/or mutation). For that purpose, we determined their statistical association with clinical parameters as well as their impact in prognosis and survival when compared with the rest of del-3′IGH and the CLL control group.

In terms of clinical features, patients carrying *TRAF3* alterations had a significant decrease of white blood cells, lymphocytes, and platelets counts and lower levels of hemoglobin. A total of 45.5% of patients exhibited Binet B/C stage and 54.5% were IGHV-UM (Table S9). Notably, all *TRAF3*-altered patients (with mutations and/or deletion) received treatment during their follow-up and showed a significantly shorter median TFT than the rest of del-3′IGH patients (6 vs. 54 months, $p < .001$) (Figure S5A). By contrast, we found no significant statistical differences between median OS of *TRAF3*-altered patients and that of the rest of del-3′IGH (68 vs. 144 months, $p = .14$) (Figure S5B).

As expected, CLL-IPI and IPS-E score systems were able to stratify patients in terms of TFT in the whole cohort ($n = 317$). However, focusing on the del-3′IGH subgroup, CLL-IPI nor IPS-E discriminate risk subgroups with different TFT. Strikingly, the presence of *TRAF3* alterations was an independent risk factor in the multivariate analyses, not only in the whole cohort but also in del-3′IGH patients ($n = 54$) (Figure S6).

In this work, we described a pathological mechanism well known in CLL, consistent with a gene dysfunction caused by a biallelic alteration (deletion and mutation). For this reason, we next carried out an integrated clinical analysis to determine the prognosis impact of biallelic *TRAF3* alterations with respect to other biallelic inactivation phenomena previously associated with an adverse prognosis (biallelic

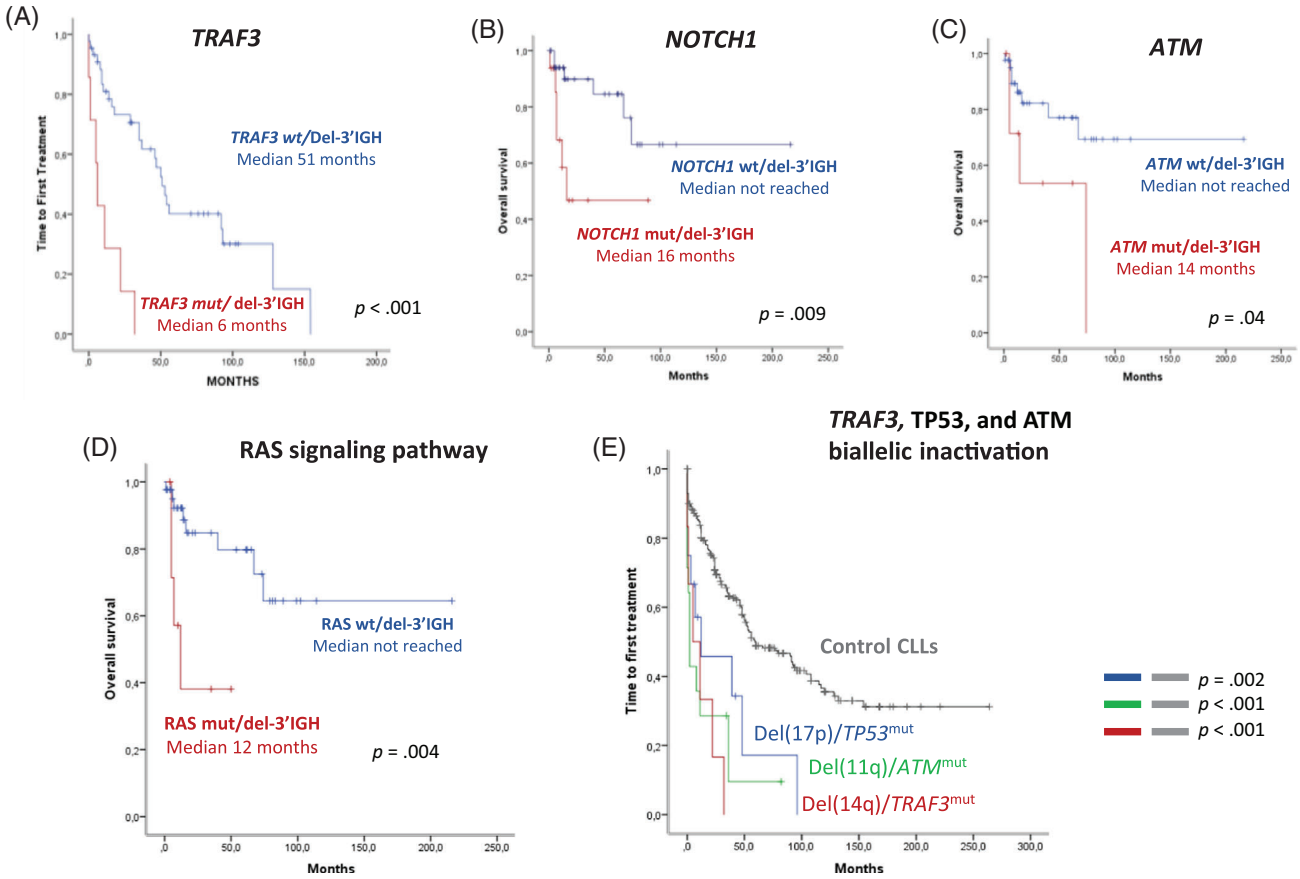

FIGURE 3 Clinical outcome of CLL patients according to the co-occurrence of del-3′IGH and different genetic alterations. (A) TFT of del-3′IGH CLL patients according to the presence of *TRAF3* mutations ($n = 54$). OS of del-3′IGH CLL patients with (B) *NOTCH1* mutations, (C) *ATM* mutations, and (D) mutations in the RAS signaling pathway ($n = 54$). (E) Clinical impact of biallelic inactivation by deletion and mutation of *TP53*, *ATM*, and *TRAF3* in the TFT of CLL patients ($n = 317$)

TP53 (del(17p) and *TP53* mutations) and *ATM* (del(11q) and *ATM* mutations) in the entire CLL cohort ($n = 317$). Our results showed that a total of 16 out of 317 CLLs had a biallelic loss of *TP53* by deletion and mutation, while 14 patients had *ATM* biallelic inactivation (Table S2). All biallelic alterations analyzed had a significant negative impact on TFT (median *TRAF3*: 5 vs. 59 months, $p < .001$, *ATM*: 2 vs. 59, $p < 0.001$ and *TP53*: 12 vs. 59, $p = .002$) (Figure 3E). Interestingly, median TFT of biallelic *TRAF3* inactivation was similar to that of biallelic *ATM* and *TP53* loss, identifying a novel subgroup with inferior outcome. Moreover, the presence of biallelic *TRAF3* alteration was an independent risk factor in the multivariate analyses, suggesting this gene as a new potential biomarker of prognosis (HR = 0.21, 95% CI = 0.05–0.85, $p = .029$) (Table 1).

TABLE 1 Multivariate Cox model analysis of TFT in CLL patients ($n = 317$)

		95% CI		
	HR	Lower	Upper	*p*
Binet stage B/C	0.16	0.08	0.32	**<.001**
IGHV-unmutated	0.36	0.20	0.62	**<.001**
CD38+	0.72	0.41	1.28	.267
High LDH	0.69	0.35	1.37	.289
High β2-M	1.00	0.56	1.80	.988
Hepatomegaly	0.32	0.10	1.04	.058
Splenomegaly	0.95	0.47	1.92	.896
Biallelic *TP53* alteration	0.19	0.04	0.88	**.034**
Biallelic *ATM* alteration	0.75	0.9	1.93	.549
Biallelic *TRAF3* alteration	0.21	0.05	0.85	**.029**

Note: Significant values are shown in bold.
Abbreviations: CI, confidence interval; CLL, chronic lymphocytic leukemia; HR, hazard ratio; LDH, lactate dehydrogenase level; TFT, time to first treatment; β2M, β2-microglobulin level.

4 | DISCUSSION

Chromosomal abnormalities involving 14q are recurrently observed in B-cell neoplasms.[6] In CLL, interstitial 14q deletions are found in ≈5% of

cases and have a variable size ranging from 14q24 to 14q32.33 regions, being the *IGH* locus the most frequent breakpoint at the telomeric side.[4,5,17] Here, we report the largest CLL cohort with a 3′IGH deletion analyzed by FISH and NGS. Specifically, 54 out of 871 CLL patients (6.2%) had a del-3′IGH, representing a group characterized by an enrichment of *TRAF3* alterations, which had a negative impact in prognosis.

According to our results, the deletion of 3′IGH was monoallelic and was present in a high percentage of cells in most cases (median: 65%). This alteration occurred simultaneously with other cytogenetic alterations in 76% of cases, being the most frequent in the del(13q) and trisomy 12. This enrichment of trisomy12 has been previously reported, not only in CLL with del(14q),[4,5,17,35] but also in other neoplasms with this aberration,[6] and furthermore, with other *IGH* abnormalities such as *IGH* translocations,[13,16,36–39] suggesting a strong cooperation between both genetic events.

With respect to the clinical characteristics of del-3′IGH CLL patients, the presence of the deletion had a negative impact on TFT, especially when compared with low-risk cytogenetics, and quite similar to that of the intermediate-risk subgroups (Figure 1C). Previous data also showed an adverse clinical impact of del(14q), although the prognosis was closer to high-risk (del(11q) and del(17p)) than to intermediate-risk cytogenetics.[5] Unlike previous studies,[5,17] we did not observe a significant association between del-3′IGH and IGHV-UM (Table S1). Nevertheless, we did find that del-3′IGH CLLs without additional cytogenetic abnormalities showed a marked poorer outcome in terms of TFT than patients with normal FISH, corroborating the clinical impact of the del-3′IGH in CLL (Figure 1E). With respect to trisomy 12, it is important to highlight that those patients with both alterations (trisomy 12 and del-3′IGH) exhibited shorter TFT than CLLs with trisomy 12 as the sole abnormality (Figure 1F), suggesting that the prognosis observed in the entire del-3′IGH cohort is independent of the trisomy 12 co-occurrence.[5,17] Therefore, this study highlights the value of including the *IGH* probe in the CLL FISH panel to improve CLL prognostic stratification, since it allows us to detect two types of *IGH* abnormalities (deletion and rearrangement), both with a clinical impact.[5,11,13,14,17,40] Thus, this study contributes a significant step forward in the improvement of CLL prognostication.[41]

For a deeper understanding of the molecular pathogenesis of del-3′IGH CLLs, we assessed the mutational profile of this subgroup by NGS. Interestingly, del-3′IGH CLLs harbored a median of two mutations per patient and a high incidence of mutations in *NOTCH1* (30%), *ATM* (20%), *TRAF3* (13%), and RAS signaling pathway genes (15%) (*BRAF*, *KRAS*, *NRAS*, *MAP2K1*) (Figure 2). These results are consistent with the enrichment of *NOTCH1* mutations previously identified in 14q-deleted CLLs.[17] The presence of *TRAF3* mutations in patients with del(14q) has also been described in some B-cell neoplasms,[20] but to our knowledge, this is the first time that it has been described a remarkably high mutational rate within del-3′IGH CLLs as well as a significant association between *TRAF3* mutations and del(14q).

As *NOTCH1* and *RAS* signaling pathway mutations have been extensively related to trisomy 12,[42–48] the mutational frequencies observed in our del-3′IGH cohort could suggest that this entity exhibits a similar mutational pattern. However, the presence of high mutational rates in *ATM* and *TRAF3* identifies a distinct genetic profile with multiple biological pathways affected, involved in proliferative and pro-survival functions as well as in DNA damage repair. Notably, the alteration of multiple pathways and the mutational burden have been previously related to shorter TFT and OS.[25] In our series, the presence of mutations in *NOTCH1*, *ATM*, and RAS pathway within del-3′IGH subgroup had a negative impact on the OS, whereas only *TRAF3* mutations were able to stratify del-3′IGH prognosis in terms of TFT (Figures 3 and S4).

TRAF3 is a negative regulator of the non-canonical NF-κB pathway, and their mutations may lead to a constitutive NF-κB activation.[49] Dysregulation of the non-canonical NF-κB signaling has been shown to play an important role in B-cell transformation and CLL pathogenesis, especially due to *BIRC3* alterations.[33,50–52] Besides *TRAF3* mutations, we also detected mutations in other genes involved in this pathway, more related to the canonical NF-κB signaling (*MYD88* and *NFKBIE*), which may indicate a deregulation of both canonical and non-canonical pathways in del-3′IGH CLL patients. Remarkably, we did not observe co-occurrences of mutations in NF-κB pathway-related genes, and most *TRAF3* mutations appeared as the only mutated gene within this pathway, suggesting mutual exclusive phenomena.

TRAF3 is located at chromosome 14q32.32, proximal to the IGH locus, and it is frequently included in the 14q deletion observed in CLL and other B-cell neoplasms.[4,20] Indeed, our results show that both loss and mutations of *TRAF3* are significantly enriched in del-3′IGH CLL patients. Additionally, we reported that *TRAF3* mutations appeared at lower VAFs than FISH IGH-deleted cells (Figure 2F), suggesting that the mutation could be an acquired secondary event in CLL evolution. The combination of deletion and mutation results in biallelic inactivation of *TRAF3*, which resembles the mechanism of other CLL driver genes dysfunction with a relevant clinical significance in the disease (*TP53* and *ATM*). Besides the clinical impact of *TP53* monoallelic alterations (deletion or mutation) in CLL patients, it has been demonstrated that double null of this gene contributes to a marked poor outcome.[53–56] Regarding *ATM* alterations, latest studies may indicate a stronger negative impact when combined *ATM* loss by 11q deletion and mutations in the remaining allele,[48,57,58] although there is still some controversy. In our cohort, our results showed that biallelic inactivation of *TP53* and *ATM* had a strong negative impact in the TFT of CLL patients and, interestingly, deletion and mutation of *TRAF3* also contributed to a poor outcome, in line with those double-hit alterations (Figure 3E). Moreover, multivariate analysis confirmed that *TRAF3* alterations constitute an independent risk factor of TFT, also in models with prognostic indexes (CLL-IPI and IPS-E) used in clinical practice (Tables 1 and S6), which could help physicians predict the prognosis of CLL patients and guide follow-up approaches. Taken together, our results also suggest that the biallelic inactivation of *TRAF3* could be driving CLL progression, especially in this subgroup of patients with del 3′-IGH.

Taking into account that this study was retrospective and more than 90% of patients received chemotherapeutic regimens, several limitations were found to answer further questions. It would be of great interest to assess the response to novel drugs according to *TRAF3* status in CLL, as well as to evaluate its potential value as a

prognostic and predictive biomarker in the era of novel agents.[41,59] In addition, performing a sequential genetic analysis during disease evolution could help to understand when the del-3′IGH usually appears and if this cytogenetic alteration plays a role as an early or late alteration in CLL. Moreover, 14q deletion including del-3′IGH may encompass other genes (apart from those analyzed in this study) that could also influence CLL pathogenesis and prognosis, and further investigations on the molecular landscape of this entity would be relevant.

In conclusion, a specific subgroup of CLLs carrying del-3′IGH was characterized by a distinct genetic profile harboring mutations affecting multiple biological pathways (NOTCH, RAS, DNA damage response, and NF-κB signaling), which also had a negative impact in CLL prognosis. Moreover, *TRAF3* biallelic inactivation by deletion and mutation, highly enriched in this del-3′IGH of CLL patients, contributes to a marked poor outcome in this subgroup of patients. Taken together, our study provides new insights into the mechanisms of pathogenesis of this CLL cytogenetic subgroup, as well as additional clinical information regarding the combination of different genetic alterations that suggests the emergence of novel molecular biomarkers. In addition, these results also manifest the importance of the IGH assessment, as it allows to classify CLL patients with poor outcomes that would be considered as low-risk cytogenetics otherwise.

ACKNOWLEDGMENTS

We are grateful to I. Rodríguez, S. González, T. Prieto, M.Á. Ramos, A. Martín, A. Díaz, A. Simón, M. del Pozo, V. Gutiérrez and S. Pujante from the Centro de Investigación del Cáncer, Salamanca, for their technical assistance.

FUNDING INFORMATION

This work was supported by grants from the Spanish Fondo de Investigaciones Sanitarias PI18/01500, PI21/00983 Instituto de Salud Carlos III (ISCIII), European Regional Development Fund (ERDF) "Una manera de hacer Europa", "Consejería de Educación, Junta de Castilla y León" (SA118P20), "Gerencia Regional de Salud, SACYL", Spain: GRS2140/A/20, GRS2385/A/21 "Fundación Memoria Don Samuel Solórzano Barruso" FS/33–2020, by grants (RD12/0036/0069) from Red Temática de Investigación Cooperativa en Cáncer (RTICC) and Centro de Investigación Biomédica en Red de Cáncer (CIBERONC CB16/12/00233). Claudia Pérez-Carretero is supported by a PFIS grant (FI19/00191) from Instituto de Salud Carlos III; María Hernández-Sánchez has been supported by a Sara Borrell post-doctoral contract (CD19/00222) from the Instituto de Salud Carlos III (ISCIII). PFIS grant and Sara Borrell post-doctoral contract is co-founded by Fondo Social Europeo (FSE) "El Fondo Social Europeo invierte en tu futuro"; Miguel Quijada-Álamo is supported by a research grant from FEHH ("Fundación Española de Hematología y Hemoterapia"; Beca de Investigación FEHH 2020), Rocío Benito is supported by a grant from the Universidad de Salamanca ("Contrato postdoctoral programa II 2020-21").

CONFLICT OF INTEREST

The authors declare no competing interests.

AUTHOR CONTRIBUTIONS

Claudia Pérez-Carretero and María Hernández-Sánchez designed research, performed sample selection, carried out NGS and statistical analyses, and drafted the manuscript. Teresa González performed sample selection, FISH analyses, and provided clinical and immunophenotypic data. Miguel Quijada-Álamo contributed to data analysis and interpretation of the results and critically reviewed the manuscript. Marta Martín-Izquierdo, Sandra Santos-Mínguez, Cristina Miguel-García performed NGS studies and data analysis. María-Jesús Vidal, Alfonso García-De-Coca, Josefina Galende, Emilia Pardal, Carlos Aguilar, Manuel Vargas-Pabón, Julio Dávila, Isabel Gascón-Y-Marín provided patients' clinical data. José-Ángel Hernández-Rivas provided clinical data and critically reviewed the manuscript. Rocío Benito designed sequencing studies and contributed to data analysis. Ana-Eugenia Rodríguez-Vicente performed SNP arrays studies, data analysis, and together with Jesús-María Hernández-Rivas conceived the study, designed and supervised the research, and critically reviewed and approved the final version of the manuscript. All authors discussed the results and revised the manuscript.

DATA AVAILABILITY STATEMENT

The data that support the findings of this study are available from the corresponding author upon reasonable request.

ORCID

Claudia Pérez-Carretero https://orcid.org/0000-0002-2089-2742
Marta Martín-Izquierdo https://orcid.org/0000-0002-5290-2116
Emilia Pardal https://orcid.org/0000-0001-7712-7876
Julio Dávila https://orcid.org/0000-0002-5185-2073
Jesús-María Hernández-Rivas https://orcid.org/0000-0002-9661-9371
Ana-Eugenia Rodríguez-Vicente https://orcid.org/0000-0001-6516-2172

REFERENCES

1. Nowakowski GS, Dewald GW, Hoyer JD, et al. Interphase fluorescence in situ hybridization with an IGH probe is important in the evaluation of patients with a clinical diagnosis of chronic lymphocytic leukaemia. *Br J Haematol*. 2005;130(1):36-42.
2. Berkova A, Pavlistova L, Babicka L, et al. Combined molecular biological and molecular cytogenetic analysis of genomic changes in 146 patients with B-cell chronic lymphocytic leukemia. *Neoplasma*. 2008;55(5):400-408.
3. Lu G, Kong Y, Yue C. Genetic and immunophenotypic profile of IGH@ rearrangement detected by fluorescence in situ hybridization in 149 cases of B-cell chronic lymphocytic leukemia. *Cancer Genet Cytogenet*. 2010;196(1):56-63.
4. Pospisilova H, Baens M, Michaux L, et al. Interstitial del(14)(q) involving IGH: a novel recurrent aberration in B-NHL. *Leukemia*. 2007;21(9):2079-2083.
5. Reindl L, Bacher U, Dicker F, et al. Biological and clinical characterization of recurrent 14q deletions in CLL and other mature B-cell neoplasms. *Br J Haematol*. 2010;151(1):25-36.
6. Mitelman F, Johanson B, Mertens F. Mitelman Database of Chromosome Aberrations in Cancer. 2014. http://cgap.nci.nih.gov/Chromosomes/Mitelman.
7. Damle RN, Wasil T, Fais F, et al. Ig V gene mutation status and CD38 expression as novel prognostic indicators in chronic lymphocytic leukemia. *Blood*. 1999;94(6):1840-1847.

8. Hamblin TJ, Davis Z, Gardiner A, Oscier DG, Stevenson FK. Unmutated Ig V(H) genes are associated with a more aggressive form of chronic lymphocytic leukemia. *Blood*. 1999;94(6):1848-1854.
9. Mayr C, Speicher MR, Kofler DM, et al. Chromosomal translocations are associated with poor prognosis in chronic lymphocytic leukemia. *Blood*. 2006;107(2):742-751.
10. Van Den Neste E, Robin V, Francart J, et al. Chromosomal translocations independently predict treatment failure, treatment-free survival and overall survival in B-cell chronic lymphocytic leukemia patients treated with cladribine. *Leukemia*. 2007;21(8):1715-1722.
11. Cavazzini F, Hernandez JA, Gozzetti A, et al. Chromosome 14q32 translocations involving the immunoglobulin heavy chain locus in chronic lymphocytic leukaemia identify a disease subset with poor prognosis. *Br J Haematol*. 2008;142(4):529-537.
12. Jimenez-Zepeda VH, Chng WJ, Schop RF, et al. Recurrent chromosome abnormalities define nonoverlapping unique subgroups of tumors in patients with chronic lymphocytic leukemia and known karyotypic abnormalities. *Clin Lymphoma Myeloma Leuk*. 2013;13(4):467-476.
13. Pérez-Carretero C, Hernández-Sánchez M, González T, et al. Chronic lymphocytic leukemia patients with IGH translocations are characterized by a distinct genetic landscape with prognostic implications. *Int J Cancer*. 2020;147(10):2780-2792.
14. Davids MS, Vartanov A, Werner L, Neuberg D, Dal Cin P, Brown JR. Controversial fluorescence in situ hybridization cytogenetic abnormalities in chronic lymphocytic leukaemia: new insights from a large cohort. *Br J Haematol*. 2015;170(5):694-703.
15. Hwang Y, Lee JY, Mun YC, Seong CM, Chung WS, Huh J. Various patterns of IgH deletion identified by FISH using combined IgH and IgH/CCND1 probes in multiple myeloma and chronic lymphocytic leukemia. *Int J Lab Hematol*. 2011;33(3):299-304.
16. Leeksma AC, Baliakas P, Moysiadis T, et al. Genomic arrays identify high-risk chronic lymphocytic leukemia with genomic complexity: a multi-center study. *Haematologica*. 2021;106(1):87-97.
17. Cosson A, Chapiro E, Belhouachi N, et al. 14q deletions are associated with trisomy 12, NOTCH1 mutations and unmutated IGHV genes in chronic lymphocytic leukemia and small lymphocytic lymphoma. *Genes Chromosomes Cancer*. 2014;53(8):657-666.
18. Wlodarska I, Matthews C, Veyt E, et al. Telomeric IGH losses detectable by fluorescence in situ hybridization in chronic lymphocytic leukemia reflect somatic VH recombination events. *J Mol Diagn*. 2007;9(1):47-54.
19. Quintero-Rivera F, Nooraie F, Rao PN. Frequency of 5'IGH deletions in B-cell chronic lymphocytic leukemia. *Cancer Genet Cytogenet*. 2009;190(1):33-39.
20. Nagel I, Bug S, Tönnies H, et al. Biallelic inactivation of TRAF3 in a subset of B-cell lymphomas with interstitial del(14)(q24.1q32.33). *Leukemia*. 2009;23(11):2153-2155.
21. Landau DA, Tausch E, Taylor-Weiner AN, et al. Mutations driving CLL and their evolution in progression and relapse. *Nature*. 2015; 526(7574):525-530.
22. Hallek M, Cheson BD, Catovsky D, et al. iwCLL guidelines for diagnosis, indications for treatment, response assessment, and supportive management of CLL. *Blood*. 2018;131(25):2745-2760.
23. Group IC-Iw. An international prognostic index for patients with chronic lymphocytic leukaemia (CLL-IPI): a meta-analysis of individual patient data. *Lancet Oncol*. 2016;17(6):779-790.
24. Condoluci A, Terzi di Bergamo L, Langerbeins P, et al. International prognostic score for asymptomatic early-stage chronic lymphocytic leukemia. *Blood*. 2020;135(21):1859-1869.
25. Puente XS, Beà S, Valdés-Mas R, et al. Non-coding recurrent mutations in chronic lymphocytic leukaemia. *Nature*. 2015;526(7574): 519-524.
26. González MB, Hernández JM, García JL, et al. The value of fluorescence in situ hybridization for the detection of 11q in multiple myeloma. *Haematologica*. 2004;89(10):1213-1218.
27. Quijada-Álamo M, Hernández-Sánchez M, Robledo C, et al. Next-generation sequencing and FISH studies reveal the appearance of gene mutations and chromosomal abnormalities in hematopoietic progenitors in chronic lymphocytic leukemia. *J Hematol Oncol*. 2017; 10(1):83.
28. Hernández-Sánchez M, Rodríguez-Vicente AE, y Marín IG, et al. DNA damage response-related alterations define the genetic background of patients with chronic lymphocytic leukemia and chromosomal gains. *Exp Hematol*. 2019;72:9-13.
29. Quijada-Álamo M, Hernández-Sánchez M, Alonso-Pérez V, et al. CRISPR/Cas9-generated models uncover therapeutic vulnerabilities of del(11q) CLL cells to dual BCR and PARP inhibition. *Leukemia*. 2020;34:1599-1612.
30. Quijada-Álamo M, Pérez-Carretero C, Hernández-Sánchez M, et al. Dissecting the role of TP53 alterations in del(11q) chronic lymphocytic leukemia. *Clin Transl Med*. 2021;11(2):e304.
31. Feng Y, Chen D, Wang GL, Zhang VW, Wong LJ. Improved molecular diagnosis by the detection of exonic deletions with target gene capture and deep sequencing. *Genet Med*. 2015;17(2):99-107.
32. Bastida JM, Lozano ML, Benito R, et al. Introducing high-throughput sequencing into mainstream genetic diagnosis practice in inherited platelet disorders. *Haematologica*. 2018;103(1):148-162.
33. Quijada-Álamo M, Hernández-Sánchez M, Rodríguez-Vicente AE, et al. Biological significance of monoallelic and biallelic BIRC3 loss in del(11q) chronic lymphocytic leukemia progression. *Blood Cancer J*. 2021;11(7):127.
34. Parker H, Rose-Zerilli MJ, Parker A, et al. 13q deletion anatomy and disease progression in patients with chronic lymphocytic leukemia. *Leukemia*. 2011;25(3):489-497.
35. Roos-Weil D, Nguyen-Khac F, Chevret S, et al. Mutational and cytogenetic analyses of 188 CLL patients with trisomy 12: a retrospective study from the French Innovative Leukemia Organization (FILO) working group. *Genes Chromosomes Cancer*. 2018;57(11):533-540.
36. Martín-Subero JI, Ibbotson R, Klapper W, et al. A comprehensive genetic and histopathologic analysis identifies two subgroups of B-cell malignancies carrying a t(14;19)(q32;q13) or variant BCL3-translocation. *Leukemia*. 2007;21(7):1532-1544.
37. Chapiro E, Radford-Weiss I, Bastard C, et al. The most frequent t(14; 19)(q32;q13)-positive B-cell malignancy corresponds to an aggressive subgroup of atypical chronic lymphocytic leukemia. *Leukemia*. 2008; 22(11):2123-2127.
38. Nguyen-Khac F, Chapiro E, Lesty C, et al. Specific chromosomal IG translocations have different prognoses in chronic lymphocytic leukemia. *Am J Blood Res*. 2011;1(1):13-21.
39. Fang H, Reichard KK, Rabe KG, et al. IGH translocations in chronic lymphocytic leukemia: clinicopathologic features and clinical outcomes. *Am J Hematol*. 2019;94(3):338-345.
40. Harris RA, Stevens JM, Pickering DL, et al. Frequency, variations, and prognostic implications of chromosome 14q32 deletions in chronic lymphocytic leukemia. *Leuk Res*. 2021;110:106665.
41. Pérez-Carretero C, González-Gascón-Y-Marín I, Rodríguez-Vicente AE, et al. The evolving landscape of chronic lymphocytic leukemia on diagnosis, prognosis and treatment. *Diagnostics*. 2021;11 (5):853.
42. López C, Delgado J, Costa D, et al. Different distribution of NOTCH1 mutations in chronic lymphocytic leukemia with isolated trisomy 12 or associated with other chromosomal alterations. *Genes Chromosomes Cancer*. 2012;51(9):881-889.
43. Del Giudice I, Rossi D, Chiaretti S, et al. NOTCH1 mutations in +12 chronic lymphocytic leukemia (CLL) confer an unfavorable prognosis, induce a distinctive transcriptional profiling and refine the intermediate prognosis of +12 CLL. *Haematologica*. 2012;97(3):437-441.
44. Balatti V, Bottoni A, Palamarchuk A, et al. NOTCH1 mutations in CLL associated with trisomy 12. *Blood*. 2012;119(2):329-331.

45. Weissmann S, Roller A, Jeromin S, et al. Prognostic impact and landscape of NOTCH1 mutations in chronic lymphocytic leukemia (CLL): a study on 852 patients. *Leukemia*. 2013;27(12):2393-2396.
46. Giménez N, Martínez-Trillos A, Montraveta A, et al. Mutations in the RAS-BRAF-MAPK-ERK pathway define a specific subgroup of patients with adverse clinical features and provide new therapeutic options in chronic lymphocytic leukemia. *Haematologica*. 2019; 104(3):576-586.
47. Vendramini E, Bomben R, Pozzo F, et al. KRAS, NRAS, and BRAF mutations are highly enriched in trisomy 12 chronic lymphocytic leukemia and are associated with shorter treatment-free survival. *Leukemia*. 2019;33(8):2111-2115.
48. Blakemore SJ, Clifford R, Parker H, et al. Clinical significance of TP53, BIRC3, ATM and MAPK-ERK genes in chronic lymphocytic leukaemia: data from the randomised UKLRF CLL4 trial. *Leukemia*. 2020;34(7): 1760-1774.
49. Moore CR, Edwards SK, Xie P. Targeting TRAF3 downstream signaling pathways in B cell neoplasms. *J Cancer Sci Ther*. 2015;7(2):67-74.
50. Moore CR, Liu Y, Shao C, Covey LR, Morse HC, Xie P. Specific deletion of TRAF3 in B lymphocytes leads to B-lymphoma development in mice. *Leukemia*. 2012;26(5):1122-1127.
51. Bushell KR, Kim Y, Chan FC, et al. Genetic inactivation of TRAF3 in canine and human B-cell lymphoma. *Blood*. 2015;125(6):999-1005.
52. Diop F, Moia R, Favini C, et al. Biological and clinical implications of. *Haematologica*. 2020;105(2):448-456.
53. Malcikova J, Smardova J, Rocnova L, et al. Monoallelic and biallelic inactivation of TP53 gene in chronic lymphocytic leukemia: selection, impact on survival, and response to DNA damage. *Blood*. 2009; 114(26):5307-5314.
54. Zenz T, Vollmer D, Trbusek M, et al. TP53 mutation profile in chronic lymphocytic leukemia: evidence for a disease specific profile from a comprehensive analysis of 268 mutations. *Leukemia*. 2010;24(12): 2072-2079.
55. Yu L, Kim HT, Kasar S, et al. Survival of Del17p CLL depends on genomic complexity and somatic mutation. *Clin Cancer Res*. 2017;23(3): 735-745.
56. Campo E, Cymbalista F, Ghia P, et al. Aberrations in chronic lymphocytic leukemia: an overview of the clinical implications of improved diagnostics. *Haematologica*. 2018;103(12):1956-1968.
57. Skowronska A, Parker A, Ahmed G, et al. Biallelic ATM inactivation significantly reduces survival in patients treated on the United Kingdom leukemia research fund chronic lymphocytic leukemia 4 trial. *J Clin Oncol*. 2012;30(36):4524-4532.
58. Lozano-Santos C, García-Vela JA, Pérez-Sanz N, et al. Biallelic ATM alterations detected at diagnosis identify a subset of treatment-naïve chronic lymphocytic leukemia patients with reduced overall survival similar to patients with p53 deletion. *Leuk Lymphoma*. 2017;58(4):859-865.
59. González-Gascón-Y-Marín I, Muñoz-Novas C, Rodríguez-Vicente AE, et al. From biomarkers to models in the changing landscape of chronic lymphocytic leukemia: evolve or become extinct. *Cancers*. 2021;13(8): 1782.

SUPPORTING INFORMATION

Additional supporting information may be found in the online version of the article at the publisher's website.

How to cite this article: Pérez-Carretero C, Hernández-Sánchez M, González T, et al. *TRAF3* alterations are frequent in del-3′IGH chronic lymphocytic leukemia patients and define a specific subgroup with adverse clinical features. *Am J Hematol*. 2022;1-12. doi:10.1002/ajh.26578

CHAPTER 4

TRAF3 alterations enhance metabolic plasticity through metabolic reprogramming in chronic lymphocytic leukemia.

Claudia Pérez Carretero[1,2], Miguel Quijada Álamo[1,2], Mariana Tannoury[3], Léa Dehgane[3], Alberto Rodríguez Sánchez[1,2], David J. Sanz[1,2], Teresa González[1,2], Rocío Benito[1,2], Élise Chapiro[4], Florence Nguyen[4], Ana E. Rodriguez Vicente[1,2], Santos A. Susin[3], Jesús María Hernández Rivas[1,2]

1. University of Salamanca, IBSAL, IBMCC, CSIC, Cancer Research Center, Salamanca, Spain
2. Department of Hematology, University Hospital of Salamanca, Salamanca, Spain
3. Drug Resistance in Hematological Malignancies, Centre de Recherche des Cordeliers, UMRS 1138, INSERM, Sorbonne Université, Université Paris Cité, F-75006 Paris, France
4. Drug Resistance in Hematological Malignancies, Centre de Recherche des Cordeliers, UMRS 1138, INSERM, Sorbonne Université, Université Paris Cité, F-75006 Paris, France; Groupe Hospitalier Pitié-Salpêtrière, Assistance Publique-Hôpitaux de Paris, F-75013 Paris, France

Manuscript in preparation.

TRAF3 alterations enhance metabolic plasticity through metabolic reprogramming in chronic lymphocytic leukemia

Claudia Pérez Carretero[1,2], Miguel Quijada Álamo[1,2], Mariana Tannoury[3], Léa Dehgane[3], Alberto Rodríguez Sanchez[1,2], David J. Sanz[1,2], Teresa González[1,2], Rocío Benito[1,2], Élise Chapiro[4], Florence Nguyen Khac[4], Ana E. Rodriguez Vicente*[1,2], Santos A. Susin[3], Jesús María Hernández Rivas[1,2]

1.University of Salamanca, IBSAL, IBMCC, CSIC, Cancer Research Center, Salamanca, Spain

2.Department of Hematology, University Hospital of Salamanca, Salamanca, Spain

3.Drug Resistance in Hematological Malignancies, Centre de Recherche des Cordeliers, UMRS 1138, INSERM, Sorbonne Université, Université Paris Cité, F-75006 Paris, France

4.Drug Resistance in Hematological Malignancies, Centre de Recherche des Cordeliers, UMRS 1138, INSERM, Sorbonne Université, Université Paris Cité, F-75006 Paris, France; Groupe Hospitalier Pitié-Salpêtrière, Assistance Publique-Hôpitaux de Paris, F-75013 Paris, France

CPC and MQA contributed equally to this work

ABSTRACT

TRAF3 is a tumor suppressor gene frequently inactivated by mutations and 14q deletions in B-cell malignancies. In chronic lymphocytic leukemia (CLL), *TRAF3* losses and mutations are rare genetic events (0.5-3%), and biallelic inactivation of this gene has been related to a dismal prognosis. However, the biological implications of *TRAF3* in CLL pathogenesis are largely unknown. In this study, we performed transcriptomic, metabolomic and functional analyses in CRISPR/Cas9-edited models harboring *TRAF3* homozygous mutation to elucidate the pathogenic functions of *TRAF3* inactivation in the disease. Our results showed that *TRAF3* mutations promoted the activation of non-canonical NF-kB signaling through p52 and RelB activation and induced significant metabolic changes in CLL cells. Metabolic studies revealed an enrichment of metabolites involved in glycolysis, tricarboxylic acid (TCA) cycle and glutamate metabolism, as well as an enhanced mitochondrial respiration and glycolysis in *TRAF3* mutated cells. Unlike in WT cells, blockade of pyruvate or glutamate import contributed to an enhanced respiration capacity of *TRAF3*-mutated cells, suggesting a metabolic reprogramming towards alternative metabolic pathways. By inhibiting pyruvate and glutamate import simultaneously, we observed a decrease in *TRAF3*-mutated CLL cells proliferation, with equal levels of the previously dysregulated metabolites to those of the WT. Altogether, these results revealed a metabolic reprogramming in CLL cells with *TRAF3* inactivation, which may be inducing a metabolic plasticity for fueling mitochondrial activity (mitochondrial glycolysis/glutaminolysis) that is potentially targetable in CLL.

*Correspondance: anerv@hotmail.com

1 INTRODUCTION

The TNF receptor-associated factor3 (TRAF3) located in 14q32.32 has been identified as a tumor suppressor gene involved in B-cell survival, immune response, and cellular metabolism(1-3). *TRAF3* is frequently encompassed within 14q deletion and affected by inactivating mutations in B-cell neoplasms, such as multiple myeloma (MM) (20%), diffuse large B-cell lymphomas (DLCBL) (15%), and other mature B-cell malignancies such as chronic lymphocytic leukemia (CLL)(4%)(4-7).

Losses on *TRAF3* are infrequent in CLL (2-5%), and mutations in this gene are present in 0.5-1% of CLL patients(8-11). Notably, 50-60% of CLL patients with *TRAF3* deletions had mutations in the remaining allele, indicating a biallelic inactivation of this gene(7, 12). Recently, our group found that CLL patients harboring biallelic *TRAF3* inactivation (deletion and mutation) showed a dismal prognosis, with a short time to first treatment (TFT)(12). Moreover, other studies have suggested *TRAF3* as a novel candidate associated with Richter transformation and ibrutinib resistance(13-15). Nevertheless, further validation in larger CLL cohorts and more investigation regarding the underlying mechanisms of these findings are needed.

Mechanistically, *TRAF3* modulates a plethora of signal transduction cascades through its ubiquitin-mediated degra-

dation activity, including NF-kB signaling(16). Specifically, *TRAF3* is a negative regulator of the non-canonical NF-KB pathway(17). *TRAF3* inactivation promotes the stabilization of NF-kB-inducing kinase (NIK) in the cytoplasm and the subsequent processing of NF-KB2 from p100 into p52, which results in the translocation of p52-RelB heterodimers into the nucleus and the activation of target gene expression(17, 18). However, how *TRAF3*-mediated NF-KB activation modulates gene expression and its implication in tumor progression and drug resistance in CLL remains to be elucidated.

It has been demonstrated that solid tumors, and more recently also hematological neoplasms, modify their metabolic preferences to provide cellular energy and favor tumor development, especially, using an aerobic glycolysis in detriment of mitochondrial oxidative phosphorylation (OXPHOS), known as the "Warburg effect"(19-21). Concretely, metabolic alterations have been identified in peripheral blood (PB) and tumor microenvironment (TME) CLL cells (22, 23). A study showed that PB cells from patients with CLL had higher OXPHOS than healthy donors (22), and other studies indicated that TME cells had an enhanced glutathione, glutamate and glucose metabolism that stimulates CLL cells survival (24-26). Notably, these metabolic changes may also influence treatment response. It has been proved that venetoclax administration induces metabolic changes in TME cells(27), and independently of BCL2 inhibition(28). Besides, venetoclax refractoriness may be accompanied by an increased OXHPOS(29). Interestingly, new therapeutic approaches based on glutamine import inhibition have been proposed as an alternative to overcome venetoclax resistance (26). In line with these findings, recent studies have suggested new roles of *TRAF3* in the metabolism and mitochondrial activity of MM cells and mice-derived B cells (30-32). However, many insights about the impact of *TRAF3* alterations on the cellular metabolism of CLL remain elusive.

The aim of this investigation was to assess the biological implications of a rare alteration recently identified as a candidate CLL driver: *TRAF3* inactivation. To reveal the role of this gene in B-cell pathogenesis within the CLL context, we performed transcriptomic, metabolomic, and functional studies in CLL cellular models and primary cells. We demonstrated that CLL-derived cell lines with *TRAF3* alterations showed a dysregulation of NF-kB transcription factors and an altered metabolism with distinct metabolic dependencies. Here, we described a new mechanism of pathogenesis based on metabolic plasticity that could be targetable in CLL cells with *TRAF3* inactivation.

2 MATERIAL AND METHODS

2.1 CRISPR/Cas9-edited CLL cell lines

PGA1 cell line, derived from a CLL patient and harboring trisomy 12, was used as the cellular model to mimic the biallelic *TRAF3* inactivation previously reported in CLL patients, as the alterations detected in this gene were significantly associated with this cytogenetic alteration (12). We designed sgRNAs that targeted exon 11 (region that clusters most of *TRAF3* mutations previously reported), generating truncating mutations in both alleles of Cas9-expressing PGA1 cells (PGA1-*TRAF3*^{mut}), and a sgRNA that not target the human genome as a negative control (PGA1-WT) (**Supplementary Figure S1**). Sequences of the selected sgRNAs are detailed in **Supplementary Table S1**. The procedures and sgRNAs used for the generation of *TRAF3* mutations in PGA1 cells were previously described (33). pLKO5 vectors (Addgene #57822) carrying the desired sgRNAs were nucleofected into PGA1-Cas9 cells and single-cell flow-sorted clones were expanded and screened. At least three different clones harboring loss-of-function mutations were chosen for each CRISPR-generated cell line to perform functional, transcriptomic and metabolomic studies.

2.2 RNA sequencing

For RNA sequencing, CLL cells were cultured for 48 hours, pelleted and lysed, and total RNA was isolated using the RNeasy micro kit (Qiagen) according to the manufacturer's protocol. RNA quality was assessed using Bioanalyzer 2100 (Agilent Technologies) and libraries were generated using the TruSeq Stranded mRNA library prep kit (Illumina) from a total amount of 200 ng of RNA. Sequencing was carried out in Nextseq500 (Illumina). Raw fastq files were first quality filtered using fastp (v0.23.2). Processed fastq files were aligned to the human genome (hg19) using the STAR aligner (v2.7.8a). FeatureCounts (v1.50) was used to summarize the read counts across the genes. Differential expression analysis between experimental groups was performed using DESeq2 (v2.11.40.6), and plotted with ggplot' heatmap.2 function. Significant differential expression was determined at FDR < 0.1. Gene set enrichment analysis (GSEA) was performed on a matrix of normalized counts using the GSEA desktop application v4.2.3. Our data was aligned with Hallmark Signatures (h.all.v2022.1), Reactome (reactome.v2022.1) and KEGG (kegg.v2022.1) gene sets using 1000 permutations.

2.3 Primary CLL samples

Viable cryopreserved peripheral blood mononuclear cells (PBMCs) from 22 CLL patients were used in the *ex vivo* studies. PBMCs were isolated by Ficoll-Paque Plus density gradient media (GE Healthcare, Life Sciences) and a complete immunophenotypic analysis was performed in all samples by flow cytometry. Only samples with a CD19 + /CD5 + fraction greater than 85% were included in the study. **Supplementary Table S2** summarizes the main biological characteristics of CLL patients. The research was conducted in accordance with the Declaration of Helsinki and prior approval by the Bioethics Committee from our institution. Written informed consent was obtained from all patients.

2.4 NF-κB family members activity ELISA

Canonical (p65/RelA, NF-κB1 p50, c-Rel) and non-canonical (NF-κB2 p52, RelB) NF-κB activity of nuclear extracts of PGA1 clones and lysates from primary CLL samples were measured using the TransAM NF-κB Transcription Factor ELISA kit (Colorimetric) (Active Motif, #43296) following manufacturer's instructions.

2.5 Seahorse stress tests

Measurement of oxygen consumption rate (OCR) and extracellular acidification rate (ECAR) was carried out in the Seahorse XF96 analyzer (Agilent). CLL cells were plated in a density of 2·105 cells/well with 5 replicates per condition and incubated for 24h (with or without treatment) at 37°C 5% CO2. For mitochondria stress test, culture medium was replaced with XF Mito stress medium (DMEM supplemented with 10mM glucose, 2mM glutamine, and 1mM pyruvate). For the glycolysis stress test, the medium was replaced with XF base medium supplemented with 2mM Glutamine (glucose-free). Cells were then transferred to a XFe96 microplate (Agilent), pre-treated with 30 ul of Cell-Tak solution (Corning™ Cell-Tak Cell and Tissue Adhesive, Fisher Scientific) in 0.1M NaHCO3 and 1N NaOH, to ensure cell adhesion. The cell microplate was incubated at 37°C in a CO2-free environment for a minimum of 1 hour before stress tests. OCR was measured after sequential injections of Oligomycin (1 uM), FCCP (1 uM), and Rotenone/Antimycin A (1uM), and ECAR was measured following the injection of glucose (10mM), oligomycin (1uM) and 2-DG (10mM) by the Seahorse analyzer, following manufacturer's instructions. OCR and ECAR rates were normalized to the amount of protein per well, determined by a BCA protein assay (Thermo Fisher, 23250). Results were analyzed using Seahorse Wave (version 2.6.3). Basal OCR, spare respiratory capacity, maximal respiration, basal glycolysis, maximal glycolytic capacity and glycolytic reserve were calculated as previously described (34).

2.6 ddPCR

Gene expression of target genes in PGA1 cell lines was assessed by droplet digital PCR (ddPCR), using Bio-Rad equipments and reagents, and following the manufacturer's instructions (see **supplementary methods**).

2.7 Targeted metabolomics

CLL cells were washed three times with ice-cold PBS, drained, snap-frozen in liquid nitrogen, and stored at –80°C until analyses. An extraction solution composed of 50% methanol, 30% acetonitrile, and 20% water was added to the cells. The supernatants were collected and separated by liquid chromatography–mass spectrometry (LC-MS) using SeQuant ZIC-pHilic column (MilliporeSigma). The aqueous mobile-phase solvent was 20 mM ammonium carbonate plus 0.1% ammonium hydroxide solution, and the organic mobile phase was acetonitrile. The metabolites were separated over a linear gradient from 80% organic to 80% aqueous for 15 minutes. The column temperature was 50°C and the flow rate was 200 µL/min. The metabolites were detected across a mass range of 75–1000 m/z using the Q-Exactive Plus mass spectrometer (Thermo Fisher Scientific) at a resolution of 35,000 (at 200 m/z) with electrospray ionization and polarity switching mode (35). Lock masses were used to ensure mass accuracy below 5 ppm. The peak areas of different metabolites were determined using Thermo Fisher Scientific TraceFinder software using the exact mass of the singly charged ion and known retention time on the HPLC column. Data analysis was performed in the MetaboAnalyst 4.0 software (36).

2.8 Statistics

Statistical analyses were carried out using GraphPad Prism software v8 (GraphPad Software). Student's t test, Mann–Whitney, ANOVA, or Kruskal–Wallis tests were used to determine statistical significance. P-values lower than 0.05 were considered statistically significant. At least three independent clones per condition were used in the functional studies. Otherwise specified, data are summarized as the mean ± standard deviation (SD).

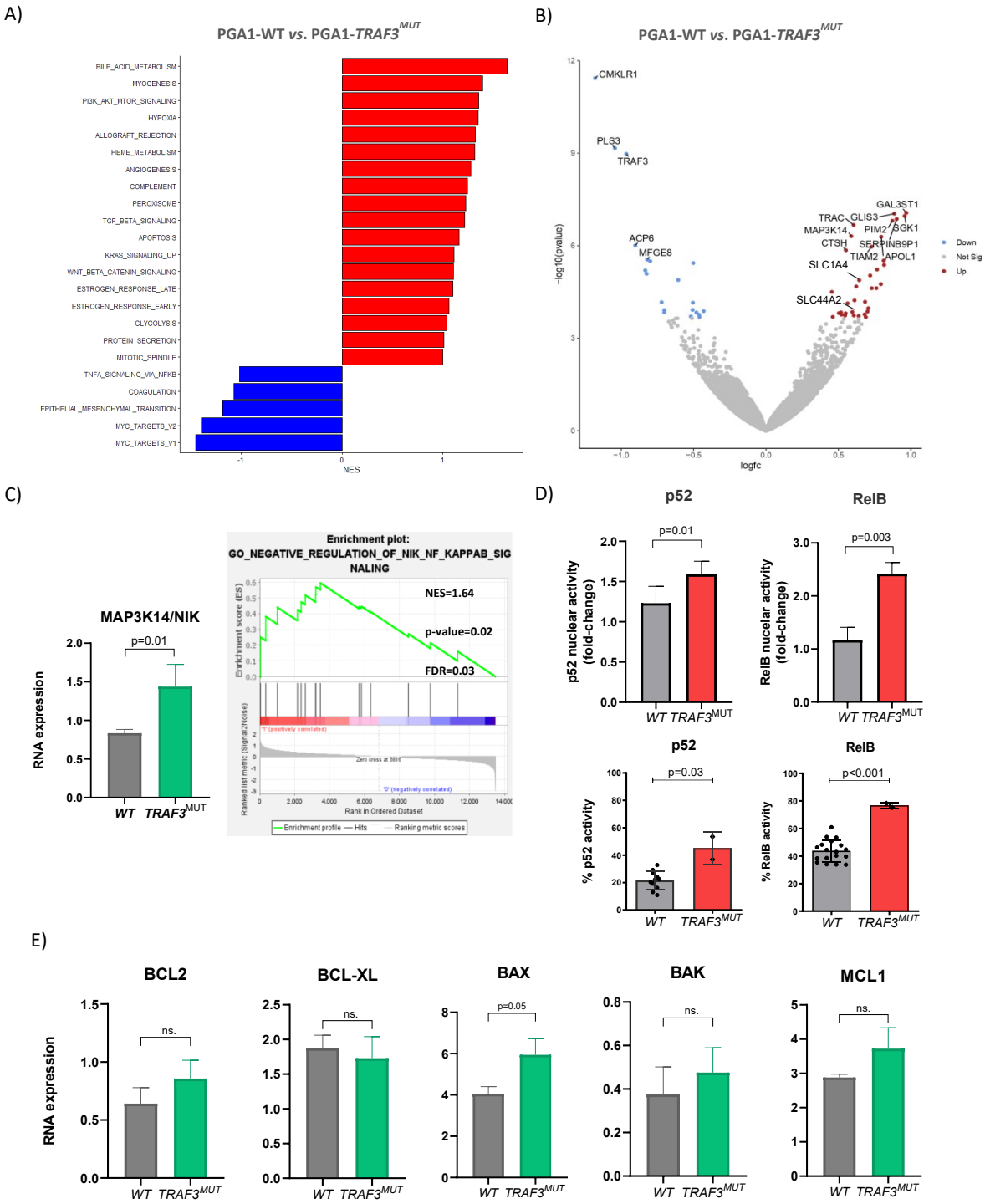

Figure 1. Transcriptomic and functional analyses of *TRAF3* inactivation in NF-κB signaling. A) RNA-seq analysis of transcriptionally upregulated (in red) and downregulated (in blue) Hallmark pathways (MSigDB) identified by Gene Set Enrichment Analysis (GSEA) for the indicated comparison. B) Volcano plot showing the significant upregulated and downregulated genes in PGA1-*TRAF3*^{mut} cells. C) Validation of MAP3K14 RNA expression by ddPCR and GSEA enrichment analysis of NF-kB signaling. D) Nuclear DNA-binding activity of the non-canonical NF-κB transcription factors p52 and RelB assessed by ELISA in nuclear and whole-cell extracts of PGA1 (top graphs) and primary cells (botton graphs; n=19 WT; n=2 *TRAF3*^{mut}) respectively. E) RNA expression of apoptotic effectors at basal state of TRAF3-mutated cells assessed by ddPCR. Data are represented as the mean ± SD.

2.9 Supplementary methods

Supplementary Methods section includes detailed protocols of cell lines, culture and ex-vivo co-culture conditions, drugs and reagents, NGS, FISH, MLPA, subcellular fractionation, Western blot, viability and MitoSOX assays.

3 RESULTS

3.1 *TRAF3* alterations promote non-canonical NF-kB pathway activation

In order to characterize the molecular mechanisms underlying *TRAF3* alterations, we performed a transcriptomic characterization of the CRISPR/Cas9-edited cellular models harboring a homozygous nonsense *TRAF3* mutation (PGA1-*TRAF3*^{mut}) and the cell lines used as a control (PGA1-WT) by RNA-seq. A total of 56 transcripts were significantly dysregulated (FDR<0.05) in *TRAF3*^{mut} cells in comparison to WT clones **(Supplementary Table S3)**. Gene-set enrichment analyses (GSEA) revealed differences in several biological pathways in PGA1-*TRAF3*^{mut} cells, including PI3K-AKT-MTOR, TGF-β signaling, apoptosis and glycolysis (**Figure 1A** and **Supplementary Table S4)**. We identified a significant upregulation of *MAP3K14* (NIK), a direct target of TRAF3-mediated degradation that stimulates NF-kB activity **(Figure 1B)**, which was further validated by ddPCR (p=0.01) **(Figure 1C)**. Considering the role of *TRAF3* in the NF-kB signaling, we analyzed the enrichment of gene sets related to this pathway and their targets (**Supplementary Figure S2**), and consequently, *TRAF3*^{mut} cells showed a global alteration of the negative regulation of NIK/NF-kB signaling (NES=1.64; p=0.02; FDR=0.03) **(Figure 1C)**.

Next, we assessed whether the dysregulation observed at the RNA level translated into changes in the DNA-binding activity of transcription factors involved in the NF-kB signaling. Regarding the non-canonical NF-kB pathway, we observed a higher nuclear activity of p52 (p=0.01) and a marked increase in RelB activity (p=0.003) **(Figure 1D)**. To further validate these results, we tested the nuclear activity of these transcription factors in a total of 14 CLL primary samples (n=19 *TRAF3*^{WT}; n=2 *TRAF3*^{mut}). Remarkably, CLL patients with *TRAF3* mutation showed higher DNA-binding activity of p52 and RelB (p=0.03, p<0.001, respectively) **(Figure 1D).** Conversely, we found no significant differences between PGA1-*TRAF3*^{mut} and PGA1-WT cells in transcription factor involved in the canonical NF-KB pathway (p50, RelA, c-Rel) **(Supplementary Figure S3)**.

As NF-kB activation has been shown to be involved in the dysregulation of apoptotic proteins, we next analyzed the expression levels of anti-apoptotic (*BCL2, MCL1, BCL-XL*) and pro-apoptotic effectors (*BAX, BAK*). Interestingly, PGA1-*TRAF3*^{mut} cells showed a higher RNA expression of *BAX* (p=0.05) **(Figure 1E)**. Moreover, we observed a trend towards higher expression levels of *BCL2* and *MCL1* in *TRAF3*-mutated cells, although it was not statistically significant.

3.2 *TRAF3* loss induces metabolic reprogramming and enhances mitochondrial activity

Previous studies have shown that B cells lacking *TRAF3* undergo metabolic reprogramming that could be mediated via NIK/NFKB signaling (30). Moreover, *TRAF3* can regulate mitochondrial activity to control B cell apoptosis (32). Taking this into account, we next sought to determine whether and how *TRAF3* inactivation mediates metabolic reprogramming in CLL cells.

To decipher the metabolic specificities of PGA1-*TRAF3*^{mut} cells, the abundance of 140 metabolites was assessed by LC-MS. The top 25 differentially enriched metabolites in PGA1-*TRAF3*^{mut} cells as well as P-values and fold-change values are shown in the heatmap and volcano plots, respectively (**Figure 2A, B**). Remarkably, PGA1-*TRAF3*^{mut} cells showed significantly higher levels of phosphoenolpyruvate, pyruvate, and lactate (glycolysis intermediates), and also increased levels of acetyl-CoA, α-ketoglutarate, and succinate (tricarboxylic acid cycle-TCA- intermediates), suggesting an enhanced mitochondrial activity (**Figure 2C**). Enrichment analysis revealed that the top 25 metabolites are involved in Warburg effect, pyruvate metabolism, TCA or citric acid cycle, and glutamate metabolism (FDR<0.01) (**Table 1**).

To further assess the metabolic activity of *TRAF3*-mutated cells, we analyzed their respiratory capacity or mitochondrial oxidative phosphorylation (OXPHOS) and glycolytic capacity by measuring the oxygen consumption rates (OCR) and extracellular acidification rates (ECAR), respectively. Interestingly, PGA1-*TRAF3*^{mut} cells showed significantly distinct mitochondrial characteristics when compared to WT: higher basal and maximal respiration levels and a more important spare capacity and generation of ATP linked to mitochondrial respiration, which is consistent with the higher abundance of TCA intermediates identified in the metabolomic study (**Figure 3A**). Considering the cellular bioenergetic profile (**Figure 3B**), we observed a shift in the presence of *TRAF3* mutations. Figure 3B shows that while the proportion of OCR for basal and non-mitochondrial respira-

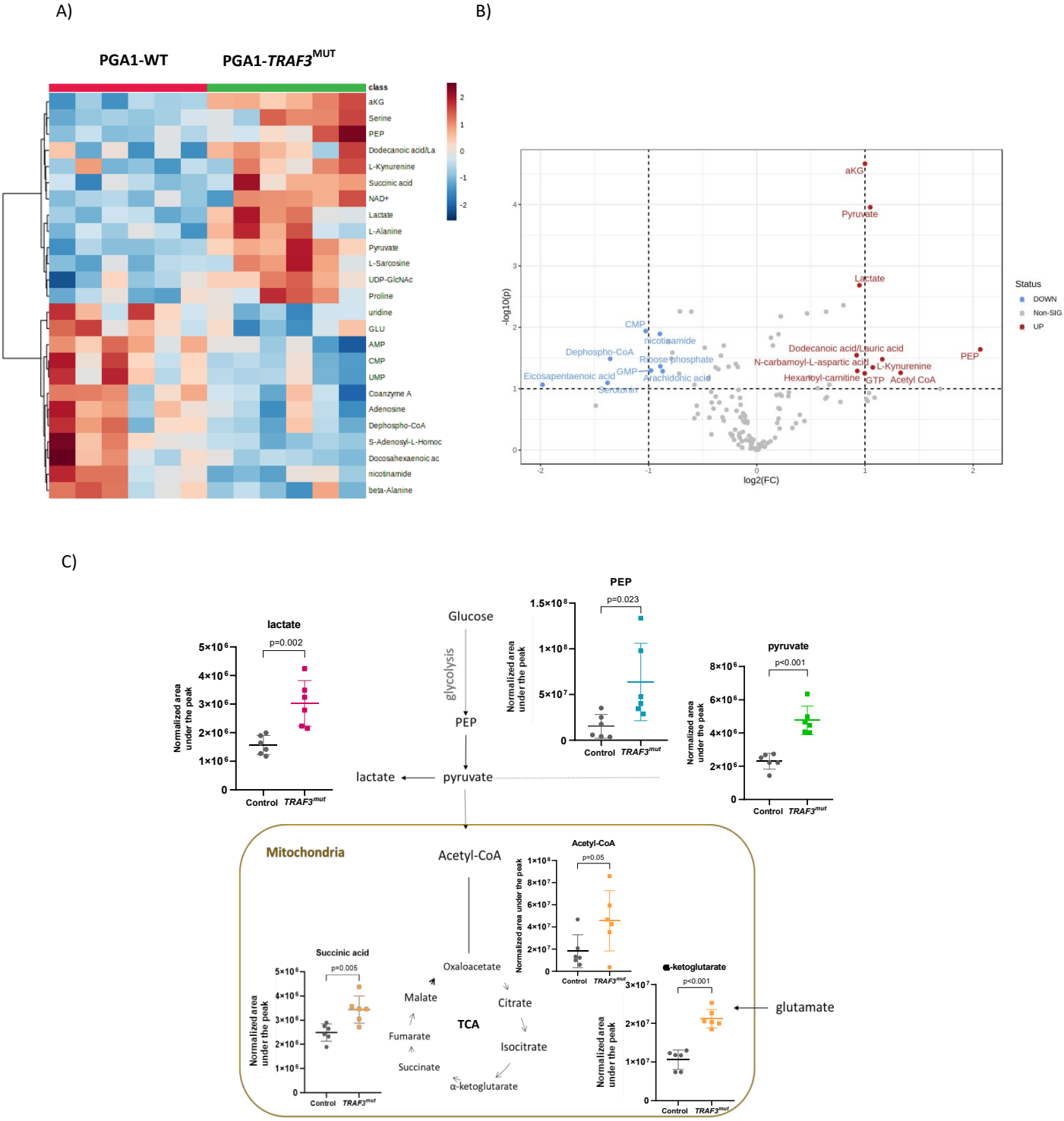

Figure 2. Metabolomic analysis of PGA1 cells with *TRAF3* biallelic inactivation. A) Heatmap top 25 significantly enriched metabolites identified by LC-MS. B) Volcano plot showing p-values and fold-changes of enriched metabolites. C) Significantly enriched metabolites in *TRAF3*-mutated cells are shown in the graph. These metabolites are involved in Warburg effect (phosphoenol-pyruvate-PEP-, pyruvate and lactate), citric acid cycle (TCA; acetyl-CoA, α-ketoglutarate and succinic acid) and glutamate metabolism (α-ketoglutarate), indicating an enhanced mitochondrial glycolytic metabolism.

Table 1. Enrichment of metabolic pathways identified in Metabolite Set Enrichment Analysis for the comparison of PGA1-*TRAF3*^{mut} *vs*. PGA1-WT cells.

Metabolic pathway	Total	Expected	Hits	Raw p	Holm p	FDR
Warburg effect	58	0.57	6	0.000	0.000	0.000
Gluconeogenesis	35	0.34	5	0.000	0.001	0.000
Pyruvate metabolism	48	0.47	5	0.000	0.004	0.001
Citric acid cycle	32	0.31	4	0.000	0.014	0.004
Amino sugar metabolism	33	0.32	3	0.003	0.295	0.061
Aspartate metabolism	35	0.34	3	0.004	0.347	0.061
Glucose-Alanine cycle	13	0.13	2	0.006	0.582	0.089
Glutamate metabolism	49	0.48	3	0.010	0.887	0.100
Beta oxidation of very long chain fatty acids	17	0.17	2	0.011	0.972	0.106
Alanine metabolism	17	0.17	2	0.011	0.972	0.106
Glycine and serine metabolism	59	0.58	3	0.016	1.000	0.135
Tryptophan metabolism	60	0.59	3	0.017	1.000	0.135
Transfer of acetyl groups into mitochondria	22	0.21	2	0.018	1.000	0.135
Cysteine metabolism	26	0.25	2	0.025	1.000	0.142
Oxidation of branched chain fatty acids	26	0.25	2	0.025	1.000	0.142
Phytanic acid peroxisomal oxidation	26	0.25	2	0.025	1.000	0.142
Mitochondrial beta-oxidation of medium chain saturated fatty acids	27	0.26	2	0.027	1.000	0.144
Lysine degradation	30	0.29	2	0.032	1.000	0.158
Ammonia recycling	32	0.31	2	0.036	1.000	0.170
Beta-Alanine metabolism	34	0.33	2	0.041	1.000	0.182
Fatty acid biosynthesis	35	0.34	2	0.043	1.000	0.183
Propanoate metabolism	42	0.41	2	0.060	1.000	0.245
Malate-Aspartate suttle	10	0.1	1	0.094	1.000	0.354
Pyruvaldehyde degradation	10	0.1	1	0.094	1.000	0.354
Valine, leucine and isoleucine degradation	60	0.59	2	0.112	1.000	0.407
Ketone body metabolism	13	0.13	1	0.120	1.000	0.422
Butyrate metabolism	19	0.19	1	0.171	1.000	0.560
Ethanol degradation	19	0.19	1	0.171	1.000	0.560
Carnitine synthesis	22	0.21	1	0.196	1.000	0.620
Caffeine metabolism	24	0.23	1	0.212	1.000	0.649
Mitochondrial beta-oxidation of short chain saturated fatty acids	27	0.26	1	0.235	1.000	0.681

tion decreased, the proportion of OCR for the spare capacity increased from 11% to 40%. Furthermore, we measured the levels of mitochondrial superoxide to assess the mitochondrial reactive oxygen species (ROS) production, and we found that PGA1-*TRAF3*^{mut} cells also had higher levels of superoxide (**Figure 3C**). Glycolysis, maximal glycolytic capacity, and glycolytic reserve measured by ECAR were slightly enhanced in the *TRAF3*-mutated cells, in line with the higher levels of anaerobic glycolysis intermediates (pyruvate and lactate) (**Figure 3D**). To further characterize this enhanced mitochondrial glycolytic metabolism, we assessed the response of our CRISPR/Cas9-generated models to 2-deoxyglucose (2-DG), a competitive hexokinase inhibitor. Interestingly, PGA1-*TRAF3*^{mut} cells had lower cell viability than the WT, which could suggest an increased dependency on glucose metabolism (**Supplementary Figure S4**).

To investigate whether the distinct metabolism of PGA1-*TRAF3*^{mut} cells was correlated to gene expression changes, we focused on the RNAseq data from key genes related to these metabolic pathways. Interestingly, we identified a dysregulation in glutathione metabolism and glutamine transport, highlighting the significant upregulation of the glutamine transporter *SLC1A4* (log2(FC)=0.643; FDR=0.007), in addition to the choline transporter *SLC44A2* (log2(FC)=0.549; FDR=0.045) (**Supplementary Figure S5**) (**Supplementary Table S3**).

Collectively, these results suggest that PGA1-*TRAF3*^{mut} cells had an increased mitochondrial glycolytic respiration through an enhanced glucose and glutamate metabolism.

3.3 *TRAF3* mutated cells showed metabolic plasticity in response to metabolic inhibitors

Since pyruvate, TCA, and glutamate metabolism were dysregulated in PGA1-*TRAF3*^{mut} cells, we next tested metabolic inhibitors that target these pathways to delve into the metabolic dependencies of these cells. Specifically, we tested the response of PGA1-*TRAF3*^{mut} cells to oxamate (lactate dehydrogenase-LDH- inhibitor, marker of anaerobic glycolysis), UK5099 (inhibitor of the mitochondrial pyruvate transporter that regulates mitochondrial glycolysis) and C968 (inhibitor of mitochondrial glutaminase that blocks glutaminolysis), by measuring viability, OCR and ECAR.

In cell viability experiments, PGA1-*TRAF3*^{mut} cells showed higher resistance to oxamate than PGA1-WT cells (**Supplementary Figure S6**). Mechanistically, oxamate significantly increased mitochondrial respiration in PGA1-WT cells, which could be explained by the favoring of pyruvate uptake by the mitochondria after LDH blockade (**Figure 4A**). Unlike WT cells, PGA1-*TRAF3*^{mut} cells displayed similar maximal respiration rates and spare capacity after oxamate treatment (**Figure 4A**). In parallel, *TRAF3*-mutated cells showed no differences in glycolysis when treated with the LDH inhibitor, while WT cells significantly increased their basal glycolysis and maximal glycolytic capacity (**Supplementary Figure S7**). These findings may indicate that PGA1-*TRAF3*^{mut} cell metabolism is independent of anaerobic glycolysis inhibition.

After UK5099 exposure, PGA1-*TRAF3*^{mut} cells exhibited similar cell viability to WT cells (**Supplementary Figure S6)**. Nevertheless, UK5099 treatment led to an increase in the maximal respiration capacity of PGA1-*TRAF3*^{mut} cells that was not observed in the WT (**Figure 4B**). Conversely, UK5099 reduced the basal glycolysis in PGA1-WT cells but we observe no effects in PGA1-*TRAF3*^{mut} cells (**Supplementary Figure S8**). Remarkably, PGA1-*TRAF3*^{mut} cells had significantly higher spare and maximal respiration capacities after C968 injection, while there were no differences in WT cells under the same conditions (**Figure 4C) (Supplementary Figure S9).**

The response of PGA1-*TRAF3*^{mut} cells to both metabolic inhibitors separately (UK5099 and C968) could indicate a greater capacity to switch their metabolism to alternative pathways and to increase their mitochondrial and glycolytic activity in restricted conditions, demonstrating an improved cellular plasticity in comparison to WT cells.

3.4 *TRAF3* mutated primary CLL cells are targetable by the combination of UK5099 and C968

Considering the metabolic dependencies and apoptosis dysregulation of PGA1-*TRAF3*^{mut} cells, we next assessed the response of primary CLL cells (n=19 *TRAF3*^{WT}, n=3 *TRAF3*^{MUT}) to a library of drugs, to explore therapeutic vulnerabilities and resistances in patients with *TRAF3* alterations. We tested CLL treatments (venetoclax, ibrutinb and idelalisib) as well as metabolic inhibitors (oxamate, UK5099 and C968), in the presence and absence of stromal co-culture with HS-5 cells, IL2 and CpG to mimic CLL microenvironment. Moreover, considering the increased respiration upon pyruvate and glutamate import inhibition, we assess the response to the combination of UK5099 and C968 to further evaluate if cells may switch from pyruvate metabolism to glutaminolysis and vice versa for fueling mitochondria metabolism **(Figure 5A)**.

Remarkably, *TRAF3* mutated CLL cells were more resistant to oxamate (as observed in the PGA1 cells: **Supplementary Figure S6**). Interestingly, these cells showed significant sensitivity to venetoclax in the absence of microen

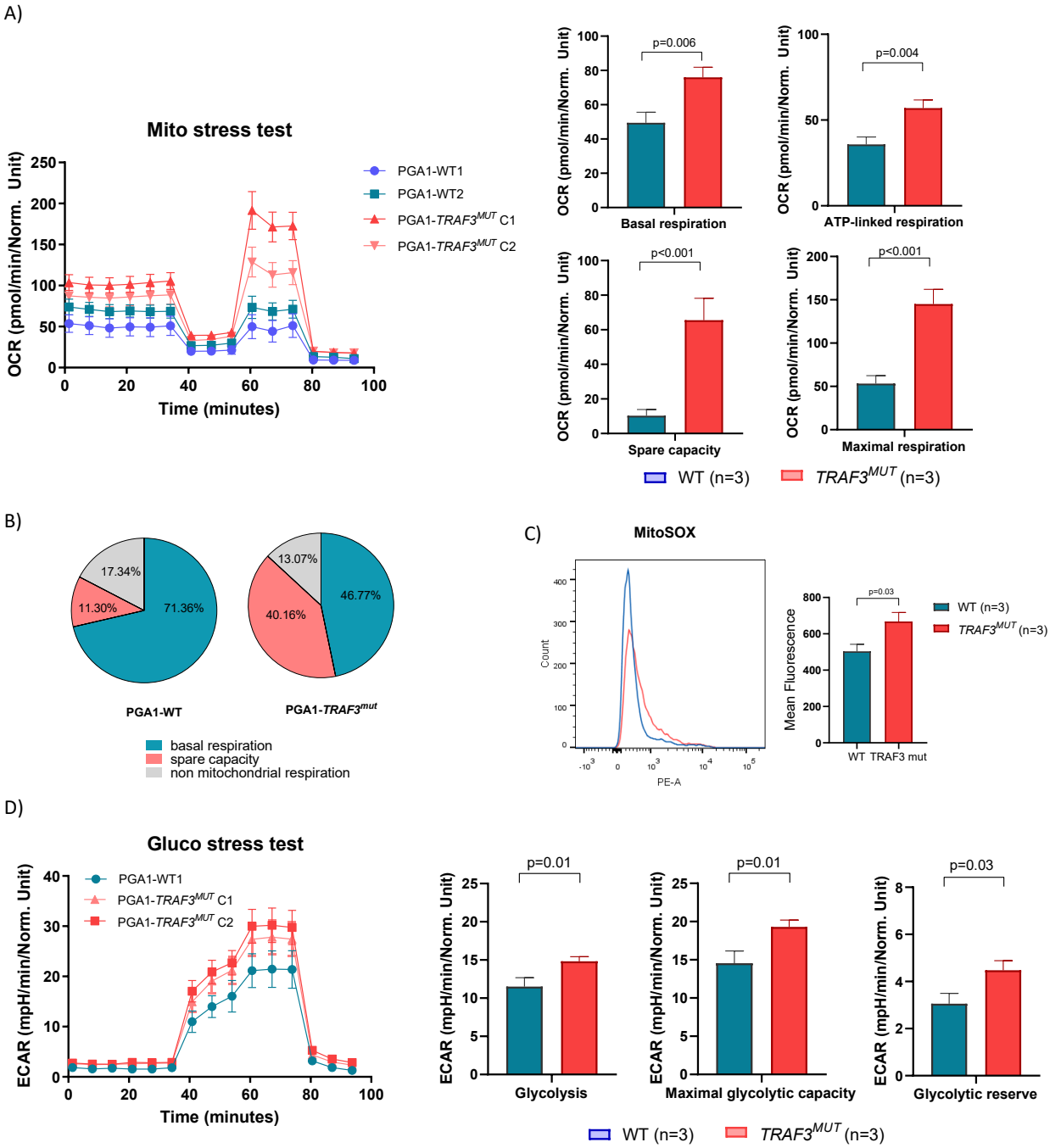

Figure 3. Bioenergetic phenotyping of PGA1-*TRAF3*^{mut} cells. A) Mito stress test. Oxygen consumption rates (OCR) of PGA1-WT and PGA1-*TRAF3*^{mut} clones are expressed by ug/protein and bar graphs show the comparison between *TRAF3*-mutated and WT cells according to spare capacity, ATP-linked, basal and maximal respiration. B) Proportions of OCR due to basal respiration, spare capacity and non-mitochodrial respiration. The proportions are relative to the highest OCR value, taken as the 100%. For this graph, two different seahorse experiments clones were used. C) Measurement of superoxide production by MitoSox staining. D) Gluco stress test. Extracellular acidification rate is expressed by ug/protein (ECAR) and bar graphs show the comparison between *TRAF3*-mutated and WT cells according to basal glycolysis, maximal glycolytic capacity and glycolytic reserve. Data represent the mean ± SD of five technical replicates from one representative experiment (out of two) in each case in mito and gluco stress test graphs. Respiratory and glycolytic indices are represented as the mean ± SD of replicates in three different PGA1-WT clones and three PGA1-*TRAF3*^{mut} clones.

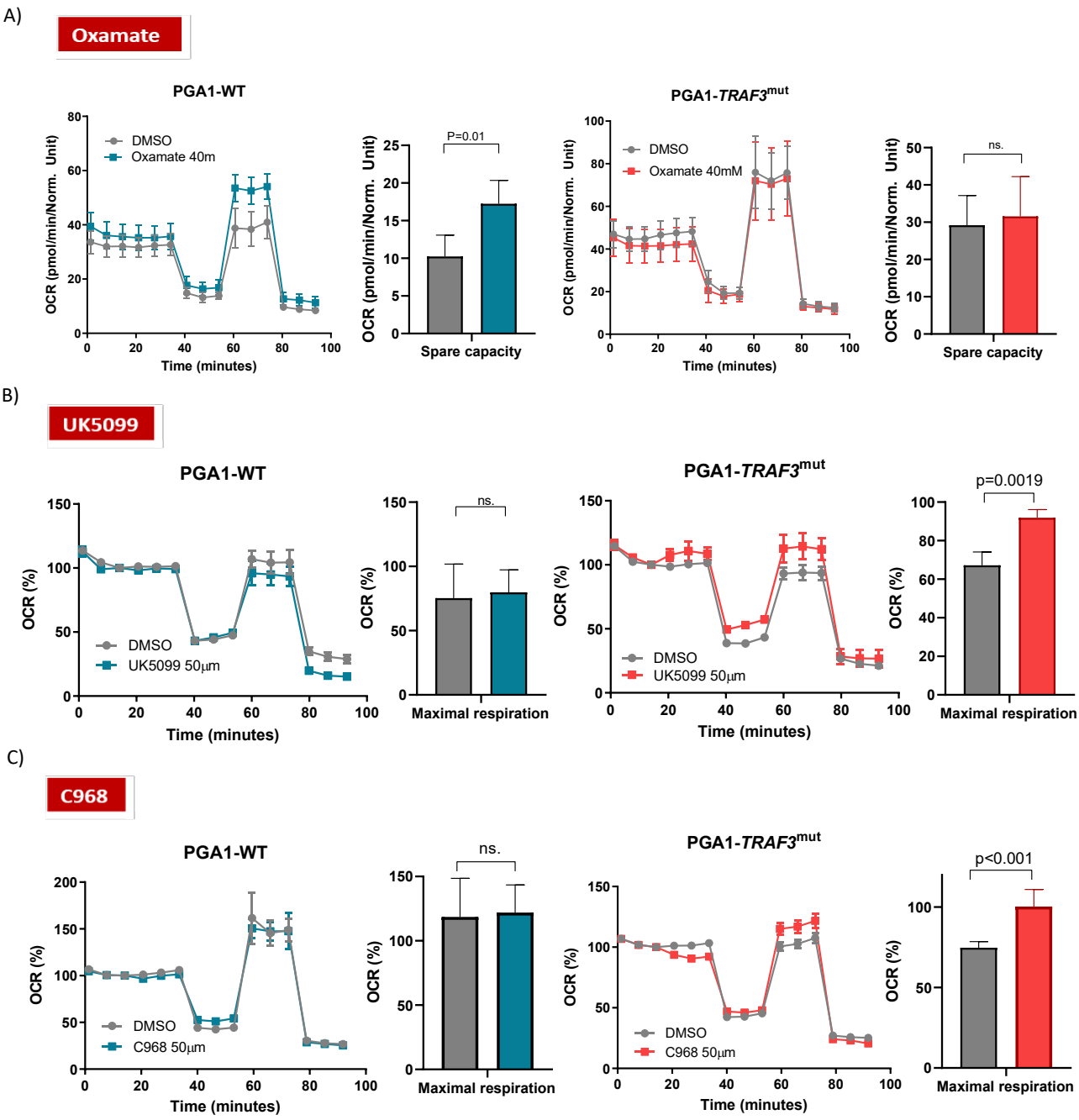

Figure 4. Analysis of mitochondrial respiration activity of PGA1-*TRAF3*^{mut} cells in response to metabolic inhibitors. A) PGA1-WT and PGA1-*TRAF3*^{MUT} cells were treated for 48h with oxamate (40 mM) and OCR was measured by seahorse technology (Mito stress test) and spare capacity is shown in the bar graphs. B) UK5099 effects on OCR (Mito stress test) in PGA1-WT and PGA1- *TRAF3*^{MUT} cells after injection in the seahorse experiment (50 µM; time: 14 min). Maximal respiration shown in the graphs. C) C968 effects on OCR (Mito stress test) in PGA1- WT and PGA1-*TRAF3*^{MUT} cells after injection in the seahorse experiment (50 µM; time: 14 min). Maximal respiration shown in the graphs. Color bars and graphs represent treated PGA1- *TRAF3*^{MUT} (red) and PGA1-WT (blue) cells, and grey bars and graphs represent untreated cells (both WT and *TRAF3* mutated as indicated). Data represent the mean ± SD. of five technical replicates from one representative experiment (out of two) in each case.

vironment, which was partially attenuated in the co-culture with stromal cells **(Figure 5A)**. Strikingly, when we compared the responses of *TRAF3*^{WT} and *TRAF3*^{MUT} CLL primary cells to the different treatments, we observed the same shift in the presence of microenvironment, except for UK5099 and C968 combination: WT cells reduced their sensitivity to this combination while *TRAF3*-mutated cells maintained a similar response when co-cultured with HS-5 (**Figure 5B**). These results suggest that UK5099 and C968 combination not only reduced cell proliferation, but also may block *TRAF3*-mediated microenvironmental stimuli in CLL cells.

3.5 Simultaneous glutaminolysis and pyruvate transport inhibition decrease *TRAF3* mutated cells proliferation by relieving metabolic plasticity

Our findings suggest enhanced mitochondrial glycolysis and an improved adaptive capacity of *TRAF3* mutated cells to pyruvate or glutaminolysis inhibition. Moreover, we hypothesize that their metabolism may fluctuate between these two pathways. As we identified a significant sensitivity to UK5099 and C968 combination in the presence and absence of microenvironment, we next tested the latter combination in *PGA1-TRAF3*^{mut} cells to explore the implications of this treatment in an isolated model. It should be noted that this combination induced more cell death in the PGA1-*TRAF3*^{mut} cells than in the PGA1-WT cells (p=0.03) (**Figure 6A**). Regarding OCR and ECAR (**Figure 6B**) **(Supplementary Figure S10)**, we no longer observe the differences that we previously identified between PGA1-WT and PGA1-*TRAF3*^{mut} cells under the single treatments, which could suggest that this combination relieves the metabolic plasticity and sensitize PGA1-*TRAF3*^{mut} cells.

To further analyze the effect of this combined treatment on the metabolome, metabolomic studies after treating the cells with UK5099 (25uM) and C968 (25 uM) were carried out. Strikingly, we identified a reprogramming in the abundance of key metabolites: pyruvate, lactate, acetyl-CoA and α-ketoglutarate. In all cases, the levels of the metabolites in PGA1-*TRAF3*^{mut} cells become equal to those of the WT cells after treatment, by decreasing, increasing or maintaining its concentration (**Figure 6C**). Collectively, our findings demonstrate that the simultaneous inhibition of pyruvate import to the mitochondria and glutaminolysis could reverse the differential metabolic reprogramming observed in *TRAF3*-mutated cells, unraveling the mechanistic insights behind this targetable dependency in CLL with these alterations.

4 DISCUSSION

Nowadays, the integration of multiomic data allows to identify novel candidate drivers with a potential role in the CLL pathogenesis and disease progression, which may contribute to develop new therapeutic strategies (10, 11). However, little is known about the implications of these new alterations at the biological level, which is indispensable to understand the underlying mechanisms and to evolve towards a better precision medicine. In this work, we deciphered new biological implications of *TRAF3*, a CLL driver, in NF-kB signaling and its role in the metabolic plasticity of CLL cells.

In line with previously reported data regarding non-canonical NF-kB activation (16, 17), our results indicated that PGA1-*TRAF3* mutated cells had an increased NIK upregulation and an enhanced activity of p52 and RelB transcription factors. Notably, we identified a dysregulation of specific apoptotic regulators, which are known NF-kB targets (Figure 1). *TRAF3* biallelic mutation in our CLL cellular models was associated with a slightly higher expression of anti-apoptotic *BCL2* and *MCL1* genes, and a significant increase of the pro-apoptotic *BAX* RNA levels. These results differ to some extent from the obtained in other study, where *BIRC3* mutated CLL cells (another negative regulator of non-canonical NF-kB signaling frequently disrupted in CLL), showed higher BCL-2 and BCL-XL expression, but a downregulation of BAX (37). It should be noted that the expression of BCL2 family proteins in other *TRAF3*-deficient models varies among studies (32, 38), suggesting that anti- and pro-apoptotic gene expression levels upon NF-kB activation could be dependent on the intermediate altered, the type and the state of the cell.

In the last few years, new potential roles of *TRAF3* in metabolism have also been described (3). Metabolomic analysis revealed a higher abundance of metabolites involved in the "Warburg effect" (PEP, pyruvate and lactate), TCA cycle (acetyl-coA, α-ketoglutarate and succinate) and glutamate metabolism (α-ketoglutarate) in PGA1-*TRAF3*^{MUT} cells (Figure 2, Table 1). This metabolic profile is consistent with the higher dependency on glucose metabolism observed in these cells, and the enhanced mitochondrial respiration and glycolysis (Figure 3), which is also in line with the previously reported (30, 32). Moreover, *TRAF3*-mutated cells were more resistant to anaerobic glycolysis inhibition by LDH blockade, to inhibition of pyruvate import to the mitochondria, and more resistant to glutaminolysis (Figure 4). Therefore, we identified for the first time a higher capacity

A)

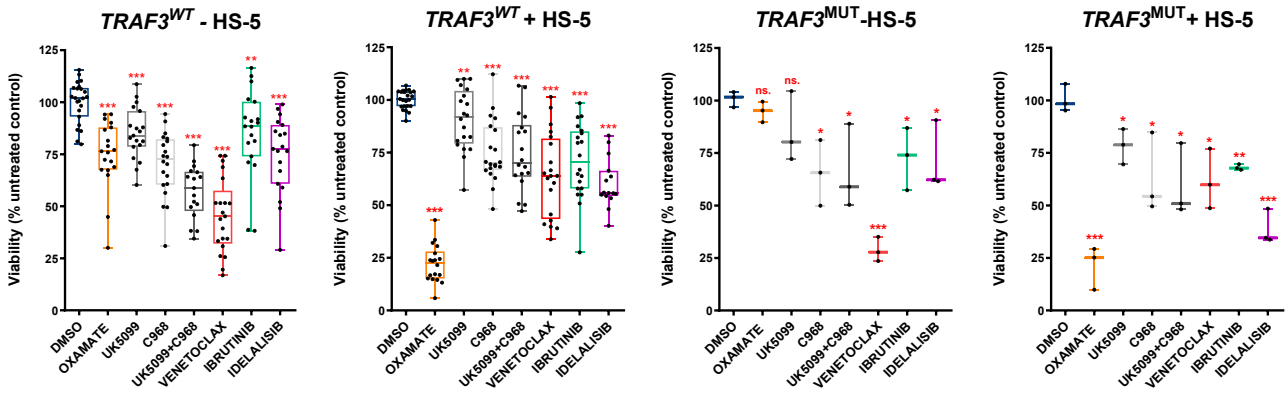

Drug	Oxamate	UK5099	C968	UK5099:C968	Venetoclax	Ibrutinib	Idelalisib
Concentration (48h)	20 mM	25 µM	25 µM	25:12 µM	2.5 nM	2 µM	2 µM

B)

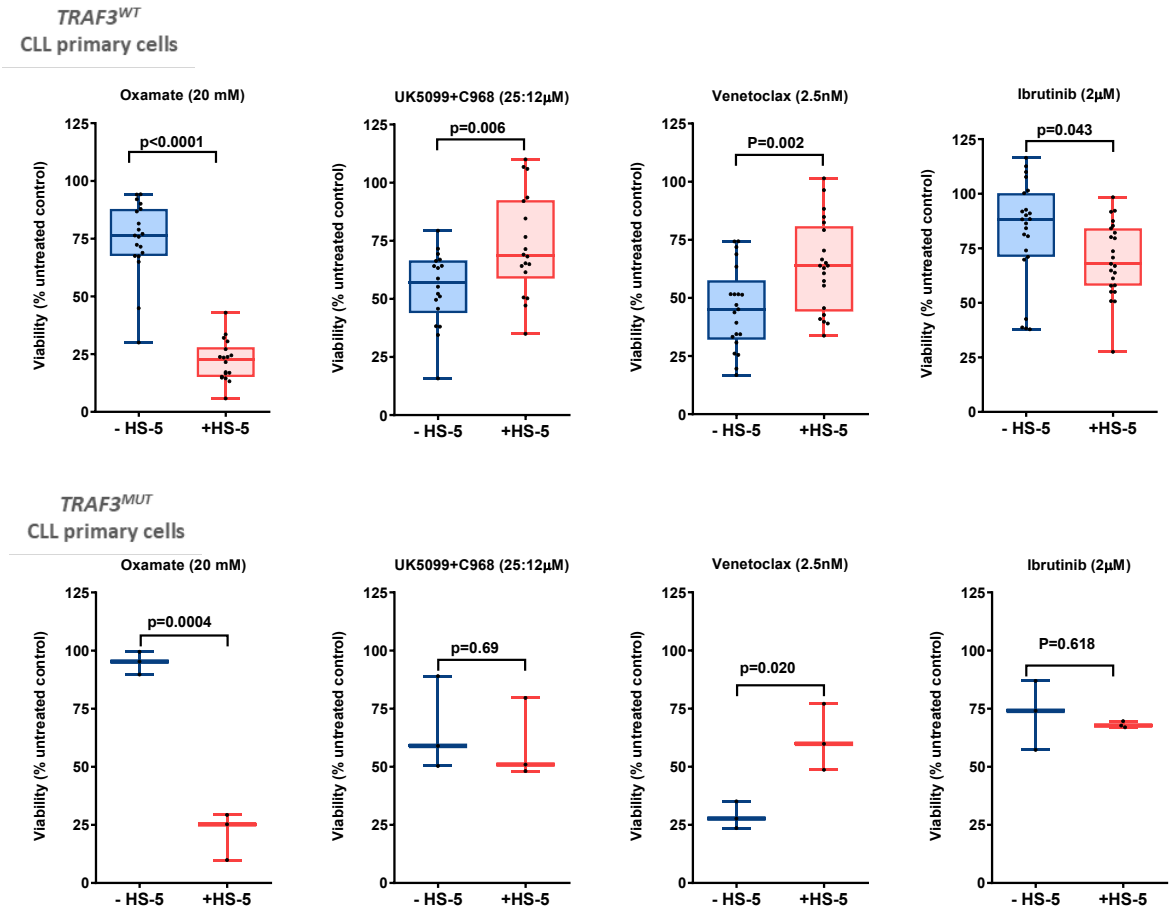

Figure 5. Response to metabolic inhibitors and CLL drugs of 22 CLL primary cells in the presence and absence of stromal stimulation. A) Viability of the *TRAF3*^{WT} (n=19) and *TRAF3*^{mut} (n=3) CLL primary cells after 48h of treatment with the inhibitors at the concentrations indicated in the panel below the graphs, seeded in co-culture with HS-5 bone marrow stromal cells, 1.5 µg/mL CpG and 50 ng/mL IL-2 (+HS-5) and without these microenvironmental stimuli (-HS-5). Statistical analysis was performed relative to the untreated cells (DMSO) in each treatment (t-student test). B) Viability of CLL primary cells with and without *TRAF3* mutations in response to oxamate, the combination of UK5099 and C968, venetoclax and ibrutinib based on the presence of microenvironmental stimuli. Normalized surviving fraction was assessed by CellTiter-Glo luminescent assay and expressed relative to untreated cells. Data is presented as the mean ± SD. ns.: not significant, *$p<0.05$, **$p<0.01$, ***$p<0.001$.

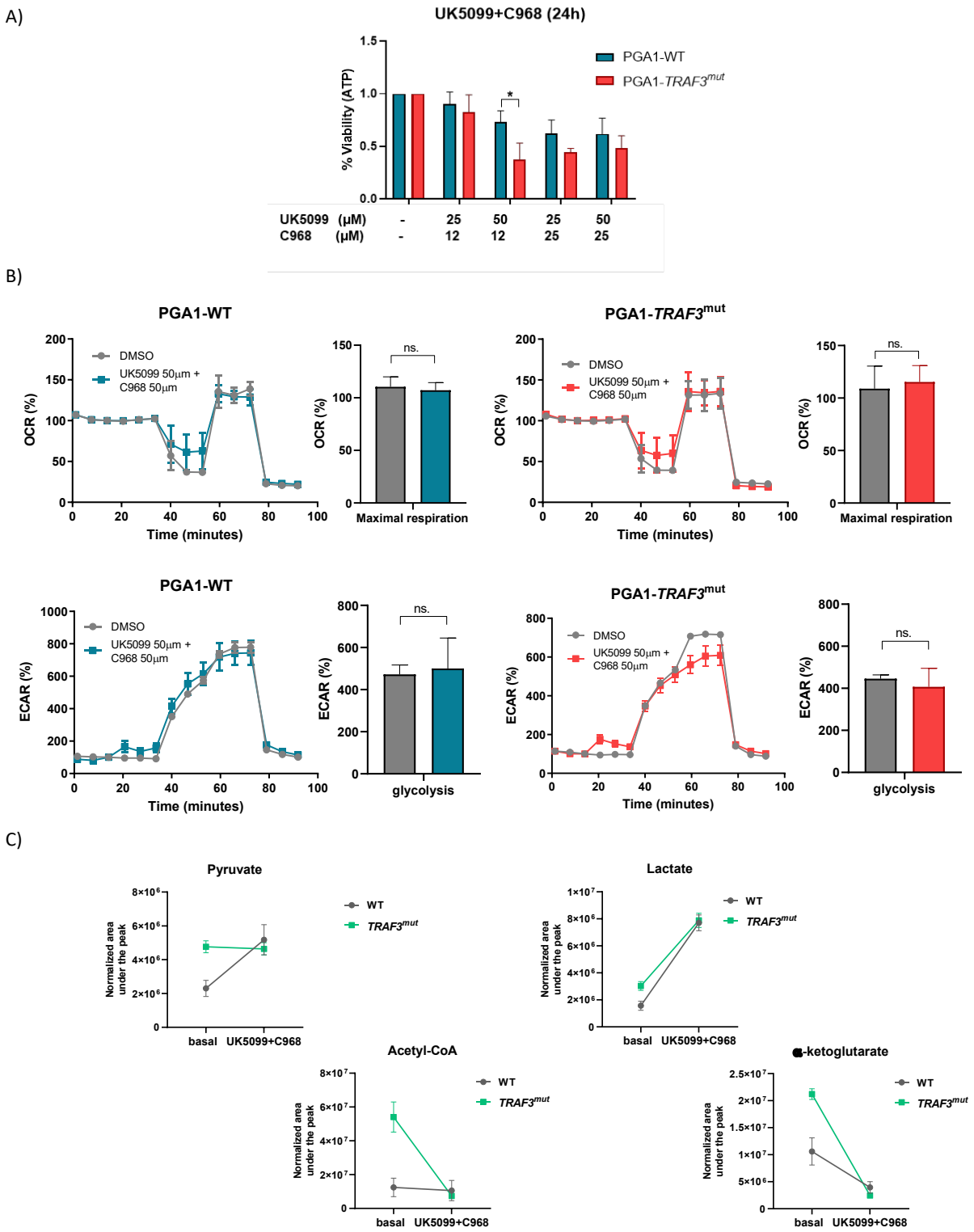

Figure 6. Metabolic analysis of PGA1-*TRAF3*^{mut} mutated cells in response to UK5099 and C968 combined treatment. A) Cell titer glo viability assay of PGA1-WT and PGA1-*TRAF3*^{mut} cells in response to the combination of UK5099 and C968 at different concentrations after 24h of treatment. B) OCR and ECAR of PGA1-WT and PGA1-*TRAF3*^{mut} cells after UK5099 and C968 injection (50:50 uM) (Mito and gluco stress test, respectively). Data represent the mean of five technical replicates from one representative experiment (out of two) in each case. Concentrations are shown below the graph. ns.:not significant. C) Changes in metabolites abundance after UK5099 and C968 treatment (25:25 uM for 24h) in PGA1-WT and PGA1-*TRAF3*^{mut} cells assessed by LC-MS. Data are represented as the mean ± SD.

of these cells to switch towards alternative metabolic pathways under stress conditions (mimicked by the administration of different metabolic inhibitors), showing an enhanced metabolic plasticity.

Intriguingly, similar metabolic dependencies and enhanced mitochondrial and glycolytic activity have been described in CLL cells upon CD40 stimulation, that subsequently activates NF-kB signaling (26). Additionally, RNAseq analysis identified an upregulation of *SLC1A4*, a glutamine transporter(39), which could be favoring the metabolic adaptation capacity to stress of PGA1-*TRAF3*^{MUT} cells(40). The main paralog of *SLC1A4* is *SCLC1A5*, a target of NF-kB signaling, which has been previously identified to be upregulated in CD40-stimulated B cells (26). It is noteworthy to mention that recent data uncovered new functions of NF-kB and more concretely, RelB activation, in metabolic reprograming in other B cell lymphomas(41, 42), which supports our findings and suggests that *TRAF3*-induced metabolic reprogramming could be dependent on NF-kB activation. Though, it is known that *TRAF3* is a *multi-faceted* gene that may activate different biological functions (43, 44), and hence, more investigations are needed to further confirm this dependency.

Given the apoptosis deregulation and metabolic dependencies of PGA1-*TRAF3*^{mut} cells, we next assessed whether these pathways could be targetable in CLL cells with *TRAF3* mutations (Figure 5). Mechanisms underlying venetoclax response often involve alterations in BCL2-family proteins, such as *BCL2* mutations, *MCL1* amplification or *BAX* expression(45-48). In our study, CLL cells with *TRAF3* mutations were more sensitive to venetoclax than the WT, which may be explained by the high expression of the pro-apoptotic regulator *BAX*. However, in the co-culture with stromal cells, primary *TRAF3*-mutated CLL cells were less sensitive to BCL2 inhibition in accordance with the effect of stromal cells in the prevention of venetoclax-induced apoptosis (49, 50). On the other hand, the use of metabolic inhibitors as a new potential approach for cancer treatment has been expanded the last few years(51-53). Interestingly, *TRAF3*-mutated CLL cells showed a reduced viability when treated with the combination of glutaminolysis and pyruvate transport inhibitors (C968 and UK5099, respectively). Strikingly, in the presence of microenvironment, primary *TRAF3*-WT cells showed an increased viability than the isolated CLL cell culture, while *TRAF3*-mutated cells remained as sensitive as isolated CLL cells to the combination. Moreover, the combined treatment (C968 and Uk5099) reverses the metabolic reprogramming reported in PGA1-*TRAF3*^{mut} cells (Figure 6). Altogether, these findings demonstrated the potential of the combination of metabolic inhibitors as a new therapeutic approach in *TRAF3*-mutated patients through its relieving effect on metabolic reprogramming.

In summary, we demonstrated the implications of *TRAF3* in different biological CLL functions, highlighting its role in metabolic reprogramming. In this work, we identified distinct metabolic dependencies and enhanced mitochondrial glycolytic metabolism in CLL cells with *TRAF3* inactivation, that could contribute to a metabolic plasticity potentially targetable in CLL.

CONFLICT OF INTEREST

The authors declare no competing financial interests.

AUTHOR CONTRIBUTIONS

CPC designed research, performed CRISPR/Cas9 experiments, carried out functional studies analyzed the data and drafted the manuscript. MQÁ designed and performed CRISPR/Cas9 and functional studies and contributed to analyze the data and interpretation of the results. MT performed functional studies and contributed to interpret the data. LD and ARS performed functional studies. DJS performed RNAseq analysis. TG performed sample selection and FISH studies. RB designed sequencing and MLPA studies and contributed to data analysis. EC and FN performed sample selection and contributed to the interpretation of the results. AERV contributed to data analysis and critically review the manuscript. SAS and JMHR conceived the study, designed and supervised the research, and critically reviewed and approved the final version of the manuscript. All authors discussed the results and revised the manuscript.

FUNDING

This work was supported by grants from Instituto de Salud Carlos III (ISCIII) &FEDER (PI21/00983) (co-funded by the European Union), Consejería de Educación-Junta de Castilla y León (SA118P20), Gerencia Regional de Salud-SACYL (GRS2140/A/20, GRS2385/A/21), Fundación Mutua Madrileña (FMM, AP176752021), Red Temática de Investigación Cooperativa en Cáncer (RTICC) (RD12/0036/0069) and Centro de Investigación Biomédica en Red de Cáncer (CIBERONC CB16/12/00233).

CPC is supported by a research grant from FEHH ("Fundación Española de Hematología y Hemoterapia"; Beca de Investigación FEHH 2022). AR is fully supported by an "Ayuda predoctoral de la Junta de Castilla y León" by the Fondo Social Europeo Plus (FSE+) (JCYL- EDU/1868/2022 PhD scholarship)

ACKNOWLEDGMENTS

We are grateful to I. Rodríguez, S. González, M.Á. Ramos, A. Martín, A. Díaz, A. Simón, M. del Pozo, V. Gutiérrez and S. Pujante from the Centro de Investigación del Cáncer, Salamanca, for

their technical assistance. We are grateful to Ivan Nemazanyy from the Metabolomics Unit in the Faculté de Médecine Paris Descartes, Paris (France), for his technical assistance.

REFERENCES

1. Xie P, Stunz LL, Larison KD, Yang B, Bishop GA. Tumor necrosis factor receptor-associated factor 3 is a critical regulator of B cell homeostasis in secondary lymphoid organs. Immunity. 2007;27(2):253-67.
2. Hildebrand JM, Yi Z, Buchta CM, Poovassery J, Stunz LL, Bishop GA. Roles of tumor necrosis factor receptor associated factor 3 (TRAF3) and TRAF5 in immune cell functions. Immunol Rev. 2011;244(1):55-74.
3. Jung J, Gokhale S, Xie P. TRAF3: A novel regulator of mitochondrial physiology and metabolic pathways in B lymphocytes Front. Oncol. 2023; 13:1081253.
4. Moore CR, Liu Y, Shao C, Covey LR, Morse HC, Xie P. Specific deletion of TRAF3 in B lymphocytes leads to B-lymphoma development in mice. Leukemia. 2012;26(5):1122-7.
5. Bushell KR, Kim Y, Chan FC, Ben-Neriah S, Jenks A, Alcaide M, et al. Genetic inactivation of TRAF3 in canine and human B-cell lymphoma. Blood. 2015;125(6):999-1005.
6. San Miguel JF. Introduction to a series of reviews on multiple myeloma. Blood. 2015;125(20):3039-40.
7. Nagel I, Bug S, Tönnies H, Ammerpohl O, Richter J, Vater I, et al. Biallelic inactivation of TRAF3 in a subset of B-cell lymphomas with interstitial del(14)(q24.1q32.33). Leukemia. 2009;23(11):2153-5.
8. Landau DA, Tausch E, Taylor-Weiner AN, Stewart C, Reiter JG, Bahlo J, et al. Mutations driving CLL and their evolution in progression and relapse. Nature. 2015;526(7574):525-30.
9. Puente XS, Beà S, Valdés-Mas R, Villamor N, Gutiérrez-Abril J, Martín-Subero JI, et al. Non-coding recurrent mutations in chronic lymphocytic leukaemia. Nature. 2015;526(7574):519-24.
10. Knisbacher BA, Lin Z, Hahn CK, Nadeu F, Duran-Ferrer M, Stevenson KE, et al. Molecular map of chronic lymphocytic leukemia and its impact on outcome. Nat Genet. 2022;54(11):1664-74.
11. Robbe P, Ridout KE, Vavoulis DV, Dréau H, Kinnersley B, Denny N, et al. Whole-genome sequencing of chronic lymphocytic leukemia identifies subgroups with distinct biological and clinical features. Nat Genet. 2022;54(11):1675-89.
12. Pérez-Carretero C, Hernández-Sánchez M, González T, Quijada-Álamo M, Martín-Izquierdo M, Santos-Mínguez S, et al. TRAF3 alterations are frequent in del-3'IGH chronic lymphocytic leukemia patients and define a specific subgroup with adverse clinical features. Am J Hematol. 2022;97(7):903-14.
13. Klintman J, Appleby N, Stamatopoulos B, Ridout K, Eyre TA, Robbe P, et al. Genomic and transcriptomic correlates of Richter transformation in chronic lymphocytic leukemia. Blood. 2021;137(20):2800-16.
14. Ondrisova L, Mraz M. Genetic and Non-Genetic Mechanisms of Resistance to BCR Signaling Inhibitors in B Cell Malignancies. Front Oncol. 2020;10:591577.
15. Nadeu F, Royo R, Massoni-Badosa R, Playa-Albinyana H, Garcia-Torre B, Duran-Ferrer M, et al. Detection of early seeding of Richter transformation in chronic lymphocytic leukemia. Nature Medicine. 2022;28(8):1662-71.
16. Moore CR, Edwards SK, Xie P. Targeting TRAF3 Downstream Signaling Pathways in B cell Neoplasms. J Cancer Sci Ther. 2015;7(2):67-74.
17. Vallabhapurapu S, Matsuzawa A, Zhang W, Tseng PH, Keats JJ, Wang H, et al. Nonredundant and complementary functions of TRAF2 and TRAF3 in a ubiquitination cascade that activates NIK-dependent alternative NF-kappaB signaling. Nat Immunol. 2008;9(12):1364-70.
18. Zarnegar BJ, Wang Y, Mahoney DJ, Dempsey PW, Cheung HH, He J, et al. Noncanonical NF-kappaB activation requires coordinated assembly of a regulatory complex of the adaptors cIAP1, cIAP2, TRAF2 and TRAF3 and the kinase NIK. Nat Immunol. 2008;9(12):1371-8.
19. Vander Heiden MG, Cantley LC, Thompson CB. Understanding the Warburg effect: the metabolic requirements of cell proliferation. Science. 2009;324(5930):1029-33.
20. Hanahan D, Weinberg RA. Hallmarks of cancer: the next generation. Cell. 2011;144(5):646-74.
21. Pavlova NN, Thompson CB. The Emerging Hallmarks of Cancer Metabolism. Cell Metab. 2016;23(1):27-47.
22. Jitschin R, Hofmann AD, Bruns H, Giessl A, Bricks J, Berger J, et al. Mitochondrial metabolism contributes to oxidative stress and reveals therapeutic targets in chronic lymphocytic leukemia. Blood. 2014;123(17):2663-72.
23. Vangapandu HV, Ayres ML, Bristow CA, Wierda WG, Keating MJ, Balakrishnan K, et al. The Stromal Microenvironment Modulates Mitochondrial Oxidative Phosphorylation in Chronic Lymphocytic Leukemia Cells. Neoplasia. 2017;19(10):762-71.
24. Zhang W, Trachootham D, Liu J, Chen G, Pelicano H, Garcia-Prieto C, et al. Stromal control of cystine metabolism promotes cancer cell survival in chronic lymphocytic leukaemia. Nat Cell Biol. 2012;14(3):276-86.
25. Jitschin R, Braun M, Qorraj M, Saul D, Le Blanc K, Zenz T, et al. Stromal cell-mediated glycolytic switch in CLL cells involves Notch-c-Myc signaling. Blood. 2015;125(22):3432-6.
26. Chen Z, Simon-Molas H, Cretenet G, Valle-Argos B, Smith LD, Forconi F, et al. Characterization of metabolic alterations of chronic lymphocytic leukemia in the lymph node microenvironment. Blood. 2022;140(6):630-43.
27. van Bruggen JAC, van der Windt GJW, Hoogendoorn M, Dubois J, Kater AP, Peters FS. Depletion of CLL cells by venetoclax treatment reverses oxidative stress and impaired glycolysis in CD4 T cells. Blood Adv. 2022;6(14):4185-95.
28. Roca-Portoles A, Rodriguez-Blanco G, Sumpton D, Cloix C, Mullin M, Mackay GM, et al. Venetoclax causes metabolic reprogramming independent of BCL-2 inhibition. Cell Death Dis. 2020;11(8):616.
29. Guièze R, Liu VM, Rosebrock D, Jourdain AA, Hernández-Sánchez M, Martinez Zurita A, et al. Mitochondrial Reprogramming Underlies Resistance to BCL-2 Inhibition in Lymphoid Malignancies. Cancer Cell. 2019;36(4):369-84.
30. Mambetsariev N, Lin WW, Wallis AM, Stunz LL, Bishop GA. TRAF3 deficiency promotes metabolic reprogramming in B cells. Sci Rep. 2016;6:35349.
31. Gokhale S, Lu W, Zhu S, Liu Y, Hart RP, Rabinowitz JD, et al. Elevated Choline Kinase α-Mediated Choline Metabolism Supports the Prolonged Survival of TRAF3-Deficient B Lymphocytes. J Immunol. 2020;204(2):459-71.
32. Liu Y, Gokhale S, Jung J, Zhu S, Luo C, Saha D, et al. Mitochondrial Fission Factor Is a Novel Interacting Protein of the Critical B Cell Survival Regulator TRAF3 in B Lymphocytes. Front Immunol. 2021;12:670338.
33. Quijada-Álamo M, Hernández-Sánchez M, Alonso-Pérez V, Rodríguez-Vicente AE, García-Tuñón I, Martín-Izquierdo M, et al. CRISPR/Cas9-generated models uncover therapeutic vulnerabilities of del(11q) CLL cells to dual BCR and PARP inhibition. Leukemia. 2020;34(6):1599-1612.
34. Yang M, Chadwick AE, Dart C, Kamishima T, Quayle JM. Bioenergetic profile of human coronary artery smooth muscle cells and effect of metabolic intervention. PLOS ONE. 2017;12(5):e0177951.

35. Bignon Y, Rinaldi A, Nadour Z, Poindessous V, Nemazanyy I, Lenoir O, et al. Cell stress response impairs de novo NAD+ biosynthesis in the kidney. JCI Insight. 2022;7(1).
36. Chong J, Wishart DS, Xia J. Using MetaboAnalyst 4.0 for Comprehensive and Integrative Metabolomics Data Analysis. Current Protocols in Bioinformatics. 2019;68(1):e86.
37. Quijada-Álamo M, Hernández-Sánchez M, Rodríguez-Vicente AE, Pérez-Carretero C, Rodríguez-Sánchez A, Martín-Izquierdo M, et al. Biological significance of monoallelic and biallelic BIRC3 loss in del(11q) chronic lymphocytic leukemia progression. Blood Cancer J. 2021;11(7):127.
38. Mambetsariev N, Lin WW, Stunz LL, Hanson BM, Hildebrand JM, Bishop GA. Nuclear TRAF3 is a negative regulator of CREB in B cells. Proc Natl Acad Sci U S A. 2016;113(4):1032-7.
39. White MA, Frigo DE. Regulation of SLC1A4 and SLC1A5 in Prostate Cancer-Response. Mol Cancer Res. 2018;16(11):1811-2.
40. Yoo HC, Park SJ, Nam M, Kang J, Kim K, Yeo JH, et al. A Variant of SLC1A5 Is a Mitochondrial Glutamine Transporter for Metabolic Reprogramming in Cancer Cells. Cell Metab. 2020;31(2):267-83.
41. Nuan-Aliman S, Bordereaux D, Thieblemont C, Baud V. The Alternative RelB NF-kB Subunit Exerts a Critical Survival Function upon Metabolic Stress in Diffuse Large B-Cell Lymphoma-Derived Cells. Biomedicines. 2022;10(2).
42. Lim SK, Peng CC, Low S, Vijay V, Budiman A, Phang BH, et al. Sustained activation of non-canonical NF-κB signalling drives glycolytic reprogramming in doxorubicin-resistant DLBCL. Leukemia. 2023;37(2):441-52.
43. Häcker H, Tseng PH, Karin M. Expanding TRAF function: TRAF3 as a tri-faced immune regulator. Nat Rev Immunol. 2011;11(7):457-68.
44. Bishop GA. TRAF3 as a powerful and multitalented regulator of lymphocyte functions. J Leukoc Biol. 2016;100(5):919-26.
45. Blombery P, Thompson ER, Nguyen T, Birkinshaw RW, Gong JN, Chen X, et al. Multiple BCL2 mutations cooccurring with Gly101Val emerge in chronic lymphocytic leukemia progression on venetoclax. Blood. 2020;135(10):773-7.
46. Thomalla D, Beckmann L, Grimm C, Oliverio M, Meder L, Herling CD, et al. Deregulation and epigenetic modification of BCL2-family genes cause resistance to venetoclax in hematologic malignancies. Blood. 2022;140(20):2113-26.
47. Thijssen R, Tian L, Anderson MA, Flensburg C, Jarratt A, Garnham AL, et al. Single-cell multiomics reveal the scale of multilayered adaptations enabling CLL relapse during venetoclax therapy. Blood. 2022;140(20):2127-41.
48. Haselager MV, Kielbassa K, Ter Burg J, Bax DJC, Fernandes SM, Borst J, et al. Changes in Bcl-2 members after ibrutinib or venetoclax uncover functional hierarchy in determining resistance to venetoclax in CLL. Blood. 2020;136(25):2918-26.
49. Panayiotidis P, Jones D, Ganeshaguru K, Foroni L, Hoffbrand AV. Human bone marrow stromal cells prevent apoptosis and support the survival of chronic lymphocytic leukaemia cells in vitro. Br J Haematol. 1996;92(1):97-103.
50. Kurtova AV, Balakrishnan K, Chen R, Ding W, Schnabl S, Quiroga MP, et al. Diverse marrow stromal cells protect CLL cells from spontaneous and drug-induced apoptosis: development of a reliable and reproducible system to assess stromal cell adhesion-mediated drug resistance. Blood. 2009;114(20):4441-50.
51. Altman BJ, Stine ZE, Dang CV. From Krebs to clinic: glutamine metabolism to cancer therapy. Nat Rev Cancer. 2016;16(11):749.
52. Schulte ML, Fu A, Zhao P, Li J, Geng L, Smith ST, et al. Pharmacological blockade of ASCT2-dependent glutamine transport leads to antitumor efficacy in preclinical models. Nat Med. 2018;24(2):194-202.
53. Luo Z, Xu J, Sun J, Huang H, Zhang Z, Ma W, et al. Co-delivery of 2-Deoxyglucose and a glutamine metabolism inhibitor V9302 via a prodrug micellar formulation for synergistic targeting of metabolism in cancer. Acta Biomater. 2020;105:239-52.

GENERAL DISCUSSION

Chronic lymphocytic leukemia (CLL) is a heterogeneous disease characterized by the presence of a wide range of genetic alterations that constitute the basis for the variable clinical outcomes observed in patients[5, 77, 78]. Chromosomal alterations are a hallmark of the disease, with an important role in CLL pathogenesis and prognosis, as well as in therapy response[58, 59, 383]. Recently, next generation sequencing (NGS) studies have led to the discovery of a great number of genetic mutations in CLL drivers that cluster into a specific set of molecular pathways, and some of these mutated genes have demonstrated a significant prognostic value that could refine patients' risk stratification[77, 78, 80, 87, 94, 96]. Moreover, CLL shows a remarkable subclonal heterogeneity, and different patterns of co-occurrence among genetic alterations may affect clonal evolution, disease progression and relapse[78, 88, 310]. Therefore, improving the molecular characterization of this disease is essential to better understand CLL pathogenesis and move towards a better precision medicine.

Chromosomal alterations are present in up to 80% of CLL patients, being the most recurrent ones 13q deletion, del(13q), 11q deletion, del(11q), 17p deletion, del(17p) and trisomy 12, +12[59, 145]. The assessment of cytogenetic alterations by FISH has become the gold standard for prognosis risk stratification, as specific abnormalities identify patients with a more aggressive disease such as del(11q) and del(17p) or an indolent one (del(13q))[59]. In addition, other cytogenetic alterations have been identified at lower but not insignificant frequencies, although their clinical significance remains controversial. These abnormalities include the 6q deletion, del(6q) and 14q rearrangements involving the *IGH* gene (14q32/*IGH* translocations (IGH*R*) and deletions (del(14q)(q32))[58, 59, 227].

In the first study of this PhD research (**Results section: *Chapter 1)*, the clinical implications** of del(6q) in CLL were addressed. The incidence of del(6q) ranges from 3 to 7%, mainly detected by conventional cytogenetics, as the 6q probe is not included in the classical 4-probe CLL FISH panel[211, 212, 215]. Besides its low incidence, the characterization of this abnormality has been limited by the co-occurrence with other factors and the small number of cases identified with del(6q) as the sole abnormality[214]. Whereas in some studies this alteration did not appear to influence outcome, in others del(6q) was associated with an adverse or intermediate prognosis[211, 214, 216, 410]. We analyzed one of the largest del(6q) series so far (N=39), being the only cytogenetic

alteration in 15 patients. To achieve this cohort size, samples were collected from three different institutions in a collaborative study. Regarding clinical characteristics, del(6q) correlated with poor prognosis makers including ZAP70 and CD38 positivity and IGHV-UM. In terms of clinical impact, del(6q) patients showed a short median time to first treatment (TFT), which was further validated in patients with del(6q) as the sole abnormality (**Results section-Chapter 1: Figure 1**). These results demonstrated the relevant clinical impact of this abnormality in prognosis, independent of the presence of additional cytogenetic alterations and similar to that of del(11q) cases. Thus, routine assessment of del(6q) could be of great utility to refine risk stratification of CLL, although there are still some limitations. First, which FISH probe should be used to assess del(6q), as the size of the deletion ranges from 6q15 to 6q27, without a specific MDR. In addition, despite conventional cytogenetic analysis has recovered its relevance and it is commonly performed, especially for clinical trials, its use is hampered by the low mitotic rate of CLL cells and the necessity of expert cytogeneticists' analyses.

In this PhD research, we also focused on the study of other less frequent cytogenetic alterations: 14q32 rearrangements and deletions involving the *IGH* gene (**Results section: chapters 2 and 3**), by screening a total of 871 CLL patients using the break-apart *IGH* FISH probe.

Although the clinical significance of 14q32/*IGH* translocations (IGH*R*) has been analyzed in several studies, the great *IGH* promiscuity and the differential prognosis regarding the translocated partner hinder the validation of their prognostic impact[206, 208, 209, 220, 224, 245, 411, 412]. In the CLL cohort analyzed in this PhD research, the median TFT of IGH*R* patients (N=46) was shorter than those of low-cytogenetic risk (del(13q)/normal FISH) and similar to that of trisomy 12 patients. Indeed, those patients with an *IGH* translocation as the only cytogenetic aberration had a shorter median TFT than patients with normal FISH (**Results section-Chapter 2: Figure 3**). By segregating IGH*R* patients according to the presence of the most common translocation t(14;18) or *IGH*::*BCL2* fusion, we identified two IGH*R* subsets with a significantly different prognosis: patients with *IGH*::*BCL2* fusion showed a better outcome, close to low-risk cytogenetics subgroups, while patients with other *IGHR* had a similar outcome to del(11q) and del(17p) cases (**Suppl. Appendix-Chapter 2:**

Figure S5). Thus, these findings corroborate and refine the intermediate-adverse outcome previously described in patients with 14q32/*IGH* translocation and shed light into the prognostic differences within the high heterogeneity of *IGH* rearrangements.

Regarding 14q32/*IGH* deletions (del(14q)(q32)), *IGH* locus has been previously identified as the telomeric breakpoint in approximately 50% of del(14q) CLLs, but few studies have investigated the real incidence and prognostic value of this alteration in CLL[189, 191, 222, 233]. The presence of del(14q) has been related to short TFT, irrespective of whether *IGH* is encompassed in the deletion[189, 191]. Therefore, the clinical impact of *IGH* deletion needs to be further assessed. In the third chapter of this thesis, we demonstrate that patients displaying del(14q)(q32) (N=54) show an intermediate prognosis, similar to that of trisomy 12. Furthermore, patients harboring del(14q)(q32) as the only cytogenetic abnormality had a significantly shorter TFT than the rest of CLL patients (**Results section-Chapter 3: Figure 1**). Thus, we determined the prognostic significance of *IGH* alterations, concretely, the negative impact of IGH*R* and *IGH* deletion, both associated with intermediate-adverse outcomes. Taken together, these results highlight the value of incorporating the *IGH* probe in the standard CLL FISH panel, in order to improve CLL prognostic stratification in an easy and cost-effective manner.

In CLL, the development of high-throughput sequencing techniques has led to the identification of genes affected by chromosomal abnormalities and revealed specific patterns of association among genetic alterations, providing a more comprehensive view of the CLL genetic landscape[66, 72, 78, 82, 86, 176]. Based on this premise, we aimed to investigate the **mutational profile of CLL patients with rare cytogenetic alterations**, to decipher the molecular underpinnings of these chromosomal abnormalities and how they may contribute to patients' prognosis refinement. For that purpose, in this PhD work we performed for the first time a molecular characterization of CLL patients with del(6q), IGH*R* and del(14q) by integrating CC and/or FISH, and NGS information.

In del(6q) cases, cytogenetic analyses by CC and FISH revealed a great genetic heterogeneity (**Results section: Chapter 1**). Del(6q) co-occurred with additional cytogenetic alterations in 24 out of 39 patients, being the most common del(17p),

followed by del(11q). Moreover, del(6q) was present in the context of complex karyotype in 39% of patients. According to the NGS analysis, 92% of del(6q) patients had mutations in at least one of the 54 CLL-related drivers evaluated, with *TP53, RPS15* and *NFKBIE* as the most recurrently mutated genes (**Results section-Chapter 1: Table 1, Figure 2**). Given this mutational burden and the presence of high-risk cytogenetics, as previously reported[212], del(6q) could be considered as a secondary abnormality that may arise as a result of the genomic instability observed in this subgroup. Nevertheless, in this PhD research, we also reported that del(6q) appeared as the sole chromosome anomaly with a significant prognostic impact in 15/39 patients, and in the major clone with abnormal karyotype of del(6q) patients with other cytogenetic alterations (16/24), thus demonstrating that del(6q) can be a primary event driving CLL pathogenesis.

NGS analysis identified distinct mutational patterns within this subgroup depending on whether del(6q) appeared alone or in combination with other abnormalities, suggesting the alteration of different molecular mechanisms. In del(6q)-only patients, the most recurrently mutated gene was *RPS15* (40%), followed by *XPO1* and *ATM* (20% each), while del(6q) patients with additional cytogenetic alterations showed higher mutational frequencies in *TP53 (38%)*, *NOTCH1* (21%) and *NFKBIE* (17%) (**Results section-Chapter 1: Figure2**). Remarkably, despite the previously reported association between *RPS15* and *TP53* mutations,[193, 254] we did not recognize these alterations as significantly concurrent events. Notably, *RPS15* mutations negatively refined TFT, while *TP53* contributed to shorter OS of del(6q) patients, which reinforces the potential cooperating role of these alterations in del(6q) pathogenesis (**Results section-Chapter 1: Figure 3**). Taken all together, we suggest the presence of two different driving forces of CLL progression within this subgroup: a) the occurrence of del(6q) as a primary event with a strong pattern of co-occurrence with gene mutations involved in RNA and ribosomal processing (*RPS15* and *XPO1*), and b) del(6q) as a second abnormality in the context of high genomic instability, probably prompted by *TP53* inactivation.

Although molecular investigations of del(6q) in CLL are scarce, its biological implications have been further analyzed in other neoplasms. Del(6q) is a cytogenetic alteration that frequently occurred in non-Hodgkin lymphomas (NHL), acute

lymphoblastic leukemia (ALL), and in solid tumors such as prostate cancer[413-415]. Regarding the molecular mechanisms of tumorigenesis underlying del(6q), *TNFAIP3,* a negative regulator of NF-kB located in 6q23, is frequently inactivated by a loss of heterozygosity and mutations in NHL[416, 417]. However, mutational analyses of *TNFAIP3* in CLL revealed the absence of mutations in this gene and suggests that *TNFAIP3* does not play a significant role in CLL pathogenesis[292, 418]. Conversely, in our research, we did identify a high frequency of mutations in *NFKBIE*, another negative regulator of NF-kB signaling. Moreover, a recent study has demonstrated that del(6q) in T-ALL encompasses *SYNCRIP* and *SNHG5* genes, located in 6q15, with biological implications in RNA and ribosomal modulation, similar to those of *RPS15* in CLL[300, 419]. In prostate cancer, *ZNF292* has been identified as a tumor suppressor gene targeted by 6q14 deletion[415] and, indeed, in our del(6q) cohort we reported *ZNF292* mutations in two patients, one of them with a 6q deletion in the proximal region of 6q14, suggesting a biallelic inactivation of this gene in CLL. These findings may indicate that multiple tumor suppressors are targeted by del(6q), with different molecular or genetic alterations among different neoplasms, which, intriguingly, seem to converge in a very specific set of common signaling pathways: RNA and ribosomal modulation and NF-kB signaling.

The main limitation of this work is the impossibility of assessing the size of the deletion and the encompassed genes with the methodology applied. Moreover, conventional cytogenetics is not accurate in evaluating the real proportion of cells affected by the deletion, and this would prevent from identifying the sequence of acquisition of genetic alterations (deletion and/or mutations) through the evolution of the disease. To overcome these issues, further investigation by applying other techniques such as genomic arrays or optical genome mapping (OGM) and single-cell sequencing would be helpful to confirm the haploinsufficiency of the candidate tumor suppressor genes and the co-occurrence among chromosomal abnormalities and mutations within the same or different clones during disease progression.

Regarding 14q32/*IGH* alterations (translocations or rearrangements), the investigation of their molecular pathomechanisms has been hampered by several factors, namely their low incidence, the heterogeneity regarding the translocated

partner, and their occurrence in leukemic forms of NHLs that may be equivocally diagnosed as CLL.

In this PhD research (**Results section: Chapter 2**), we assessed for the first time the mutational profile of a large cohort of IGH*R* CLLs by targeted NGS (N=46). Notably, IGH*R* CLLs showed a distinct mutational profile with high mutational frequency of *NOTCH1, IGLL5, POT1, BCL2, FBXW7, ZMYM3, MGA, BRAF* and *HIST1H1E* genes, being *BCL2* and *FBXW7* mutations significantly associated with the IGH*R* (**Results section- Chapter 2: Figure 1**). Considering the significant association of 14q32/*IGH* translocation and trisomy 12 previously described[178, 230], and also observed in this work, the high incidence of *NOTCH1* mutations (a well-known trisomy 12-associated mutated gene[178, 182, 190]) could be ascertained by the presence of the trisomy 12 rather than the IGH*R*. However, these mutations were also present in patients with IGH*R* as the sole abnormality, whose mutational pattern did not significantly differ from the reported in the whole IGH*R* cohort, demonstrating the association between IGH*R* and *NOTCH1* mutations. Moreover, a subsequent study to this thesis has explored the mutational profile of a Chinese CLL population with *IGHR,* identifying a similar genetic profile to the reported in this research, and also the statistically significant association between *FBXW7* mutations and IGH*R*, further validating and demonstrating the relevance of our findings[420].

Notably, the mutational pattern varied according to the translocated partner within this subgroup of patients. In our study, thirteen patients showed the t(14;18) or *IGH/BCL2* rearrangement. From the remaining IGH*R* CLLs, two cases rearranged with *BCL6*, a common *IGH* rearrangement described. Given the small number of cases with this rearrangement and the great heterogeneity previously reported, we differentiate two IGH*R* subgroups: those with *IGH::BCL2* fusion and the rest of IGH*R*s (non-*IGH::BCL2*). Of note, cases with *IGH::CCND1* fusion were excluded to avoid the inclusion of leukemic forms of mantle cell lymphoma. IGH*R* without *IGH::BCL2* showed a higher mutational burden and recurrent mutations in *NOTCH1, SF3B1, POT1, TP53* and *FBXW7*, whereas patients with *IGH::BCL2* fusion showed a higher incidence of mutations in *BCL2, IGLL5, NOTCH1* and *HIST1H1E* (**Suppl. Appendix-Chapter 2: Figure S3)**. *BCL2* and *NOTCH1* mutations had been previously identified in a cohort of nine *IGH::BCL2* cases by *Puente et al.*[77], while *TP53* and *FBXW7* mutations were

observed in a study of three CLL cases with *IGH::BCL3* fusion, thus corroborating the robustness of our results[421]. Interestingly, these mutational patterns are consistent with the worse prognosis observed in the group of non-*IGH::BCL2* IGH*R* CLLs, which associated with bad-prognosis genes, and the longer TFT of patients with *IGH::BCL2* fusion[188, 224, 227, 230, 231]. It should be noted that most mutations appeared at lower variant allele frequencies (VAFs) than the *IGH* translocations, indicating that mutations are likely acquired as secondary events during CLL clonal evolution. Altogether, these observations contribute to unravel the molecular mechanisms that could be responsible for the clinical outcome of IGH*R* patients.

Additionally, mutations in non-coding regions were identified in IGH*R* CLLs, located not only in the hotspot of the 3'UTR region of *NOTCH1*, but also in 5'UTR *IGLL5* and 5'UTR *BCL2* (**Results section-Chapter 2: Figure 2**). Although these mutations had been previously described in CLL[77, 257], here we newly reported the association between these non-coding mutations and *IGH* translocations, as well as examined their clinical relevance. To date, there is a lack of functional studies assessing the implications of non-coding mutations in the disease, albeit recent findings such as those from the Pan-Cancer Analysis of Whole Genomes Consortium have revealed an increased number of driver candidates with mutations in UTR regions, which have a potential role in CLL pathogenesis[422, 423]. Regarding 3'UTR *NOTCH1* mutations, their functional consequence in the protein and clinical impact have been demonstrated to be similar to those of the hotspot *NOTCH1* coding mutations[77, 85, 276]. *Puente et al.* showed that patients harboring *IGH::BCL2* fusion, with a high incidence of 5'UTR *BCL2* mutations, presented higher levels of *BCL2* expression[77]. However, it was difficult to determine whether this *BCL2* overexpression was a consequence of the translocation or the UTR mutations. In a contemporary study to this thesis, *Robbe et al.* specifically demonstrated the association between 5'UTR *BCL2* mutations and *BCL2* overexpression[296].

In the present PhD work, we found that 5'UTR *BCL2* mutations were also present in IGH*R* CLLs different from *IGH::BCL2* fusions, indicating that these mutations are not just restricted to these rearrangements. Moreover, we demonstrated for the first time that the occurrence of *IGLL5* and *BCL2* mutations (including coding and UTR mutations) within this subgroup was associated with a longer TFT than that of the rest

of IGH*R* CLLs, which could point to these mutations as good prognostic markers (**Results section-Chapter 2: Figure 3**). Nevertheless, more investigations are still needed to decipher the molecular implications of UTR regions in CLL. This issue could be addressed through the characterization of the translocated *IGH* partners and other UTR regions altered in this disease by using techniques such as OGM and WGS, and then mimicking these mutations in *in vitro* and *in vivo* CRISPR/Cas9-edited models to discover their functional and biological consequences.

Another important and novel aspect that we identified regarding the molecular features of IGH*R* in CLL, is the presence of mutations previously reported in NHL[424-426]. Whereas *IGH* translocations occur at low frequencies in CLL, the incidence of IGH*R* in NHL significantly increases according to the hematological malignancy and the IGH-translocated partner. For instance, *IGH::BCL2* or t(14;18) appeared in the 70-95% of cases of follicular lymphoma (FL), *IGH::MYC* or t(8;14) in the 60-70% of Burkitt lymphomas, and one third of diffuse large B-cell lymphomas (DLBCL) present t(3;14) or *IGH::BCL6* fusion[427, 428]. We detected mutations previously reported in lymphomas, especially in FL and DLCBL[426, 429-432], such as mutations in *IGLL5, BCL2* and *HIST1H1E,* within the IGH*R* CLL subgroup (**Results section-Chapter 2: Table 1**). Strikingly, the clinical implications of some of these mutations are different in CLL and NHL: *BCL2* mutations are related to a higher risk of transformation and aggressive disease in FL, while they associated with a better prognosis in our IGH*R* cohort[433]. Moreover, IGH*R* CLLs also showed mutations in well-known CLL driver genes, indicating that this entity displays a distinct and intermediate mutational profile between CLL and lymphoma, with multiple genetic mechanisms underlying pathogenesis, which may affect Notch signaling (*NOTCH1, FBXW7*), cell cycle and apoptotic processes (*TP53, BCL2*) or chromatin modification (*HIST1H1E, ZMYM3*).

In the chapter 3 of this PhD research, we delved into the molecular characteristics of 14q32/*IGH* deletion (del(14q)(q32)) which affects the 3' flanking site of the *IGH*, detected as the loss of one red signal using the *IGH* break-apart FISH probe (N=54). As in the previously analyzed rare cytogenetics subgroups, del(14q)(q32) CLLs showed a high frequency of mutations in specific genes, standing out *NOTCH1, ATM*, genes involved in the RAS signaling pathway (*BRAF, MAP2K1, KRAS, NRAS*) and *TRAF3* (**Results section-Chapter 3: Figure 2**). In terms of additional cytogenetic alterations,

del(14q)(q32) patients displayed a high incidence of trisomy 12, further corroborating the high concurrence of this chromosomal abnormality, 14q32/*IGH* alterations (translocations and deletions) and *NOTCH1* mutations in CLL and suggesting a cooperation between these genetic events in the pathogenesis of the disease[178, 189, 191].

Undoubtedly, the major finding in chapter 3 was the significant enrichment of *TRAF3* mutations in del(14q)(q32) (**Results section-Chapter 3: Figure 2)**. This gene appears to be mutated in 0.5-1% of patients in unselected CLL cohorts[77, 78, 296], whereas its mutational frequency increased up to 13% in our cohort. Intriguingly, *TRAF3* is located in 14q32.32, proximal to the *IGH* locus, suggesting that the *IGH* deletion observed could extend to *TRAF3*. *Nagel et al*, demonstrated that 14q deletions in different B-cell malignancies may encompass *TRAF3*, and reported two CLL cases with a heterozygous deletion and *TRAF3* mutations in the remaining allele[205]. In this PhD work, we identified a *TRAF3* loss in 20% of patients with del(14q)(q32) (11/54), 64% of them harboring mutations in this gene. In terms of clinical significance, the presence of *TRAF3* alterations associated with shorter TFT than the rest of del(14q)(q32). Besides, *TRAF3* mutations appeared at lower VAFs than FISH *IGH*-deleted cells, which may indicate that the mutation is an acquired secondary event in CLL evolution, resulting in **the biallelic inactivation of *TRAF3*** in this subgroup of patients.

TRAF3 biallelic inactivation by deletion and mutation resembles the mechanism of other CLL driver genes dysfunction with a relevant clinical significance in the disease, such as *TP53*/del(17p) and *ATM*/del(11q)[67, 71, 72, 86]. Within the whole cohort analyzed during this PhD research by NGS and FISH (N=317), the biallelic inactivation of *TP53* and *ATM* had a strong negative impact in the TFT of CLL patients and, interestingly, deletion and mutation of *TRAF3* also contributed to a poor outcome, in line with those double-hit alterations**.** Moreover, multivariate analysis confirmed that *TRAF3* alterations constitute an independent risk factor of TFT (**Results section-Chapter 3: Figure 3, Table 1)**, and recent studies have proposed this gene as a candidate CLL driver involved in Richter transformation[315, 434]**.** Taken all this together, in this PhD work we identified a molecular mechanism based on the biallelic inactivation of the candidate CLL driver *TRAF3* that could be driving CLL progression, specifically in a specific CLL subset with del(14q)(q32).

Despite the prognostic relevance of biallelic *TRAF3* inactivation found in this PhD work, little is known about the biological role of *TRAF3* in CLL pathogenesis and how it can affect therapy response. *TRAF3* is a negative regulator of NF-kB signaling, with multiple additional functions described in B and T cells, involving immune and inflammatory response[435-438]. Recently, it has been demonstrated that *TRAF3* may modulate metabolic pathways and mitochondrial physiology in MM and NHL in *in vitro* and *in vivo* models[239, 402, 439]. In the last chapter of this thesis, we investigated **the biological role of *TRAF3* in NF-kB signaling and metabolism in CLL** through CRISPR/cas9-edited cellular models that mimic the *TRAF3* mutations reported in CLL patients (**Results section: Chapter 4)**.

CLL cells harboring biallelic *TRAF3* mutation showed a transcriptional dysregulation of non-canonical NF-kB signaling. Concretely, the inactivation of this gene prompted NIK upregulation, a direct target of TRAF3-mediated proteasomal degradation (**Results section-Chapter 4: Figure 1**). According to previous studies, NIK stabilization triggers non-canonical NF-kB activation by processing the transcription factor NF-kB2 or p100 to p52, which subsequently translocates into the nucleus in the form of p52-RelB heterodimers and activates gene expression[237, 438]. By measuring the DNA binding activity of p52 and RelB, we reported a higher activity of these NF-kB transcription factors in *TRAF3* mutated CLL cells, in line with previous CLL studies regarding NF-kB activation[237, 438]. *BIRC3*, a well-known CLL driver, is frequently inactivated in CLL by mutations and/or del(11q)[86, 176]. This gene, together with *TRAF3*, *BIRC2* and *TRAF2* assembles a complex that constitutively targets *NIK*, and its inactivation also promoted non-canonical NF-kB activation via p52 and RelB nuclear translocation[177, 237, 267]. Here, we demonstrated that the dysfunction of *TRAF3* gene in CLL may have a similar functional consequence to *BIRC3* inactivation in NF-kB signaling.

In a previous study, *TRAF3* inactivation has been associated with a subgroup of DLBCL showing a constitutive RelB activation, which is consistent with the marked correlation observed in our research[440]. Conversely, other studies have proposed that *TRAF3* deficiency may coordinate also canonical NF-kB pathway[291, 441]. However, we did not find any statistically significant correlation in our study, although we noticed a trend towards higher p50 activity in *TRAF3*-mutated CLL cells.

This PhD work also explored new functional consequences of the inactivation of this gene in cellular metabolism. Thus, metabolomic analyses revealed a distinct metabolic profile in *TRAF3*-mutated CLL cells, with a higher abundance of metabolites involved in "Warburg Effect" (phosphoenol-pyruvate, pyruvate and lactate), tricarboxylic acid cycle (TCA) (acetyl-CoA, α-ketoglutarate and succinate) and glutamate metabolism (α-ketoglutarate) (**Results section-Chapter 4: Figure 2, Table 1)**. The enrichment of these metabolites suggests a higher dependency of glucose uptake to uncover the enhanced metabolism of the intermediates involved. Indeed, we identified that *TRAF3*-mutated cells were more sensitive to the inhibition of glucose metabolism by the administration of a glucose analogue. However, in the transcriptional analyses we did not observe an upregulation of the glucose transporter *GLUT1*, or the glycolytic enzyme hexokinase 2, previously reported in a *TRAF3*-deficient B-cell murine model[439], suggesting that the dysregulation of other genes might be responsible for this altered glucose metabolism.

In accordance with these findings and previous data, *TRAF3*-mutated CLL cells showed an enhanced mitochondrial respiration and glycolysis[239, 402, 439]. Moreover, we identified that *TRAF3*-mutant cells were more resistant to anaerobic glycolysis inhibition by lactate-dehydrogenase (LDH) blockade, suggesting a more pronounced mitochondrial glycolytic metabolism. Additionally, *TRAF3*-mutated cells showed a higher maximal respiration in response to the mitochondrial pyruvate carrier inhibitor UK5099, as well as to the glutaminolysis inhibitor C968, which may indicate a higher resistance to pyruvate import and glutaminolysis inhibition in comparison to CLL cells without *TRAF3* mutations (**Results section-Chapter 4: Figure 3 and 4**). Based on these results, we hypothesized that *TRAF3* inactivation in CLL may enhance metabolic plasticity through metabolic reprogramming, allowing cells to fluctuate between mitochondrial glycolysis and glutaminolysis for fueling mitochondrial metabolism. Hence, in this thesis we reported for the first time that *TRAF3* inactivation may induce an improved adaptive capacity of CLL cells to switch to alternative metabolic pathways under stress conditions.

After demonstrating the *TRAF3*-dependent metabolic reprogramming and considering the potential role of *TRAF3* in modulating gene expression via NF-kB activation, we next wondered whether these metabolic changes would be correlated

with a specific gene expression dysregulation. To address this question, in this PhD work we analyzed the gene expression profile of *TRAF3*-mutated CLL cells. Transcriptional studies revealed a dysregulation of glutathione metabolism and glutamine transport (**Suppl. Appendix-Chapter 4: Figure S2)**. Concretely, *TRAF3*-mutated cells presented a significant upregulation of the choline transporter *SLC44A2* and the glutamine transporter *SLC1A4*. Intriguingly, both genes are greatly related to glutamine metabolism[442]. Choline can be metabolized into cysteine and glutathione and, in parallel, glutathione can be derived from glutamine and glutamate metabolism[442]. Previous studies identified elevated choline metabolism in *TRAF3*-deficient cells, which is consistent with our results[239, 443]. Thus, the upregulation of *SLC44A2* and *SLC1A4* could be favoring the metabolic adaption capacity to glutaminolysis inhibition in *TRAF3*-mutated CLL cells.

Furthermore, *SLC1A4* is the main paralog of *SLC1A5,* a target of NF-kB signaling, previously identified to be upregulated in CD40-stimulated B cells[379, 444]. CD40 stimulation subsequently activate NF-kB signaling, and interestingly, similar metabolic dependencies and enhanced mitochondrial and glycolytic activity to *TRAF3*-mutated cells has been described upon CD40 stimulation of B cells[379]. Notably, contemporary works to this thesis uncovered new functions of NF-kB and more concretely, RelB activation, in metabolic reprograming in other B cell lymphomas, which supports our findings and suggests that *TRAF3*-induced metabolic reprogramming could be dependent on NF-kB activation[445, 446]. Even though, *TRAF3* is a multi-faceted gene that may activate different biological functions, and hence, more investigations are needed to further confirm this dependency[447].

Given the dysregulated molecular pathways identified in *TRAF3*-mutated CLL cells, we explored if they could be potentially targetable by CLL drugs and metabolic inhibitors in primary CLL cells with *TRAF3* mutations, in the presence and absence of microenvironment (**Results section-Chapter 4: Figure 5)**. Moreover, considering the metabolic plasticity (mitochondrial glycolysis/glutaminolysis), we also assessed the response to the combined treatment of the metabolic inhibitors UK5099 and C968. The results of this PhD research showed a higher sensitivity of *TRAF3*-mutated cells to venetoclax, as well as a reduced viability after the combined treatment of glutaminolysis and pyruvate transport inhibitors. However, in the presence of

microenvironment, *TRAF3*-mutated CLL primary cells were less sensitive to BCL2 inhibition, in accordance with the effect of stromal cells in the prevention of venetoclax-induced apoptosis[448], whereas *TRAF3*-mutated cells remained as sensitive to the combination of the metabolic inhibitors as isolated CLL cells. These results suggest that the simultaneous inhibition could be blocking *TRAF3*-mediated microenvironmental stimuli. Remarkably, the combined treatment (C968 and UK5099) targeting pyruvate import and glutaminolysis reverses the differential metabolic reprogramming reported in *TRAF3*-mutated cells with respect to the WT (**Results section-Chapter 4: Figure 6)**, further corroborating their metabolic specificities and plasticity that we have described in this work. Altogether, these findings demonstrate the potential of the combination of metabolic inhibitors as a new therapeutic approach in *TRAF3*-mutated patients through its relieving effect on metabolic reprogramming.

All in all, this PhD research contributes to **an improved molecular characterization of rare cytogenetic alterations in CLL**. Despite the low incidence of the alterations analyzed, we achieved a sufficient number of cases to determine relevant molecular alterations underlying CLL pathogenesis of each subgroup. Concretely, we identified distinct mutational patterns within del(6q), IGH*R* and del(14q)(q32) subsets, which shed light into the specific set of molecular pathways altered. In this PhD work we reported a high incidence of biallelic inactivation of *TRAF3* gene in a specific CLL subset del(14q)(q32), with a relevant biological role in NF-kB and metabolism. Furthermore, we described a novel pathomechanism in CLL based on an enhanced tumor adaptive capacity mediated by metabolic reprogramming, and dependent on the inactivation of a specific driver gene.

Additionally, we determined the **prognostic impact of rare cytogenetic alterations and candidate CLL drivers** that could contribute to refine traditional risk stratification models. *RPS15* mutations have been previously associated with high-risk subsets (del(17p) and refractory CLL)[193, 254], and here, we demonstrate that their co-occurrence with 6q deletion could further aggravate CLL outcome. In parallel, the presence of well-established poor prognosis genes (*NOTCH1, SF3B1, TP53, BIRC3* and *BRAF)* not only negatively refined TFT in intermediate risk subgroups such as *IGH* translocations or trisomy 12, but also prompted a shift to a more aggressive outcome in low-risk subsets of patients (del(13q) and normal FISH). And last but not least, we

firstly reported the clinical implication of the biallelic inactivation of the candidate CLL driver *TRAF3*, identified as an independent risk prognostic factor with similar statistically significance to the biallelic *TP53* inactivation, also in patients already stratified according to CLL-IPI and IPS-E prognostic indexes. Altogether, these findings could mean a step forward in CLL prognostication.

In addition to the prognostic implications, this PhD research shed light into the **molecular mechanisms that could affect therapy response of CLL patients with these rare cytogenetic abnormalities.** Concretely, the presence of *RPS15* has been identified in ibrutinib-refractory patients and in our study, two patients with del(6q) and *RPS15* mutations relapsed to subsequent ibrutinib treatment, which may suggest an alternative treatment indication to ibrutinib in this CLL subgroup[449]. Moreover, the high incidence of *NOTCH1* mutations in CLL patients within IGH*R* and del(14q)(q32) CLLs could affect the response to anti-CD20 therapy, and *BCL2* overexpression in *IGH::BCL2* patients could suggest venetoclax as the better treatment option[270]. Furthermore, we proposed a novel therapeutic approach based on the combination of metabolic inhibitors in those patients with *TRAF3* alterations. However, further investigations are needed to confirm the potential clinical implications of this research.

In summary, the results of this PhD research reinforce the statement that the co-occurrence or accumulation of genetic alterations have a relevant implication on CLL pathogenesis and prognosis, highlighting the importance of the assessment of different genetic alterations and their interpretation from a global and integrative point of view, to improve the understanding of CLL pathogenesis and move towards a more efficient personalized medicine.

FUTURE PERSPECTIVES

In the last years, the study of cancer metabolism has significantly expanded the comprehension of the pathogenic mechanisms involved in tumorigenesis, identifying metabolic reprogramming as a promising therapeutic target[333]. Recent investigations suggest that metabolic changes in CLL could be mediating cell proliferation or survival[372]. However, the specific roles of metabolic reprogramming in CLL pathogenesis are currently under investigation.

Thanks to my research stay abroad at Dr. Santos A. Susin lab in the Sorbonne Université in Paris, we were able to demonstrate the implications of the CLL driver *TRAF3* in cellular metabolism, with a relevant role in metabolic reprogramming. Concretely, *TRAF3*-mutated cells showed an enrichment of certain glycolytic and TCA cycle intermediates, as well as an enhanced metabolic plasticity under stress conditions. Nevertheless, many questions regarding the functional consequences of *TRAF3* inactivation in CLL metabolism remain to be elucidated.

Our findings revealed an upregulation of genes related to glutamine metabolism in *TRAF3*-mutated cells, which would explain the abundance of certain intermediates related to this pathway and the resistance to glutaminolysis inhibition. However, at basal state, we did not detect any statistically significant transcriptional change regarding glycolysis or pyruvate mitochondrial metabolism, which could explain the metabolic alterations observed in these cells. To decipher the **additional genetic and/or metabolic changes that might be occurring in *TRAF3*-mutated cells** and overcome RNAseq limitations, I propose to apply a **multiplexed CRISPR/Cas9 screening (Figure 12)** using CLL cellular models. This methodology is based on targeting simultaneously several genes by a sgRNAs lentiviral library, and generating a pool of cells where each one harbors a different loss-of function gene mutation[393]. By using this technique, we could identify gene essentialities of *TRAF3*-mutated cells in the absence or presence of certain treatments. Hence, we could design two sgRNAs libraries targeting 1) genes involved in **glycolysis**, and 2) genes involved in **pyruvate metabolism**. At the end of the experiment, the underrepresentation of certain sgRNAs in *TRAF3*-mutated cells but not in the WT cells would indicate that genes targeted by those sgRNA are essential for proliferation in these models and therefore, for metabolic reprogramming. Moreover, those genes could be potential targets, revealing novel therapeutic approaches in CLLs with *TRAF3* alteration.

CRISPR/Cas9-based screening has already been used for the study of cancer metabolism, identifying novel metabolic dependencies in specific cellular models[404] (**Figure 12**). Our group has recently implemented this technology to study vulnerabilities and resistances of CLL cell lines to PI3K inhibitors (*Pérez-Carretero et al, SEHH-SETH Congress 2022*), uncovering the potential of mTOR inhibitors to overcame PI3Ki resistances. Thus, the next step will be to apply this methodology to decipher *TRAF3*-mediated metabolic alterations in CLL, as described above.

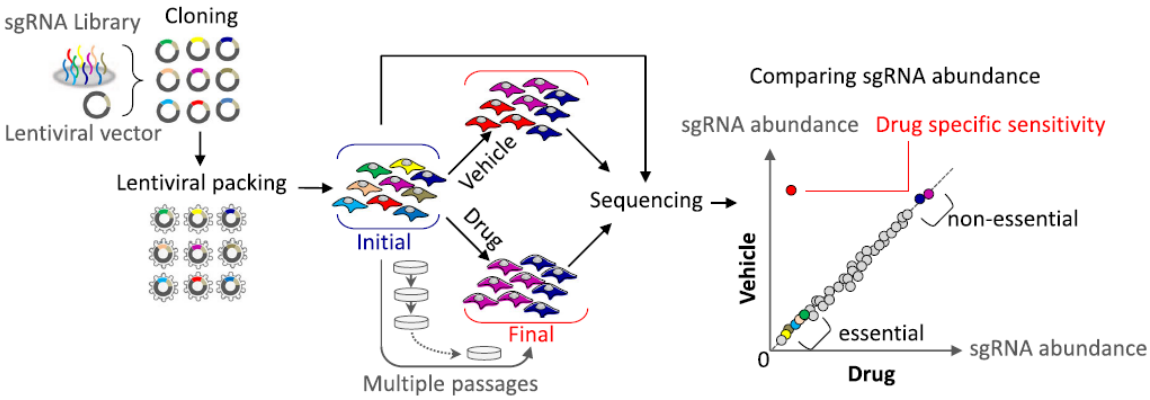

Figure 12. CRISPR/Cas9 loss-of-function screening for the study of metabolic dependencies. A library of sgRNAs targeting the regions of interest will be cloned into a lentiviral vector, followed by packaging into lentiviral particles that will be used to infect cells expressing the nuclease Cas9. Subsequently, cells will be treated with a vehicle or a metabolic inhibitor, passaged, and sequenced. By comparing the abundance of sgRNAs at the end of the experiment to their initial representation, the selective depletion of sgRNAs in the inhibitor treated population can be determined (negative selection) (*adapted from Kang et al. 2018)*[404].

In the light of our results, we suggested that the **metabolism of *TRAF3*-mutated cells may fluctuate between two different pathways** (mitochondrial pyruvate metabolism/glutaminolysis) for fueling mitochondrial activity under stress conditions. However, to further demonstrate this, it would be necessary to perform metabolomics after the treatment with each metabolic inhibitor, and **trace glutamine and glucose** to assess the flux or through which pathways they are metabolized. For that purpose, the use of **isotope-labeled substrates Glucose (^{13}C) and glutamine (^{13}C, ^{15}N)** has been extensively described in metabolomics, as it allows to determine the changes of bioenergetic demands in tumor cells[404]. RNAseq analyses of *TRAF3*-mutated cells treated with the metabolic inhibitors would be of great interest to further investigate

the metabolic reprogramming and the dysregulation of other pathways in these cell lines. Altogether, these approaches would contribute to unravel the *TRAF3*-medited metabolic changes in CLL.

Additionally, this PhD research shows that the combination of certain metabolic drugs may inhibit a *TRAF3*-dependent microenvironmental stimulation in CLL primary cells, which suggests that the *TRAF3*-mediated metabolic reprograming affects TME cells survival and proliferation. However, due to the low incidence of *TRAF3* in CLL patients, these experiments could be performed in just three *TRAF3*-mutated CLL samples. Recent studies have demonstrated that secretion of certain metabolites may alter TME[333], thus, it would be of great interest to analyze if the metabolic reprogramming observed in *TRAF3*-mutated cells could promote the secretion of specific metabolites that activate TME cells. In parallel, recent data demonstrated that CD40 or BCR stimulation results in a metabolic reprogramming of CLL cells[379]. Altogether, these findings may indicate a **metabolic reprogramming upon TME-tumor cells interaction in both cell types**, which could also influence proliferation and treatment response. To investigate the metabolic implications of these cell-cell interactions, metabolomics could be performed in both stromal and CLL cell lines with and without *TRAF3* mutations after co-culture, an also after the administration of CLL or metabolic drugs.

Finally, our findings and recent data suggest that *TRAF3* inactivation could induce **metabolic reprograming through non-canonical NF-kB activation**[445, 446]. In addition, activation of this pathway has been related to the appearance of resistances to venetoclax and ibrutinib[330, 450]. In CLL, this molecular pathway is frequently activated by inactivating mutations, mainly in ***BIRC3***, but also by less frequent mutations or CNA losses in ***TRAF2*** and ***NFKB2***, respectively, in addition to the ***TRAF3*** gene, extensively described in this thesis[78]. In our laboratory, we have generated CRISPR/Cas9-edited cellular models harboring truncating mutations in *BIRC3*, *TRAF2* and *NFKB2*, mimicking the reported ones in CLL patients. Given the potential implication of non-canonical NF-kB signaling in metabolic reprogramming, and also in treatment response, we believe it is worth deepening into the biological implication of these drivers in cellular metabolism through metabolomic, transcriptional and functional approaches, in order to expand the characterization of metabolic changes in CLL.

CONCLUDING REMARKS

1. The presence of the rare cytogenetic abnormalities del(6q), IGH*R* and del(14q)(q32) significantly impacts CLL prognosis, identifying intermediate/adverse-risk subgroups with similar times to first treatment to trisomy 12 or del(11q).
2. Patients with del(6q) as the sole abnormality present a distinct mutational profile with a high incidence of *RPS15* mutations, which impairs CLL outcome within del(6q) subset. Conversely, patients with del(6q) and additional cytogenetic abnormalities have recurrent mutations in *TP53* and show a higher karyotype complexity.
3. The mutational landscape of patients with IGH*R* is characterized by the presence of *NOTCH1, FBXW7, POT1, IGLL5, BCL2* and *HIST1H1E* mutations, indicating an intermediate mutational profile between CLL and NHL. Moreover, the IGH*R* subgroup displays mutations in the 5'UTR non-coding regions of *IGLL5* and *BCL2,* which is associated with a better prognosis.
4. The mutational pattern and clinical outcome of IGH*R* patients varies depending on the type of the IGH rearrangement. *IGH*::*BCL2* fusion associates with *IGLL5, BCL2* and *HIST1H1E* mutations and a longer time to first treatment, while the other CLLs showing IGH*R* present higher frequencies of mutation in poor-prognosis genes (*TP53, SF3B1).*
5. Patients harboring del(14)(q32) display a high frequency of mutations in *NOTCH1, ATM*, genes involved in the RAS signaling pathway (*BRAF, MAP2K1* and *KRAS*), and a high incidence of *TRAF3* biallelic inactivation by deletion and mutation. Furthermore, *TRAF3* biallelic inactivation has a negative impact in prognosis, being an independent risk factor of the time to first treatment.
6. *TRAF3* homozygous mutation in CLL cells promotes the activation of non-canonical NF-kB signaling, through the upregulation of NIK, a target of proteasomal *TRAF3*-mediated degradation, and higher DNA-binding activity of the transcription factors p52 and RelB.
7. CLL cells harboring *TRAF3* inactivation show a metabolic reprogramming based on an enrichment of metabolites involved in the "Warburg effect", tricarboxylic acid (TCA) cycle and glutamate metabolism, and an enhanced mitochondrial respiration. Moreover, *TRAF3*-mutated CLL cells present a higher respiration activity than *TRAF3-wild type* cells after inhibition of the glycolytic pyruvate metabolism,

glutaminolysis and pyruvate import to the mitochondria, indicating a metabolic plasticity and an enhanced adaptive capacity of *TRAF3*-mutated cells to stress conditions.

8. Simultaneous inhibition of glutaminolysis and pyruvate import decreases *TRAF3*-mutated CLL proliferation by relieving *TRAF3*-dependent metabolic reprogramming. Thus, these findings would indicate that the metabolic plasticity relies on the ability of *TRAF3*-mutated cells to switch towards alternative metabolic pathways (mitochondrial glycolysis/glutaminolysis) for fueling mitochondrial activity, being potentially targetable in CLL.

9.

RESUMEN EN CASTELLANO

RESUMEN EN CASTELLANO

VNiVERSiDAD D SALAMANCA

CAMPUS OF INTERNATIONAL EXCELLENCE

Tesis doctoral

Análisis molecular de alteraciones citogenéticas poco frecuentes en la leucemia linfática crónica: de las alteraciones genómicas a la reprogramación metabólica

Directores:

Prof. Dr. Jesús M. Hernández Rivas

Dra. Ana E. Rodríguez Vicente

Claudia Pérez Carretero

2023

INTRODUCCIÓN

La leucemia linfocítica crónica (LLC) consiste en una proliferación de linfocitos B maduros en sangre periférica, médula ósea o ganglios linfáticos, caracterizada por un comportamiento clínico muy heterogéneo, debido a la gran heterogeneidad genética subyacente. En la última década, los grandes avances en técnicas moleculares de alto rendimiento han mejorado significativamente la comprensión de la patogénesis de la enfermedad, ofreciendo nuevas perspectivas que pueden finalmente traducirse en la identificación de nuevos biomarcadores pronósticos y nuevas estrategias terapéuticas para mejorar el manejo de los pacientes.

Las alteraciones cromosómicas son un sello distintivo de la LLC y cada alteración citogenética se asocia con un pronóstico diferente, lo que permite estratificar a los pacientes en distintos subgrupos de riesgo. Durante las últimas décadas, las alteraciones citogenéticas más recurrentes (deleción de 13q, del(13q), deleción de 11q, del(11q), deleción de 17p, del(17p) y trisomía del cromosoma 12, +12) se han evaluado de forma rutinaria mediante el panel clásico de FISH de 4 sondas diseñado para la LLC. Con respecto a las anomalías cromosómicas menos frecuentes que no se incluyen en este panel de FISH, se ha observado que la deleción 6q21, las deleciones 14q32 o las traslocaciones 14q32 pueden influir en el pronóstico, aunque todavía existe cierta controversia entre distintos estudios. Además, la prevalencia de estas alteraciones está probablemente infravalorada, ya que no se evalúan de manera rutinaria, lo que dificulta establecer su incidencia real y, por tanto, su importancia pronóstica.

La expansión de las técnicas de secuenciación de nueva generación (NGS) ha permitido identificar un gran número de alteraciones genéticas, donde se incluyen mutaciones y alteraciones del número de copias que afectan a genes *driver* de la LLC, de manera que no existe una única aberración genética específica de la enfermedad. En los últimos años, se han llevado a cabo multitud de estudios para obtener una caracterización exhaustiva del panorama molecular de la LLC, integrando tanto información cromosómica como mutacional. Estos enfoques han demostrado que ciertas mutaciones genéticas tienen un impacto clínico, lo que puede contribuir a refinar mejor el pronóstico de la LLC, especialmente dentro del modelo de

estratificación de riesgo citogenético. Aunque la gran mayoría son mutaciones codificantes, algunos estudios demostraron que las mutaciones no codificantes también pueden afectar a la patobiología y la clínica de la enfermedad, como las mutaciones en 3'UTR de *NOTCH1*. Cabe destacar que apenas se ha investigado un número reducido de mutaciones genéticas como posibles marcadores pronósticos, y el impacto clínico de varias alteraciones aún está por determinar.

Del mismo modo, la NGS ha permitido investigar más a fondo la patogénesis de la LLC, identificando patrones de concurrencia entre alteraciones cromosómicas y mutaciones somáticas, que pueden estar implicados en la progresión de la LLC. Un mecanismo patogénico frecuente relacionado con estos eventos concurrentes es la inactivación bialélica de genes mediante deleción y mutación, como la inactivación de *ATM* mediante mutaciones y la deleción de 11q, y la de *TP53* mediante mutaciones in la deleción de 17p. En cuanto a las deleciones y traslocaciones 6q y 14q, se ha sugerido la inactivación de ciertos genes supresores por haploinsuficiencia, pero no se ha validado la inactivación bialélica de estos genes. *TRAF3* es un supresor de tumores localizado en 14q32, y se ha observado que puede estar inactivado por una alteración doble (deleción y mutación) en otras neoplasias malignas de células B como el mieloma múltiple (MM) o el linfoma no Hodgkin (NHL). Sin embargo, a pesar de la identificación de deleciones 14q en LLC, la incidencia y asociación de mutaciones de *TRAF3* con esta alteración, así como su impacto en la biología de la enfermedad se desconocen, probablemente debido a su baja incidencia y a la ausencia de estudios que hayan profundizado en ello.

En los últimos años, para superar las limitaciones de disponibilidad de muestras y la dificultad de manipular células de LLC *ex vivo*, los modelos *in vitro* e *in vivo* editados con CRISPR/Cas9 se han convertido en una herramienta muy útil para evaluar las implicaciones biológicas de las alteraciones de la LLC. Además, los recientes avances en el estudio del metabolismo celular en cáncer han demostrado que las neoplasias hematológicas pueden alterar sus especificidades metabólicas para mantener un fenotipo proliferativo y, concretamente, se han identificado alteraciones metabólicas en la LLC, especialmente tras la recaída. Sin embargo, a pesar de estos avances, aún no se ha estudiado si los cambios metabólicos pueden verse influidos por las mutaciones en genes *driver* observadas en la LLC, ni cómo pueden afectar a la

patogénesis y a la progresión de la enfermedad. Así pues, el estudio del metabolismo podría contribuir a mejorar el conocimiento de los mecanismos patogénicos de la LLC y a identificar nuevas vulnerabilidades y resistencias terapéuticas.

En resumen, a la vista de lo descrito anteriormente, es esencial ampliar la caracterización molecular de la LLC, teniendo en cuenta las alteraciones cromosómicas poco frecuentes, las alteraciones en el número de copias, las mutaciones codificantes y no codificantes, así como evaluar las implicaciones de los genes drivers en nuevas funciones biológicas no estudiadas hasta el momento en la LLC. Teniendo esto en cuenta, un análisis que integre estudios de edición genómica, genómica y metabolómica sería de gran utilidad para abordar estas cuestiones y comprender mejor el papel de las alteraciones genéticas raras en la patogénesis, la progresión, y en la respuesta a tratamiento en la LLC.

OBJETIVOS

OBJETIVO GENERAL

Caracterizar el impacto pronóstico y el perfil mutacional de los pacientes con LLC con alteraciones citogenéticas poco frecuentes que afectan a las regiones cromosómicas 6q y 14q32, así como evaluar las implicaciones clínicas y biológicas de los genes *drivers* de la LLC más frecuentemente alterados en estos subgrupos mediante la combinación de secuenciación de nueva generación, edición del genoma y estudios metabólicos.

OBJETIVOS ESPECÍFICOS

1. Evaluar la relevancia pronóstica y las implicaciones clínicas de la deleción 6q, del(6q), las traslocaciones 14q32/*IGH* (IGHR) y las deleciones 14q32/*IGH* en la evolución de la LLC.

2. Caracterizar el perfil mutacional de los pacientes con LLC que presentan del(6q), centrándonos en aquellos con del(6q) como única alteración, y su capacidad para definir el pronóstico de los pacientes con LLC.

3. Analizar el perfil mutacional de los pacientes con LLC y IGH*R*, y evaluar el impacto pronóstico de las mutaciones identificadas dentro de este subgrupo.

4. Determinar las características moleculares de los pacientes con LLC que presentan deleción de *IGH*, así como la incidencia e importancia clínica de la inactivación bialélica de *TRAF3* en este subgrupo de pacientes.

5. Dilucidar las consecuencias biológicas de la inactivación bialélica de *TRAF3* en la señalización de NF-κB y el metabolismo celular mediante modelos celulares editados con CRISPR/Cas9 que imitan las mutaciones de *TRAF3* observadas en pacientes con LLC.

6. Evaluar el impacto de la inactivación de *TRAF3* en la respuesta al tratamiento con fármacos para la LLC y nuevas combinaciones de inhibidores metabólicos en modelos celulares y células primarias de LLC.

CAPÍTULO 1: RESUMEN

Los pacientes con leucemia linfática crónica y deleción de la región cromosómica 6q como única alteración presentan una alta incidencia de mutaciones en *RPS15* y pronóstico adverso

Claudia Pérez Carretero[1,2], Teresa González[1,2], Miguel Quijada Álamo[1,2], Gian Matteo Rigolin[3], Adrian Dubuc[4], Ángela Villaverde Ramiro[1,2,] Alberto Rodríguez[1,2], Juan Nicolás Rodríguez[5], Araceli Rubio[6], Julio Dávila[7], Mª Jesús Vidal[8], Isabel González Gascón y Marín[9], José Ángel Hernández Rivas[9], Rocío Benito[1,2], Matt Davids[10], Jeremy Abrasom[11], Antonio Cuneo[3], Paola Dal Cin[4], Ana-Eugenia Rodríguez-Vicente[1,2] Jesús-María Hernández-Rivas[1,2]

12. University of Salamanca, IBSAL, IBMCC, CSIC, Cancer Research Center, Salamanca, Spain.
13. Department of Hematology, University Hospital of Salamanca, Salamanca, Spain.
14. Hematology Section, St. Anna University Hospital, Ferrara, Italy
15. Department of Pathology, Brigham and Women's Hospital, Boston, MA, USA
16. Department of Hematology. Hospital Juan Ramon Jimenez, Huelva, Spain
17. Department of Hematology, Hospital Miguel Servet, Zaragoza, Spain
18. Department of Hematology, Hospital Nuestra Señora de Sonsoles, Ávila, Spain
19. Department of Hematology, Hospital Universitario, León, Spain.
20. Department of Hematology, Hospital Universitario Infanta Leonor. Universidad Complutense, Madrid, Spain.
21. Dana Farber Cancer Institute, Boston, MA, USA
22. Massachusetts General Hospital, Boston, MA, USA.

INTRODUCCIÓN Y OBJETIVOS

La deleción de 6q del(6q) es una alteración citogenética poco frecuente que aparece en un 3-7% de los enfermos de Leucemia Linfática Crónica (LLC). Aunque en algunos estudios se asocia a una menor supervivencia global, su impacto pronóstico y las características moleculares de los pacientes con esta deleción aún no se han establecido, debido en parte a su baja frecuencia, la variabilidad de la deleción, o la detección de esta alteración tras la administración del tratamiento. Los obejtivos de este estudio son evaluar el impacto pronóstico de esta deleción y analizar perfil mutacional en enfermos de LLC con del(6q) para elucidar los mecanismos de patogenicidad y su impacto clínico.

PACIENTES Y MÉTODOS

Se analizaron un total de 39 muestras de pacientes con LLC y del(6q) y 315 como grupo control. El cariotipo se analizó mediante citogenética convencional y se evaluó el estado mutacional de 54 genes relacionados con la patogénesis de la LLC, mediante un panel personalizado de NGS de captura (Agilent, SureSelect) en la plataforma NextSeq (Illumina). Los resultados se correlacionaron con las características clínicas de los pacientes mediantelos correspondientes tests estadísticos.

RESULTADOS

El análisis citogenético de los pacientes con LLC y del(6q) reveló que ésta era la única alteración en 15 casos, mientras que 24 presentaban otras alteraciones citogenéticas (15 de ellas con cariotipo complejo). El 40% de los enfermos con 6q- presentaban un estadio Binet B/C, y tenían con más frecuencia parámetros biológicos de mal pronóstico con respecto al grupo control: IGHV-UM (76% *vs.* 46%, p=0,003), ZAP70 positivo (63% *vs.* 7,6%, p<0,001) y CD38 positivo (52% *vs.* 28%, p=0,017).

En cuanto al perfil mutacional de los pacientes con del(6q), el 92% de los pacientes (36/39) presentaban al menos una mutación en alguno de los genes analizados. Los genes más frecuentemente mutados en este subgrupo fueron *TP53* (28%), *RPS15* (25%), *NFKBIE* (15%) y *ATM* (15%), todos ellos asociados a mal pronóstico y recaída. De manera interesante, *RPS15* era el gen más mutado en las

LLCs con del(6q) como alteración única (6/15, 40%), mientras que en las LLCs con del(6q) y otras alteraciones fueron *TP53* (9/24, 38%) y *NFKBIE* (4/24, 17%).

Los pacientes con LLC y del(6q) presentaban un menor tiempo hasta el primer tratamiento (TPT) (6 *vs.* 36 meses, p=0,002), independientemente de la presencia de alteraciones citogenéticas adicionales. Cabe destacar que los pacientes con del(6q) y mutaciones en *RPS15* presentaban un menor TPT que las LLCs con del(6q) y *RPS15 wild-type* (5 *vs.* 13 meses, p=0,042), permitiendo definir el pronóstico de este subgrupo de pacientes.

CONCLUSIONES

Los enfermos de LLC con del(6q) presentan menor tiempo hasta el primer tratamiento y un mayor porcentaje de mutaciones en *RPS15* y *TP53*, asociadas a mal pronóstico. Su perfil mutacional varía dependiendo de si del(6q) aparece como alteración única o en combinación con otras alteraciones citogenéticas. Las mutaciones en *RPS15* permiten definir el pronóstico de las LLC con del(6q).

CAPÍTULO 2: RESUMEN

Los pacientes con leucemia linfática crónica y traslocación de *IGH* presentan un perfil genético característico con implicaciones pronósticas

Claudia Pérez-Carretero[1,2], María Hernández-Sánchez[1,2,3], Teresa González[1,2], Miguel Quijada-Álamo[1,2], Marta Martín-Izquierdo[1,2], Jesús-María Hernández-Sánchez[1,2], María-Jesús Vidal[4], Alfonso García de Coca[5], Carlos Aguilar[6], Manuel Vargas-Pabón[7], Sara Alonso[8], Magdalena Sierra[9], Araceli Rubio-Martínez[10], Julio Dávila[11], José R. Díaz-Valdés[12], José-Antonio Queizán[12], José-Ángel Hernández-Rivas[13], Rocío Benito[1,2], Ana E. Rodríguez-Vicente[1,2] and Jesús-María Hernández-Rivas[1,2]

14. Universidad de Salamanca, IBSAL, Centro de Investigación del Cáncer, IBMCC-CSIC, Salamanca, Spain.
15. Servicio de Hematología, Hospital Universitario de Salamanca, Salamanca, Spain.
16. Department of Medical Oncology, Dana Farber Cancer Institute, Boston, Massachusetts, USA.
17. Servicio de Hematología, Hospital Universitario, León, Spain.
18. Servicio de Hematología, Hospital Clínico, Valladolid, Spain.
19. Servicio de Hematología, Complejo Hospitalario de Soria, Soria, Spain.
20. Servicio de Hematología, Hospital Jarrio, Asturias, Spain.
21. Servicio de Hematología, Hospital Universitario Central de Asturias, Oviedo, Spain.
22. Servicio de Hematología, Hospital Virgen de la Concha, Zamora, Spain.
23. Servicio de Hematología, Hospital Miguel Servet, Zaragoza, Spain.
24. Servicio de Hematología, Hospital Nuestra Señora de Sonsoles, Ávila, Spain.
25. Servicio de Hematología, Hospital General de Segovia, Segovia, Spain.
26. Servicio de Hematología. Hospital Universitario Infanta Leonor. Universidad Complutense. Madrid, Spain.

INTRODUCCIÓN Y OBJETIVOS

La traslocación de la región 14q32, que contiene el gen de la cadena pesada de las inmunoglobulinas (*IGH*), aparece en el 5-15% de pacientes de leucemia linfática crónica (LLC). Aunque algunos estudios le atribuyen a este subgrupo un pronóstico desfavorable, sus características clínicas y biológicas no se conocen en profundidad. La secuenciación masiva (NGS) ha mejorado notablemente el conocimiento de la heterogeneidad genética y clínica de la LLC, por lo que nos planteamos el análisis del perfil mutacional de estos pacientes para profundizar en sus mecanismos moleculares de patogenicidad y para definir mejor su pronóstico.

PACIENTES Y MÉTODOS

Se analizaron 233 muestras de pacientes con LLC, de los cuales 46 presentaban traslocación de 14q32. En todos los casos se disponía de datos clínicos y FISH para las 4 sondas del panel de LLC (del(11)(q22)/ATM, del(13)(q14.3), del(17)(p13)/TP53 y +12) además de la sonda *break-apart* para el gen *IGH* (Vysis). Se diseñó un panel de captura personalizado de 54 genes para el análisis mediante NGS, seleccionados por su frecuencia e implicación en la patogenia de la enfermedad. La secuenciación se realizó en la plataforma NextSeq (Illumina). El panel cubre el 97% de las regiones (>100X) con una profundidad de 606 lecturas/base, permitiendo la detección de variantes presentes en >3% de las células.

RESULTADOS

El análisis del tiempo hasta el primer tratamiento (TPT) mostró que los pacientes con reordenamiento de *IGH* tienen un pronóstico intermedio-adverso, con una mediana inferior a la de los pacientes con del(13q) (19 meses *vs.* 120 meses, p<0,001) y más próxima a las LLCs con +12 (19 meses *vs.* 28 meses, p=0,37).

En el estudio mutacional, el 82% de los pacientes (38/46) tenía al menos una mutación. Se identificaron 109 mutaciones en 35 genes, siendo la mediana de mutaciones por paciente 2 (0-6). Los genes más frecuentemente mutados fueron *NOTCH1* (30%), *IGLL5* (17%), *SF3B1* (13%), *POT1* (13%), *TP53, BCL2, FBXW7, ZMYM3* and *MGA* (9% cada uno). Además, las mutaciones en *BCL2* (Q=0,048) y *FBXW7* (Q=0,06) se asociaban exclusivamente a este subgrupo. De manera

interesante, la frecuencia de mutación en los genes *IGLL5, BCL2* y *HIST1H1E* era significativamente mayor a la descrita en estudios previos de LLC y algunas de las mutaciones se habían observado en otros tipos de NHL. Además, no solo se identificaron mutaciones en las regiones codificantes, sino también en las regiones 5'UTR de *IGLL5* y *BCL2,* asociadas con un mayor TPT que los pacientes con reordenamiento de *IGH* sin estas mutaciones (mediana de TPT no alcanzada vs. 9 meses, p=0,001). Además, la incorporación del análisis mutacional en la evaluación del impacto clínico permitió demostrar que la presencia de mutaciones en los genes más frecuentemente mutados en estos pacientes (*NOTCH1, POT1, TP53, SF3B1 y BRAF*) reduce significativamente el TPT en este subgrupo de LLC (2 meses *vs.* 88 meses, p<0.0001), siendo un factor de riesgo independiente (HR=0,255, 95%CI=0,07-0,9, p=0,030).

Por otro lado, el 28% de pacientes con reordenamiento de *IGH* (13/46) presentaban la t(14;18), siendo la mediana de mutaciones por paciente significativamente menor que el resto de traslocaciones (1 vs 2, p=0,03). En el subgrupo con t(14;18), los genes más frecuentemente mutados fueron *BCL2* (23%), *IGLL5* (23%), *HIST1H1E* (15%), *NOTCH1* (15%), mientras que en el resto fueron *NOTCH1* (36%), *SF3B1* (18%), *POT1* (18%) y *TP53* (12%). Estas diferencias podrían explicar el hecho de que las t(14;18) se asocien a marcadores de buen pronóstico como IGHV-M (p=0,001) y mayor TPT que el resto de traslocaciones (56 meses *vs.* 4 meses, p=0,05).

CONCLUSIONES

Los pacientes de LLC con reordenamiento de *IGH* se caracterizan por: a) una elevada frecuencia de mutación; b) la presencia de un alto porcentaje de mutaciones en genes que mutan con poca frecuencia en LLC: *POT1, BCL2, FBXW7, IGLL5, ZMYM3, MGA, BRAF* and *HIST1H1E* y c) presentar un pronóstico intermedio-malo que se agrava en presencia de mutaciones genéticas. Además, los pacientes con t(14;18) tienen una frecuencia de mutación menor que el resto de reordenamientos, presentan mutaciones en *BCL2* e *HIST1H1E* y se asocian con marcadores de buen pronóstico como IGHV-M y menor TPT.

CAPÍTULO 3: RESUMEN

Las alteraciones de *TRAF3* son frecuentes en pacientes con leucemia linfática crónica y del-3'IGH y definen un subgrupo con características clínicas de mal pronóstico

Claudia Pérez-Carretero[1,2], María Hernández-Sánchez[1,2,3], Teresa González[1,2], Miguel Quijada-Álamo[1,2], Marta Martín-Izquierdo[1,2], Sandra Santos-Mínguez[1,2], Cristina Miguel-García[1,2], María-Jesús Vidal[4], Alfonso García-De-Coca[5], Josefina Galende[6], Emilia Pardal[7], Carlos Aguilar[8], Manuel Vargas-Pabón[9], Julio Dávila[10], Isabel Gascón-Y-Marín[11], José-Ángel Hernández-Rivas[11], Rocío Benito[1,2], Jesús-María Hernández-Rivas[1,2] and Ana-Eugenia Rodríguez-Vicente[1,2]

12. Universidad de Salamanca, IBSAL, Centro de Investigación del Cáncer (IBMCC-CSIC), Salamanca, Spain.
13. Servicio de Hematología, Hospital Universitario de Salamanca, Salamanca, Spain.
14. Departamento de Bioquímica y Biología Molecular, Facultad de Farmacia. Universidad Complutense de Madrid, Madrid, Spain (Present affiliation).
15. Servicio de Hematología, Hospital Universitario, León, Spain.
16. Servicio de Hematología, Hospital Clínico, Valladolid, Spain.
17. Servicio de Hematología, Hospital El Bierzo, Ponferrada, Spain
18. Servicio de Hematología, Hospital Virgen del Puerto, Plasencia, Spain
19. Servicio de Hematología, Complejo Hospitalario de Soria, Soria, Spain.
20. Servicio de Hematología, Hospital Jarrio, Asturias, Spain.
21. Servicio de Hematología, Hospital Nuestra Señora de Sonsoles, Ávila, Spain.
22. Servicio de Hematología. Hospital Universitario Infanta Leonor. Universidad Complutense. Madrid, Spain.

INTRODUCCIÓN Y OBJETIVOS

Los reordenamientos del gen *IGH* son un evento poco común en la Leucemia Linfática Crónica (LLC). Además de estas traslocaciones, se han descrito deleciones intersticiales que incluyen este gen (localizado en la región 14q32.33). Sin embargo, no se conoce en profundidad su impacto clínico ni los mecanismos moleculares subyacentes a estas alteraciones. El objetivo de este estudio es analizar el perfil mutacional en enfermos de LLC con deleción parcial o intersticial de *IGH* para elucidar los mecanismos de patogenicidad y su impacto clínico.

PACIENTES Y MÉTODOS

Un total de 871 muestras de pacientes con LLC se analizaron mediante FISH con una sonda 'break-apart' (Vysis) que cubre el gen IGH. Se consideró la presencia de microdeleción de IGH en aquellas muestras con una pérdida de un extremo de la sonda con un 'cut off'>20% de las células de sangre (del-3'IGH). Además, se utilizó el panel de 4 sondas de LLC para del(11)(q22)/ATM, del(13)(q14.3), del(17)(p13)/TP53 y +12. Se evaluó mediante un panel personalizado de NGS el estado mutacional de 54 genes relacionados con la patogénesis de la LLC en muestras no tratadas de 317 LLCs (54 con microdeleción de *IGH* y 263 controles), con la plataforma NextSeq (Illumina). La pérdida de *TRAF3* se analizó mediante el análisis de variación en el número de copias (CNVs) mediante NGS, validadas mediante SNP arrays 6.0.

RESULTADOS

Un total de 54 LLCs presentaban una deleción del extremo 3' de 300kb del gen *IGH* mediante FISH (del-3'IGH). La presencia de esta alteración se asociaba con un menor tiempo hasta el primer tratamiento (TPT) respecto a las LLCs con alteraciones citogenéticas de buen pronóstico (13q- o FISH normal) (45 vs. 184, 116 meses; p<0,001, p<0,001 respectivamente), y similar al de aquellas con pronóstico intermedio (+12) (45 vs 75 meses; p=0,004).

En cuanto al perfil mutacional, el 93% de los pacientes del-3'IGH presentaban al menos una mutación en alguno de los genes analizados. Además, la mediana de mutaciones por paciente fue 2 (0-6). El 30% tenían mutaciones en *NOTCH1*, el 20% en *ATM*, 15% en algún gen de la vía de señalización de RAS (*BRAF, KRAS, NRAS* y

MAP2K1) y el 13% presentaba mutaciones en *TRAF3*. Las mutaciones en *ATM* Y *TRAF3* se asociaban con la presencia de del-3'IGH (p=0,037, p<0,0001 respectivamente). Los pacientes con *TRAF3* mutado presentaban más de una mutación en dicho gen siendo al menos una mutación truncadora. De manera interesante, este gen se localiza en la región 14q32, una zona muy próxima al gen *IGH*, por lo que analizamos si estaba incluido en la deleción. En los análisis de CNV se identificaron 11 pacientes con pérdida de *TRAF3,* siete de ellos con mutaciones en el otro alelo. Además, la frecuencia de variación alélica (VAF) de las mutaciones era inferior al porcentaje de células con la deleción (media: 15,6±4.7 *vs*. 70,5±6.5), indicando que la aparición de las mutaciones es un evento secundario que resulta en la inactivación bialélica de *TRAF3*.

En cuanto al impacto clínico, la presencia de las mutaciones en *NOTCH1*, *ATM*, vía de RAS y *TRAF3* permitía definir el pronóstico de los pacientes con del-3'IGH. Aquellos con mutaciones en *NOTCH1, ATM* y vía de RAS presentaban una menor supervivencia global que el resto de pacientes con del-3'IGH, mientras que los pacientes con mutaciones en *TRAF3* presentaban un menor tiempo hasta primer tratamiento (6 vs. 51 meses, p<0,001). Además, la inactivación bialélica de *TRAF3* se asociaba con un pronóstico desfavorable, similar al de los pacientes con inactivación bialélica de *ATM* o *TP53,* siendo un factor de riesgo independiente en el análisis multivariante (HR=0,21, 95%CI=0,05–0,85, p=0,029).

CONCLUSIONES

Los enfermos de LLC con microdeleción del extremo 3' de IGH presentan un menor tiempo hasta el primer tratamiento que las LLCs con del(13q) o FISH normal. Los pacientes con esta alteración citogenética presentan un perfil mutacional característico con mayor frecuencia de mutaciones en *NOTCH1*, *ATM* y via de RAS, cuya concurrencia podría agravar el pronóstico de los pacientes, y una alta incidencia de la inactivación bialélica de *TRAF3* mediante mutación y deleción, contribuyendo a un menor tiempo hasta el primer tratamiento siendo un factor de riesgo independiente.

CAPÍTULO 4: RESUMEN

Las alteraciones de *TRAF3* potencian la plasticidad del metabolismo celular mediante reprogramación metabólica en la leucemia linfática crónica

Claudia Pérez Carretero[1,2], Miguel Quijada Álamo[1,2], Mariana Tannoury[3], Léa Dehgane[3], Alberto Rodríguez Sánchez[1,2], David J. Sanz[1,2], Teresa González[1,2], Rocío Benito[1,2], Élise Chapiro[4], Florence Nguyen[4], Ana E. Rodriguez Vicente[1,2], Santos A. Susin[3], Jesús María Hernández Rivas[1,2]

5. University of Salamanca, IBSAL, IBMCC, CSIC, Cancer Research Center, Salamanca, Spain
6. Department of Hematology, University Hospital of Salamanca, Salamanca, Spain
7. Drug Resistance in Hematological Malignancies, Centre de Recherche des Cordeliers, UMRS 1138, INSERM, Sorbonne Université, Université Paris Cité, F-75006 Paris, France
8. Drug Resistance in Hematological Malignancies, Centre de Recherche des Cordeliers, UMRS 1138, INSERM, Sorbonne Université, Université Paris Cité, F-75006 Paris, France; Groupe Hospitalier Pitié-Salpêtrière, Assistance Publique-Hôpitaux de Paris, F-75013 Paris, France

INTRODUCCIÓN Y OBJETIVOS

El gen *TRAF3* (*TNF receptor-associated factor 3*), localizado en 14q32, está frecuentemente alterado por deleción y/o mutación en el mieloma múltiple, el linfoma y otras neoplasias malignas de células B como la leucemia linfocítica crónica (LLC). Este gen aparece mutado en el 0.5-1% de pacientes con LLC, y delecionado en alrededor del 2% de casos, ya que puede estar afectado por la deleción 14q. En concreto, nuestro grupo ha descrito recientemente una alta incidencia de la inactivación bialélica de *TRAF3* (13%) en un subgrupo de pacientes con deleción de 14q32/*IGH*, asociada con un pronóstico desfavorable. En cuanto a su función biológica, *TRAF3* es un regulador negativo de la ruta no canónica NF-kB, y datos recientes han descubierto funciones adicionales de este gen en la inflamación, la inmunidad antiviral o el metabolismo celular en neoplasias como mieloma múltiple o linfoma no Hodgkin. Sin embargo, se desconoce la importancia a nivel funcional de las alteraciones de *TRAF3* en la LLC. Por ello, el objetivo de este estudio fue evaluar la implicación biológica de las alteraciones de *TRAF3* en la patogénesis de la LLC mediante modelos generados con CRISPR/Cas9.

PACIENTES Y MÉTODOS

Se utilizó el sistema CRISPR/Cas9 para reproducir mutaciones homocigóticas de pérdida de función de *TRAF3* en la línea celular PGA1 derivada de CLL. Posteriormente, caracterizamos estas células mediante análisis transcriptómico con la tecnología de RNAseq (Illumina), análisis metabolómico mediante cromatograífa líquida (MilliporeSigma) acoplada a espectrometría de masas (Thermo Fisher Scientific) (LC-MS) y estudios funcionales. Los estudios funcionales incluyen el análisis de la expresión de genes antiapoptóticos mediante PCR digital (Bio-Rad), análisis de la actividad de unión de factores de transcripción al DNA mediante ELISA (Active Motif), y la evaluación de la respiración mitocondrial y glicólisis midiendo las tasas de consumo de oxígeno (OCR) y de acidificación del medio extracelular (ECAR) en estos modelos mediante la tecnología Seahorse (Agilent). Además, se analizó la viabilidad celular de un total de 22 muestras de células primarias de LLC en respuesta a distintos tratamientos e inhibidores metabólicos (CellTiter-Glo, Promega).

RESULTADOS

Los análisis RNA-seq identificaron 54 genes desregulados enriquecidos en vías como la señalización NIK/NF-kB (FDR=0,029). Concretamente, NIK (una diana directa de la degradación mediada por *TRAF3*) aumentó significativamente (Q<0,001) en los clones *TRAF3*-mutados, lo que se correlacionó con una mayor actividad nuclear de los factores de transcripción NF-kB no canónicos p52 (p=0,05) y RelB (p=0,02). Además, las células PGA1-*TRAF3* mutadas mostraron mayores niveles de BAX (p=0,05).

En el estudio metabolómico, se encontró un enriquecimiento de metabolitos implicados en el efecto Warburg, el ciclo del ácido cítrico (TCA) y el metabolismo del glutamato (FDR<0,001, 0,003, 0,1 resp.), con niveles significativamente mayores de α-cetoglutarato (intermediario del TCA sintetizado a partir del glutamato), piruvato y lactato (productos de la glucólisis) (p<0,001, p<0,001, p=0,002) en las células PGA1-*TRAF3* mutadas. Cabe destacar que estas células mostraron características mitocondriales distintas: mayores niveles de respiración basal y máxima y una mayor capacidad de reserva y generación de ATP ligada a la respiración mitocondrial, así como una mayor glicólisis.

Así, las células con mutación de *TRAF3* eran más sensibles a la 2-deoxi-D-glucosa (inhibidor de la captación de glucosa) y más resistentes al oxamato (inhibidor de la lactato-deshidrogenasa, marcador de la glucólisis anaeróbica). En general, estos resultados indican que, a diferencia de las células WT, las *TRAF3* mutadas utilizan un metabolismo glucolítico mitocondrial. Sorprendentemente, al utilizar UK5099 (inhibidor del transportador mitocondrial de piruvato que regula la glucólisis mitocondrial) las células mutantes mostraron niveles máximos de respiración superiores a las WT, lo que sugiere una reprogramación metabólica hacia una vía metabólica alternativa que alimenta el metabolismo mitocondrial. Por lo tanto, probamos el efecto del C968 (inhibidor de la glutaminólisis) y descubrimos que las células *TRAF3* mutadas también eran más resistentes a este fármaco, lo que revela una plasticidad metabólica específica (glucólisis mitocondrial/ glutaminólisis) en las células PGA1-*TRAF3* mutadas que no existe en las WT.

Curiosamente, el tratamiento combinado (UK5099 y C968) indujo más muerte celular en las células *TRAF3* mutadas que en las WT (p=0,03). De manera interesante, esta combinación revertía la reprogramación metabólica observada en estado basal (tras el tratamiento combinado, los niveles de metabolitos previamente alterados eran ya igual en las WT y en las *TRAF3*-mutadas), y las *TRAF3*-mutadas presentaban el mismo nivel de respiración y glicólisis que las WT. Además, las células primarias de LLC con mutaciones de *TRAF3* también eran sensibles a esta combinación (p<0,05), lo que sugiere una nueva oportunidad potencial para tratar a pacientes con alteraciones de *TRAF3*.

CONCLUSIONES

Las células con *TRAF3* mutado presentan una mayor activación de la vía no canónica de NF-kB y una reprogramación metabólica hacia un aumento de la glucólisis mitocondrial y la glutaminólisis. La inhibición simultánea de estas dos vías revierte dicha reprogamación metabólica y disminuye la proliferación en las células con mutación de *TRAF3*. Por lo tanto, en este estudio identificamos un mecanismo de adaptación celular potenciado en las células *TRAF3* mutadas, basado en una mayor plasticidad metabólica, que puede ser una potencial diana terapéutica en pacientes con LLC.

CONCLUSIONES

1. La presencia de las alteraciones cromosómicas poco frecuentes del(6q), IGHR y del(14q)(q32) influye significativamente en el pronóstico de la LLC, identificando subgrupos de riesgo intermedio/adverso con tiempos hasta el primer tratamiento similares a los de la trisomía 12 o del(11q).
2. Los pacientes con del(6q) como única alteración presentan un perfil mutacional distinto con una alta incidencia de mutaciones *RPS15*, lo que agrava el pronóstico de la LLC dentro del subgrupo del(6q). Por el contrario, los pacientes con del(6q) y alteraciones citogenéticas adicionales presentan mutaciones recurrentes en *TP53* y muestran una mayor complejidad del cariotipo.
3. El perfil mutacional de los pacientes con IGH*R* se caracteriza por la presencia de mutaciones en *NOTCH1, FBXW7, POT1, IGLL5, BCL2* e *HIST1H1E*, lo que indica un perfil mutacional intermedio entre la LLC y el LNH. Además, el subgrupo IGH*R* presenta mutaciones en las regiones no codificantes 5'UTR de *IGLL5* y *BCL2*, asociadas a un mejor pronóstico.
4. El perfil mutacional y el curso clínico de los pacientes con IGH*R* varían en función del tipo de reordenamiento *IGH*. La fusión *IGH::BCL2* se asocia a mutaciones en *IGLL5, BCL2* e *HIST1H1E* y a un mayor tiempo hasta el primer tratamiento, mientras que el resto de LLC que presentan IGH*R* presentan mayores frecuencias de mutación en genes de mal pronóstico (*TP53, SF3B1*).
5. Los pacientes que presentan del(14)(q32) muestran una alta frecuencia de mutaciones en *NOTCH1, ATM*, genes implicados en la vía de señalización RAS (*BRAF, MAP2K1* y *KRAS*), y una alta incidencia de inactivación bialélica de *TRAF3* por deleción y mutación. Además, la inactivación bialélica de *TRAF3* tiene un impacto negativo en el pronóstico, siendo un factor de riesgo independiente del tiempo hasta el primer tratamiento.
6. La mutación homocigota de *TRAF3* en células de LLC promueve la activación de la ruta no canónica de NF-kB, a través de la sobreexpresión de NIK, una diana de la degradación proteasomal mediada por *TRAF3*, y una mayor actividad de unión al ADN de los factores de transcripción p52 y RelB.

7. Las células de LLC que presentan inactivación de *TRAF3* muestran una reprogramación metabólica basada en un enriquecimiento de metabolitos implicados en el "efecto Warburg", el ciclo del ácido tricarboxílico (TCA) y el metabolismo del glutamato, y una mayor respiración mitocondrial. Además, las células de LLC con *TRAF3* mutado presentan una mayor actividad respiratoria que las células *TRAF3-wild type* tras la inhibición del metabolismo glucolítico del piruvato, la glutaminolisis y la importación de piruvato a la mitocondria, lo que indica una plasticidad metabólica y una mayor capacidad de adaptación de las células mutadas con *TRAF3* a condiciones de estrés.
8. La inhibición simultánea de la glutaminolisis y la importación de piruvato disminuye la proliferación de las células de LLC con mutación de *TRAF3* al revertir la reprogramación metabólica dependiente de *TRAF3*. Por lo tanto, estos hallazgos indicarían que la plasticidad metabólica se basa en la capacidad de las células con mutación *TRAF3* para cambiar hacia vías metabólicas alternativas (glucólisis mitocondrial/glutaminólisis) para impulsar la actividad mitocondrial, siendo potenciales dianas terapéuticas en la LLC.

REFERENCES

1. Swerdlow SH, Campo E, Pileri SA, et al. The 2016 revision of the World Health Organization classification of lymphoid neoplasms. *Blood*. 05 2016;127(20):2375-90. doi:10.1182/blood-2016-01-643569

2. Chiorazzi N, Rai KR, Ferrarini M. Chronic Lymphocytic Leukemia. *New England Journal of Medicine*. 2005;352(8):804-815. doi:10.1056/NEJMra041720

3. Kipps TJ, Stevenson FK, Wu CJ, et al. Chronic lymphocytic leukaemia. *Nature Reviews Disease Primers*. 2017;3(1):16096. doi:10.1038/nrdp.2016.96

4. Strati P, Jain N, O'Brien S. Chronic Lymphocytic Leukemia: Diagnosis and Treatment. *Mayo Clinic Proceedings*. 2018;93(5):651-664. doi:10.1016/j.mayocp.2018.03.002

5. Hallek M. Chronic lymphocytic leukemia: 2020 update on diagnosis, risk stratification and treatment..*American Journal of Hematology*. 2019;94(11):1266-1287. doi:https://doi.org/10.1002/ajh.25595

6. Berndt SI, Skibola CF, Joseph V, et al. Genome-wide association study identifies multiple risk loci for chronic lymphocytic leukemia. *Nature Genetics*. 2013;45(8):868-876. doi:10.1038/ng.2652

7. Cerhan JR, Slager SL. Familial predisposition and genetic risk factors for lymphoma. *Blood*. 2015;126(20):2265-2273. doi:10.1182/blood-2015-04-537498

8. Speedy HE, Sava G, Houlston RS. Inherited Susceptibility to CLL. In: Malek S, ed. *Advances in Chronic Lymphocytic Leukemia*. Springer New York; 2013:293-308.

9. Cheson BD, Bennett JM, Rai KR, et al. Guidelines for clinical protocols for chronic lymphocytic leukemia: Recommendations of the national cancer institute-sponsored working group.. *American Journal of Hematology*. 1988;29(3):152-163. doi:https://doi.org/10.1002/ajh.2830290307

10. Hallek M, Cheson BD, Catovsky D, et al. Guidelines for the diagnosis and treatment of chronic lymphocytic leukemia: a report from the International Workshop on Chronic Lymphocytic Leukemia updating the National Cancer Institute-Working Group 1996 guidelines. *Blood*. Jun 2008;111(12):5446-56. doi:10.1182/blood-2007-06-093906

11. Hallek M, Cheson BD, Catovsky D, et al. iwCLL guidelines for diagnosis, indications for treatment, response assessment, and supportive management of CLL. *Blood*. 2018;131(25):2745-2760. doi:10.1182/blood-2017-09-806398

12. Matutes E, Owusu-Ankomah K, Morilla R, et al. The immunological profile of B-cell disorders and proposal of a scoring system for the diagnosis of CLL. *Leukemia*. 1994;8(10):1640-1645.

13. Moreau EJ, Matutes E, A'Hern RP, et al. Improvement of the chronic lymphocytic leukemia scoring system with the monoclonal antibody SN8 (CD79b). *Am J Clin Pathol*. 1997;108(4):378-82. doi:10.1093/ajcp/108.4.378

14. Rawstron AC, Kreuzer K-A, Soosapilla A, et al. Reproducible diagnosis of chronic lymphocytic leukemia by flow cytometry: An European Research Initiative on CLL (ERIC) & European Society for Clinical Cell Analysis (ESCCA) Harmonisation project. *Cytometry Part B: Clinical Cytometry*. 2018;94(1):121-128. doi:https://doi.org/10.1002/cyto.b.21595

15. Melo JV, Catovsky D, Galton DAG. The relationship between chronic lymphocytic leukaemia and prolymphocytic leukaemia. *British Journal of Haematology*. 1986;64(1):77-86. doi:https://doi.org/10.1111/j.1365-2141.1986.tb07575.x

16. Schlette E, Medeiros LJ, Keating M, Lai R. CD79b Expression in Chronic Lymphocytic Leukemia: Association With Trisomy 12 and Atypical Immunophenotype. *Archives of Pathology & Laboratory Medicine*. 2003;127(5):561-566. doi:10.5858/2003-127-0561-CEICLL

17. Quijano S, López A, Rasillo A, et al. Impact of trisomy 12, del(13q), del(17p), and del(11q) on the immunophenotype, DNA ploidy status, and proliferative rate of leukemic B-cells in chronic lymphocytic leukemia. *Cytometry Part B: Clinical Cytometry*. 2008;74B(3):139-149. doi:https://doi.org/10.1002/cyto.b.20390

18. Cro L, Ferrario A, Lionetti M, et al. The clinical and biological features of a series of immunophenotypic variant of B-CLL.. *European Journal of Haematology*. 2010;85(2):120-129. doi:https://doi.org/10.1111/j.1600-0609.2010.01454.x

19. Rawstron AC, Bennett FL, O'Connor SJM, et al. Monoclonal B-Cell Lymphocytosis and Chronic Lymphocytic Leukemia. *New England Journal of Medicine*. 2008;359(6):575-583. doi:10.1056/NEJMoa075290

20. Ignacio C, Arancha R-C, Gutiérrez ML, et al. Low-count monoclonal B-cell lymphocytosis persists after seven years of follow up and is associated with a poorer outcome. *Haematologica*. 2018;103(7):1198-1208. doi:10.3324/haematol.2017.183954

21. Vardi A, Dagklis A, Scarfò L, et al. Immunogenetics shows that not all MBL are equal: the larger the clone, the more similar to CLL. *Blood*. 2013;121(22):4521-4528. doi:10.1182/blood-2012-12-471698

22. Nieto WG, Almeida J, Romero A, et al. Increased frequency (12%) of circulating chronic lymphocytic leukemia–like B-cell clones in healthy subjects using a highly sensitive multicolor flow cytometry approach. *Blood*. 2009;114(1):33-37. doi:https://doi.org/10.1182/blood-2009-01-197368

23. Campo E, Swerdlow SH, Harris NL, Pileri S, Stein H, Jaffe ES. The 2008 WHO classification of lymphoid neoplasms and beyond: evolving concepts and practical applications. *Blood*. 2011;117(19):5019-5032. doi:10.1182/blood-2011-01-293050

24. Parikh SA, Habermann TM, Chaffee KG, et al. Hodgkin transformation of chronic lymphocytic leukemia: Incidence, outcomes, and comparison to de novo Hodgkin lymphoma. *American Journal of Hematology*. 2015;90(4):334-338. doi:https://doi.org/10.1002/ajh.23939

25. Rossi D, Gaidano G. Richter syndrome: pathogenesis and management. *Seminars in Oncology*. 2016;43(2):311-319. doi:https://doi.org/10.1053/j.seminoncol.2016.02.012

26. Tsimberidou A-M, O'Brien S, Kantarjian HM, et al. Hodgkin transformation of chronic lymphocytic leukemia. *Cancer*. 2006;107(6):1294-1302. doi:https://doi.org/10.1002/cncr.22121

27. Parikh SA, Rabe KG, Call TG, et al. Diffuse large B-cell lymphoma (Richter syndrome) in patients with chronic lymphocytic leukaemia (CLL): a cohort study of newly diagnosed patients. *British Journal of Haematology*. 2013;162(6):774-782. doi:https://doi.org/10.1111/bjh.12458

28. Mouhssine S, Gaidano G. Richter Syndrome: From Molecular Pathogenesis to Druggable Targets. *Cancers*. 2022;14(19). doi:10.3390/cancers14194644

29. Rossi D, Spina V, Deambrogi C, et al. The genetics of Richter syndrome reveals disease heterogeneity and predicts survival after transformation. *Blood*. 2011;117(12):3391-3401. doi:10.1182/blood-2010-09-302174

30. Sharma S, Rai KR. Chronic lymphocytic leukemia (CLL) treatment: So many choices, such great options. *Cancer*. 2019;125(9):1432-1440. doi:https://doi.org/10.1002/cncr.31931

31. Pérez-Carretero C, González-Gascón-Y-Marín I, Rodríguez-Vicente AE, et al. The Evolving Landscape of Chronic Lymphocytic Leukemia on Diagnosis, Prognosis and Treatment. *Diagnostics (Basel)*. 2021;11(5)doi:10.3390/diagnostics11050853

32. Rai KR, Sawitsky A, Cronkite EP, Chanana AD, Levy RN, Pasternack BS. Clinical staging of chronic lymphocytic leukemia. *Blood*. 1975;46(2):219-234. doi:10.1182/blood.V46.2.219.219

33. Binet JL, Auquier A, Dighiero G, et al. A new prognostic classification of chronic lymphocytic leukemia derived from a multivariate survival analysis. *Cancer*. 1981;48(1):198-206.

34. Rai KR, Jain P. Chronic lymphocytic leukemia (CLL)-Then and now. *Am J Hematol*. 2016;91(3):330-40. doi:10.1002/ajh.24282

35. Viñolas N, Reverter JC, Urbano-Ispizua A, Montserrat E, Rozman C. Lymphocyte doubling time in chronic lymphocytic leukemia: an update of its prognostic significance. *Blood cells*. 1987 1987;12(2):457-470.

36. Rozman C, Hernandez-Nieto L, Montserrat E, Brugues R. Prognostic Significance of Bone-Marrow Patterns in Chronic Lymphocytic Leukaemia. *British Journal of Haematology*.1981;47(4):529-537. doi:https://doi.org/10.1111/j.1365-2141.1981.tb02681.x

37. González-Gascón-Y-Marín I, Muñoz-Novas C, Rodríguez-Vicente AE, et al. From Biomarkers to Models in the Changing Landscape of Chronic Lymphocytic Leukemia: Evolve or Become Extinct. *Cancers (Basel)*. 2021;13(8)doi:10.3390/cancers13081782

38. Hallek M, Wanders L, Ostwald M, et al. Serum β2-Microglobulin and Serum Thymidine Kinase are Independent Predictors of Progression-Free Survival in Chronic Lymphocytic Leukemia and Immunocytoma. *Leukemia & Lymphoma*. 1996;22(5-6):439-447. doi:10.3109/10428199609054782

39. Magnac C, Porcher R, Davi F, et al. Predictive value of serum thymidine kinase level for Ig-V mutational status in B-CLL. *Leukemia*. 2003;17(1):133-137. doi:10.1038/sj.leu.2402780

40. Piñeyroa JA, Magnano L, Rivero A, et al. Serum soluble CD23 levels are an independent predictor of time to first treatment in chronic lymphocytic leukemia. *Hematological Oncology*. 2022;40(4):588-595. doi:https://doi.org/10.1002/hon.3027

41. Damle RN, Wasil T, Fais F, et al. Ig V gene mutation status and CD38 expression as novel prognostic indicators in chronic lymphocytic leukemia. *Blood*. Sep 1999;94(6):1840-7.

42. Orchard JA, Ibbotson RE, Davis Z, et al. ZAP-70 expression and prognosis in chronic lymphocytic leukaemia. *The Lancet*. 2004;363(9403):105-111. doi:10.1016/S0140-6736(03)15260-9

43. Davide R, Antonella Z, Francesca Maria R, et al. CD49d expression is an independent risk factor of progressive disease in early stage chronic lymphocytic leukemia. *Haematologica*. 2008;93(10):1575-1579. doi:10.3324/haematol.13103

44. Rassenti LZ, Jain S, Keating MJ, et al. Relative value of ZAP-70, CD38, and immunoglobulin mutation status in predicting aggressive disease in chronic lymphocytic leukemia. *Blood*. 2008;112(5):1923-1930. doi:10.1182/blood-2007-05-092882

45. Gattei V, Bulian P, Del Principe MI, et al. Relevance of CD49d protein expression as overall survival and progressive disease prognosticator in chronic lymphocytic leukemia. *Blood*. 2008;111(2):865-873. doi:10.1182/blood-2007-05-092486

46. Lesley-Ann S, Anastasia H, Panagiotis B, et al. Immunoglobulin genes in chronic lymphocytic leukemia: key to understanding the disease and improving risk stratification. *Haematologica*. 2017;102(6):968-971. doi:10.3324/haematol.2017.165605

47. Fais F, Ghiotto F, Hashimoto S, et al. Chronic lymphocytic leukemia B cells express restricted sets of mutated and unmutated antigen receptors. *The Journal of Clinical Investigation*. 1998;102(8):1515-1525. doi:10.1172/JCI3009

48. Hamblin TJ, Davis Z, Gardiner A, Oscier DG, Stevenson FK. Unmutated Ig V(H) genes are associated with a more aggressive form of chronic lymphocytic leukemia. *Blood*. 1999;94(6):1848-54.

49. Young C, Brink R. The unique biology of germinal center B cells. *Immunity*. 2021;54(8):1652-1664. doi:10.1016/j.immuni.2021.07.015

50. Fabbri G, Dalla-Favera R. The molecular pathogenesis of chronic lymphocytic leukaemia. *Nat Rev Cancer*. 2016;16(3):145-62. doi:10.1038/nrc.2016.8

51. Cramer P, Hallek M. Prognostic factors in chronic lymphocytic leukemia—what do we need to know? *Nature Reviews Clinical Oncology*. 2011;8(1):38-47. doi:10.1038/nrclinonc.2010.167

52. Stamatopoulos K, Belessi C, Moreno C, et al. Over 20% of patients with chronic lymphocytic leukemia carry stereotyped receptors: pathogenetic implications and clinical correlations. *Blood*. 2006;109(1):259-270. doi:10.1182/blood-2006-03-012948

53. Agathangelidis A, Darzentas N, Hadzidimitriou A, et al. Stereotyped B-cell receptors in one-third of chronic lymphocytic leukemia: a molecular classification with implications for targeted therapies. *Blood*. 2012;119(19):4467-4475. doi:10.1182/blood-2011-11-393694

54. Baliakas P, Hadzidimitriou A, Sutton L-A, et al. Clinical effect of stereotyped B-cell receptor immunoglobulins in chronic lymphocytic leukaemia: a retrospective multicentre study. *The Lancet Haematology*. 2014;1(2):e74-e84. doi:10.1016/S2352-3026(14)00005-2

55. Stamatopoulos K, Agathangelidis A, Rosenquist R, Ghia P. Antigen receptor stereotypy in chronic lymphocytic leukemia. *Leukemia*. 2017;31(2):282-291. doi:10.1038/leu.2016.322

56. Agathangelidis A, Chatzidimitriou A, Gemenetzi K, et al. Higher-order connections between stereotyped subsets: implications for improved patient classification in CLL. *Blood*. 2021;137(10):1365-1376. doi:10.1182/blood.2020007039

57. Sonia J, Andreas A, Christof S, et al. Prognostic impact of prevalent chronic lymphocytic leukemia stereotyped subsets: analysis within prospective clinical trials of the German CLL Study Group (GCLLSG). *Haematologica*. 2019;105(11):2598-2607. doi:10.3324/haematol.2019.231027

58. Puiggros A, Blanco G, Espinet B. Genetic Abnormalities in Chronic Lymphocytic Leukemia: Where We Are and Where We Go. *BioMed Research International*. 2014;2014:435983. doi:10.1155/2014/435983

59. Döhner H, Stilgenbauer S, Benner A, et al. Genomic aberrations and survival in chronic lymphocytic leukemia. *N Engl J Med*. 2000;343(26):1910-6. doi:10.1056/NEJM200012283432602

60. Juliusson G, Oscier DG, Fitchett M, et al. Prognostic Subgroups in B-Cell Chronic Lymphocytic Leukemia Defined by Specific Chromosomal Abnormalities. *New England Journal of Medicine*. 1990;323(11):720-724. doi:10.1056/NEJM199009133231105

61. Van Dyke DL, Werner L, Rassenti LZ, et al. The Dohner fluorescence in situ hybridization prognostic classification of chronic lymphocytic leukaemia (CLL): the CLL Research Consortium experience. *British Journal of Haematology*. 2016;173(1):105-113. doi:https://doi.org/10.1111/bjh.13933

62. Dewald GW, Brockman SR, Paternoster SF, et al. Chromosome anomalies detected by interphase fluorescence in situ hybridization: correlation with significant biological features of B-cell chronic lymphocytic leukaemia. *British Journal of Haematology*. 2003;121(2):287-295. doi:https://doi.org/10.1046/j.1365-2141.2003.04265.x

63. Geisler C, Jurlander J, Bullinger L, et al. Danish CLL2-Study revisited: FISH on a cohort with a 20-yr follow-up confirms the validity of the hierarchical model of genomic aberrations in chronic lymphocytic leukaemia. *European Journal of Haematology*. 2009;83(2):156-158. doi:https://doi.org/10.1111/j.1600-0609.2009.01258.x

64. Byrd JC, Gribben JG, Peterson BL, et al. Select High-Risk Genetic Features Predict Earlier Progression Following Chemoimmunotherapy With Fludarabine and Rituximab in Chronic Lymphocytic Leukemia: Justification for Risk-Adapted Therapy. *Journal of Clinical Oncology*. 2006;24(3):437-443. doi:10.1200/JCO.2005.03.1021

65. Kipps TJ, Fraser G, Coutre SE, et al. Long-Term Studies Assessing Outcomes of Ibrutinib Therapy in Patients With Del(11q) Chronic Lymphocytic Leukemia. *Clinical Lymphoma, Myeloma and Leukemia*. 2019;19(11):715-722.e6. doi:10.1016/j.clml.2019.07.004

66. Austen B, Skowronska A, Baker C, et al. Mutation status of the residual ATM allele is an important determinant of the cellular response to chemotherapy and survival in patients with chronic lymphocytic leukemia containing an 11q deletion. *J Clin Oncol*. 2007;25(34):5448-57. doi:10.1200/JCO.2007.11.2649

67. Skowronska A, Parker A, Ahmed G, et al. Biallelic ATM inactivation significantly reduces survival in patients treated on the United Kingdom Leukemia Research Fund Chronic Lymphocytic Leukemia 4 trial. *J Clin Oncol*. 2012;30(36):4524-32. doi:10.1200/JCO.2011.41.0852

68. Stankovic T, Skowronska A. The role of ATM mutations and 11q deletions in disease progression in chronic lymphocytic leukemia. *Leuk Lymphoma*. 2014;55(6):1227-39. doi:10.3109/10428194.2013.829919

69. Rosenwald A, Chuang EY, Davis RE, et al. Fludarabine treatment of patients with chronic lymphocytic leukemia induces a p53-dependent gene expression response. *Blood*. 2004;104(5):1428-1434. doi:10.1182/blood-2003-09-3236

70. Zenz T, Häbe S, Denzel T, et al. Detailed analysis of p53 pathway defects in fludarabine-refractory chronic lymphocytic leukemia (CLL): dissecting the contribution of 17p deletion, TP53 mutation, p53-p21 dysfunction, and miR34a in a prospective clinical trial. *Blood*. 2009;114(13):2589-97. doi:10.1182/blood-2009-05-224071

71. Zenz T, Vollmer D, Trbusek M, et al. TP53 mutation profile in chronic lymphocytic leukemia: evidence for a disease specific profile from a comprehensive analysis of 268 mutations. *Leukemia*. 2010;24(12):2072-9. doi:10.1038/leu.2010.208

72. Malcikova J, Smardova J, Rocnova L, et al. Monoallelic and biallelic inactivation of TP53 gene in chronic lymphocytic leukemia: selection, impact on survival, and response to DNA damage. *Blood*. 2009;114(26):5307-14. doi:10.1182/blood-2009-07-234708

73. Gonzalez D, Martinez P, Wade R, et al. Mutational Status of the TP53 Gene As a Predictor of Response and Survival in Patients With Chronic Lymphocytic Leukemia: Results From the LRF CLL4 Trial. *Journal of Clinical Oncology*. 2011;29(16):2223-2229. doi:10.1200/JCO.2010.32.0838

74. Eichhorst B, Robak T, Montserrat E, et al. Chronic lymphocytic leukaemia: ESMO Clinical Practice Guidelines for diagnosis, treatment and follow-up. *Annals of Oncology*. 2021;32(1):23-33. doi:10.1016/j.annonc.2020.09.019

75. Malcikova J, Tausch E, Rossi D, et al. ERIC recommendations for TP53 mutation analysis in chronic lymphocytic leukemia—update on methodological approaches and results interpretation. *Leukemia*. 2018;32(5):1070-1080. doi:10.1038/s41375-017-0007-7

76. Thompson PA, O'Brien SM, Wierda WG, et al. Complex karyotype is a stronger predictor than del(17p) for an inferior outcome in relapsed or refractory chronic lymphocytic leukemia patients treated with ibrutinib-based regimens. *Cancer*. 2015;121(20):3612-3621. doi:https://doi.org/10.1002/cncr.29566

77. Puente XS, Beà S, Valdés-Mas R, et al. Non-coding recurrent mutations in chronic lymphocytic leukaemia. *Nature*. 2015;526(7574):519-24. doi:10.1038/nature14666

78. Landau DA, Tausch E, Taylor-Weiner AN, et al. Mutations driving CLL and their evolution in progression and relapse. *Nature*. 2015;526(7574):525-30. doi:10.1038/nature15395

79. Guièze R, Wu CJ. Genomic and epigenomic heterogeneity in chronic lymphocytic leukemia. *Blood*. 2015;126(4):445-53. doi:10.1182/blood-2015-02-585042

80. Baliakas P, Hadzidimitriou A, Sutton LA, et al. Recurrent mutations refine prognosis in chronic lymphocytic leukemia. *Leukemia*. 2015;29(2):329-36. doi:10.1038/leu.2014.196

81. Knisbacher BA, Lin Z, Hahn CK, et al. Molecular map of chronic lymphocytic leukemia and its impact on outcome. *Nat Genet*. Nov 2022;54(11):1664-1674. doi:10.1038/s41588-022-01140-w

82. Jeromin S, Weissmann S, Haferlach C, et al. SF3B1 mutations correlated to cytogenetics and mutations in NOTCH1, FBXW7, MYD88, XPO1 and TP53 in 1160 untreated CLL patients. *Leukemia*. 2014;28(1):108-17. doi:10.1038/leu.2013.263

83. Weissmann S, Roller A, Jeromin S, et al. Prognostic impact and landscape of NOTCH1 mutations in chronic lymphocytic leukemia (CLL): a study on 852 patients. *Leukemia*. 2013;27(12):2393-6. doi:10.1038/leu.2013.218

84. Villamor N, Conde L, Martínez-Trillos A, et al. NOTCH1 mutations identify a genetic subgroup of chronic lymphocytic leukemia patients with high risk of transformation and poor outcome. *Leukemia*. 2013;27(5):1100-6. doi:10.1038/leu.2012.357

85. Nadeu F, Delgado J, Royo C, et al. Clinical impact of clonal and subclonal TP53, SF3B1, BIRC3, NOTCH1, and ATM mutations in chronic lymphocytic leukemia. *Blood*. 2016;127(17):2122-30. doi:10.1182/blood-2015-07-659144

86. Blakemore SJ, Clifford R, Parker H, et al. Clinical significance of TP53, BIRC3, ATM and MAPK-ERK genes in chronic lymphocytic leukaemia: data from the randomised UK LRF CLL4 trial. *Leukemia*. 2020;34(7):1760-1774. doi:10.1038/s41375-020-0723-2

87. Mansouri L, Thorvaldsdottir B, Sutton L-A, et al. Different prognostic impact of recurrent gene mutations in chronic lymphocytic leukemia depending on IGHV gene somatic hypermutation status: a study by ERIC in HARMONY. *Leukemia*. 2023;37(2):339-347. doi:10.1038/s41375-022-01802-y

88. Landau DA, Carter SL, Stojanov P, et al. Evolution and impact of subclonal mutations in chronic lymphocytic leukemia. *Cell*. 2013;152(4):714-26. doi:10.1016/j.cell.2013.01.019

89. Martínez-Trillos A, Pinyol M, Navarro A, et al. Mutations in TLR/MYD88 pathway identify a subset of young chronic lymphocytic leukemia patients with favorable outcome. *Blood*. 2014;123(24):3790-3796. doi:10.1182/blood-2013-12-543306

90. Shuai W, Lin P, Strati P, et al. Clinicopathological characterization of chronic lymphocytic leukemia with MYD88 mutations: L265P and non-L265P mutations are associated with different features. *Blood Cancer Journal*. 2020;10(8):86. doi:10.1038/s41408-020-00351-w

91. Wierda WG, O'Brien S, Wang X, et al. Prognostic nomogram and index for overall survival in previously untreated patients with chronic lymphocytic leukemia. *Blood*. 2007;109(11):4679-4685. doi:10.1182/blood-2005-12-051458

92. Pflug N, Bahlo J, Shanafelt TD, et al. Development of a comprehensive prognostic index for patients with chronic lymphocytic leukemia. *Blood*. 2014;124(1):49-62. doi:10.1182/blood-2014-02-556399

93. Delgado J, Doubek M, Baumann T, et al. Chronic lymphocytic leukemia: A prognostic model comprising only two biomarkers (IGHV mutational status and FISH cytogenetics) separates patients with different outcome and simplifies the CLL-IPI. *American Journal of Hematology*. 2017;92(4):375-380. doi:https://doi.org/10.1002/ajh.24660

94. group IC-Iw. An international prognostic index for patients with chronic lymphocytic leukaemia (CLL-IPI): a meta-analysis of individual patient data. *Lancet Oncol*. 2016;17(6):779-790. doi:10.1016/S1470-2045(16)30029-8

95. Condoluci A, Terzi di Bergamo L, Langerbeins P, et al. International prognostic score for asymptomatic early-stage chronic lymphocytic leukemia. *Blood*. 2020;135(21):1859-1869. doi:10.1182/blood.2019003453

96. Rossi D, Rasi S, Spina V, et al. Integrated mutational and cytogenetic analysis identifies new prognostic subgroups in chronic lymphocytic leukemia. *Blood*. 2013;121(8):1403-12. doi:10.1182/blood-2012-09-458265

97. Panagiotis B, Theodoros M, Anastasia H, et al. Tailored approaches grounded on immunogenetic features for refined prognostication in chronic lymphocytic leukemia. *Haematologica*. 2019;104(2):360-369. doi:10.3324/haematol.2018.195032

98. Visentin A, Bonaldi L, Rigolin GM, et al. The combination of complex karyotype subtypes and IGHV mutational status identifies new prognostic and predictive groups in chronic lymphocytic leukaemia. *British Journal of Cancer*. 2019;121(2):150-156. doi:10.1038/s41416-019-0502-x

99. Rawstron AC, Fazi C, Agathangelidis A, et al. A complementary role of multiparameter flow cytometry and high-throughput sequencing for minimal residual disease detection in chronic lymphocytic leukemia: an European Research Initiative on CLL study. *Leukemia*. 2016;30(4):929-936. doi:10.1038/leu.2015.313

100. Thompson PA, Wierda WG. Eliminating minimal residual disease as a therapeutic end point: working toward cure for patients with CLL. *Blood*. 2016;127(3):279-286. doi:10.1182/blood-2015-08-634816

101. Kovacs G, Robrecht S, Fink AM, et al. Minimal Residual Disease Assessment Improves Prediction of Outcome in Patients With Chronic Lymphocytic Leukemia (CLL) Who Achieve Partial Response: Comprehensive Analysis of Two Phase III Studies of the German CLL Study Group. *Journal of Clinical Oncology*. 2016;34(31):3758-3765. doi:10.1200/JCO.2016.67.1305

102. CollaborativeGroup CLLT. Chemotherapeutic Options in Chronic Lymphocytic Leukemia: a Meta-analysis of the Randomized Trials. *JNCI: Journal of the National Cancer Institute*. 1999;91(10):861-868. doi:10.1093/jnci/91.10.861

103. Goede V, Fischer K, Busch R, et al. Obinutuzumab plus Chlorambucil in Patients with CLL and Coexisting Conditions. *New England Journal of Medicine*. 2014;370(12):1101-1110. doi:10.1056/NEJMoa1313984

104. Hillmen P, Robak T, Janssens A, et al. Chlorambucil plus ofatumumab versus chlorambucil alone in previously untreated patients with chronic lymphocytic leukaemia (COMPLEMENT 1): a randomised, multicentre, open-label phase 3 trial. *The Lancet*. 2015;385(9980):1873-1883. doi:10.1016/S0140-6736(15)60027-7

105. Eichhorst B, Fink A-M, Bahlo J, et al. First-line chemoimmunotherapy with bendamustine and rituximab versus fludarabine, cyclophosphamide, and rituximab in patients with advanced chronic lymphocytic leukaemia (CLL10): an international, open-label, randomised, phase 3, non-inferiority trial. *The Lancet Oncology*. 2016;17(7):928-942. doi:10.1016/S1470-2045(16)30051-1

106. Burger JA, O'Brien S. Evolution of CLL treatment — from chemoimmunotherapy to targeted and individualized therapy. *Nature Reviews Clinical Oncology*. 2018;15(8):510-527. doi:10.1038/s41571-018-0037-8

107. Burger JA. Treatment of Chronic Lymphocytic Leukemia. *New England Journal of Medicine*. 2020;383(5):460-473. doi:10.1056/NEJMra1908213

108. Stevenson FK, Krysov S, Davies AJ, Steele AJ, Packham G. B-cell receptor signaling in chronic lymphocytic leukemia. *Blood*. 2011;118(16):4313-4320. doi:10.1182/blood-2011-06-338855

109. Burger JA, Chiorazzi N. B cell receptor signaling in chronic lymphocytic leukemia. *Trends in Immunology*. 2013;34(12):592-601. doi:10.1016/j.it.2013.07.002

110. ten Hacken E, Burger JA. Microenvironment interactions and B-cell receptor signaling in Chronic Lymphocytic Leukemia: Implications for disease pathogenesis and treatment. *Biochimica et Biophysica Acta (BBA) - Molecular Cell Research*. 2016;1863(3):401-413. doi:https://doi.org/10.1016/j.bbamcr.2015.07.009

111. Petlickovski A, Laurenti L, Li X, et al. Sustained signaling through the B-cell receptor induces Mcl-1 and promotes survival of chronic lymphocytic leukemia B cells. *Blood*. 2005;105(12):4820-4827. doi:10.1182/blood-2004-07-2669

112. Hampel PJ, Parikh SA. Chronic lymphocytic leukemia treatment algorithm 2022. *Blood Cancer Journal*. 2022;12(11):161. doi:10.1038/s41408-022-00756-9

113. Herman SEM, Gordon AL, Hertlein E, et al. Bruton tyrosine kinase represents a promising therapeutic target for treatment of chronic lymphocytic leukemia and is effectively targeted by PCI-32765. *Blood*. 2011;117(23):6287-6296. doi:10.1182/blood-2011-01-328484

114. de Rooij MFM, Kuil A, Geest CR, et al. The clinically active BTK inhibitor PCI-32765 targets B-cell receptor– and chemokine-controlled adhesion and migration in chronic lymphocytic leukemia. *Blood*. 2012;119(11):2590-2594. doi:10.1182/blood-2011-11-390989

115. Byrd JC, Furman RR, Coutre SE, et al. Targeting BTK with Ibrutinib in Relapsed Chronic Lymphocytic Leukemia. *New England Journal of Medicine*. 2013;369(1):32-42. doi:10.1056/NEJMoa1215637

116. Burger JA, Tedeschi A, Barr PM, et al. Ibrutinib as Initial Therapy for Patients with Chronic Lymphocytic Leukemia. *New England Journal of Medicine*. 2015;373(25):2425-2437. doi:10.1056/NEJMoa1509388

117. Woyach JA, Ruppert AS, Heerema NA, et al. Ibrutinib Regimens versus Chemoimmunotherapy in Older Patients with Untreated CLL. *New England Journal of Medicine*. 2018;379(26):2517-2528. doi:10.1056/NEJMoa1812836

118. Moreno C, Greil R, Demirkan F, et al. Ibrutinib plus obinutuzumab versus chlorambucil plus obinutuzumab in first-line treatment of chronic lymphocytic leukaemia (iLLUMINATE): a multicentre, randomised, open-label, phase 3 trial. *The Lancet Oncology*. 2019;20(1):43-56. doi:10.1016/S1470-2045(18)30788-5

119. Byrd JC, Harrington B, O'Brien S, et al. Acalabrutinib (ACP-196) in Relapsed Chronic Lymphocytic Leukemia. *New England Journal of Medicine*. 2015;374(4):323-332. doi:10.1056/NEJMoa1509981

120. Sharman JP, Egyed M, Jurczak W, et al. Acalabrutinib with or without obinutuzumab versus chlorambucil and obinutuzumab for treatment-naive chronic lymphocytic leukaemia (ELEVATE-TN): a randomised, controlled, phase 3 trial. *The Lancet*. 2020;395(10232):1278-1291. doi:10.1016/S0140-6736(20)30262-2

121. Tam CS, Brown JR, Kahl BS, et al. Zanubrutinib versus bendamustine and rituximab in untreated chronic lymphocytic leukaemia and small lymphocytic lymphoma (SEQUOIA): a randomised, controlled, phase 3 trial. *The Lancet Oncology*. 2022;23(8):1031-1043. doi:10.1016/S1470-2045(22)00293-5

122. Danilov AV, Herbaux C, Walter HS, et al. Phase Ib Study of Tirabrutinib in Combination with Idelalisib or Entospletinib in Previously Treated Chronic Lymphocytic Leukemia. *Clinical Cancer Research*. 2020;26(12):2810-2818. doi:10.1158/1078-0432.CCR-19-3504

123. Reiff SD, Mantel R, Smith LL, et al. The BTK Inhibitor ARQ 531 Targets Ibrutinib-Resistant CLL and Richter Transformation. *Cancer Discovery*. 2018;8(10):1300-1315. doi:10.1158/2159-8290.CD-17-1409

124. Mato AR, Shah NN, Jurczak W, et al. Pirtobrutinib in relapsed or refractory B-cell malignancies (BRUIN): a phase 1/2 study. *The Lancet*. 2021;397(10277):892-901. doi:10.1016/S0140-6736(21)00224-5

125. Hoellenriegel J, Meadows SA, Sivina M, et al. The phosphoinositide 3′-kinase delta inhibitor, CAL-101, inhibits B-cell receptor signaling and chemokine networks in chronic lymphocytic leukemia. *Blood*. 2011;118(13):3603-3612. doi:10.1182/blood-2011-05-352492

126. Furman RR, Sharman JP, Coutre SE, et al. Idelalisib and Rituximab in Relapsed Chronic Lymphocytic Leukemia. *New England Journal of Medicine*. 2014;370(11):997-1007. doi:10.1056/NEJMoa1315226

127. Ghia P, Pluta A, Wach M, et al. ASCEND: Phase III, Randomized Trial of Acalabrutinib Versus Idelalisib Plus Rituximab or Bendamustine Plus Rituximab in Relapsed or Refractory Chronic Lymphocytic Leukemia. *Journal of Clinical Oncology*. 2020;38(25):2849-2861. doi:10.1200/JCO.19.03355

128. Flinn IW, Hillmen P, Montillo M, et al. The phase 3 DUO trial: duvelisib vs ofatumumab in relapsed and refractory CLL/SLL. *Blood*. 2018;132(23):2446-2455. doi:10.1182/blood-2018-05-850461

129. Mato AR, Ghosh N, Schuster SJ, et al. Phase 2 study of the safety and efficacy of umbralisib in patients with CLL who are intolerant to BTK or PI3Kδ inhibitor therapy. *Blood*. 2021;137(20):2817-2826. doi:10.1182/blood.2020007376

130. Hus I, Puła B, Robak T. PI3K Inhibitors for the Treatment of Chronic Lymphocytic Leukemia: Current Status and Future Perspectives. *Cancers*. 2022;14(6). doi:10.3390/cancers14061571

131. Ferrer G, Montserrat E. Critical molecular pathways in CLL therapy. *Molecular Medicine*. 2018;24(1):9. doi:10.1186/s10020-018-0001-1

132. Kale J, Osterlund EJ, Andrews DW. BCL-2 family proteins: changing partners in the dance towards death. *Cell Death & Differentiation*. 2018;25(1):65-80. doi:10.1038/cdd.2017.186

133. Souers AJ, Leverson JD, Boghaert ER, et al. ABT-199, a potent and selective BCL-2 inhibitor, achieves antitumor activity while sparing platelets. *Nature Medicine*. 2013;19(2):202-208. doi:10.1038/nm.3048

134. Anderson MA, Deng J, Seymour JF, et al. The BCL2 selective inhibitor venetoclax induces rapid onset apoptosis of CLL cells in patients via a TP53-independent mechanism. *Blood*. 2016;127(25):3215-3224. doi:10.1182/blood-2016-01-688796

135. Roberts AW, Davids MS, Pagel JM, et al. Targeting BCL2 with Venetoclax in Relapsed Chronic Lymphocytic Leukemia. *New England Journal of Medicine*. 2015;374(4):311-322. doi:10.1056/NEJMoa1513257

136. Seymour JF, Kipps TJ, Eichhorst B, et al. Venetoclax–Rituximab in Relapsed or Refractory Chronic Lymphocytic Leukemia. *New England Journal of Medicine*. 2018;378(12):1107-1120. doi:10.1056/NEJMoa1713976

137. Fischer K, Al-Sawaf O, Bahlo J, et al. Venetoclax and Obinutuzumab in Patients with CLL and Coexisting Conditions. *New England Journal of Medicine*. 2019;380(23):2225-2236. doi:10.1056/NEJMoa1815281

138. Al-Sawaf O, Zhang C, Tandon M, et al. Venetoclax plus obinutuzumab versus chlorambucil plus obinutuzumab for previously untreated chronic lymphocytic leukaemia (CLL14): follow-up results from a multicentre, open-label, randomised, phase 3 trial. *The Lancet Oncology*. 2020;21(9):1188-1200. doi:10.1016/S1470-2045(20)30443-5

139. Kharfan-Dabaja MA, Kumar A, Hamadani M, et al. Clinical Practice Recommendations for Use of Allogeneic Hematopoietic Cell Transplantation in Chronic Lymphocytic Leukemia on Behalf of the Guidelines Committee of the American Society for Blood and Marrow Transplantation. *Biology of Blood and Marrow Transplantation*. 2016;22(12):2117-2125. doi:10.1016/j.bbmt.2016.09.013

140. Roeker LE, Dreger P, Brown JR, et al. Allogeneic stem cell transplantation for chronic lymphocytic leukemia in the era of novel agents. *Blood Advances*. 2020;4(16):3977-3989. doi:10.1182/bloodadvances.2020001956

141. Dreger P, Schetelig J, Andersen N, et al. Managing high-risk CLL during transition to a new treatment era: stem cell transplantation or novel agents? *Blood*. 2014;124(26):3841-3849. doi:10.1182/blood-2014-07-586826

142. Porter DL, Hwang W-T, Frey NV, et al. Chimeric antigen receptor T cells persist and induce sustained remissions in relapsed refractory chronic lymphocytic leukemia. *Science Translational Medicine*. 2015;7(303):303ra139-303ra139. doi:10.1126/scitranslmed.aac5415

143. Liu E, Marin D, Banerjee P, et al. Use of CAR-Transduced Natural Killer Cells in CD19-Positive Lymphoid Tumors. *New England Journal of Medicine*. 2020;382(6):545-553. doi:10.1056/NEJMoa1910607

144. Gauthier J, Hirayama AV, Purushe J, et al. Feasibility and efficacy of CD19-targeted CAR T cells with concurrent ibrutinib for CLL after ibrutinib failure. *Blood*. 2020;135(19):1650-1660. doi:10.1182/blood.2019002936

145. Juliusson G, Gahrton G. Chromosome aberrations in B-cell chronic lymphocytic leukemia: Pathogenetic and clinical implications. *Cancer Genetics and Cytogenetics*. 1990;45(2):143-160. doi:10.1016/0165-4608(90)90079-P

146. Juliusson G, Gahrton G. Cytogenetics in CLL and related disorders. *Baillieres Clin Haematol*. 1993;6(4):821-48.

147. Baliakas P, Iskas M, Gardiner A, et al. Chromosomal translocations and karyotype complexity in chronic lymphocytic leukemia: a systematic reappraisal of classic cytogenetic data. *Am J Hematol*. 2014;89(3):249-55. doi:10.1002/ajh.23618

148. Leeksma AC, Baliakas P, Moysiadis T, et al. Genomic arrays identify high-risk chronic lymphocytic leukemia with genomic complexity: a multi-center study. *Haematologica*. 2021;106(1):87-97. doi:10.3324/haematol.2019.239947

149. Puiggros A, Ramos-Campoy S, Kamaso J, et al. Optical Genome Mapping: A Promising New Tool to Assess Genomic Complexity in Chronic Lymphocytic Leukemia (CLL). *Cancers*. 2022;14(14). doi:10.3390/cancers14143376

150. Rigolin GM, Cibien F, Martinelli S, et al. Chromosome aberrations detected by conventional karyotyping using novel mitogens in chronic lymphocytic leukemia with "normal" FISH: correlations with clinicobiologic parameters. *Blood*. 2012;119(10):2310-2313. doi:10.1182/blood-2011-11-395269

151. Baliakas P, Jeromin S, Iskas M, et al. Cytogenetic complexity in chronic lymphocytic leukemia: definitions, associations, and clinical impact. *Blood*. 2019;133(11):1205-1216. doi:10.1182/blood-2018-09-873083

152. Reddy KS. Chronic lymphocytic leukaemia profiled for prognosis using a fluorescence in situ hybridisation panel. *Br J Haematol*. 2006;132(6):705-22. doi:10.1111/j.1365-2141.2005.05919.x

153. Van Dyke DL, Shanafelt TD, Call TG, et al. A comprehensive evaluation of the prognostic significance of 13q deletions in patients with B-chronic lymphocytic leukaemia. *British Journal of Haematology*. 2010;148(4):544-550. doi:https://doi.org/10.1111/j.1365-2141.2009.07982.x

154. Calin GA, Dumitru CD, Shimizu M, et al. Frequent deletions and down-regulation of micro- RNA genes miR15 and miR16 at 13q14 in chronic lymphocytic leukemia. *Proceedings of the National Academy of Sciences*. 2002;99(24):15524-15529. doi:10.1073/pnas.242606799

155. Hammarsund M, Corcoran MM, Wilson W, et al. Characterization of a novel B-CLL candidate gene – DLEU7 – located in the 13q14 tumor suppressor locus. *FEBS Letters*. 2004;556(1-3):75-80. doi:https://doi.org/10.1016/S0014-5793(03)01371-1

156. Klein U, Lia M, Crespo M, et al. The DLEU2/miR-15a/16-1 Cluster Controls B Cell Proliferation and Its Deletion Leads to Chronic Lymphocytic Leukemia. *Cancer Cell*. 2010;17(1):28-40. doi:10.1016/j.ccr.2009.11.019

157. Cimmino A, Calin GA, Fabbri M, et al. miR-15 and miR-16 induce apoptosis by targeting BCL2. *Proceedings of the National Academy of Sciences*. 2005;102(39):13944-13949. doi:10.1073/pnas.0506654102

158. Liu Y, Szekely L, Grandér D, et al. Chronic lymphocytic leukemia cells with allelic deletions at 13q14 commonly have one intact RB1 gene: evidence for a role of an adjacent locus. *Proceedings of the National Academy of Sciences*. 1993;90(18):8697-8701. doi:10.1073/pnas.90.18.8697

159. José Ángel H, Ana Eugenia R, Marcos G, et al. A high number of losses in 13q14 chromosome band is associated with a worse outcome and biological differences in patients with B-cell chronic lymphoid leukemia. *Haematologica*. 2009;94(3):364-371. doi:10.3324/haematol.13862

160. Mosca L, Fabris S, Lionetti M, et al. Integrative Genomics Analyses Reveal Molecularly Distinct Subgroups of B-Cell Chronic Lymphocytic Leukemia Patients with 13q14 Deletion. *Clinical Cancer Research*. 2010;16(23):5641-5653. doi:10.1158/1078-0432.CCR-10-0151

161. Ouillette P, Collins R, Shakhan S, et al. The Prognostic Significance of Various 13q14 Deletions in Chronic Lymphocytic Leukemia. *Clinical Cancer Research*. 2011;17(21):6778-6790. doi:10.1158/1078-0432.CCR-11-0785

162. Dal Bo M, Rossi FM, Rossi D, et al. 13q14 Deletion size and number of deleted cells both influence prognosis in chronic lymphocytic leukemia.. *Genes, Chromosomes and Cancer*. 2011;50(8):633-643. doi:https://doi.org/10.1002/gcc.20885

163. Rodríguez AE, Hernández JÁ, Benito R, et al. Molecular Characterization of Chronic Lymphocytic Leukemia Patients with a High Number of Losses in 13q14. *PLOS ONE*. 2012;7(11):e48485. doi:10.1371/journal.pone.0048485

164. Puiggros A, Delgado J, Rodriguez-Vicente A, et al. Biallelic losses of 13q do not confer a poorer outcome in chronic lymphocytic leukaemia: analysis of 627 patients with isolated 13q deletion. *British Journal of Haematology*. 2013;163(1):47-54. doi:https://doi.org/10.1111/bjh.12479

165. Garg R, Wierda W, Ferrajoli A, et al. The prognostic difference of monoallelic versus biallelic deletion of 13q in chronic lymphocytic leukemia. *Cancer*. 2012;118(14):3531-3537. doi:https://doi.org/10.1002/cncr.26593

166. Neilson JR, Auer R, White D, et al. Deletions at 11q identify a subset of patients with typical CLL who show consistent disease progression and reduced survival. *Leukemia*. 1997;11(11):1929-1932. doi:10.1038/sj.leu.2400819

167. Döhner H, Stilgenbauer S, James MR, et al. 11q Deletions Identify a New Subset of B-Cell Chronic Lymphocytic Leukemia Characterized by Extensive Nodal Involvement and Inferior Prognosis. *Blood*. 1997;89(7):2516-2522. doi:10.1182/blood.V89.7.2516

168. Kern W, Dicker F, Schnittger S, Haferlach C, Haferlach T. Correlation of flow cytometrically determined expression of ZAP-70 using the SBZAP antibody with IgVH mutation status and cytogenetics in 1,229 patients with chronic lymphocytic leukemia. *Cytometry Part B: Clinical Cytometry*. 2009;76B(6):385-393. doi:https://doi.org/10.1002/cyto.b.20483

169. Hernández JÁ, Hernández-Sánchez M, Rodríguez-Vicente AE, et al. A Low Frequency of Losses in 11q Chromosome Is Associated with Better Outcome and Lower Rate of Genomic Mutations in Patients with Chronic Lymphocytic Leukemia. *PLOS ONE*. 2015;10(11):e0143073. doi:10.1371/journal.pone.0143073

170. Stilgenbauer S, Liebisch P, James MR, et al. Molecular cytogenetic delineation of a novel critical genomic region in chromosome bands 11q22.3-923.1 in lymphoproliferative disorders. *Proceedings of the National Academy of Sciences*. 1996;93(21):11837-11841. doi:10.1073/pnas.93.21.11837

171. Edelmann J, Holzmann K, Miller F, et al. High-resolution genomic profiling of chronic lymphocytic leukemia reveals new recurrent genomic alterations. *Blood*. 2012;120(24):4783-4794. doi:10.1182/blood-2012-04-423517

172. Jennifer E, Karlheinz H, Eugen T, et al. Genomic alterations in high-risk chronic lymphocytic leukemia frequently affect cell cycle key regulators and NOTCH1-regulated transcription. *Haematologica*. 2020;105(5):1379-1390. doi:10.3324/haematol.2019.217307

173. Stankovic T, Skowronska A. The role of ATM mutations and 11q deletions in disease progression in chronic lymphocytic leukemia. *Leukemia & Lymphoma*. 2014;55(6):1227-1239. doi:10.3109/10428194.2013.829919

174. Lozano-Santos C, García-Vela JA, Pérez-Sanz N, et al. Biallelic ATM alterations detected at diagnosis identify a subset of treatment-naïve chronic lymphocytic leukemia patients with reduced overall survival similar to patients with p53 deletion. *Leuk Lymphoma*. 2017;58(4):859-865. doi:10.1080/10428194.2016.1213829

175. Matthew JJR-Z, Jade F, Helen P, et al. ATM mutation rather than BIRC3 deletion and/or mutation predicts reduced survival in 11q-deleted chronic lymphocytic leukemia: data from the UK LRF CLL4 trial. *Haematologica*. 2014;99(4):736-742. doi:10.3324/haematol.2013.098574

176. Raponi S, Del Giudice I, Ilari C, et al. Biallelic BIRC3 inactivation in chronic lymphocytic leukaemia patients with 11q deletion identifies a subgroup with very aggressive disease. *British Journal of Haematology*. 2019;185(1):156-159. doi:https://doi.org/10.1111/bjh.15405

177. Fary D, Riccardo M, Chiara F, et al. Biological and clinical implications of BIRC3 mutations in chronic lymphocytic leukemia. *Haematologica*. 2020;105(2):448-456. doi:10.3324/haematol.2019.219550

178. Roos-Weil D, Nguyen-Khac F, Chevret S, et al. Mutational and cytogenetic analyses of 188 CLL patients with trisomy 12: A retrospective study from the French Innovative Leukemia Organization (FILO) working group. *Genes Chromosomes Cancer*. 2018;57(11):533-540. doi:10.1002/gcc.22650

179. Matutes E, Oscier D, Garcia-Marco J, et al. Trisomy 12 defines a group of CLL with atypical morphology: correlation between cytogenetic, clinical and laboratory features in 544 patients. *British Journal of Haematology*. 1996;92(2):382-388. doi:https://doi.org/10.1046/j.1365-2141.1996.d01-1478.x

180. Francesco A, Paolo S, Luca L, Alessandra F. Morphological, immunophenotypic, and genetic features of chronic lymphocytic leukemia with trisomy 12: a comprehensive review. *Haematologica*. 2018;103(6):931-938. doi:10.3324/haematol.2017.186684

181. Balatti V, Bottoni A, Palamarchuk A, et al. NOTCH1 mutations in CLL associated with trisomy 12. *Blood*. 2012;119(2):329-31. doi:10.1182/blood-2011-10-386144

182. Del Giudice I, Rossi D, Chiaretti S, et al. NOTCH1 mutations in +12 chronic lymphocytic leukemia (CLL) confer an unfavorable prognosis, induce a distinctive transcriptional profiling and refine the intermediate prognosis of +12 CLL. *Haematologica*. 2012;97(3):437-41. doi:10.3324/haematol.2011.060129

183. Balatti V, Lerner S, Rizzotto L, et al. Trisomy 12 CLLs progress through NOTCH1 mutations. *Leukemia*. 2013;27(3):740-743. doi:10.1038/leu.2012.239

184. Vendramini E, Bomben R, Pozzo F, et al. KRAS, NRAS, and BRAF mutations are highly enriched in trisomy 12 chronic lymphocytic leukemia and are associated with shorter treatment-free survival. *Leukemia*. 2019;33(8):2111-2115. doi:10.1038/s41375-019-0444-6

185. Giménez N, Martínez-Trillos A, Montraveta A, et al. Mutations in the RAS-BRAF-MAPK-ERK pathway define a specific subgroup of patients with adverse clinical features and provide new therapeutic options in chronic lymphocytic leukemia. *Haematologica*. 2019;104(3):576-586. doi:10.3324/haematol.2018.196931

186. Sen F, Lai R, Albitar M. Chronic lymphocytic leukemia with t(14;18) and trisomy 12. *Arch Pathol Lab Med*. 2002;126(12):1543-6. doi:10.1043/0003-9985(2002)1262.0.CO;2

187. Sellmann L, Gesk S, Walter C, et al. Trisomy 19 is associated with trisomy 12 and mutated IGHV genes in B-chronic lymphocytic leukaemia. *British Journal of Haematology*. 2007;138(2):217-220. doi:https://doi.org/10.1111/j.1365-2141.2007.06636.x

188. Martín-Subero JI, Ibbotson R, Klapper W, et al. A comprehensive genetic and histopathologic analysis identifies two subgroups of B-cell malignancies carrying a t(14;19)(q32;q13) or variant BCL3-translocation. *Leukemia*. 2007;21(7):1532-44. doi:10.1038/sj.leu.2404695

189. Reindl L, Bacher U, Dicker F, et al. Biological and clinical characterization of recurrent 14q deletions in CLL and other mature B-cell neoplasms. *Br J Haematol*. 2010;151(1):25-36. doi:10.1111/j.1365-2141.2010.08299.x

190. López C, Delgado J, Costa D, et al. Different distribution of NOTCH1 mutations in chronic lymphocytic leukemia with isolated trisomy 12 or associated with other chromosomal alterations. *Genes Chromosomes Cancer*. 2012;51(9):881-9. doi:10.1002/gcc.21972

191. Cosson A, Chapiro E, Belhouachi N, et al. 14q deletions are associated with trisomy 12, NOTCH1 mutations and unmutated IGHV genes in chronic lymphocytic leukemia and small lymphocytic lymphoma. *Genes Chromosomes Cancer*. 2014;53(8):657-66. doi:10.1002/gcc.22176

192. Panagiotis B, Anna P, Aliki X, et al. Additional trisomies amongst patients with chronic lymphocytic leukemia carrying trisomy 12: the accompanying chromosome makes a difference. *Haematologica*. 2016;101(7):e299-e302. doi:10.3324/haematol.2015.140202

193. Yu L, Kim HT, Kasar S, et al. Survival of Del17p CLL Depends on Genomic Complexity and Somatic Mutation. *Clin Cancer Res*. 2017;23(3):735-745. doi:10.1158/1078-0432.CCR-16-0594

194. Tam CS, Shanafelt TD, Wierda WG, et al. De novo deletion 17p13.1 chronic lymphocytic leukemia shows significant clinical heterogeneity: the M. D. Anderson and Mayo Clinic experience. *Blood*. 2009;114(5):957-964. doi:10.1182/blood-2009-03-210591

195. Fabbri G, Khiabanian H, Holmes AB, et al. Genetic lesions associated with chronic lymphocytic leukemia transformation to Richter syndrome. *J Exp Med*. Oct 2013;210(11):2273-88. doi:10.1084/jem.20131448

196. Julio D, Itziar S, Tycho B, et al. Genomic complexity and IGHV mutational status are key predictors of outcome of chronic lymphocytic leukemia patients with TP53 disruption. *Haematologica*. 2014;99(11):e231-e234. doi:10.3324/haematol.2014.108365

197. Rossi D, Khiabanian H, Spina V, et al. Clinical impact of small TP53 mutated subclones in chronic lymphocytic leukemia. *Blood*. 2014;123(14):2139-2147. doi:10.1182/blood-2013-11-539726

198. Catovsky D, Richards S, Matutes E, et al. Assessment of fludarabine plus cyclophosphamide for patients with chronic lymphocytic leukaemia (the LRF CLL4 Trial): a randomised controlled trial. *The Lancet*. 2007;370(9583):230-239. doi:10.1016/S0140-6736(07)61125-8

199. Zenz T, Eichhorst B, Busch R, et al. TP53 Mutation and Survival in Chronic Lymphocytic Leukemia. *Journal of Clinical Oncology*. 2010;28(29):4473-4479. doi:10.1200/JCO.2009.27.8762

200. Stilgenbauer S, Schnaiter A, Paschka P, et al. Gene mutations and treatment outcome in chronic lymphocytic leukemia: results from the CLL8 trial. *Blood*. 2014;123(21):3247-3254. doi:10.1182/blood-2014-01-546150

201. Lazarian G, Tausch E, Eclache V, et al. TP53 mutations are early events in chronic lymphocytic leukemia disease progression and precede evolution to complex karyotypes. *International Journal of Cancer*. 2016;139(8):1759-1763. doi:https://doi.org/10.1002/ijc.30222

202. Haferlach C, Dicker F, Schnittger S, Kern W, Haferlach T. Comprehensive genetic characterization of CLL: a study on 506 cases analysed with chromosome banding analysis, interphase FISH, IgV(H) status and immunophenotyping. *Leukemia*. 2007;21(12):2442-51. doi:10.1038/sj.leu.2404935

203. Cosson A, Chapiro E, Bougacha N, et al. Gain in the short arm of chromosome 2 (2p+) induces gene overexpression and drug resistance in chronic lymphocytic leukemia: analysis of the central role of XPO1. *Leukemia*. 2017;31(7):1625-1629. doi:10.1038/leu.2017.100

204. Brown JR, Hanna M, Tesar B, et al. Integrative Genomic Analysis Implicates Gain of PIK3CA at 3q26 and MYC at 8q24 in Chronic Lymphocytic Leukemia. *Clinical Cancer Research*. 2012;18(14):3791-3802. doi:10.1158/1078-0432.CCR-11-2342

205. Nagel I, Bug S, Tönnies H, et al. Biallelic inactivation of TRAF3 in a subset of B-cell lymphomas with interstitial del(14)(q24.1q32.33). *Leukemia*. 2009;23(11):2153-5. doi:10.1038/leu.2009.149

206. Mayr C, Speicher MR, Kofler DM, et al. Chromosomal translocations are associated with poor prognosis in chronic lymphocytic leukemia. *Blood*. 2006;107(2):742-51. doi:10.1182/blood-2005-05-2093

207. Van Den Neste E, Robin V, Francart J, et al. Chromosomal translocations independently predict treatment failure, treatment-free survival and overall survival in B-cell chronic lymphocytic leukemia patients treated with cladribine. *Leukemia*. 2007;21(8):1715-22. doi:10.1038/sj.leu.2404764

208. Cavazzini F, Hernandez JA, Gozzetti A, et al. Chromosome 14q32 translocations involving the immunoglobulin heavy chain locus in chronic lymphocytic leukaemia identify a disease subset with poor prognosis. *Br J Haematol*. 2008;142(4):529-37. doi:10.1111/j.1365-2141.2008.07227.x

209. Gerrie AS, Bruyere H, Chan MJ, et al. Immunoglobulin heavy chain (IGH@) translocations negatively impact treatment-free survival for chronic lymphocytic leukemia patients who have an isolated deletion 13q abnormality. *Cancer Genet*. 2012;205(10):523-7. doi:10.1016/j.cancergen.2012.05.011

210. DE Braekeleer M, Tous C, Guéganic N, et al. Immunoglobulin gene translocations in chronic lymphocytic leukemia: A report of 35 patients and review of the literature. *Mol Clin Oncol*. 2016;4(5):682-694. doi:10.3892/mco.2016.793

211. Stilgenbauer S, Bullinger L, Benner A, et al. Incidence and clinical significance of 6q deletions in B cell chronic lymphocytic leukemia. *Leukemia*. 1999;13(9):1331-1334. doi:10.1038/sj.leu.2401499

212. Finn WG, Kay NE, Kroft SH, Church S, Peterson LC. Secondary Abnormalities of Chromosome 6q in B-Cell Chronic Lymphocytic Leukemia: A Sequential Study of Karyotypic Instability in 51 Patients. *American Journal of Hematology*. 1998;59(3):223-229. doi:https://doi.org/10.1002/(SICI)1096-8652(199811)59:3

213. Dalsass A, Mestichelli F, Ruggieri M, et al. 6q deletion detected by fluorescence in situ hybridization using bacterial artificial chromosome in chronic lymphocytic leukemia. *European Journal of Haematology*.2013;91(1):10-19. doi:https://doi.org/10.1111/ejh.12115

214. Audil HY, Hampel PJ, Van Dyke DL, et al. The prognostic significance of del6q23 in chronic lymphocytic leukemia.. *American Journal of Hematology*. 2021;96(6):E203-E206. doi:https://doi.org/10.1002/ajh.26168

215. Cuneo A, Rigolin GM, Bigoni R, et al. Chronic lymphocytic leukemia with 6q− shows distinct hematological features and intermediate prognosis. *Leukemia*. 2004;18(3):476-483. doi:10.1038/sj.leu.2403242

216. Wang D-M, Miao K-R, Fan L, et al. Intermediate prognosis of 6q deletion in chronic lymphocytic leukemia. *Leukemia & Lymphoma*. 2011;52(2):230-237. doi:10.3109/10428194.2010.542599

217. Mosaad Zaki E, Mohamed Zahran A, Abdelazeem Metwaly A, Hafez R, Hussein S, Elaiw Mohammed A. Impact of CD39 expression on CD4+ T lymphocytes and 6q deletion on outcome of patients with chronic lymphocytic leukemia. *Hematology/Oncology and Stem Cell Therapy*. 2019;12(1):26-31. doi:https://doi.org/10.1016/j.hemonc.2018.09.002

218. Jarosova M, Hruba M, Oltova A, et al. Chromosome 6q deletion correlates with poor prognosis and low relative expression of FOXO3 in chronic lymphocytic leukemia patients. *American Journal of Hematology*. 2017;92(10):E604-E607. doi:https://doi.org/10.1002/ajh.24852

219. Zhang X, Tang N, Hadden TJ, Rishi AK. Akt, FoxO and regulation of apoptosis. *Biochimica et Biophysica Acta (BBA) - Molecular Cell Research*. 2011;1813(11):1978-1986. doi:https://doi.org/10.1016/j.bbamcr.2011.03.010

220. Nowakowski GS, Dewald GW, Hoyer JD, et al. Interphase fluorescence in situ hybridization with an IGH probe is important in the evaluation of patients with a clinical diagnosis of chronic lymphocytic leukaemia. *Br J Haematol*. 2005;130(1):36-42. doi:10.1111/j.1365-2141.2005.05548.x

221. Nelson BP, Gupta R, Dewald GW, Paternoster SF, Rosen ST, Peterson LC. Chronic lymphocytic leukemia FISH panel: impact on diagnosis. *Am J Clin Pathol*. 2007;128(2):323-32. doi:10.1309/21TN2RUWKR827UW2

222. Berkova A, Pavlistova L, Babicka L, et al. Combined molecular biological and molecular cytogenetic analysis of genomic changes in 146 patients with B-cell chronic lymphocytic leukemia. *Neoplasma*. 2008;55(5):400-8.

223. Lu G, Kong Y, Yue C. Genetic and immunophenotypic profile of IGH@ rearrangement detected by fluorescence in situ hybridization in 149 cases of B-cell chronic lymphocytic leukemia. *Cancer Genet Cytogenet*. 2010;196(1):56-63. doi:10.1016/j.cancergencyto.2009.08.021

224. Fang H, Reichard KK, Rabe KG, et al. IGH translocations in chronic lymphocytic leukemia: Clinicopathologic features and clinical outcomes. *Am J Hematol*. 2019;94(3):338-345. doi:10.1002/ajh.25385

225. Huh YO, Lin KIC, Vega F, et al. MYC translocation in chronic lymphocytic leukaemia is associated with increased prolymphocytes and a poor prognosis. *British Journal of Haematology*. 2008;142(1):36-44. doi:https://doi.org/10.1111/j.1365-2141.2008.07152.x

226. Hwang Y, Lee JY, Mun YC, Seong CM, Chung WS, Huh J. Various patterns of IgH deletion identified by FISH using combined IgH and IgH/CCND1 probes in multiple myeloma and chronic lymphocytic leukemia. *Int J Lab Hematol*. 2011;33(3):299-304. doi:10.1111/j.1751-553X.2010.01290.x

227. Davids MS, Vartanov A, Werner L, Neuberg D, Dal Cin P, Brown JR. Controversial fluorescence in situ hybridization cytogenetic abnormalities in chronic lymphocytic leukaemia: new insights from a large cohort. *Br J Haematol*. 2015;170(5):694-703. doi:10.1111/bjh.13498

228. Put N, Van Roosbroeck K, Konings P, et al. Chronic lymphocytic leukemia and prolymphocytic leukemia with MYC translocations: a subgroup with an aggressive disease course. *Annals of Hematology*. 2012;91(6):863-873. doi:10.1007/s00277-011-1393-y

229. Jimenez-Zepeda VH, Chng WJ, Schop RF, et al. Recurrent chromosome abnormalities define nonoverlapping unique subgroups of tumors in patients with chronic lymphocytic leukemia and known karyotypic abnormalities. *Clin Lymphoma Myeloma Leuk*. 2013;13(4):467-76. doi:10.1016/j.clml.2013.05.003

230. Nguyen-Khac F, Chapiro E, Lesty C, et al. Specific chromosomal IG translocations have different prognoses in chronic lymphocytic leukemia. *Am J Blood Res*. 2011;1(1):13-21.

231. Put N, Meeus P, Chatelain B, et al. Translocation t(14;18) is not associated with inferior outcome in chronic lymphocytic leukemia. *Leukemia*. 2009;23(6):1201-1204. doi:10.1038/leu.2009.44

232. Willis TG, Dyer MJ. The role of immunoglobulin translocations in the pathogenesis of B-cell malignancies. *Blood*. 2000;96(3):808-22.

233. Pospisilova H, Baens M, Michaux L, et al. Interstitial del(14)(q) involving IGH: a novel recurrent aberration in B-NHL. *Leukemia*. 2007;21(9):2079-83. doi:10.1038/sj.leu.2404739

234. Wlodarska I, Matthews C, Veyt E, et al. Telomeric IGH losses detectable by fluorescence in situ hybridization in chronic lymphocytic leukemia reflect somatic VH recombination events. *J Mol Diagn*. 2007;9(1):47-54. doi:10.2353/jmoldx.2007.060088

235. Bushell KR, Kim Y, Chan FC, et al. Genetic inactivation of TRAF3 in canine and human B-cell lymphoma. *Blood*. 2015;125(6):999-1005. doi:10.1182/blood-2014-10-602714

236. San Miguel JF. Introduction to a series of reviews on multiple myeloma. *Blood*. 2015;125(20):3039-40. doi:10.1182/blood-2015-01-613596

237. Zarnegar BJ, Wang Y, Mahoney DJ, et al. Noncanonical NF-kappaB activation requires coordinated assembly of a regulatory complex of the adaptors cIAP1, cIAP2, TRAF2 and TRAF3 and the kinase NIK. *Nat Immunol*. 2008;9(12):1371-8. doi:10.1038/ni.1676

238. Häcker H, Tseng PH, Karin M. Expanding TRAF function: TRAF3 as a tri-faced immune regulator. *Nat Rev Immunol*. 2011;11(7):457-68. doi:10.1038/nri2998

239. Jung J, Gokhale S, Xie P. TRAF3: A novel regulator of mitochondrial physiology and metabolic pathways in B lymphocytes *Front. Oncol*. 2023;13:1081253. doi: 10.3389/fonc.2023.1081253.

240. Zheng J. Oncogenic chromosomal translocations and human cancer (Review). *Oncol Rep*. 2013;30(5):2011-2019. doi:10.3892/or.2013.2677

241. Puiggros A, Collado R, José Calasanz M, et al. Patients with chronic lymphocytic leukemia and complex karyotype show an adverse outcome even in absence of TP53/ATM FISH deletions. *Oncotarget;* 2017;*8, No 33*.

242. Cavallari M, Cavazzini F, Bardi A, et al. Biological significance and prognostic/predictive impact of complex karyotype in chronic lymphocytic leukemia. *Oncotarget;* 2018; *9, No 76*.

243. Visentin A, Bonaldi L, Rigolin GM, et al. The complex karyotype landscape in chronic lymphocytic leukemia allows the refinement of the risk of Richter syndrome transformation. *Haematologica*. 2021;107(4):868-876. doi:10.3324/haematol.2021.278304

244. Rigolin GM, Saccenti E, Guardalben E, et al. In chronic lymphocytic leukaemia with complex karyotype, major structural abnormalities identify a subset of patients with inferior outcome and distinct biological characteristics.. *British Journal of Haematology*. 2018;181(2):229-233. doi:https://doi.org/10.1111/bjh.15174

245. Costa D, Granada I, Espinet B, et al. Balanced and unbalanced translocations in a multicentric series of 2843 patients with chronic lymphocytic leukemia. *Genes, Chromosomes and Cancer*. 2022;61(1):37-43. doi:https://doi.org/10.1002/gcc.22994

246. Herling CD, Klaumünzer M, Rocha CK, et al. Complex karyotypes and KRAS and POT1 mutations impact outcome in CLL after chlorambucil-based chemotherapy or chemoimmunotherapy. *Blood*. 2016;128(3):395-404. doi:10.1182/blood-2016-01-691550

247. Ramos-Campoy S, Puiggros A, Kamaso J, et al. TP53 Abnormalities Are Underlying the Poor Outcome Associated with Chromothripsis in Chronic Lymphocytic Leukemia Patients with Complex Karyotype. *Cancers*. 2022;14(15). doi:10.3390/cancers14153715

248. Jarošová M, Plevová K, Kotašková J, Doubek M, Pospíšilová Š. The importance of complex karyotype in prognostication and treatment of chronic lymphocytic leukemia (CLL): a comprehensive review of the literature. *Leukemia & Lymphoma*. 2019;60(10):2348-2355. doi:10.1080/10428194.2019.1576038

249. Mato AR, Hill BT, Lamanna N, et al. Optimal sequencing of ibrutinib, idelalisib, and venetoclax in chronic lymphocytic leukemia: results from a multicenter study of 683 patients. *Annals of Oncology*. 2017;28(5):1050-1056. doi:10.1093/annonc/mdx031

250. Badoux XC, Keating MJ, Wang X, et al. Fludarabine, cyclophosphamide, and rituximab chemoimmunotherapy is highly effective treatment for relapsed patients with CLL. *Blood*. 2011;117(11):3016-3024. doi:10.1182/blood-2010-08-304683

251. Ratnaparkhe M, Wong JKL, Wei P-C, et al. Defective DNA damage repair leads to frequent catastrophic genomic events in murine and human tumors. *Nature Communications*. 2018;9(1):4760. doi:10.1038/s41467-018-06925-4

252. Quesada V, Conde L, Villamor N, et al. Exome sequencing identifies recurrent mutations of the splicing factor SF3B1 gene in chronic lymphocytic leukemia. *Nat Genet*. 2011;44(1):47-52. doi:10.1038/ng.1032

253. Puente XS, Pinyol M, Quesada V, et al. Whole-genome sequencing identifies recurrent mutations in chronic lymphocytic leukaemia. *Nature*. 2011;475(7354):101-5. doi:10.1038/nature10113

254. Ljungström V, Cortese D, Young E, et al. Whole-exome sequencing in relapsing chronic lymphocytic leukemia: clinical impact of recurrent RPS15 mutations. *Blood*. 2016;127(8):1007-16. doi:10.1182/blood-2015-10-674572

255. Rodríguez-Vicente AE, Bikos V, Hernández-Sánchez M, Malcikova J, Hernández-Rivas JM, Pospisilova S. Next-generation sequencing in chronic lymphocytic leukemia: recent findings and new horizons. *Oncotarget*. 2017;8(41):71234-71248. doi:10.18632/oncotarget.19525

256. Lawrence MS, Stojanov P, Mermel CH, et al. Discovery and saturation analysis of cancer genes across 21 tumour types. *Nature*. 2014;505(7484):495-501. doi:10.1038/nature12912

257. Kasar S, Kim J, Improgo R, et al. Whole-genome sequencing reveals activation-induced cytidine deaminase signatures during indolent chronic lymphocytic leukaemia evolution. *Nat Commun*. 2015;6:8866. doi:10.1038/ncomms9866

258. Alexandrov LB, Nik-Zainal S, Wedge DC, et al. Signatures of mutational processes in human cancer. *Nature*. 2013;500(7463):415-421. doi:10.1038/nature12477

259. Fabbri G, Rasi S, Rossi D, et al. Analysis of the chronic lymphocytic leukemia coding genome: role of NOTCH1 mutational activation. *Journal of Experimental Medicine*. 2011;208(7):1389-1401. doi:10.1084/jem.20110921

260. Rossi D, Fangazio M, Rasi S, et al. Disruption of BIRC3 associates with fludarabine chemorefractoriness in TP53 wild-type chronic lymphocytic leukemia. *Blood*. 2012;119(12):2854-62. doi:10.1182/blood-2011-12-395673

261. Rossi D, Bruscaggin A, Spina V, et al. Mutations of the SF3B1 splicing factor in chronic lymphocytic leukemia: association with progression and fludarabine-refractoriness. *Blood*. 2011;118(26):6904-6908. doi:10.1182/blood-2011-08-373159

262. Silvia R, Hossein K, Carmela C, et al. Clinical impact of small subclones harboring NOTCH1, SF3B1 or BIRC3 mutations in chronic lymphocytic leukemia. *Haematologica*. 2016;101(4):e135-e138. doi:10.3324/haematol.2015.136051

263. Wang L, Brooks Angela N, Fan J, et al. Transcriptomic Characterization of SF3B1 Mutation Reveals Its Pleiotropic Effects in Chronic Lymphocytic Leukemia. *Cancer Cell*. 2016;30(5):750-763. doi:https://doi.org/10.1016/j.ccell.2016.10.005

264. Wan Y, Wu CJ. SF3B1 mutations in chronic lymphocytic leukemia. *Blood*. 2013;121(23):4627-4634. doi:10.1182/blood-2013-02-427641

265. Elias C, Florence C, Paolo G, et al. TP53 aberrations in chronic lymphocytic leukemia: an overview of the clinical implications of improved diagnostics. *Haematologica*. 2018;103(12):1956-1968. doi:10.3324/haematol.2018.187583

266. Quijada-Álamo M, Pérez-Carretero C, Hernández-Sánchez M, et al. Dissecting the role of TP53 alterations in del(11q) chronic lymphocytic leukemia. *Clin Transl Med*. 2021;11(2):e304. doi:10.1002/ctm2.304

267. Quijada-Álamo M, Hernández-Sánchez M, Rodríguez-Vicente AE, et al. Biological significance of monoallelic and biallelic BIRC3 loss in del(11q) chronic lymphocytic leukemia progression. *Blood Cancer J*. 2021;11(7):127. doi:10.1038/s41408-021-00520-5

268. Oscier DG, Rose-Zerilli MJJ, Winkelmann N, et al. The clinical significance of NOTCH1 and SF3B1 mutations in the UK LRF CLL4 trial. *Blood*. 2013;121(3):468-475. doi:10.1182/blood-2012-05-429282

269. Guièze R, Robbe P, Clifford R, et al. Presence of multiple recurrent mutations confers poor trial outcome of relapsed/refractory CLL. *Blood*. 2015;126(18):2110-2117. doi:10.1182/blood-2015-05-647578

270. Pozzo F, Bittolo T, Arruga F, et al. NOTCH1 mutations associate with low CD20 level in chronic lymphocytic leukemia: evidence for a NOTCH1 mutation-driven epigenetic dysregulation. *Leukemia*. 2016;30(1):182-189. doi:10.1038/leu.2015.182

271. Delgado J, Nadeu F, Colomer D, Campo E. Chronic lymphocytic leukemia: from molecular pathogenesis to novel therapeutic strategies. *Haematologica*. 2020;105(9):2205-2217. doi:10.3324/haematol.2019.236000

272. Mansouri L, Sutton L-A, Ljungström V, et al. Functional loss of IκBε leads to NF-κB deregulation in aggressive chronic lymphocytic leukemia. *Journal of Experimental Medicine*. 2015;212(6):833-843. doi:10.1084/jem.20142009

273. Young E, Noerenberg D, Mansouri L, et al. EGR2 mutations define a new clinically aggressive subgroup of chronic lymphocytic leukemia. *Leukemia*. 2017;31(7):1547-1554. doi:10.1038/leu.2016.359

274. Martínez-Trillos A, Navarro A, Aymerich M, et al. Clinical impact of MYD88 mutations in chronic lymphocytic leukemia. *Blood*. 2016;127(12):1611-1613. doi:10.1182/blood-2015-10-678490

275. Spina V, Rossi D. Overview of non-coding mutations in chronic lymphocytic leukemia. *Molecular Oncology*. 2019;13(1):99-106. doi:https://doi.org/10.1002/1878-0261.12416

276. Tamara B, Federico P, Riccardo B, et al. Mutations in the 3′ untranslated region of NOTCH1 are associated with low CD20 expression levels chronic lymphocytic leukemia. *Haematologica*. 2017;102(8):e305-e309. doi:10.3324/haematol.2016.162594

277. Burns A, Alsolami R, Becq J, et al. Whole-genome sequencing of chronic lymphocytic leukaemia reveals distinct differences in the mutational landscape between IgHVmut and IgHVunmut subgroups. *Leukemia*. 2018;32(2):332-342. doi:10.1038/leu.2017.177

278. Larrayoz M, Rose-Zerilli MJJ, Kadalayil L, et al. Non-coding NOTCH1 mutations in chronic lymphocytic leukemia; their clinical impact in the UK CLL4 trial. *Leukemia*. 2017;31(2):510-514. doi:10.1038/leu.2016.298

279. Cui B, Chen L, Zhang S, et al. MicroRNA-155 influences B-cell receptor signaling and associates with aggressive disease in chronic lymphocytic leukemia. *Blood*. 2014;124(4):546-554. doi:10.1182/blood-2014-03-559690

280. Mraz M, Malinova K, Kotaskova J, et al. miR-34a, miR-29c and miR-17-5p are downregulated in CLL patients with TP53 abnormalities. *Leukemia*. 2009;23(6):1159-1163. doi:10.1038/leu.2008.377

281. Zenz T, Mohr J, Eldering E, et al. miR-34a as part of the resistance network in chronic lymphocytic leukemia. *Blood*. 2009;113(16):3801-3808. doi:10.1182/blood-2008-08-172254

282. Asslaber D, Piñón JD, Seyfried I, et al. microRNA-34a expression correlates with MDM2 SNP309 polymorphism and treatment-free survival in chronic lymphocytic leukemia. *Blood*. 2010;115(21):4191-4197. doi:10.1182/blood-2009-07-234823

283. Kulis M, Martin-Subero JI. Integrative epigenomics in chronic lymphocytic leukaemia: Biological insights and clinical applications. *British Journal of Haematology*. 2023;200(3):280-290. doi:https://doi.org/10.1111/bjh.18465

284. Kulis M, Heath S, Bibikova M, et al. Epigenomic analysis detects widespread gene-body DNA hypomethylation in chronic lymphocytic leukemia. *Nature Genetics*. 2012;44(11):1236-1242. doi:10.1038/ng.2443

285. Landau Dan A, Clement K, Ziller Michael J, et al. Locally Disordered Methylation Forms the Basis of Intratumor Methylome Variation in Chronic Lymphocytic Leukemia. *Cancer Cell*. 2014;26(6):813-825. doi:10.1016/j.ccell.2014.10.012

286. Kulis M, Merkel A, Heath S, et al. Whole-genome fingerprint of the DNA methylome during human B cell differentiation. *Nature Genetics*. 2015;47(7):746-756. doi:10.1038/ng.3291

287. Queirós AC, Villamor N, Clot G, et al. A B-cell epigenetic signature defines three biologic subgroups of chronic lymphocytic leukemia with clinical impact. *Leukemia*. 2015;29(3):598-605. doi:10.1038/leu.2014.252

288. Wojdacz TK, Amarasinghe HE, Kadalayil L, et al. Clinical significance of DNA methylation in chronic lymphocytic leukemia patients: results from 3 UK clinical trials. *Blood Advances*. 2019;3(16):2474-2481. doi:10.1182/bloodadvances.2019000237

289. Beekman R, Chapaprieta V, Russiñol N, et al. The reference epigenome and regulatory chromatin landscape of chronic lymphocytic leukemia. *Nature Medicine*. 2018;24(6):868-880. doi:10.1038/s41591-018-0028-4

290. Rendeiro AF, Krausgruber T, Fortelny N, et al. Chromatin mapping and single-cell immune profiling define the temporal dynamics of ibrutinib response in CLL. *Nature Communications*. 2020;11(1):577. doi:10.1038/s41467-019-14081-6

291. Mansouri L, Papakonstantinou N, Ntoufa S, Stamatopoulos K, Rosenquist R. NF-κB activation in chronic lymphocytic leukemia: A point of convergence of external triggers and intrinsic lesions. *Seminars in Cancer Biology*. 2016;39:40-48. doi:https://doi.org/10.1016/j.semcancer.2016.07.005

292. Philipp C, Edelmann J, Bühler A, Winkler D, Stilgenbauer S, Küppers R. Mutation analysis of the TNFAIP3 (A20) tumor suppressor gene in CLL. *International Journal of Cancer*. 2011;128(7):1747-1750. doi:https://doi.org/10.1002/ijc.25497

293. Fabbri G, Holmes AB, Viganotti M, et al. Common nonmutational NOTCH1 activation in chronic lymphocytic leukemia. *Proceedings of the National Academy of Sciences*. 2017;114(14):E2911-E2919. doi:10.1073/pnas.1702564114

294. Quijada-Álamo M, Hernández-Sánchez M, Alonso-Pérez V, et al. CRISPR/Cas9-generated models uncover therapeutic vulnerabilities of del(11q) CLL cells to dual BCR and PARP inhibition. *Leukemia*. 2020;doi:10.1038/s41375-020-0714-3

295. Stankovic T, Hubank M, Cronin D, et al. Microarray analysis reveals that TP53- and ATM-mutant B-CLLs share a defect in activating proapoptotic responses after DNA damage but are distinguished by major differences in activating prosurvival responses. *Blood*. 2004;103(1):291-300. doi:10.1182/blood-2003-04-1161

296. Robbe P, Ridout KE, Vavoulis DV, et al. Whole-genome sequencing of chronic lymphocytic leukemia identifies subgroups with distinct biological and clinical features. *Nat Genet*. 2022;54(11):1675-1689. doi:10.1038/s41588-022-01211-y

297. Ramsay AJ, Quesada V, Foronda M, et al. POT1 mutations cause telomere dysfunction in chronic lymphocytic leukemia. *Nat Genet*. 2013;45(5):526-30. doi:10.1038/ng.2584

298. Rodríguez D, Bretones G, Quesada V, et al. Mutations in CHD2 cause defective association with active chromatin in chronic lymphocytic leukemia. *Blood*. 2015;126(2):195-202. doi:10.1182/blood-2014-10-604959

299. Walker JS, Hing ZA, Harrington B, et al. Recurrent XPO1 mutations alter pathogenesis of chronic lymphocytic leukemia. *Journal of Hematology & Oncology*. 2021;14(1):17. doi:10.1186/s13045-021-01032-2

300. Bretones G, Álvarez MG, Arango JR, et al. Altered patterns of global protein synthesis and translational fidelity in RPS15-mutated chronic lymphocytic leukemia. *Blood*. 2018;132(22):2375-2388. doi:10.1182/blood-2017-09-804401

301. Burger JA, Burger M, Kipps TJ. Chronic Lymphocytic Leukemia B Cells Express Functional CXCR4 Chemokine Receptors That Mediate Spontaneous Migration Beneath Bone Marrow Stromal Cells. *Blood*. 1999;94(11):3658-3667. doi:10.1182/blood.V94.11.3658

302. Burger JA, Zvaifler NJ, Tsukada N, Firestein GS, Kipps TJ. Fibroblast-like synoviocytes support B-cell pseudoemperipolesis via a stromal cell–derived factor-1– and CD106 (VCAM-1)–dependent mechanism. *The Journal of Clinical Investigation*. 2001;107(3):305-315. doi:10.1172/JCI11092

303. Bürkle A, Niedermeier M, Schmitt-Gräff A, Wierda WG, Keating MJ, Burger JA. Overexpression of the CXCR5 chemokine receptor, and its ligand, CXCL13 in B-cell chronic lymphocytic leukemia. *Blood*. 2007;110(9):3316-3325. doi:10.1182/blood-2007-05-089409

304. Nishio M, Endo T, Tsukada N, et al. Nurselike cells express BAFF and APRIL, which can promote survival of chronic lymphocytic leukemia cells via a paracrine pathway distinct from that of SDF-1α. *Blood*. 2005;106(3):1012-1020. doi:10.1182/blood-2004-03-0889

305. Deaglio S, Vaisitti T, Bergui L, et al. CD38 and CD100 lead a network of surface receptors relaying positive signals for B-CLL growth and survival. *Blood*. 2005;105(8):3042-3050. doi:10.1182/blood-2004-10-3873

306. Chen Y, Chen L, Yu J, et al. Cirmtuzumab blocks Wnt5a/ROR1 stimulation of NF-κB to repress autocrine STAT3 activation in chronic lymphocytic leukemia. *Blood*. 2019;134(13):1084-1094. doi:10.1182/blood.2019001366

307. Burger JA, Quiroga MP, Hartmann E, et al. High-level expression of the T-cell chemokines CCL3 and CCL4 by chronic lymphocytic leukemia B cells in nurselike cell cocultures and after BCR stimulation. *Blood*. 2009;113(13):3050-3058. doi:10.1182/blood-2008-07-170415

308. Kitada S, Zapata JM, Andreeff M, Reed JC. Bryostatin and CD40-ligand enhance apoptosis resistance and induce expression of cell survival genes in B-cell chronic lymphocytic leukaemia. *British Journal of Haematology*. 1999;106(4):995-1004. doi:https://doi.org/10.1046/j.1365-2141.1999.01642.x

309. Leeksma AC, Taylor J, Wu B, et al. Clonal diversity predicts adverse outcome in chronic lymphocytic leukemia. *Leukemia*. 2019;33(2):390-402. doi:10.1038/s41375-018-0215-9

310. Nadeu F, Clot G, Delgado J, et al. Clinical impact of the subclonal architecture and mutational complexity in chronic lymphocytic leukemia. *Leukemia*. 2018;32(3):645-653. doi:10.1038/leu.2017.291

311. Ojha J, Ayres J, Secreto C, et al. Deep sequencing identifies genetic heterogeneity and recurrent convergent evolution in chronic lymphocytic leukemia. *Blood*. 2015;125(3):492-498. doi:10.1182/blood-2014-06-580563

312. Gruber M, Bozic I, Leshchiner I, et al. Growth dynamics in naturally progressing chronic lymphocytic leukaemia. *Nature*. 2019;570(7762):474-479. doi:10.1038/s41586-019-1252-x

313. Kwok M, Wu CJ. Clonal Evolution of High-Risk Chronic Lymphocytic Leukemia: A Contemporary Perspective. Review. *Frontiers in Oncology*. 2021;11, doi.org/10.3389/fonc.2021.790004

314. Hernández-Sánchez M, Kotaskova J, Rodríguez AE, et al. CLL cells cumulate genetic aberrations prior to the first therapy even in outwardly inactive disease phase. *Leukemia*. 2019;33(2):518-558. doi:10.1038/s41375-018-0255-1

315. Klintman J, Appleby N, Stamatopoulos B, et al. Genomic and transcriptomic correlates of Richter transformation in chronic lymphocytic leukemia. *Blood*. 2021;137(20):2800-2816. doi:10.1182/blood.2020005650

316. Schuh A, Becq J, Humphray S, et al. Monitoring chronic lymphocytic leukemia progression by whole genome sequencing reveals heterogeneous clonal evolution patterns. *Blood*. 2012;120(20):4191-4196. doi:10.1182/blood-2012-05-433540

317. Condoluci A, Rossi D. Genomic Instability and Clonal Evolution in Chronic Lymphocytic Leukemia: Clinical Relevance. *Journal of the National Comprehensive Cancer Network*. 2021 2021;19(2):227-233. doi:10.6004/jnccn.2020.7623

318. Landau DA, Sun C, Rosebrock D, et al. The evolutionary landscape of chronic lymphocytic leukemia treated with ibrutinib targeted therapy. *Nature Communications*. 2017;8(1):2185. doi:10.1038/s41467-017-02329-y

319. Herling CD, Abedpour N, Weiss J, et al. Clonal dynamics towards the development of venetoclax resistance in chronic lymphocytic leukemia. *Nat Commun*. 2018;9(1):727. doi:10.1038/s41467-018-03170-7

320. Burger JA, Landau DA, Taylor-Weiner A, et al. Clonal evolution in patients with chronic lymphocytic leukaemia developing resistance to BTK inhibition. *Nature Communications*. 2016;7(1):11589. doi:10.1038/ncomms11589

321. Ahn IE, Underbayev C, Albitar A, et al. Clonal evolution leading to ibrutinib resistance in chronic lymphocytic leukemia. *Blood*. 2017;129(11):1469-1479. doi:10.1182/blood-2016-06-719294

322. Woyach JA, Furman RR, Liu T-M, et al. Resistance Mechanisms for the Bruton's Tyrosine Kinase Inhibitor Ibrutinib. *New England Journal of Medicine*. 2014;370(24):2286-2294. doi:10.1056/NEJMoa1400029

323. Woyach JA, Ruppert AS, Guinn D, et al. BTKC481S-Mediated Resistance to Ibrutinib in Chronic Lymphocytic Leukemia. *Journal of Clinical Oncology*. 2017;35(13):1437-1443. doi:10.1200/JCO.2016.70.2282

324. Wang E, Mi X, Thompson MC, et al. Mechanisms of Resistance to Noncovalent Bruton's Tyrosine Kinase Inhibitors. *New England Journal of Medicine*. 2022;386(8):735-743. doi:10.1056/NEJMoa2114110

325. Liu T-M, Woyach JA, Zhong Y, et al. Hypermorphic mutation of phospholipase C, γ2 acquired in ibrutinib-resistant CLL confers BTK independency upon B-cell receptor activation. *Blood*. 2015;126(1):61-68. doi:10.1182/blood-2015-02-626846

326. Jones D, Woyach JA, Zhao W, et al. PLCG2 C2 domain mutations co-occur with BTK and PLCG2 resistance mutations in chronic lymphocytic leukemia undergoing ibrutinib treatment. *Leukemia*. 2017;31(7):1645-1647. doi:10.1038/leu.2017.110

327. Blombery P, Anderson MA, Gong J-n, et al. Acquisition of the Recurrent Gly101Val Mutation in BCL2 Confers Resistance to Venetoclax in Patients with Progressive Chronic Lymphocytic Leukemia. *Cancer Discovery*. 2019;9(3):342-353. doi:10.1158/2159-8290.CD-18-1119

328. Blombery P, Thompson ER, Nguyen T, et al. Multiple BCL2 mutations cooccurring with Gly101Val emerge in chronic lymphocytic leukemia progression on venetoclax. *Blood*. 2020;135(10):773-777. doi:10.1182/blood.2019004205

329. Eugen T, William C, Anna D, et al. Venetoclax resistance and acquired BCL2 mutations in chronic lymphocytic leukemia. *Haematologica*. 2019;104(9):e434-e437. doi:10.3324/haematol.2019.222588

330. Thijssen R, Tian L, Anderson MA, et al. Single-cell multiomics reveal the scale of multilayered adaptations enabling CLL relapse during venetoclax therapy. *Blood*. 2022;140(20):2127-2141. doi:10.1182/blood.2022016040

331. Guièze R, Liu VM, Rosebrock D, et al. Mitochondrial Reprogramming Underlies Resistance to BCL-2 Inhibition in Lymphoid Malignancies. *Cancer Cell*. 2019;36(4):369-384.e13. doi:10.1016/j.ccell.2019.08.005

332. Thomalla D, Beckmann L, Grimm C, et al. Deregulation and epigenetic modification of BCL2-family genes cause resistance to venetoclax in hematologic malignancies. *Blood*. 2022;140(20):2113-2126. doi:10.1182/blood.2021014304

333. Pavlova NN, Thompson CB. The Emerging Hallmarks of Cancer Metabolism. *Cell Metab*. 2016;23(1):27-47. doi:10.1016/j.cmet.2015.12.006

334. Boroughs LK, DeBerardinis RJ. Metabolic pathways promoting cancer cell survival and growth. *Nature Cell Biology*. 2015;17(4):351-359. doi:10.1038/ncb3124

335. Vander Heiden MG, Cantley LC, Thompson CB. Understanding the Warburg effect: the metabolic requirements of cell proliferation. *Science*. 2009;324(5930):1029-33. doi:10.1126/science.1160809

336. DeBerardinis RJ, Mancuso A, Daikhin E, et al. Beyond aerobic glycolysis: Transformed cells can engage in glutamine metabolism that exceeds the requirement for protein and nucleotide synthesis. *Proceedings of the National Academy of Sciences*. 2007;104(49):19345-19350. doi:10.1073/pnas.0709747104

337. Zhang J, Pavlova NN, Thompson CB. Cancer cell metabolism: the essential role of the nonessential amino acid, glutamine. *The EMBO Journal*. 2017;36(10):1302-1315. doi:https://doi.org/10.15252/embj.201696151

338. Bertout JA, Patel SA, Simon MC. The impact of O2 availability on human cancer. *Nature Reviews Cancer*. 2008;8(12):967-975. doi:10.1038/nrc2540

339. Boya P, Reggiori F, Codogno P. Emerging regulation and functions of autophagy. *Nature Cell Biology*. 2013;15(7):713-720. doi:10.1038/ncb2788

340. Le A, Lane Andrew N, Hamaker M, et al. Glucose-Independent Glutamine Metabolism via TCA Cycling for Proliferation and Survival in B Cells. *Cell Metabolism*. 2012;15(1):110-121. doi:10.1016/j.cmet.2011.12.009

341. Yang C, Ko B, Hensley Christopher T, et al. Glutamine Oxidation Maintains the TCA Cycle and Cell Survival during Impaired Mitochondrial Pyruvate Transport. *Molecular Cell*. 2014;56(3):414-424. doi:10.1016/j.molcel.2014.09.025

342. Zhang J, Fan J, Venneti S, et al. Asparagine Plays a Critical Role in Regulating Cellular Adaptation to Glutamine Depletion. *Molecular Cell*. 2014;56(2):205-218. doi:10.1016/j.molcel.2014.08.018

343. Menendez JA, Lupu R. Fatty acid synthase and the lipogenic phenotype in cancer pathogenesis. *Nature Reviews Cancer*. 2007;7(10):763-777. doi:10.1038/nrc2222

344. Lee Joyce V, Carrer A, Shah S, et al. Akt-Dependent Metabolic Reprogramming Regulates Tumor Cell Histone Acetylation. *Cell Metabolism*. 2014;20(2):306-319. doi:10.1016/j.cmet.2014.06.004

345. Cai L, Sutter Benjamin M, Li B, Tu Benjamin P. Acetyl-CoA Induces Cell Growth and Proliferation by Promoting the Acetylation of Histones at Growth Genes. *Molecular Cell*. 2011;42(4):426-437. doi:10.1016/j.molcel.2011.05.004

346. Sonveaux P, Copetti T, De Saedeleer CJ, et al. Targeting the Lactate Transporter MCT1 in Endothelial Cells Inhibits Lactate-Induced HIF-1 Activation and Tumor Angiogenesis. *PLOS ONE*. 2012;7(3):e33418. doi:10.1371/journal.pone.0033418

347. Yun J, Rago C, Cheong I, et al. Glucose Deprivation Contributes to the Development of KRAS Pathway Mutations in Tumor Cells. *Science*. 2009;325(5947):1555-1559. doi:10.1126/science.1174229

348. Schwartzenberg-Bar-Yoseph F, Armoni M, Karnieli E. The Tumor Suppressor p53 Down-Regulates Glucose Transporters GLUT1 and GLUT4 Gene Expression. *Cancer Research*. 2004;64(7):2627-2633. doi:10.1158/0008-5472.CAN-03-0846

349. Wahlström T, Arsenian Henriksson M. Impact of MYC in regulation of tumor cell metabolism. *Biochimica et Biophysica Acta (BBA) - Gene Regulatory Mechanisms*. 2015;1849(5):563-569. doi:https://doi.org/10.1016/j.bbagrm.2014.07.004

350. Nicklin P, Bergman P, Zhang B, et al. Bidirectional Transport of Amino Acids Regulates mTOR and Autophagy. *Cell*. 2009;136(3):521-534. doi:10.1016/j.cell.2008.11.044

351. Jewell JL, Kim YC, Russell RC, et al. Differential regulation of mTORC1 by leucine and glutamine. *Science*. 2015;347(6218):194-198. doi:10.1126/science.1259472

352. Dalva-Aydemir S, Bajpai R, Martinez M, et al. Targeting the Metabolic Plasticity of Multiple Myeloma with FDA-Approved Ritonavir and Metformin. *Clinical Cancer Research*. 2015;21(5):1161-1171. doi:10.1158/1078-0432.CCR-14-1088

353. Raez LE, Papadopoulos K, Ricart AD, et al. A phase I dose-escalation trial of 2-deoxy-d-glucose alone or combined with docetaxel in patients with advanced solid tumors. *Cancer Chemotherapy and Pharmacology*. 2013;71(2):523-530. doi:10.1007/s00280-012-2045-1

354. Zhai X, Yang Y, Wan J, Zhu R, Wu Y. Inhibition of LDH-A by oxamate induces G2/M arrest, apoptosis and increases radiosensitivity in nasopharyngeal carcinoma cells. *Oncol Rep*. 2013;30(6):2983-2991. doi:10.3892/or.2013.2735

355. Xia M, Li X, Diao Y, Du B, Li Y. Targeted inhibition of glutamine metabolism enhances the antitumor effect of selumetinib in KRAS-mutant NSCLC. *Translational Oncology*. 2021;14(1):100920. doi:https://doi.org/10.1016/j.tranon.2020.100920

356. Yu W, Yang X, Zhang Q, Sun L, Yuan S, Xin Y. Targeting GLS1 to cancer therapy through glutamine metabolism. *Clinical and Translational Oncology*. 2021;23(11):2253-2268. doi:10.1007/s12094-021-02645-2

357. Yap TA, Daver N, Mahendra M, et al. Complex I inhibitor of oxidative phosphorylation in advanced solid tumors and acute myeloid leukemia: phase I trials. *Nature Medicine*. 2023;29(1):115-126. doi:10.1038/s41591-022-02103-8

358. Varghese S, Pramanik S, Williams LJ, et al. The Glutaminase Inhibitor CB-839 (Telaglenastat) Enhances the Antimelanoma Activity of T-Cell–Mediated Immunotherapies. *Molecular Cancer Therapeutics*. 2021;20(3):500-511. doi:10.1158/1535-7163.MCT-20-0430

359. Halestrap AP. The mitochondrial pyruvate carrier. Kinetics and specificity for substrates and inhibitors. *Biochemical Journal*. 1975;148(1):85-96. doi:10.1042/bj1480085

360. Divakaruni AS, Wiley SE, Rogers GW, et al. Thiazolidinediones are acute, specific inhibitors of the mitochondrial pyruvate carrier. *Proceedings of the National Academy of Sciences*. 2013;110(14):5422-5427. doi:10.1073/pnas.1303360110

361. Rais R, Jančařík A, Tenora L, et al. Discovery of 6-Diazo-5-oxo-l-norleucine (DON) Prodrugs with Enhanced CSF Delivery in Monkeys: A Potential Treatment for Glioblastoma. *Journal of Medicinal Chemistry*. 2016;59(18):8621-8633. doi:10.1021/acs.jmedchem.6b01069

362. Robinson Mary M, McBryant Steven J, Tsukamoto T, et al. Novel mechanism of inhibition of rat kidney-type glutaminase by bis-2-(5-phenylacetamido-1,2,4-thiadiazol-2-yl)ethyl sulfide (BPTES). *Biochemical Journal*. 2007;406(3):407-414. doi:10.1042/BJ20070039

363. Wang J-B, Erickson JW, Fuji R, et al. Targeting Mitochondrial Glutaminase Activity Inhibits Oncogenic Transformation. *Cancer Cell*. 2010;18(3):207-219. doi:10.1016/j.ccr.2010.08.009

364. Hassanein M, Hoeksema MD, Shiota M, et al. SLC1A5 Mediates Glutamine Transport Required for Lung Cancer Cell Growth and Survival. *Clinical Cancer Research*. 2013;19(3):560-570. doi:10.1158/1078-0432.CCR-12-2334

365. Hu K, Li K, Lv J, et al. Suppression of the SLC7A11/glutathione axis causes synthetic lethality in KRAS-mutant lung adenocarcinoma. *The Journal of Clinical Investigation*. 2020;130(4):1752-1766. doi:10.1172/JCI124049

366. Schulte ML, Fu A, Zhao P, et al. Pharmacological blockade of ASCT2-dependent glutamine transport leads to antitumor efficacy in preclinical models. *Nat Med*. 2018;24(2):194-202. doi:10.1038/nm.4464

367. Galicia-Vázquez G, Aloyz R. Ibrutinib Resistance Is Reduced by an Inhibitor of Fatty Acid Oxidation in Primary CLL Lymphocytes. Original Research. *Frontiers in Oncology*. 2018;8 doi.org/10.3389/fonc.2018.00411

368. Ricciardi MR, Mirabilii S, Allegretti M, et al. Targeting the leukemia cell metabolism by the CPT1a inhibition: functional preclinical effects in leukemias. *Blood*. 2015;126(16):1925-1929. doi:10.1182/blood-2014-12-617498

369. Pallasch CP, Schwamb J, Königs S, et al. Targeting lipid metabolism by the lipoprotein lipase inhibitor orlistat results in apoptosis of B-cell chronic lymphocytic leukemia cells. *Leukemia*. 2008;22(3):585-592. doi:10.1038/sj.leu.2405058

370. Janku F, LoRusso P, Mansfield AS, et al. First-in-human evaluation of the novel mitochondrial complex I inhibitor ASP4132 for treatment of cancer. *Investigational New Drugs*. 2021;39(5):1348-1356. doi:10.1007/s10637-021-01112-7

371. Janku F, Beom S-H, Moon YW, et al. First-in-human study of IM156, a novel potent biguanide oxidative phosphorylation (OXPHOS) inhibitor, in patients with advanced solid tumors. *Investigational New Drugs*. 2022;40(5):1001-1010. doi:10.1007/s10637-022-01277-9

372. Nie Y, Yun X, Zhang Y, Wang X. Targeting metabolic reprogramming in chronic lymphocytic leukemia. *Experimental Hematology & Oncology*. 2022;11(1):39. doi:10.1186/s40164-022-00292-z

373. Jitschin R, Braun M, Qorraj M, et al. Stromal cell-mediated glycolytic switch in CLL cells involves Notch-c-Myc signaling. *Blood*. 2015;125(22):3432-6. doi:10.1182/blood-2014-10-607036

374. Jitschin R, Hofmann AD, Bruns H, et al. Mitochondrial metabolism contributes to oxidative stress and reveals therapeutic targets in chronic lymphocytic leukemia. *Blood*. 2014;123(17):2663-72. doi:10.1182/blood-2013-10-532200

375. Rozovski U, Hazan-Halevy I, Barzilai M, Keating MJ, Estrov Z. Metabolism pathways in chronic lymphocytic leukemia. *Leukemia & Lymphoma*. 2016;57(4):758-765. doi:10.3109/10428194.2015.1106533

376. Galicia-Vázquez G, Smith S, Aloyz R. Del11q-positive CLL lymphocytes exhibit altered glutamine metabolism and differential response to GLS1 and glucose metabolism inhibition. *Blood Cancer Journal*. 2018;8(1):13. doi:10.1038/s41408-017-0039-2

377. Vangapandu HV, Ayres ML, Bristow CA, et al. The Stromal Microenvironment Modulates Mitochondrial Oxidative Phosphorylation in Chronic Lymphocytic Leukemia Cells. *Neoplasia*. 2017;19(10):762-771. doi:10.1016/j.neo.2017.07.004

378. Zhang W, Trachootham D, Liu J, et al. Stromal control of cystine metabolism promotes cancer cell survival in chronic lymphocytic leukaemia. *Nat Cell Biol*. 2012;14(3):276-86. doi:10.1038/ncb2432

379. Chen Z, Simon-Molas H, Cretenet G, et al. Characterization of metabolic alterations of chronic lymphocytic leukemia in the lymph node microenvironment. *Blood*. 2022;140(6):630-643. doi:10.1182/blood.2021013990

380. van Bruggen JAC, van der Windt GJW, Hoogendoorn M, Dubois J, Kater AP, Peters FS. Depletion of CLL cells by venetoclax treatment reverses oxidative stress and impaired glycolysis in CD4 T cells. *Blood Adv*. 2022;6(14):4185-4195. doi:10.1182/bloodadvances.2022007034

381. Liu J, Zhang C, Hu W, Feng Z. Tumor suppressor p53 and metabolism. *Journal of Molecular Cell Biology*. 2019;11(4):284-292. doi:10.1093/jmcb/mjy070

382. Lu J, Cannizzaro E, Meier-Abt F, et al. Multi-omics reveals clinically relevant proliferative drive associated with mTOR-MYC-OXPHOS activity in chronic lymphocytic leukemia. *Nature Cancer*. 2021;2(8):853-864. doi:10.1038/s43018-021-00216-6

383. Baliakas P, Espinet B, Mellink C, et al. Cytogenetics in Chronic Lymphocytic Leukemia: ERIC Perspectives and Recommendations. *HemaSphere*. 2022;6(4):e707. doi: 10.1097/HS9.0000000000000707

384. Bishop R. Applications of fluorescence in situ hybridization (FISH) in detecting genetic aberrations of medical significance. *Bioscience Horizons: The International Journal of Student Research*. 2010;3(1):85-95. doi:10.1093/biohorizons/hzq009

385. Neveling K, Mantere T, Vermeulen S, et al. Next-generation cytogenetics: Comprehensive assessment of 52 hematological malignancy genomes by optical genome mapping. *The American Journal of Human Genetics*. 2021;108(8):1423-1435. doi:10.1016/j.ajhg.2021.06.001

386. Feng Y, Chen D, Wang GL, Zhang VW, Wong LJ. Improved molecular diagnosis by the detection of exonic deletions with target gene capture and deep sequencing. *Genet Med*. 2015;17(2):99-107. doi:10.1038/gim.2014.80

387. Lesley-Ann S, Viktor L, Anna E, et al. Comparative analysis of targeted next-generation sequencing panels for the detection of gene mutations in chronic lymphocytic leukemia: an ERIC multi-center study. *Haematologica*. 2020;106(3):682-691. doi:10.3324/haematol.2019.234716

388. Bewicke-Copley F, Arjun Kumar E, Palladino G, Korfi K, Wang J. Applications and analysis of targeted genomic sequencing in cancer studies. *Computational and Structural Biotechnology Journal*. 2019;17:1348-1359. doi:https://doi.org/10.1016/j.csbj.2019.10.004

389. Davi F, Langerak AW, de Septenville AL, et al. Immunoglobulin gene analysis in chronic lymphocytic leukemia in the era of next generation sequencing. *Leukemia*. 2020;34(10):2545-2551. doi:10.1038/s41375-020-0923-9

390. McCafferty N, Stewart JP, Darzentas N, et al. A novel next-generation sequencing capture-based strategy to report somatic hypermutation status using genomic regions downstream to immunoglobulin rearrangements. *Haematologica*. 2022;doi:10.3324/haematol.2022.281928

391. Lanemo Myhrinder A, Hellqvist E, Bergh A-C, et al. Molecular characterization of neoplastic and normal "sister" lymphoblastoid B-cell lines from chronic lymphocytic leukemia. *Leukemia & Lymphoma*. 2013;54(8):1769-1779. doi:10.3109/10428194.2013.764418

392. Hsu Patrick D, Lander Eric S, Zhang F. Development and Applications of CRISPR-Cas9 for Genome Engineering. *Cell*. 2014;157(6):1262-1278. doi:https://doi.org/10.1016/j.cell.2014.05.010

393. Shalem O, Sanjana NE, Hartenian E, et al. Genome-Scale CRISPR-Cas9 Knockout Screening in Human Cells. *Science*. 2014;343(6166):84-87. doi:10.1126/science.1247005

394. Montaño A, Forero-Castro M, Hernández-Rivas J-M, García-Tuñón I, Benito R. Targeted genome editing in acute lymphoblastic leukemia: a review. *BMC Biotechnology*. 2018;18(1):45. doi:10.1186/s12896-018-0455-9

395. Close V, Close W, Kugler SJ, et al. FBXW7 mutations reduce binding of NOTCH1, leading to cleaved NOTCH1 accumulation and target gene activation in CLL. *Blood*. 2019;133(8):830-839. doi:10.1182/blood-2018-09-874529

396. Arruga F, Gizdic B, Bologna C, et al. Mutations in NOTCH1 PEST domain orchestrate CCL19-driven homing of chronic lymphocytic leukemia cells by modulating the tumor suppressor gene DUSP22. *Leukemia*. 2017;31(9):1882-1893. doi:10.1038/leu.2016.383

397. ten Hacken E, Sewastianik T, Yin S, et al. In Vivo Modeling of CLL Transformation to Richter Syndrome Reveals Convergent Evolutionary Paths and Therapeutic Vulnerabilities. *Blood Cancer Discovery*. 2023;4(2):150-169. doi:10.1158/2643-3230.BCD-22-0082

398. Dranka BP, Benavides GA, Diers AR, et al. Assessing bioenergetic function in response to oxidative stress by metabolic profiling. *Free Radical Biology and Medicine*. 2011;51(9):1621-1635. doi:https://doi.org/10.1016/j.freeradbiomed.2011.08.005

399. Yang M, Chadwick AE, Dart C, Kamishima T, Quayle JM. Bioenergetic profile of human coronary artery smooth muscle cells and effect of metabolic intervention. *PLOS ONE*. 2017;12(5):e0177951. doi:10.1371/journal.pone.0177951

400. Underwood E, Redell JB, Zhao J, Moore AN, Dash PK. A method for assessing tissue respiration in anatomically defined brain regions. *Scientific Reports*. 2020;10(1):13179. doi:10.1038/s41598-020-69867-2

401. Cheng G, Zielonka J, McAllister D, Tsai S, Dwinell MB, Kalyanaraman B. Profiling and targeting of cellular bioenergetics: inhibition of pancreatic cancer cell proliferation. *British Journal of Cancer*. 2014;111(1):85-93. doi:10.1038/bjc.2014.272

402. Liu Y, Gokhale S, Jung J, et al. Mitochondrial Fission Factor Is a Novel Interacting Protein of the Critical B Cell Survival Regulator TRAF3 in B Lymphocytes. *Front Immunol*. 2021;12:670338. doi:10.3389/fimmu.2021.670338

403. Roca-Portoles A, Rodriguez-Blanco G, Sumpton D, et al. Venetoclax causes metabolic reprogramming independent of BCL-2 inhibition. *Cell Death Dis*. 2020;11(8):616. doi:10.1038/s41419-020-02867-2

404. Kang YP, Ward NP, DeNicola GM. Recent advances in cancer metabolism: a technological perspective. *Experimental & Molecular Medicine*. 2018;50(4):1-16. doi:10.1038/s12276-018-0027-z

405. Mayers JR, Torrence ME, Danai LV, et al. Tissue of origin dictates branched-chain amino acid metabolism in mutant Kras-driven cancers. *Science*. 2016;353(6304):1161-1165. doi:10.1126/science.aaf5171

406. Dang L, White DW, Gross S, et al. Cancer-associated IDH1 mutations produce 2-hydroxyglutarate. *Nature*. 2009;462(7274):739-744. doi:10.1038/nature08617

407. Yang K, Han X. Lipidomics: Techniques, Applications, and Outcomes Related to Biomedical Sciences. *Trends in Biochemical Sciences*. 2016;41(11):954-969. doi:10.1016/j.tibs.2016.08.010

408. Thurgood LA, Dwyer ES, Lower KM, Chataway TK, Kuss BJ. Altered expression of metabolic pathways in CLL detected by unlabelled quantitative mass spectrometry analysis. *British Journal of Haematology*. 2019;185(1):65-78. doi:https://doi.org/10.1111/bjh.15751

409. Piszcz J, Armitage EG, Ferrarini A, et al. To treat or not to treat: metabolomics reveals biomarkers for treatment indication in chronic lymphocytic leukaemia patients. *Oncotarget;* 2016;*Vol 7, No 16*.

410. Cuneo A, Roberti MG, Bigoni R, et al. Four novel non-random chromosome rearrangements in B-cell chronic lymphocytic leukaemia: 6p24–25 and 12p12–13 translocations, 4q21 anomalies and monosomy 21. *British Journal of Haematology*. 2000;108(3):559-564. doi:https://doi.org/10.1046/j.1365-2141.2000.01898.x

411. Chapiro E, Radford-Weiss I, Bastard C, et al. The most frequent t(14;19)(q32;q13)-positive B-cell malignancy corresponds to an aggressive subgroup of atypical chronic lymphocytic leukemia. *Leukemia*. 2008;22(11):2123-7. doi:10.1038/leu.2008.102

412. Nyla AH, Natarajan M, Qiuhong Z, et al. Prognostic significance of translocations in the presence of mutated IGHV and of cytogenetic complexity at diagnosis of chronic lymphocytic leukemia. *Haematologica*. 2020;106(6):1608-1615. doi:10.3324/haematol.2018.212571

413. Merup M, Moreno TC, Heyman M, et al. 6q Deletions in Acute Lymphoblastic Leukemia and Non-Hodgkin's Lymphomas. *Blood*. 1998;91(9):3397-3400. doi:https://doi.org/10.1182/blood.V91.9.3397

414. Thelander EF, Ichimura K, Corcoran M, et al. Characterization of 6q deletions in mature B cell lymphomas and childhood acute lymphoblastic leukemia. *Leuk Lymphoma*. 2008;49(3):477-87. doi:10.1080/10428190701817282

415. Kluth M, Jung S, Habib O, et al. Deletion lengthening at chromosomes 6q and 16q targets multiple tumor suppressor genes and is associated with an increasingly poor prognosis in prostate cancer. *Oncotarget;* 2017;*Vol 8, No 65*.

416. Honma K, Tsuzuki S, Nakagawa M, et al. TNFAIP3/A20 functions as a novel tumor suppressor gene in several subtypes of non-Hodgkin lymphomas. *Blood*. 2009;114(12):2467-2475. doi:10.1182/blood-2008-12-194852

417. Kato M, Sanada M, Kato I, et al. Frequent inactivation of A20 in B-cell lymphomas. *Nature*. 2009;459(7247):712-716. doi:10.1038/nature07969

418. Frenzel LP, Claus R, Plume N, et al. Sustained NF-kappaB activity in chronic lymphocytic leukemia is independent of genetic and epigenetic alterations in the TNFAIP3 (A20) locus. *International Journal of Cancer*. 2011;128(10):2495-2500. doi:https://doi.org/10.1002/ijc.25579

419. Gachet S, El-Chaar T, Avran D, et al. Deletion 6q Drives T-cell Leukemia Progression by Ribosome Modulation. *Cancer Discovery*. 2018;8(12):1614-1631. doi:10.1158/2159-8290.CD-17-0831

420. Li Q, Xing S, Zhang H, Mao X, Xiao M, Wang Y. IGH Translocations in Chinese Patients With Chronic Lymphocytic Leukemia: Clinicopathologic Characteristics and Genetic Profile. Original Research. *Frontiers in Oncology*. 2022;12:858523. doi: 10.3389/fonc.2022.858523

421. Li Q, Xing S, Zhang H, et al. Case Report: Chronic Lymphocytic Leukemia With a Rare Translocation t(14;19)(q32;q13) Involving IGH/BCL3 Rearrangements: Report of Three Chinese Cases and Literature Review. Case Report. *Frontiers in Oncology*. 2020;10:594732. doi: 10.3389/fonc.2020.594732.

422. Rheinbay E, Nielsen MM, Abascal F, et al. Analyses of non-coding somatic drivers in 2,658 cancer whole genomes. *Nature*. 2020;578(7793):102-111. doi:10.1038/s41586-020-1965-x

423. Mosquera Orgueira A, Rodríguez Antelo B, Díaz Arias J, et al. Novel Mutation Hotspots within Non-Coding Regulatory Regions of the Chronic Lymphocytic Leukemia Genome. *Sci Rep*. Feb 2020;10(1):2407. doi:10.1038/s41598-020-59243-5

424. de Miranda NF, Georgiou K, Chen L, et al. Exome sequencing reveals novel mutation targets in diffuse large B-cell lymphomas derived from Chinese patients. *Blood*. 2014;124(16):2544-53. doi:10.1182/blood-2013-12-546309

425. Pasqualucci L, Khiabanian H, Fangazio M, et al. Genetics of follicular lymphoma transformation. *Cell Rep*. 2014;6(1):130-40. doi:10.1016/j.celrep.2013.12.027

426. Okosun J, Bödör C, Wang J, et al. Integrated genomic analysis identifies recurrent mutations and evolution patterns driving the initiation and progression of follicular lymphoma. *Nat Genet*. 2014;46(2):176-181. doi:10.1038/ng.2856

427. Roix JJ, McQueen PG, Munson PJ, Parada LA, Misteli T. Spatial proximity of translocation-prone gene loci in human lymphomas. *Nature Genetics*. 2003;34(3):287-291. doi:10.1038/ng1177

428. Salam DSDA, Thit EE, Teoh SH, Tan SY, Peh SC, Cheah S-C. C-MYC, BCL2 and BCL6 Translocation in B-cell Non-Hodgkin Lymphoma Cases. Research Paper. *Journal of Cancer*. 2020;11(1):190-198. doi:10.7150/jca.36954

429. Morin RD, Mendez-Lago M, Mungall AJ, et al. Frequent mutation of histone-modifying genes in non-Hodgkin lymphoma. *Nature*. 2011;476(7360):298-303. doi:10.1038/nature10351

430. Li H, Kaminski MS, Li Y, et al. Mutations in linker histone genes HIST1H1 B, C, D, and E; OCT2 (POU2F2); IRF8; and ARID1A underlying the pathogenesis of follicular lymphoma. *Blood*. 2014;123(10):1487-98. doi:10.1182/blood-2013-05-500264

431. Zhang J, Grubor V, Love CL, et al. Genetic heterogeneity of diffuse large B-cell lymphoma. *Proc Natl Acad Sci U S A*. 2013;110(4):1398-403. doi:10.1073/pnas.1205299110

432. Batmanov K, Wang W, Bjørås M, Delabie J, Wang J. Integrative whole-genome sequence analysis reveals roles of regulatory mutations in BCL6 and BCL2 in follicular lymphoma. *Sci Rep*. 2017;7(1):7040. doi:10.1038/s41598-017-07226-4

433. Correia C, Schneider PA, Dai H, et al. BCL2 mutations are associated with increased risk of transformation and shortened survival in follicular lymphoma. *Blood*. 2015;125(4):658-67. doi:10.1182/blood-2014-04-571786

434. Nadeu F, Royo R, Massoni-Badosa R, et al. Detection of early seeding of Richter transformation in chronic lymphocytic leukemia. *Nature Medicine*. 2022;28(8):1662-1671. doi:10.1038/s41591-022-01927-8

435. Hildebrand JM, Yi Z, Buchta CM, Poovassery J, Stunz LL, Bishop GA. Roles of tumor necrosis factor receptor associated factor 3 (TRAF3) and TRAF5 in immune cell functions. *Immunol Rev*. 2011;244(1):55-74. doi:10.1111/j.1600-065X.2011.01055.x

436. Xie P, Stunz LL, Larison KD, Yang B, Bishop GA. Tumor necrosis factor receptor-associated factor 3 is a critical regulator of B cell homeostasis in secondary lymphoid organs. *Immunity*. 2007;27(2):253-67. doi:10.1016/j.immuni.2007.07.012

437. Moore CR, Edwards SK, Xie P. Targeting TRAF3 Downstream Signaling Pathways in B cell Neoplasms. *J Cancer Sci Ther*. 2015;7(2):67-74. doi:10.4172/1948-5956.1000327

438. Vallabhapurapu S, Matsuzawa A, Zhang W, et al. Nonredundant and complementary functions of TRAF2 and TRAF3 in a ubiquitination cascade that activates NIK-dependent alternative NF-kappaB signaling. *Nat Immunol*. 2008;9(12):1364-70. doi:10.1038/ni.1678

439. Mambetsariev N, Lin WW, Wallis AM, Stunz LL, Bishop GA. TRAF3 deficiency promotes metabolic reprogramming in B cells. *Sci Rep*. 2016;6:35349. doi:10.1038/srep35349

440. Eluard B, Nuan-Aliman S, Faumont N, et al. The alternative RelB NF-κB subunit is a novel critical player in diffuse large B-cell lymphoma. *Blood*. 2022;139(3):384-398. doi:10.1182/blood.2020010039

441. Zarnegar B, Yamazaki S, He JQ, Cheng G. Control of canonical NF-kappaB activation through the NIK-IKK complex pathway. *Proc Natl Acad Sci U S A*. 2008;105(9):3503-8. doi:10.1073/pnas.0707959105

442. Xiao Y, Meierhofer D. Glutathione Metabolism in Renal Cell Carcinoma Progression and Implications for Therapies. *International Journal of Molecular Sciences*. 2019;20(15). doi:10.3390/ijms20153672

443. Gokhale S, Lu W, Zhu S, et al. Elevated Choline Kinase α-Mediated Choline Metabolism Supports the Prolonged Survival of TRAF3-Deficient B Lymphocytes. *J Immunol*. 2020;204(2):459-471. doi:10.4049/jimmunol.1900658

444. White MA, Frigo DE. Regulation of SLC1A4 and SLC1A5 in Prostate Cancer-Response. *Mol Cancer Res*. 2018;16(11):1811-1812. doi:10.1158/1541-7786.MCR-18-0240

445. Nuan-Aliman S, Bordereaux D, Thieblemont C, Baud V. The Alternative RelB NF-kB Subunit Exerts a Critical Survival Function upon Metabolic Stress in Diffuse Large B-Cell Lymphoma-Derived Cells. *Biomedicines*. 2022;10(2)doi:10.3390/biomedicines10020348

446. Lim SK, Peng CC, Low S, et al. Sustained activation of non-canonical NF-κB signalling drives glycolytic reprogramming in doxorubicin-resistant DLBCL. *Leukemia*. 2023;37(2):441-452. doi:10.1038/s41375-022-01769-w

447. Bishop GA. TRAF3 as a powerful and multitalented regulator of lymphocyte functions. *J Leukoc Biol*. 2016;100(5):919-926. doi:10.1189/jlb.2MR0216-063R

448. Kurtova AV, Balakrishnan K, Chen R, et al. Diverse marrow stromal cells protect CLL cells from spontaneous and drug-induced apoptosis: development of a reliable and reproducible system to assess stromal cell adhesion-mediated drug resistance. *Blood*. 2009;114(20):4441-50. doi:10.1182/blood-2009-07-233718

449. Machnicki MM, Górniak P, Pępek M, et al. Predictive significance of selected gene mutations in relapsed and refractory chronic lymphocytic leukemia patients treated with ibrutinib. *European Journal of Haematology*. 2021;106(3):320-326. doi:https://doi.org/10.1111/ejh.13550

450. Ondrisova L, Mraz M. Genetic and Non-Genetic Mechanisms of Resistance to BCR Signaling Inhibitors in B Cell Malignancies. *Front Oncol*. 2020;10:591577. doi:10.3389/fonc.2020.591577

SUPPLEMENTARY APPENDIXES

SUPPLEMENTARY APPENDIX: CHAPTER 1

Chronic Lymphocytic Leukemia patients with chromosome 6q deletion as the sole cytogenetic abnormality display a high frequency of *RPS15* mutations and have a dismal prognosis

Claudia Pérez Carretero[1,2], Teresa González[1,2], Miguel Quijada Álamo[1,2], Gian Matteo Rigolin[3], Adrian Dubuc[4], Ángela Villaverde Ramiro[1,2,] Alberto Rodríguez[1,2], Juan Nicolás Rodríguez[5], Araceli Rubio[6], Julio Dávila[7], Mª Jesús Vidal[8], Isabel González Gascón y Marín[9], José Ángel Hernández Rivas[9], Rocío Benito[1,2], Matt Davids[10], Jeremy Abrasom[11], Antonio Cuneo[3], Paola Dal Cin[4], Ana-Eugenia Rodríguez-Vicente*[1,2], Jesús-María Hernández-Rivas[1,2]

1. University of Salamanca, IBSAL, IBMCC, CSIC, Cancer Research Center, Salamanca, Spain.
2. Department of Hematology, University Hospital of Salamanca, Salamanca, Spain.
3. Hematology Section, St. Anna University Hospital, Ferrara, Italy
4. Department of Pathology, Brigham and Women's Hospital, Boston, MA, USA
5. Department of Hematology. Hospital Juan Ramon Jimenez, Huelva, Spain
6. Department of Hematology, Hospital Miguel Servet, Zaragoza, Spain
7. Department of Hematology, Hospital Nuestra Señora de Sonsoles, Ávila, Spain
8. Department of Hematology, Hospital Universitario, León, Spain.
9. Department of Hematology, Hospital Universitario Infanta Leonor. Universidad Complutense, Madrid, Spain.
10. Dana Farber Cancer Institute, Boston, MA, USA
11. Massachusetts General Hospital, Boston, MA, USA.

AERV and JMHR shared senior authorship

Table of contents of supplementary appendix Chapter 1

SUPPLEMENTARY METHODS

Target deep sequencing

All genomic DNA samples underwent targeted-deep sequencing using an in-house 54 gene custom capture-enrichment panel (682 regions) designed using Agilent SureDesign and previously validated[1,2,3,4]. A SureSelectXT Custom 416.393 kbp target enrichment library containing 8951 oligonucleotide probes against *H.sapiens* hg19 GRCh37 sequence was prepared by Agilent for use with Illumina multiplexed sequencing platforms.

Patient genomic DNA was isolated from blood and prepared for sequencing using the SureSelectQXT Reagent Kit (G9681B) according to the manufacturer's instructions. Targeted DNA sequencing libraries were constructed using SureSelect^{QXT} Reagent Kit (Agilent Technologies, Santa Clara, CA) with 50 ng of genomic DNA. Briefly, tumor DNA was enzymatically fragmented and tagged to generate adapter-tagged libraries. Biotin-labeled probes specific to the targeted regions of interest) via hybridization, and libraries were enriched for regions of interest using streptavidin beads, then amplified, dual-indexed, and pooled for sequencing; quality of the libraries were measured with 4200 TapeStation (Agilent) and quantified using Qubit 3.0 (ThermoFisher Scientific, Waltham, MA).

NGS data analysis

Raw data quality control was performed with FastQC (v0.11.8) and Picard tools (v2.2.4) to collect sequencing metrics. Demultiplexed files (FASTQ) were aligned to the reference genome (GRCh37/hg19 genome), read duplicates were marked with SAMTools (v1.3.1) and post-alignment was performed with GATK (v3.5). Coverage for each region was assessed using BEDTools (v.2.26.0). A minimum quality score of Q30 was required for ensuring high-quality sequencing results. Finally, somatic variant calling, and annotation were performed using an in-house pipeline, based on VarScan (v2.4) and ANNOVAR (v.2017Jul16), respectively.

Median coverage of target regions was 600 reads/base, with at least 100X in 97% of them. To validate variants detected with VAF <5% using the custom panel, samples were conducted to resequencing using different amplicon-based approaches (Illumina Nextera XT/454 Roche) with read depth above 1000X, allowing to report variants down to 2% previously described by our group[3,4,5].

Data was then filtered according to the severity of the consequence, considering variants that lead to an amino acid change in the protein sequence (missense, nonsense, frameshift) and those in the splice site and UTRs. To discard single nucleotide polymorphisms (SNPs), minor allelic frequencies (MAFs) were consulted in several databases (dbSNP, 1000 genomes, ExAC and our in-house database) and only variants with a MAF of <0.01 were selected for further analysis. In addition, variants with a VAF between 40-60% or greater than 90% were manually reviewed prioritizing variants described in *in silico* tools (Polymorphism Phenotyping v2 (PolyPhen-2), Sorting Intolerant From Tolerant (SIFT) and ClinVar) as deleterious, damaging, pathogenic or likely pathogenic.

Variants were annotated using automated pipelines and potential pathogenic variants were identified. Further validation was performed by manual review using the Integrative Genomics Viewer (IGV)[6]. Variants were classified, and the pathogenicity analyzed using ClinVar and Varsome web tool[7].

REFERENCES

1. Hernández-Sánchez M, Rodríguez-Vicente AE, González-Gascón Y Marín I, Quijada-Álamo M, Hernández-Sánchez JM, Martín-Izquierdo M, et al. DNA damage response-related alterations define the genetic background of patients with chronic lymphocytic leukemia and chromosomal gains. Exp Hematol. 2019. 72:9-13.

2. Quijada-Álamo M, Hernández-Sánchez M, Alonso-Pérez V, Rodríguez-Vicente AE, García-Tuñón I, Martín-Izquierdo M, et al. CRISPR/Cas9-generated models uncover therapeutic vulnerabilities of del(11q) CLL cells to dual BCR and PARP inhibition. Leukemia. 2020. 34(6):1599-1612.

3. Pérez-Carretero C, Hernández-Sánchez M, González T, Quijada-Álamo M, Martín-Izquierdo M, Hernández-Sánchez JM, et al. Chronic lymphocytic leukemia patients with IGH translocations are characterized by a distinct genetic landscape with prognostic implications. Int J Cancer. 2020;147(10):2780-92.

4. Quijada-Álamo M, Pérez-Carretero C, Hernández-Sánchez M, Rodríguez-Vicente AE, Herrero AB, Hernández-Sánchez JM, et al. Dissecting the role of TP53 alterations in del(11q) chronic lymphocytic leukemia. Clin Transl Med. 2021;11(2):e304.

5. Quijada-Álamo M, Hernández-Sánchez M, Robledo C, Hernández-Sánchez JM, Benito R, Montaño A, et al. Next-generation sequencing and FISH studies reveal the appearance of gene mutations and chromosomal abnormalities in hematopoietic progenitors in chronic lymphocytic leukemia. J Hematol Oncol. 2017;10(1):83.

6. Robinson JT, Thorvaldsdóttir H, Wenger AM, Zehir A, Mesirov JP. Variant Review with the Integrative Genomics Viewer. Cancer Res. 2017;77(21):e31-e4.

7. Kopanos C, Tsiolkas V, Kouris A, Chapple CE, Albarca Aguilera M, Meyer R, et al. VarSome: the human genomic variant search engine. Bioinformatics. 2019;35(11):1978-80.

SUPPLEMENTARY TABLES

Supplementary Table S1. Clinical and biological features of CLL patients with 6q deletion (N=39) and the control group (n=317).

Characteristic	Del(6q) CLLs (n=39)	Control group (n=317)	*p*
Age of diagnosis, median	**61**	**72**	**<0,001**
Male, %	53,8(21/39)	65,6(208/317)	0,194
Leucocytes (10^9/L), median (range)	18,7 (5,6-238)	18,9 (7,3-369)	0,752
Lymphocytes (10^9/L), median (range)	15,1 (2,4-101)	14,3 (6,6-355)	0,908
Platelets (10^9/L), median (range)	192 (55-442)	177 (23-456)	0,231
Binet stage B/C, %	37,8 (14/37)	26,8(82/305)	0,177
Hepatomegaly, %	2,7(1/37)	4,9(14/284)	1
Splenomegaly, %	16,2(6/37)	19,2(55/287)	0,824
Adenopaties, %	57,14 (20/35)	42,55 (120/282)	0,108
ZAP70+, %	**63,6 (14/22)**	**15,9(48/301)**	**<0,001**
CD38+, %	**51,7(15/29)**	**28,3(58/205)**	**0,017**
High β2-M, %	45,5(15/33)	41,3(104/252)	0,709
High LDH, %	11,4(4/35)	19(53/278)	0,355
IGHV-unmutated, %	**75,8(22/29)**	**45,7 (123/269)**	**0,003**
del(13q), %	**23 (9/39)**	**57,4(181/315)**	**0,001**
Tri12, %	8 (3/39)	19,1(60/314)	0,165
del(11q), %	18(7/39)	16,8(53/315)	0,814
del(17p), %	21(8/39)	9,2(29/315)	0,063
Treatment, %	**82(32/39)**	**54,3(170/313)**	**0,001**
Death, %	28,2(11/39)	27,4(87/317)	0,694

SUPPLEMENTARY FIGURES

A)

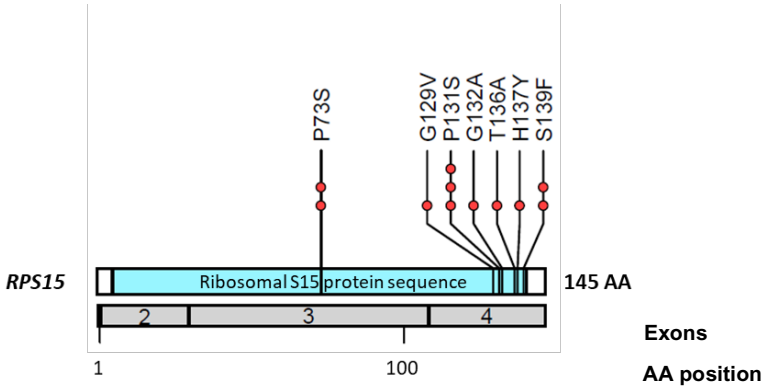

B)

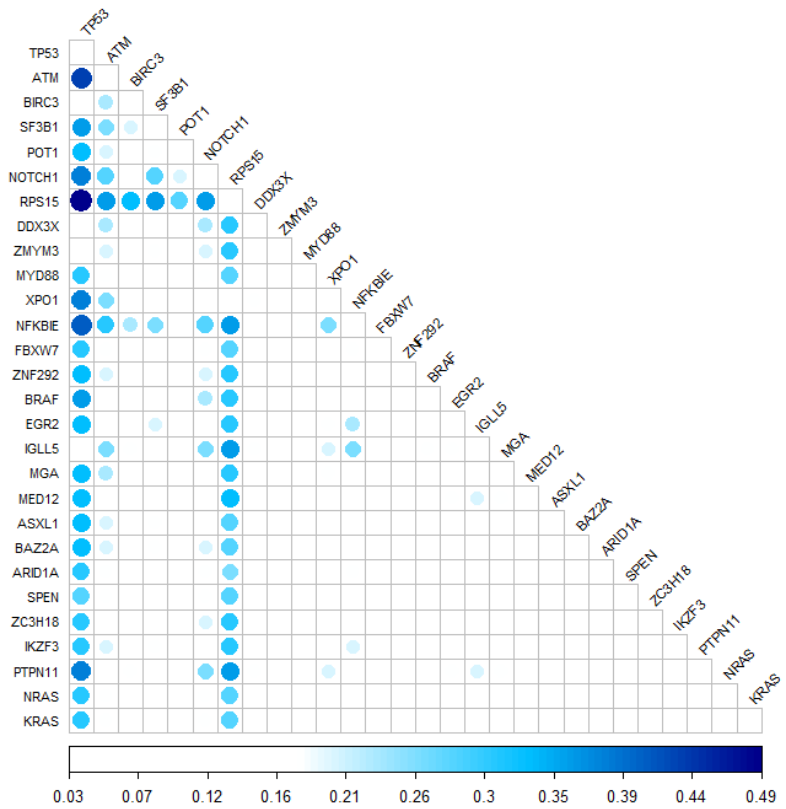

Supplementary Figure S1. *RPS15* mutations in CLL patients with del(6q). A) Diagram of *RPS15* mutations representing the position of the mutations in the aminoacid (AA) sequence and the AA change induced. Ref transcript: NM_001018. B) Mutual-exclusivity diagram of mutated genes in CLL patients with del(6q). Color and size of the circles are plotted in the graph based on the proportion of events involved in the analysis (from white (3%) to dark blue (50%), percentage related to the whole cohort, n=39) and level of significance per interaction, respectively.

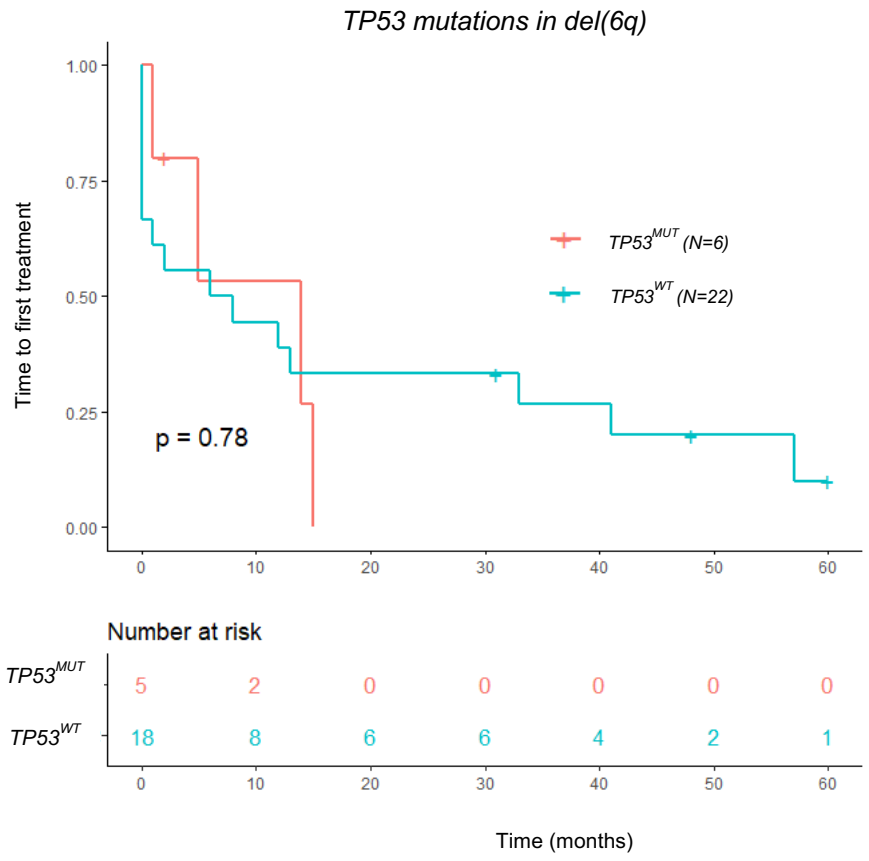

Supplementary Figure S2. Clinical impact of *TP53* mutations on the time to first treatment of del(6q) CLL patients.

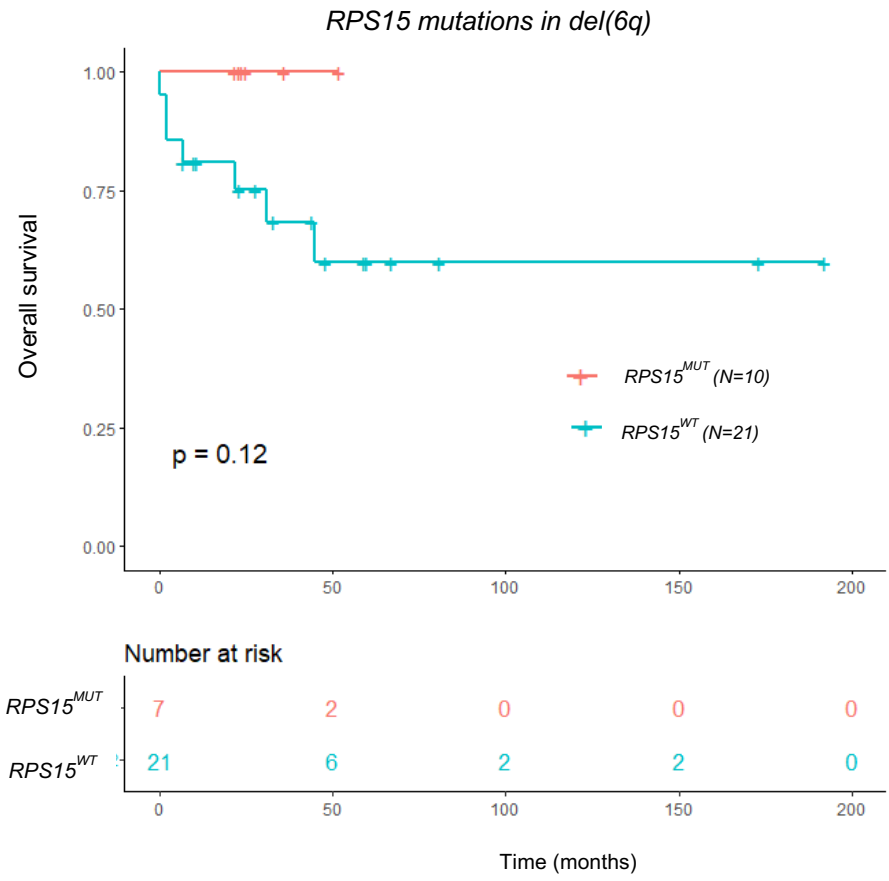

Supplementary Figure S3. Clinical impact of *RPS15* mutations on the overall survival of del(6q) CLL patients.

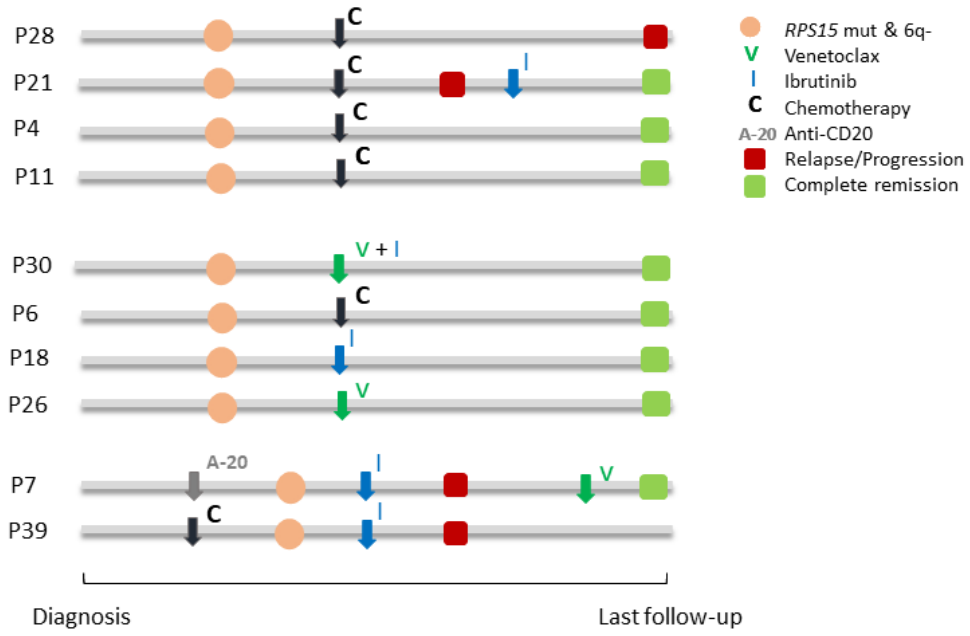

Supplementary Figure S4. Diagram follow-up of CLL patients with 6q deletion and *RPS15* mutations. The presence of alterations, treatment indication and response to therapy from the date of diagnosis to the last follow-up are shown in the graph. *RPS15* mutations and del(6q) are represented with circles, treatment indication with arrows and response to therapy with squares.

SUPPLEMENTARY APPENDIX: CHAPTER 2

Received: 16 January 2020 | Revised: 19 June 2020 | Accepted: 7 July 2020
DOI: 10.1002/ijc.33235

CANCER GENETICS AND EPIGENETICS

IJC International Journal of Cancer

Chronic lymphocytic leukemia patients with *IGH* translocations are characterized by a distinct genetic landscape with prognostic implications

Claudia Pérez-Carretero[1,2] | María Hernández-Sánchez[1,2,3] | Teresa González[1,2] | Miguel Quijada-Álamo[1,2] | Marta Martín-Izquierdo[1,2] | Jesús-María Hernández-Sánchez[1,2] | María-Jesús Vidal[4] | Alfonso García de Coca[5] | Carlos Aguilar[6] | Manuel Vargas-Pabón[7] | Sara Alonso[8] | Magdalena Sierra[9] | Araceli Rubio-Martínez[10] | Julio Dávila[11] | José R. Díaz-Valdés[12] | José-Antonio Queizán[12] | José-Ángel Hernández-Rivas[13] | Rocío Benito[1,2] | Ana E. Rodríguez-Vicente[1,2] | Jesús-María Hernández-Rivas[1,2]

[1]Universidad de Salamanca, IBSAL, Centro de Investigación del Cáncer, IBMCC-CSIC, Salamanca, Spain
[2]Servicio de Hematología, Hospital Universitario de Salamanca, Salamanca, Spain
[3]Department of Medical Oncology, Dana Farber Cancer Institute, Boston, Massachusetts
[4]Servicio de Hematología, Hospital Universitario, León, Spain
[5]Servicio de Hematología, Hospital Clínico, Valladolid, Spain
[6]Servicio de Hematología, Complejo Hospitalario de Soria, Soria, Spain
[7]Servicio de Hematología, Hospital Jarrio, Asturias, Spain
[8]Servicio de Hematología, Hospital Universitario Central de Asturias, Oviedo, Spain
[9]Servicio de Hematología, Hospital Virgen de la Concha, Zamora, Spain
[10]Servicio de Hematología, Hospital Miguel Servet, Zaragoza, Spain
[11]Servicio de Hematología, Hospital Nuestra Señora de Sonsoles, Ávila, Spain
[12]Servicio de Hematología, Hospital General de Segovia, Segovia, Spain
[13]Servicio de Hematología, Hospital Universitario Infanta Leonor, Universidad Complutense, Madrid, Spain

Table of contents supplementary appendix Chapter 2

Supplementary Figure S4

Kaplan-Meier analysis in CLL patients included in the study according to the presence of FISH aberrations.

Supplementary Figure S5

Kaplan-Meier analysis of TFT and OS in IGH*R*-CLL patients according to the *IGH* translocation (*IGH/BCL2 vs*. non-*IGH/BCL2*).

Supplementary Figure S6

Kaplan-Meier analysis of TFT in IGHR-CLL patients according to *BRAF* and *TP53* mutation status.

Supplementary Figure S7

Kaplan-Meier analysis of TFT in non-IGH*R* CLL patients according to the presence of mutations in *NOTCH1, SF3B1, TP53, BIRC3* and *BRAF*.

SUPPLEMENTARY METHODS

Patients' exclusion and risk classification criteria

Patients with clinical features, histopathology or immunophenotype inconsistent with CLL or Matutes Score >3 were excluded[1]. As distinction of *IGH/CCND1* translocation-associated CLL and mantle cell lymphoma (MCL) leukemic forms might not be unequivocal, we also excluded all *IGH/CCND1* positive cases.

Within control group, the cytogenetic risk classification of patients that carried more than one chromosomal alteration was determined by the worst risk abnormality, according to the Döhner hierarchy[2]. For example, patients carrying 13q- and 11q- were categorized in the 11q group, while patients with 11q- and 17p- were characterized as 17p-. Patients with *IGH* rearrangements/translocations were included in the CLL-IGHR group, irrespective of the presence of additional abnormalities.

Cell isolation and DNA extraction

B lymphocytes (CD19-positive cells) extracted from bone marrow or peripheral blood samples of CLL patients were positively selected using magnetically activated cell sorting (MACS) CD19 MicroBeads (Miltenyi Biotec, Bergisch Gladbach, Germany) and frozen in RLT plus at 80°C. DNA was isolated using a commercial kit (Qiagen, Valencia, CA, USA). To assess

DNA quantity and quality we used the Qubit dsDNA HS Assay kit (Invitrogen, Life Technologies, Carlsbad, CA, USA), and the TapeStation 4200 system (Agilent Technologies, Santa Clara, CA, USA). The required concentration and quality to ensure optimal sequencing were 25 ng/µl and DIN>6 respectively (as specified in the Illumina/Agilent protocols).

Target deep sequencing

All genomic DNA samples underwent targeted-deep sequencing using an in-house 54 gene custom capture-enrichment panel (682 regions) designed using Agilent SureDesign and previously validated[3,4] (**Supplementary Table S2**). A SureSelectXT Custom 416.393 kbp target enrichment library containing 8951 oligonucleotide probes against *H.sapiens* hg19 GRCh37 sequence was prepared by Agilent for use with Illumina multiplexed sequencing platforms.

Patient genomic DNA was isolated from blood and prepared for sequencing using the SureSelectQXT Reagent Kit (G9681B) according to the manufacturer's instructions. Targeted DNA sequencing libraries were constructed using SureSelect^{QXT} Reagent Kit (Agilent Technologies, Santa Clara, CA) with 50 ng of genomic DNA. Briefly, tumor DNA was enzymatically fragmented and tagged to generate adapter-tagged libraries. Biotin-labeled probes specific to the targeted regions of interest) via hybridization, and libraries were enriched for regions of interest using streptavidin beads, then amplified, dual-indexed, and pooled for sequencing; quality of the libraries were measured with 2200 TapeStation (Agilent) and quantified using Qubit 2.0 (ThermoFisher Scientific, Waltham, MA).

PCR amplification-based methods were applied for validating mutations detected at low frequencies (**Supplementary Table S7**). Validation assays using the 454 Titanium Amplicon system (Roche Applied Science) were carried out for a previous study of our group[5]. For the new validations, PCR libraries were prepared using Nextera XT DNA Sample Preparation Kit (Illumina) and indexed using Nextera XT Index Kit (Illumina). The indexed libraries were then purified using Agencourt AMPure XP beads, quality checked on a Bioanalyzer DNA 1000 chip and then quantified by fluorometry using Qubit HS dsDNA assay kit. The libraries were then diluted to an equimolar concentration of 4 nM before pooling for sequencing. A final confirmation of the pooled library concentration was done by a fluorometric measurement before denaturing and sequencing. The pooled genomic libraries were then sequenced using the Illumina NextSeq or MiSeq platform (Ilumina). Resequencing was also performed in the CD19- cell fraction of patients carrying *BCL2* mutations, to further validate they were somatic.

REFERENCES

1. Moreau EJ, Matutes E, A'Hern RP, Morilla AM, Morilla RM, Owusu-Ankomah KA, et al. Improvement of the chronic lymphocytic leukemia scoring system with the monoclonal antibody SN8 (CD79b). Am J Clin Pathol. 1997;108(4):378-82.

2. Döhner H, Stilgenbauer S, Benner A, Leupolt E, Kröber A, Bullinger L, et al. Genomic aberrations and survival in chronic lymphocytic leukemia. N Engl J Med. 2000;343(26):1910-6.

3. Hernández-Sánchez M, Rodríguez-Vicente AE, González-Gascón Y Marín I, Quijada-Álamo M, Hernández-Sánchez JM, Martín-Izquierdo M, et al. DNA damage response-related alterations define the genetic background of patients with chronic lymphocytic leukemia and chromosomal gains. Exp Hematol. 2019. 72:9-13.

4. Quijada-Álamo M, Hernández-Sánchez M, Alonso-Pérez V, Rodríguez-Vicente AE, García-Tuñón I, Martín-Izquierdo M, et al. CRISPR/Cas9-generated models uncover therapeutic vulnerabilities of del(11q) CLL cells to dual BCR and PARP inhibition. Leukemia. 2020. 34(6):1599-1612

5. Quijada-Álamo M, Hernández-Sánchez M, Robledo C, Hernández-Sánchez JM, Benito R, Montaño A, et al. Next-generation sequencing and FISH studies reveal the appearance of gene mutations and chromosomal abnormalities in hematopoietic progenitors in chronic lymphocytic leukemia. J Hematol Oncol. 2017;10(1):83.

SUPPLEMENTARY TABLES

Supplementary Table S1. Clinical and biological characteristics of CLL patients depending on the presence of *IGH* rearrangements (N=233).

Characteristic	*IGH*-translocation (N=46)	no *IGH*-translocation (N=187)	*P*	*Q*
Median age at diagnosis, years (range)	69 (43-89)	67 (28-91)	0.310[b]	0.691
Gender Male, %	63	65.2	0.780[c]	0.78
Median time from diagnosis to FISH, months (range)	1 (0-117)	0 (0-221)	0.579[b]	0.691
Binet B or C, %	38.6	24.6	0.060[c]	0.135
Median WBC[a] count, $\cdot 10^9$/L (range)	17.6 (2.3-196)	19 (5.7-964)	0.691[b]	0.691
Median lymphocytes count, $\cdot 10^9$/L (range)	11.6 (0.6-186)	14.4 (1.1-960)	0.564[b]	0.691
Median platelet count, $\cdot 10^9$/L (range)	172 (55-295)	177 (2-587)	0.451[b]	0.691
Median hemoglobin level, g/dL (range)	14.1 (6.6-16.5)	14.2 (4.4-18.9)	0.618[b]	0.691
High β2-microglobulin level, %	67.4	36.3	**0.0002[c]**	**0.002**
High lactate dehydrogenase level, %	27.3	17.7	0.150[c]	0.25
Hepatomegaly, %	7.1	5.4	0.668[c]	0.771
Splenomegaly, %	15.9	17.9	0.751[c]	0.78
B Symptoms, %	11.1	8.9	0.655[c]	0.771
Richter transformation	4.3	1.6	0.257[c]	0.385
IGHV-Unmutated*, %*	60.6	40	**0.028[c]**	**0.084**
13q deletion, %	26.1	62	**<0.0001[c]**	**0.0002**
trisomy 12, %	34.8	13.9	**0.001[c]**	**0.005**
11q deletion, %	4.3	14.4	0.063[c]	0.135
17p deletion, %	6.5	2.1	0.119[c]	0.223
TP53 disruption (deletion/mutation),%	8.7	11.2	0.619[c]	0.771
Need for treatment	67.4	45.5	0.008[c]	**0.03**
Median follow-up, months (range)	57 (1-157)	60 (0-264)	0.344[b]	0.691

[a] WBC: white blood cells, [b]Mann Whitney U test, [c]$\chi 2$ test

Supplementary Table S2. List of regions and mean coverage of genes included in the custom-designed panel of NGS**.**

Gene	Transcript	Regions	Mean coverage (reads/base)	Gene	Transcript	Regions	Mean coverage (reads/base)
ARID1A	ENST00000324856	Exons 1-20	808	***KLHL6***	ENST00000341319	Exons 1-7	707
ASXL1	ENST00000375687	Exons 1-13	691	***KRAS***	ENST00000311936	Exons 2-5	522
ATM	ENST00000278616	Exons 2-63	443	***MAP2K1***	ENST00000307102	Exons 1-11	553
ATRX	ENST00000373344	Exons 1-35	274	***MED12***	ENST00000374080	Exons 1-4	356
BAX	ENST00000345358	Exon 2-6	815	***MGA***	ENST00000570161	Exons 2-23	680
BAZ2A	ENST00000551812	Exons 2-28	829	***MYD88***	ENST00000396334	Exons 2-5	781
BCL2	ENST00000398117	Exons 2-3 and 5'UTR	629	***NFKBIE***	ENST00000275015	Exons 1-2	969
BCOR	ENST00000378444	Exons 2-15	448	***NOTCH1***	ENST00000277541	Exon 34 and 3'UTR	1183
BIRC3	ENST00000263464	Exons 2-9	479	***NRAS***	ENST00000369535	Exons 2-3	601
BRAF	ENST00000288602	Exons 11-16	503	***NXF1***	ENST00000294172	Exons 3-21	644
BTK	ENST00000308731	Exons 2-19	418	***PAX5***	ENST00000358127	enhancer	783
CARD11	ENST00000396946	Exons 3-17	801	***PCDH10***	ENST00000264360	Exons 1-5	550
CCND2	ENST00000261254	Exons 1-5	814	***PIK3CD***	ENST00000377346	Exons 3-24	848
CD19	ENST00000324662	Exons 1-6	856	***PLCG2***	ENST00000564138	Exons 2-33	618
CDC73	ENST00000367435	Exons 1-16	440	***POT1***	ENST00000357628	Exons 5-19	405
CHD2	ENST00000394196	Exons 2-39	475	***PTPN11***	ENST00000351677	Exonso 2-15	641
DDX3X	ENST00000399959	Exons 1-16	356	***RPS15***	ENST00000593052	Exons 2-4	676
EGR2	ENST00000242480	Exons 1-2	1001	***SAMHD1***	ENST00000262878	Exons 1-16	504
FAM50A	ENST00000393600	Exons 2-12	528	***SETD2***	ENST00000409792	Exons 1-21	506
FAT1	ENST00000441802	Exons 2-27	765	***SF3B1***	ENST00000335508	Exons 14-16	519
FBXW7	ENST00000281708	Exons 7-12	710	***SORCS2***	ENST00000507866	Exons 1-27	894
FUBP1	ENST00000370768	Exons 1-19	451	***TP53***	ENST00000269305	Exons 4-10	650
HIST1H1B	ENST00000331442	Exon 1	963	***TRAF3***	ENST00000392745	Exons 1-12	610
HIST1H1E	ENST00000304218	Exon 1	669	***XPO1***	ENST00000401558	Exons 15-16	540
IGLL5	ENST00000526893	Exons 1-3, 5'UTR	553	***ZC3H18***	ENST00000301011	Exons 2-18	770
IKZF3	ENST00000346872	Exon 5	696	***ZMYM3***	ENST00000373998	Exons 2-25	499
IRF4	ENST00000380956	Exons 2-9	691	***ZNF292***	ENST00000339907	Exons 1-8	395

Supplementary Table S3. Distribution of mutations according to the presence of *IGH* rearrangements detected by FISH in untreated CLL patients (N=233).

Gene	CLLs with *IGH* rearrangement (N=46)		CLLs without *IGH* rearrangement (N=187)		*P*	*Q*
	Mutated cases (N)	Frequency (%)	Mutated cases (N)	Frequency (%)		
NOTCH1	14	30.4	31	16.6	**0.033***	0.154
IGLL5	8	17.4	27	14.4	0.616	0.894
SF3B1	6	13.0	19	10.2	0.571	0.894
POT1	6	13.0	14	7.5	0.228	0.532
TP53	4	8.7	19	10.2	0.765	0.913
BCL2	4	8.7	1	0.5	**0.006***	**0.048*****
FBXW7	4	8.7	2	1.1	**0.015***	**0.060****
ZMYM3	4	8.7	4	2.1	**0.029***	0.154
MGA	4	8.7	4	2.1	**0.029***	0.154
BRAF	3	6.5	2	1.1	0.054	0.108
EGR2	3	6.5	2	1.1	0.054	0.108
RPS15	3	6.5	13	7.0	0.918	0.972
NFKBIE	3	6.5	9	4.8	0.639	0.894
HIST1H1E	2	4.3	1	0.5	0.100	0.160
BIRC3	2	4.3	10	5.3	0.783	0.913
ATM	2	4.3	19	10.2	0.217	0.532
FUBP1	2	4.3	3	1.6	0.257	0.293
MAP2K1	2	4.3	4	2.1	0.338	0.338
IRF4	2	4.3	3	1.6	0.257	0.293
ZNF292	2	4.3	5	2.7	0.551	0.894
MYD88	1	2.2	4	2.1	0.972	0.972
CHD2	1	2.2	13	7.0	0.222	0.532

*P<0.05
** Q<0.1
*** Q<0.05

Supplementary Table S4. Frequencies of recurrent gene mutations according to the presence of additional cytogenetic aberrations in untreated IGH*R-CLLs.*

Gene	t(IGH)+ 13q- (N=8)	Rest of t(IGH) (N=38)			t(IGH)+ 11q/17p- (N=5)	Rest of t(IGH) (N=41)			t(IGH) + tri12 (N=15)	Rest of t(IGH) (N=31)			t(IGH) only (N=18)	Rest of t(IGH) (N=28)		
	%	%	*P*	*Q*	%	%	*P*	*Q*	%	%	*P*	*Q*	%	%	*P*	*Q*
NOTCH1	12.5	34.2	0.403	1.000	40.0	29.3	0.633	1.000	33.3	29.0	1.000	1.000	33.3	28.6	0.753	0.927
SF3B1	25.0	10.5	0.277	1.000	0.0	14.6	1.000	1.000	6.7	16.1	0.647	1.000	16.7	10.7	0.666	0.888
IGLL5	25.0	13.2	0.613	1.000	0.0	17.1	0.569	1.000	6.7	19.4	0.243	0.768	27.8	10.7	0.232	0.864
POT1	12.5	13.2	1.000	1.000	20.0	12.2	0.520	1.000	20.0	9.7	0.375	0.857	5.6	17.8	0.380	0.888
TP53	0.0	10.5	1.000	1.000	**60.0**	2.4	**0.003**	**0.048***	6.7	9.7	1.000	1.000	0.0	14.3	0.144	0.864
BCL2	0.0	10.5	1.000	1.000	0.0	9.8	1.000	1.000	13.3	6.5	0.587	1.000	11.1	7.1	0.639	0.888
ZMYM3	12.5	7.9	0.548	1.000	0.0	9.8	1.000	1.000	6.7	9.7	1.000	1.000	11.1	7.1	0.639	0.888
MGA	25.0	5.3	0.134	1.000	0.0	9.8	1.000	1.000	0.0	12.9	0.288	0.768	11.1	7.1	0.639	0.888
FBXW7	0.0	10.5	1.000	1.000	20.0	7.3	0.379	1.000	13.3	6.5	0.587	1.000	5.6	10.7	1.000	1.000
BRAF	0.0	7.9	1.000	1.000	0.0	7.3	1.000	1.000	13.3	3.2	0.244	0.768	5.6	7.1	1.000	1.000
EGR2	0.0	7.9	1.000	1.000	0.0	7.3	1.000	1.000	20.0	0.0	0.030	0.480	0.0	10.7	0.270	0.864
RPS15	12.5	5.3	0.444	1.000	0.0	7.3	1.000	1.000	13.3	3.2	0.244	0.768	0.0	10.7	0.270	0.864
HIST1H1E	0.0	5.3	1.000	1.000	0.0	4.9	1.000	1.000	13.3	0.0	0.101	0.768	0.0	7.1	0.513	0.888
BIRC3	12.5	2.6	0.321	1.000	20.0	2.4	0.208	1.000	0.0	6.5	1.000	1.000	0.0	7.1	0.513	0.888
ATM	0.0	5.3	1.000	1.000	0.0	4.9	1.000	1.000	6.7	3.2	1.000	1.000	5.6	3.6	1.000	1.000
FUBP1	0.0	5.3	1.000	1.000	0.0	4.9	1.000	1.000	0.0	6.5	1.000	1.000	11.1	0.0	0.148	0.864

*Q<0.05

Supplementary Table S7. List of mutations detected at low frequency and validated by amplicon-based NGS systems (Illumina Nextera XT/454 Roche).

Group	ID Patient	Gene	Chromosome	Start	End	Reference	Altered	Frequency (Capture-NGS)	Frequency (Amplicon-NGS)	Amplicon-based NGS system	Previously reported in CLL[7,8,31]
Control	94	*ATM*	chr11	108186590	108186590	A	G	4.35	4.85	Illumina Nextera XT	
Control	84	*ATM*	chr11	108186742	108186742	C	T	4.47	4.5	Illumina Nextera XT	YES
Control	53	*ATM*	chr11	108201020	108201020	T	-	4.7	4.8	Illumina Nextera XT	
Control	53	*ATM*	chr11	108206581	108206581	G	A	5.26	4.8	Illumina Nextera XT	YES
Control	49	*ATM*	chr11	108141874	108141874	G	A	6	3	Illumina Nextera XT	YES
Control	94	*ATM*	chr11	108142079	108142079	-	T	6.03	5.5	454 Roche	YES
Control	91	*ATM*	chr11	108098515	108098515	A	T	6.92	13	454 Roche	YES
Control	46	*BIRC3*	chr11	102207657	102207657	C	-	4.92	5.15	Illumina Nextera XT	YES
Control	24	*BIRC3*	chr11	102207657	102207657	C	-	5.17	4.98	Illumina Nextera XT	YES
Control	3	*NFKBIE*	chr6	44232739	44232742	GTAA	-	2.44	1.9	Illumina Nextera XT	YES
Control	7	*NFKBIE*	chr6	44232739	44232742	GTAA	-	2.45	2.4	Illumina Nextera XT	YES
Control	101	*NOTCH1*	chr9	139390649	139390650	AG	-	2.64	3	454 Roche	YES
Control	58	*NOTCH1*	chr9	139390649	139390650	AG	-	2.83	2.9	454 Roche	YES
Control	44	*SF3B1*	chr2	198267360	198267360	T	A	3.27	4.55	Illumina Nextera XT	YES
Control	87	*SF3B1*	chr2	198266769	198266769	G	C	3.84	4.76	Illumina Nextera XT	
Control	24	*SF3B1*	chr2	198266611	198266611	C	T	2.7	4.42	Illumina Nextera XT	YES
Control	100	*SF3B1*	chr2	198266834	198266834	T	C	3.97	3	454 Roche	YES
Control	109	*SF3B1*	chr2	198267361	198267361	T	C	4.61	8.93	Illumina Nextera XT	YES
Control	33	*TP53*	chr17	7577569	7577569	A	T	2.03	2.01	Illumina Nextera XT	
Control	58	*TP53*	chr17	7577570	7577570	C	A	3.85	5.58	Illumina Nextera XT	
Control	33	*TP53*	chr17	7578406	7578406	C	T	3.86	5	Illumina Nextera XT	YES
IGHR	12	*BIRC3*	chr11	102207676	102207679	AAGA	-	3.08	4.9	Illumina Nextera XT	
IGHR	26	*FBXW7*	chr4	153249385	153249385	G	A	4	3.21	Illumina Nextera XT	YES
IGHR	34	*KRAS*	chr12	25378647	25378647	T	A	4.23	7.92	Illumina Nextera XT	YES
IGHR	34	*MYD88*	chr3	38182641	38182641	T	C	3.29	6.09	Illumina Nextera XT	YES
IGHR	22	*NFKBIE*	chr6	44232739	44232742	GTAA	-	2.4	1.47	Illumina Nextera XT	YES
IGHR	13	*NFKBIE*	chr6	44232739	44232742	GTAA	-	4.41	2.28	Illumina Nextera XT	YES
IGHR	29	*NOTCH1*	chr9	139390649	139390650	AG	-	2.75	5.72	Illumina Nextera XT	YES
IGHR	20	*NOTCH1*	chr9	139390649	139390650	AG	-	3.47	8.6	Illumina Nextera XT	YES
IGHR	20	*POT1*	chr7	124532398	124532398	G	A	4.52	4.53	Illumina Nextera XT	YES
IGHR	41	*SETD2*	chr3	47164048	47164048	-	C	3.12	5	Illumina Nextera XT	
IGHR	13	*SF3B1*	chr2	198266611	198266611	C	T	4.92	4.98	Illumina Nextera XT	YES
IGHR	13	*SF3B2*	chr3	198266834	198266834	T	C	5.85	6.04	Illumina Nextera XT	YES

Supplementary Table S8. Frequencies of the most recurrently mutated genes according to the *IGH* translocation in untreated patients: *IGH/BCL2* vs non-*IGH/BCL2*.

Gene	*IGH/BCL2* (N=13), %	*non-IGH/BCL2* (N=33), %	*P*	*Q*
NOTCH1	15.38	36.36	0.286	0.487
SF3B1	0.00	18.18	0.163	0.487
IGLL5	23.08	12.12	0.196	0.487
POT1	0.00	18.18	0.163	0.487
TP53	0.00	12.12	0.313	0.487
MGA	0.00	12.12	0.313	0.487
FBXW7	0.00	12.12	0.313	0.487
BRAF	0.00	9.09	0.548	0.590
EGR2	0.00	9.09	0.548	0.590
BCL2	23.08	3.03	**0.062**	0.487
ZMYM3	7.69	9.09	1.000	1.000
RPS15	0.00	9.09	0.548	0.590
HIST1H1E	15.38	0.00	**0.075**	0.487
ZNF292	7.69	3.03	0.490	0.590

SUPPLEMENTARY FIGURES

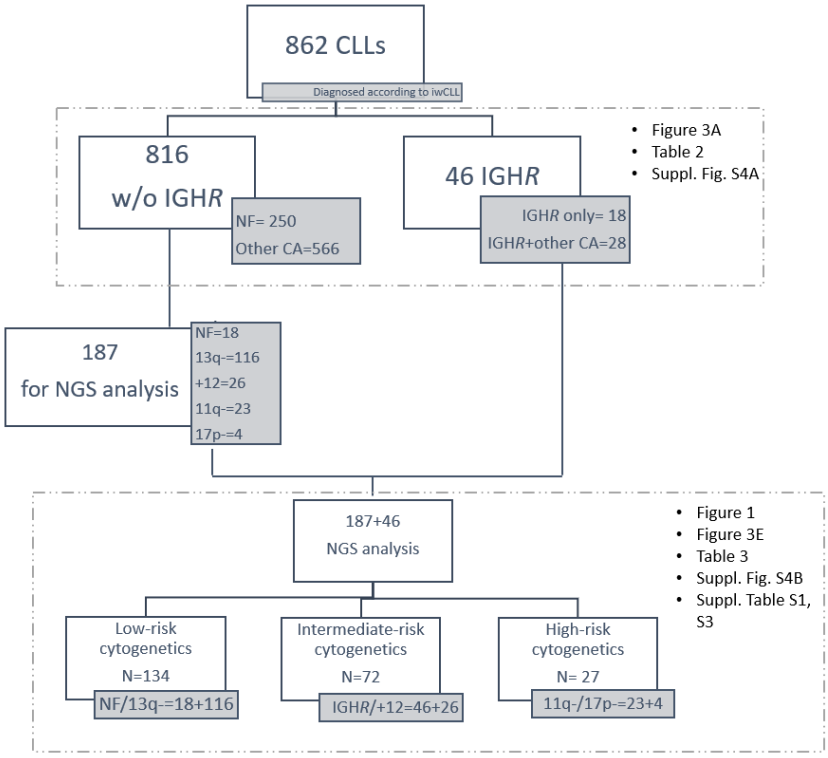

Supplementary Figure S1. Consort diagram of patients included in the study for outcome and mutational analyses. IGH*R*: *IGH* rearrangement/translocation, CA: cytogenetic abnormalities, NF: normal FISH, 13q-: 13q deletion, +12: trisomy 12, 11q-: 11q deletion, 17p-: 17p deletion.

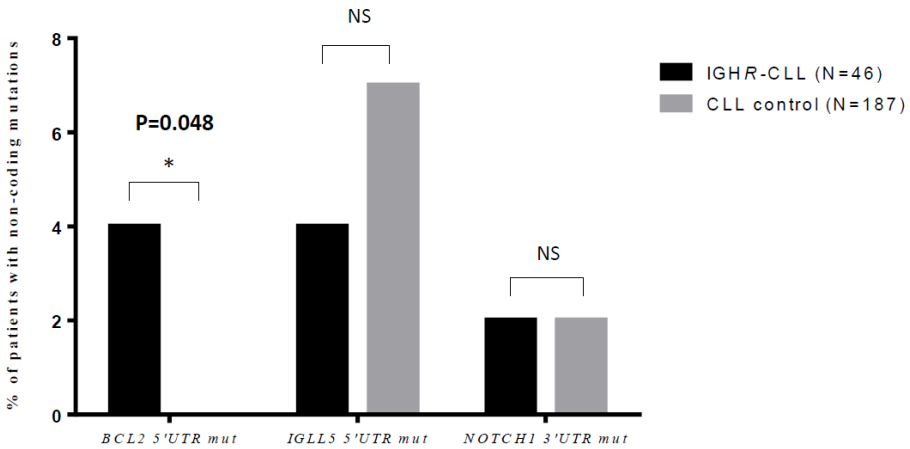

Supplementary Figure S2. Frequencies of *BCL2, IGLL5* and *NOTCH1* UTR mutations according to the presence of an *IGH* rearrangement in 233 CLL patients.

A)

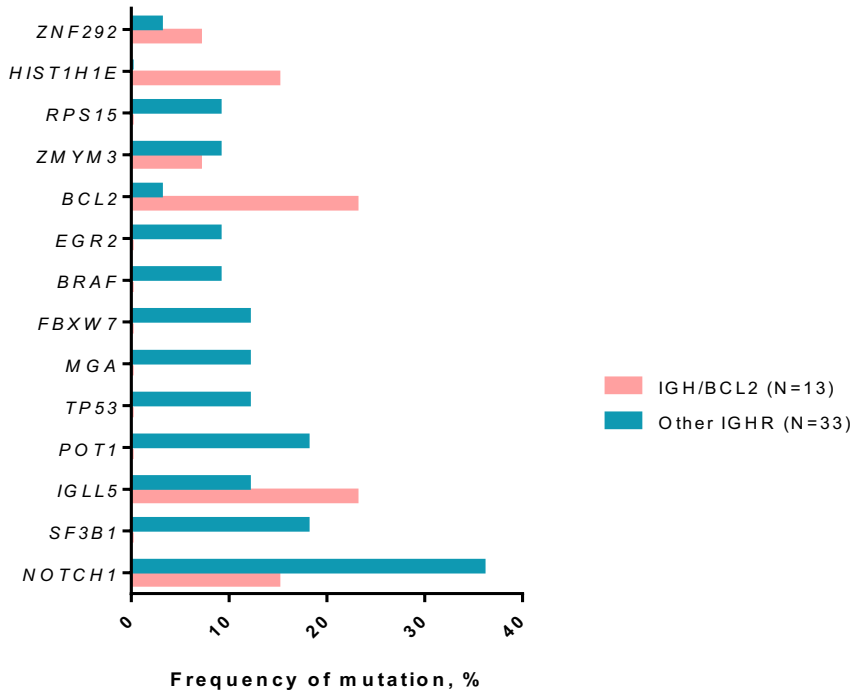

B)

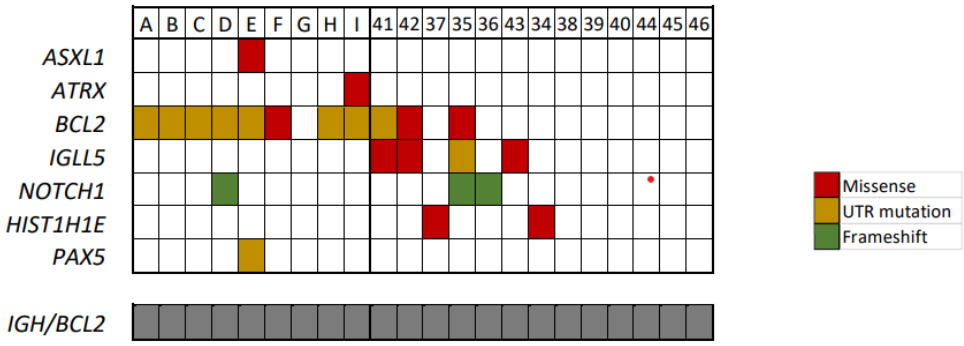

Supplementary Figure S3. Mutational landscape of *IGH/BCL2* rearrangements. A) Mutational frequencies in *IGH/BCL2* cases with respect to the rest of rearrangements (p/q values; see Supplementary Table S8). B) Mutational profile of *IGH/BCL2* rearrangements. Each column represents a patient; numbers referes to the patient ID in our study while alphabet letters corresponds to the cases reported in Puente el *al.*[8]; each row corresponds to a genetic alteration.Mutations shown in Puente et al. samples are restricted to the gene regions included in our panel (Supplementary Table S2).

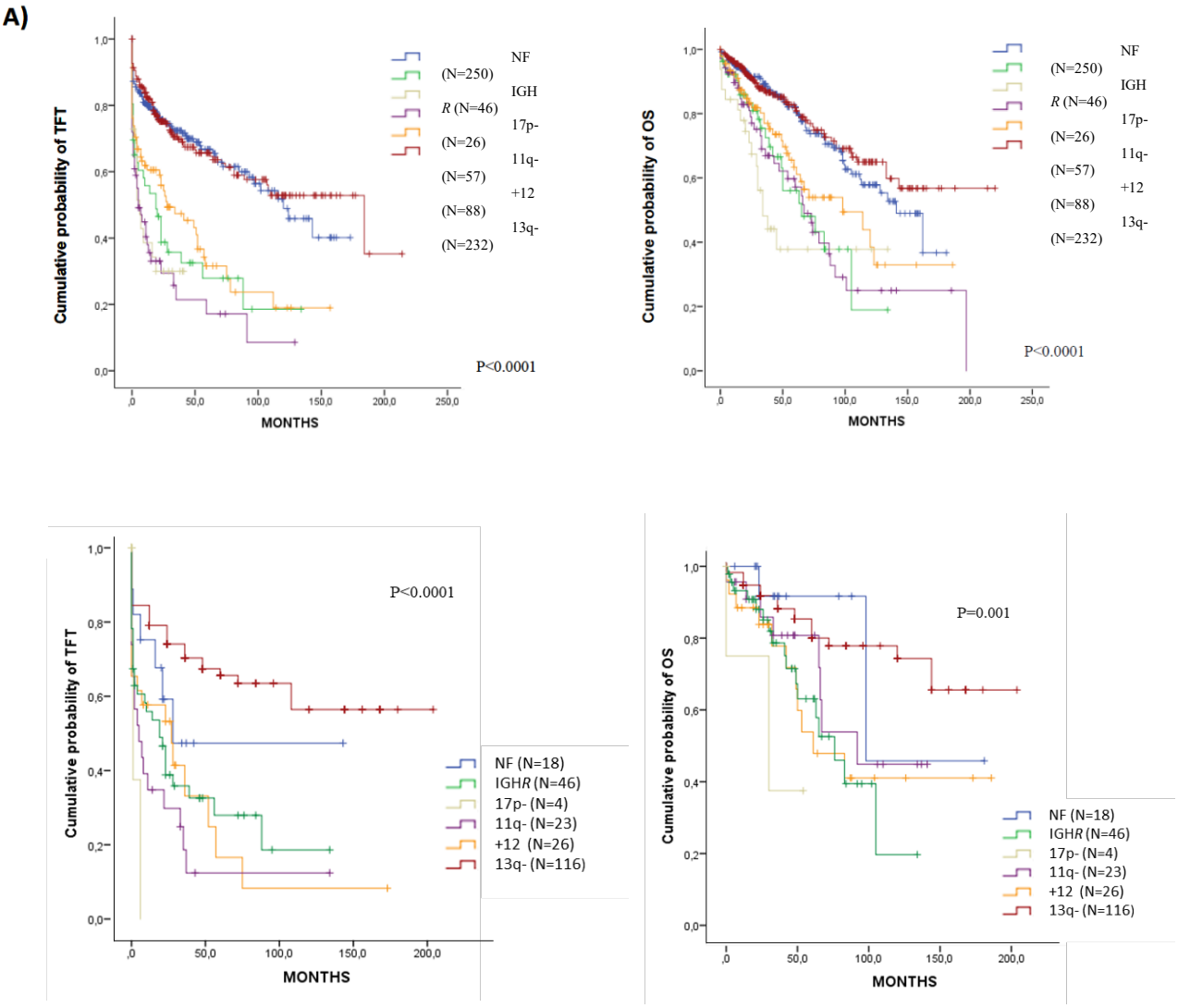

Supplementary Figure S4. Kaplan-Meier analysis in CLL patients included in the study according to the presence of FISH aberrations (13q- as sole aberration, normal FISH, +12, IGH*R*, 11q- and 17p-). (A) TFT and OS of the entire cohort (N=862); B) TFT and OS of patients included in the mutational analysis (N=233).

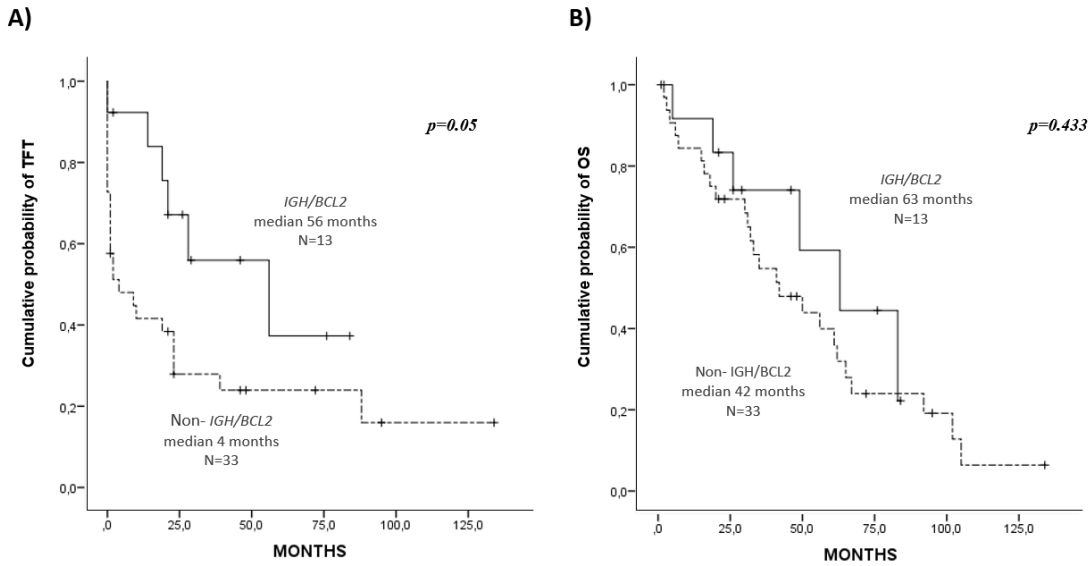

Supplementary Figure S5. Kaplan-Meier analysis of TFT and OS in IGH*R*-CLL patients according to the *IGH* translocation (*IGH / BCL2 vs.* non-*IGH / BCL2*).

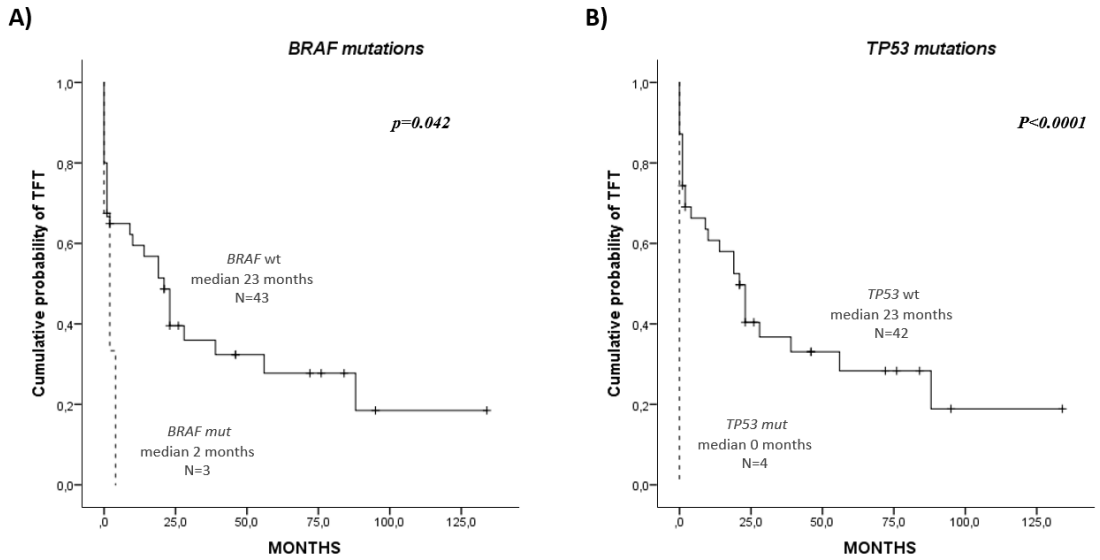

Supplementary Figure S6. Kaplan-Meier analysis of TFT in IGHR-CLL patients according to (A) *BRAF* and (B) *TP53* mutation status.

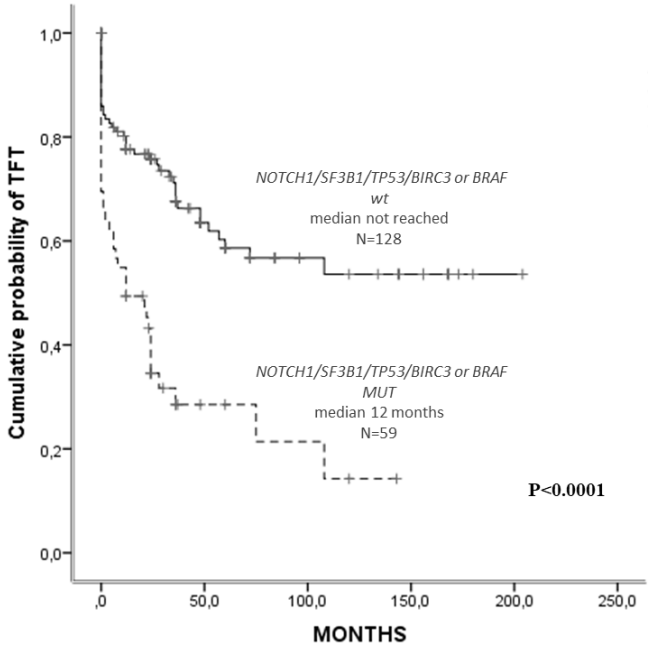

Supplementary Figure S7. Kaplan-Meier analysis of TFT in non-IGH*R* CLL patients according to the presence of mutations in *NOTCH1, SF3B1, TP53, BIRC3* and *BRAF* (N=187).

SUPPLEMENTARY APPENDIX: CHAPTER 3

Received: 2 February 2022 | Revised: 11 April 2022 | Accepted: 17 April 2022
DOI: 10.1002/ajh.26578

RESEARCH ARTICLE

AJH WILEY

TRAF3 alterations are frequent in del-3′IGH chronic lymphocytic leukemia patients and define a specific subgroup with adverse clinical features

Claudia Pérez-Carretero[1,2] | María Hernández-Sánchez[1,2] | Teresa González[1,2] | Miguel Quijada-Álamo[1,2] | Marta Martín-Izquierdo[1,2] | Sandra Santos-Mínguez[1,2] | Cristina Miguel-García[1,2] | María-Jesús Vidal[3] | Alfonso García-De-Coca[4] | Josefina Galende[5] | Emilia Pardal[6] | Carlos Aguilar[7] | Manuel Vargas-Pabón[8] | Julio Dávila[9] | Isabel Gascón-Y-Marín[10] | José-Ángel Hernández-Rivas[10] | Rocío Benito[1,2] | Jesús-María Hernández-Rivas[1,2] | Ana-Eugenia Rodríguez-Vicente[1,2]

[1]Universidad de Salamanca, IBSAL, IBMCC- Centro de Investigación del Cáncer (USAL-CSIC), Salamanca, Spain
[2]Servicio de Hematología, Hospital Universitario de Salamanca, Salamanca, Spain
[3]Servicio de Hematología, Hospital Universitario, León, Spain
[4]Servicio de Hematología, Hospital Clínico, Valladolid, Spain
[5]Servicio de Hematología, Hospital El Bierzo, Ponferrada, Spain
[6]Servicio de Hematología, Hospital Virgen del Puerto, Plasencia, Spain
[7]Servicio de Hematología, Complejo Hospitalario de Soria, Soria, Spain
[8]Servicio de Hematología, Hospital Jarrio, Asturias, Spain
[9]Servicio de Hematología, Hospital Nuestra Señora de Sonsoles, Ávila, Spain
[10]Servicio de Hematología, Hospital Universitario Infanta Leonor, Universidad Complutense, Madrid, Spain

Table of contents supplementary appendix Chapter 3

Supplementary Figure S3

TRAF3 losses detected using targeted-capture NGS data in CLL patients with del-3'IGH.

Supplementary Figure S4

Clinical impact of genetic mutations and del-3'IGH on 317 CLLs.

Supplementary Figure S5

Clinical impact of *TRAF3* alterations (deletion/mutations) on del-3'IGH CLLs.

Supplementary Figure S6

Multivariate analyses in the entire CLL cohort and del-3'IGH CLLs.

SUPPLEMENTARY METHODS

Patients' exclusion and risk classification criteria

Patients with clinical features, histopathology or immunophenotype inconsistent with CLL or Matutes Score ≥3 were excluded[1]. Within control group, the cytogenetic risk classification of patients that carried more than one chromosomal alteration was determined by the worst risk abnormality, according to the Döhner hierarchy[2]. For example, patients carrying 13q- and 11q- were categorized in the 11q group, while patients with 11q- and 17p- were characterized as 17p-. Patients with *IGH* deletion were included in the del-3'IGH group, irrespective of the presence of additional abnormalities.

Target deep sequencing

All genomic DNA samples underwent targeted-deep sequencing using an in-house 54 gene custom capture-enrichment panel (682 regions) designed using Agilent SureDesign and previously validated[3,4,5] (**Table S3**). A SureSelectXT Custom 416.393 kbp target enrichment library containing 8951 oligonucleotide probes against *H.sapiens* hg19 GRCh37 sequence was prepared by Agilent for use with Illumina multiplexed sequencing platforms.

Patient genomic DNA was isolated from blood and prepared for sequencing using the SureSelectQXT Reagent Kit (G9681B) according to the manufacturer's instructions. Targeted DNA sequencing libraries were constructed using

SureSelect^{QXT} Reagent Kit (Agilent Technologies, Santa Clara, CA) with 50 ng of genomic DNA. Briefly, tumor DNA was enzymatically fragmented and tagged to generate adapter-tagged libraries. Biotin-labeled probes specific to the targeted regions of interest) via hybridization, and libraries were enriched for regions of interest using streptavidin beads, then amplified, dual-indexed, and pooled for sequencing; quality of the libraries were measured with 4200 TapeStation (Agilent) and quantified using Qubit 3.0 (ThermoFisher Scientific, Waltham, MA).

NGS data analysis

Raw data quality control was performed with FastQC (v0.11.8) and Picard tools (v2.2.4) to collect sequencing metrics. Demultiplexed files (FASTQ) were aligned to the reference genome (GRCh37/hg19 genome), read duplicates were marked with SAMTools (v1.3.1) and post-alignment was performed with GATK (v3.5). Coverage for each region was assessed using BEDTools (v.2.26.0). A minimum quality score of Q30 was required for ensuring high-quality sequencing results. Finally, somatic variant calling, and annotation were performed using an in-house pipeline, based on VarScan (v2.4) and ANNOVAR (v.2017Jul16), respectively.

Median coverage of target regions was 600 reads/base, with at least 100X in 97% of them. To validate variants detected with VAF <5% using the custom panel, samples were conducted to resequencing using different amplicon-based approaches (Illumina Nextera XT/454 Roche) with read depth above 1000X, allowing to report variants down to 2% previously described by our group[6,7].

Data was then filtered according to the severity of the consequence, considering variants that lead to an amino acid change in the protein sequence (missense, nonsense, frameshift) and those in the splice site and UTRs. To discard single nucleotide polymorphisms (SNPs), minor allelic frequencies (MAFs) were consulted in several databases (dbSNP, 1000 genomes, ExAC and our in-house database) and only variants with a MAF of <0.01 were selected for further analysis. In addition, variants with a VAF between 40-60% or greater than 90% were manually reviewed prioritizing variants described in *in silico* tools (Polymorphism Phenotyping v2 (PolyPhen-2), Sorting Intolerant From Tolerant (SIFT) and ClinVar) as deleterious, damaging, pathogenic or likely pathogenic.

Variants were annotated using automated pipelines and potential pathogenic variants were identified. Further validation was performed by manual review using the Integrative Genomics Viewer (IGV)[8]. Variants were classified, and the pathogenicity analyzed using ClinVar and Varsome web tool[9].

REFERENCES

1. Moreau EJ, Matutes E, A'Hern RP, et al. Improvement of the chronic lymphocytic leukemia scoring system with the monoclonal antibody SN8 (CD79b). Am J Clin Pathol. 1997;108(4):378-382.
2. Döhner H, Stilgenbauer S, Benner A, et al. Genomic aberrations and survival in chronic lymphocytic leukemia. N Engl J Med. 2000;343(26):1910-1916.
3. Hernández-Sánchez M, Rodríguez-Vicente AE, González-Gascón Y Marín I, et al. DNA damage response-related alterations define the genetic background of patients with chronic lymphocytic leukemia and chromosomal gains. Exp Hematol. 2019. 72:9-13.
4. Quijada-Álamo M, Hernández-Sánchez M, Alonso-Pérez V, et al. CRISPR/Cas9-generated models uncover therapeutic vulnerabilities of del(11q) CLL cells to dual BCR and PARP inhibition. Leukemia. 2020. 34(6):1599-1612
5. Pérez-Carretero C, Hernández-Sánchez M, González T, et al. Chronic lymphocytic leukemia patients with IGH translocations are characterized by a distinct genetic landscape with prognostic implications. Int J Cancer. 2020;147(10):2780-2792.
6. Quijada-Álamo M, Pérez-Carretero C, Hernández-Sánchez M, et al. Dissecting the role of TP53 alterations in del(11q) chronic lymphocytic leukemia. Clin Transl Med. 2021;11(2):e304.
7. Quijada-Álamo M, Hernández-Sánchez M, Robledo C, et al. Next-generation sequencing and FISH studies reveal the appearance of gene mutations and chromosomal abnormalities in hematopoietic progenitors in chronic lymphocytic leukemia. J Hematol Oncol. 2017;10(1):83.
8. Robinson JT, Thorvaldsdóttir H, Wenger AM, Zehir A, Mesirov JP. Variant Review with the Integrative Genomics Viewer. Cancer Res. 2017;77(21):e31-e34.
9. Kopanos C, Tsiolkas V, Kouris A, et al. VarSome: the human genomic variant search engine. Bioinformatics. 2019;35(11):1978-1980.

SUPPLEMENTARY TABLES

Supplementary Table S1. Clinical and biological characteristics of the whole cohort of CLL patients (n=871) depending on the presence of 3'IGH deletion (del-3'IGH).

Characteristic	Del-3'IGH (n=54)	Non del-3'IGH (n=817)	*P*
Median age at diagnosis, years (range)	64.5 (43-89)	66 (25-97)	0.585[b]
Gender Male, n (%)	36/54 (66.7)	528/817 (64.6)	0.883[c]
Binet B or C, n (%)	12/51 (23.5)	177/806 (22.0)	0.862[c]
Median WBC[a] count, $\cdot 10^9$/L (range)	16.9 (4.5-93.8)	17.8 (2.4-964)	0.115[b]
Median lymphocytes count, $\cdot 10^9$/L (range)	11.0 (2.7-84)	12.2 (0.8-960)	0.160[b]
Median platelet count, $\cdot 10^9$/L (range)	190.5 (17-376)	187 (2-587)	0.914[b]
Median hemoglobin level, g/dL (range)	13.8 (7.7-17.1)	14.2 (4.4-18.9)	0.185[b]
CD38 positivity, n (%)	9/38 (23.7)	138/533 (25.9)	0.850
High β2-microglobulin level, n (%)	17/39 (43.6)	279/728 (38.3)	0.505[c]
High lactate dehydrogenase level, n (%)	8/50 (16.0)	127/799 (15.9)	1[c]
Hepatomegaly, n (%)	1/48 (2.1)	57/793 (7.2)	0.244[c]
Splenomegaly, n (%)	**14/49 (28.6)**	**127/800 (15.9)**	**0.028[c]**
Lymphoadenopathy, n (%)	17/47 (36.2)	232/718 (32.3)	0.630
B Symptoms, n (%)	4/47 (8.5)	64/787 (8.1)	0.788[c]
Richter transformation, n (%)	2/54 (3.7)	14/817 (1.7)	0.253[c]
IGHV-Unmutated, n (%)	24/47 (51.1)	283/622 (45.5)	0.536[c]
13q deletion, n (%)	24/54 (44.4)	352/817 (43.1)	1[c]
trisomy 12, n (%)	12/54 (22.2)	129/817 (15.7)	0.250[c]
11q deletion, n (%)	6/54 (11.1)	90/817 (11.0)	1[c]
17p deletion, n (%)	5/54 (9.3)	37/817 (4.5)	0.175[c]
Need for treatment, n (%)	**35/54 (64.8)**	**379/817 (46.4)**	**0.011[c]**
Second neoplasms, n (%)	7/54 (12.9)	97/779 (12.4)	0.831[c]
Median follow-up, months (range)	60 (2-217)	59 (1-340)	0.433

[a] WBC: white blood cells

[b] Mann Whitney U test
[c] $\chi 2$ test

Supplementary Table S2. Clinical and biological features of CLL patients analyzed by NGS (n=317).

Characteristic		Del-3'IGH (n=54)	Non del-3'IGH (n=263)	*P*
Median age at diagnosis, years (range)		**64.5 (43-89)**	**72 (38-97)**	**<0.001[b]**
Gender Male, n (%)		36/54 (66.7)	173/263 (65.8)	0.509[c]
Binet B or C, n (%)		12/51 (23.5)	70/259 (27.0)	0.860[c]
Median WBC[a] count, $\cdot 10^9$/L (range)		**16.9 (4.5-93.8)**	**18.9 (2.4-369)**	**0.015[b]**
Median lymphocytes count, $\cdot 10^9$/L (range)		**11.0 (2.7-84)**	**14.2 (0.8-355)**	**0.012[b]**
Median platelet count, $\cdot 10^9$/L (range)		190.5 (17-376)	176.5 (23-456)	0.552[b]
Median hemoglobin level, g/dL (range)		13.8 (7.7-17.1)	14.2 (4.4-18.9)	0.185[b]
CD38 positivity, n (%)		9/38 (23.7)	49/172 (28.4)	1[c]
High β2-microglobulin level, n (%)		17/39 (43.6)	129/219 (41.1)	1[c]
High lactate dehydrogenase level, n (%)		8/50 (16.0)	186/234 (20.5)	0.211[c]
Hepatomegaly, n (%)		1/48 (2.1)	13/242 (5.4)	0.702[c]
Splenomegaly, n (%)		14/49 (28.6)	42/244 (17.2)	0.063[c]
Lymphoadenopathy, n (%)		17/47 (36.2)	104/236 (44.0)	0.258[c]
B Symptoms, n (%)		4/47 (8.5)	23/234 (9.8)	0.658[c]
IGHV-Unmutated, n (%)		24/47 (51.1)	103/228 (45.1)	0.615[c]
CLL-IPI	Low risk	16/47 (34.0)	78/188 (41.3)	0.407[c]
	Intermediate risk	21/47 (44.7)	55/188 (29.1)	0.055[c]
	High/Very high risk	10/47 (21.3)	55/188 (29.1)	0.362[c]
IPS-E (Binet A)	Low risk	10/30 (33.3)	58/151 (38.4)	0.683[c]
	Intermediate risk	11/30 (36.7)	62/151 (41.1)	0.689[c]
	High risk	9/30 (30.0)	31/151 (20.5)	0.334[c]
FISH	13q deletion	**24/54 (44.4)**	**159/263 (60.4)**	**0.023[c]**
	trisomy 12	12/54 (22.2)	48/263 (18.3)	0.567[c]
	11q deletion	6/54 (11.1)	47/263 (17.9)	0.316[c]
	17p deletion	5/54 (9.3)	25/263 (9.5)	1[c]
NGS	*NOTCH1*	16/54 (29.6)	50/263 (19.6)	0.097[c]
	SF3B1	7/54 (12.9)	29/263 (11.0)	0.642[c]
	ATM	**11/54 (20.4)**	**26/263 (9.8)**	**0.037[c]**
	TP53	5/54 (9.2)	35/263 (13.3)	0.505[c]
	TRAF3	**7/54 (13.0)**	**1/263 (0.4)**	**<0.001[c]**
Biallelic *ATM* inactivation (del(11q) & mutation)		4/54 (7.4)	16/263 (6.0)	0.758[c]
Biallelic *TP53* inactivation (del(17q) & mutation)		4/54 (7.4)	15/263 (5.7)	0.544[c]
Biallelic *TRAF3* inactivation (loss & mutation)		**7/54 (13.0)**	**0/263 (0)**	**< 0.001[c]**
Need for treatment, n (%)		35/54 (64.8)	137/263 (52.1)	0.094[c]
Median follow-up, months (range)		60 (2-217)	60 (0-264)	0.550[b]

[a] WBC: white blood cells
[b] Mann Whitney U test
[c] $\chi 2$ test

Supplementary Table S3. List of genes and their genomic regions included in the custom-designed panel of NGS**.**

Gene	Transcript	Regions	Gene	Transcript	Regions
ARID1A	ENST00000324856	Exons 1-20	***KLHL6***	ENST00000341319	Exons 1-7
ASXL1	ENST00000375687	Exons 1-13	***KRAS***	ENST00000311936	Exons 2-5
ATM	ENST00000278616	Exons 2-63	***MAP2K1***	ENST00000307102	Exons 1-11
ATRX	ENST00000373344	Exons 1-35	***MED12***	ENST00000374080	Exons 1-4
BAX	ENST00000345358	Exon 2-6	***MGA***	ENST00000570161	Exons 2-23
BAZ2A	ENST00000551812	Exons 2-28	***MYD88***	ENST00000396334	Exons 2-5
BCL2	ENST00000398117	Exons 2-3 and 5'UTR	***NFKBIE***	ENST00000275015	Exons 1-2
BCOR	ENST00000378444	Exons 2-15	***NOTCH1***	ENST00000277541	Exon 34 and 3'UTR
BIRC3	ENST00000263464	Exons 2-9	***NRAS***	ENST00000369535	Exons 2-3
BRAF	ENST00000288602	Exons 11-16	***NXF1***	ENST00000294172	Exons 3-21
BTK	ENST00000308731	Exons 2-19	***PAX5***	ENST00000358127	enhancer
CARD11	ENST00000396946	Exons 3-17	***PCDH10***	ENST00000264360	Exons 1-5
CCND2	ENST00000261254	Exons 1-5	***PIK3CD***	ENST00000377346	Exons 3-24
CD19	ENST00000324662	Exons 1-6	***PLCG2***	ENST00000564138	Exons 2-33
CDC73	ENST00000367435	Exons 1-16	***POT1***	ENST00000357628	Exons 5-19
CHD2	ENST00000394196	Exons 2-39	***PTPN11***	ENST00000351677	Exonso 2-15
DDX3X	ENST00000399959	Exons 1-16	***RPS15***	ENST00000593052	Exons 2-4
EGR2	ENST00000242480	Exons 1-2	***SAMHD1***	ENST00000262878	Exons 1-16
FAM50A	ENST00000393600	Exons 2-12	***SETD2***	ENST00000409792	Exons 1-21
FAT1	ENST00000441802	Exons 2-27	***SF3B1***	ENST00000335508	Exons 14-16
FBXW7	ENST00000281708	Exons 7-12	***SORCS2***	ENST00000507866	Exons 1-27
FUBP1	ENST00000370768	Exons 1-19	***TP53***	ENST00000269305	Exons 4-10
HIST1H1B	ENST00000331442	Exon 1	***TRAF3***	ENST00000392745	Exons 1-12
HIST1H1E	ENST00000304218	Exon 1	***XPO1***	ENST00000401558	Exons 15-16
IGLL5	ENST00000526893	Exons 1-3, 5'UTR	***ZC3H18***	ENST00000301011	Exons 2-18
IKZF3	ENST00000346872	Exon 5	***ZMYM3***	ENST00000373998	Exons 2-25
IRF4	ENST00000380956	Exons 2-9	***ZNF292***	ENST00000339907	Exons 1-8

Supplementary Table S4. Regions of losses in 14q detected by SNP arrays in CLL patients A and B (GRCh37 (hg19) reference genome).

Patient	Cytogenetic band	Start (Kb)	End (Kb)	Size (Kb)	Microarray Nomenclature (ISCN 2016)
A (ID 23)	14q11.2	22922238	22997833	75	arr[GRCh37] 14q11.2(22922238_22997833)x1
	14q32.33	106401664	106603507	202	arr[GRCh37] 14q32.33(106401664_106603507)x1
	14q32.33	106629557	106777331	148	arr[GRCh37] 14q32.33(106629557_106777331)x0
	14q32.33	106825904	107198332	372	arr[GRCh37] 14q32.33(106825904_107198332)x1
B (ID 28)	14q24.1-q24.3	69246576	77613858	8367	arr[GRCh37] 14q24.1q24.3(69246576_77613858)x1
	14q24.3-q32.33	77617307	106199364	28582	arr[GRCh37] 14q24.3q32.33(77617307_106199364)x1
	14q32.33	106401664	106603507	202	arr[GRCh37] 14q32.33(106401664_106603507)x1

Supplementary Table S6. *TRAF3* alterations detected in del-3'IGH CLL patients.

Patient ID	Del 3'IGH, % of cells	*TRAF3* del, CNV	*TRAF3* alterations (del/mut)	AA change (Transcript: ENST00000392745)	VAF *TRAF3* mut, %	Other cytogenetic alterations	Other mutated genes
6	38	YES	del/wt	-	-	tri12 (83%)	*NOTCH1, BCOR*
12	78	YES	del/wt	-	-	del(17p) (32%)	*NOTCH1, BRAF, TP53, SF3B1*
14	30	YES	del/wt	-	-	-	*NOTCH1, NRAS, MAP2K1, IGLL5, PTPN11*
18	97	YES	del/wt	-	-	-	*ATM, BRAF, FBXW7, ZNF292*
2	62	YES	del/mut	W266X	2.0	tri12 (74%)	*NOTCH1, ZNF292*
16	90	YES	del/mut	G416E	2.62	-	*NRAS, ATM, NOTCH1*
27	60	YES	del/mut	E109fs; Q443K	88.36; 2.98	tri12 (64%)	-
28	95	YES	del/mut	C76G; G123D; Q501X; G533S	15.42; 28.12; 2.87; 13.7	tri12 (9%)	-
29	68	YES	del/mut	C105fs; Q384X	6.92; 48.24	tri12 (69%)	-
30	79	YES	del/mut	K107X; E109X; K331X; G416V	9.2; 6.19; 38.18; 4.14	tri12 (70%)	-
31	78	YES	del/mut	K52X; P63L; N312fs; Q443X; Y452C; V494G	7.64; 5.13; 8.97; 6.02; 11.15; 3.42	-	*SAMHD1*

CNV: copy number variations
VAF: variant allele frequency

Supplementary Table S8. Region of losses in 14q and *TRAF3* mutations detected in the validation cohort (GRCh37 (hg19) reference genome) (Puente et al. Nature 2015).

ID Patient	Chromosome	Band	Start	End	Copy Number (CN)	*TRAF3* loss	*TRAF3* mutation	AA change (Transcript: ENST00000392745)
33	14	q24.1 - q31.1	68572622	82357949	CN Loss	no	no	-
53	14	q23.3 - q24.2	67079108	71399987	CN Loss	no	no	-
53	14	q24.3	77853149	78299641	CN Loss	no	no	-
141	14	q23.1	58585617	58808196	CN Loss	no	no	-
155	14	q11.2 - q13.2	23966322	36014644	CN Loss	no	no	-
155	14	q21.1	39423632	41532448	CN Loss	no	no	-
155	14	q22.1	51407824	52035583	CN Loss	no	no	-
176	14	q23.2 - q24.3	62327857	78130190	CN Loss	no	no	-
339	14	q12	27457476	28352792	CN Loss	no	no	-
382	14	q24.1 - q32.33	69220906	107262283	CN Loss	yes	yes	N285fs
386	14	q23.3 - q24.3	67231548	79167253	CN Loss	no	no	-
519	14	q24.1	69124632	69205672	CN Loss	no	no	-
733	14	q24.1-q24.3	69930247	75930247	CN Loss	no	no	-
760	14	q24.2 - q24.3	73532123	74439436	CN Loss	no	no	-
802	14	q24.1-q32.33	69250915	107171764	CN Loss	yes	no	-
804	14	q23.2-q32.33	62767057	106505314	CN Loss	yes	yes	W420X
813	14	q24.1-q32.33	68930247	107171764	CN Loss	yes	yes	Y452C
1076	14	q32.2 - q32.33	99770435	106221093	CN Loss	yes	no	-
1169	14	q24.1 - q32.33	69263470	106235413	CN Loss	yes	no	-
1191	14	q24.1 - q32.33	69258318	107276012	CN Loss	yes	no	-
1191	14	q24.1 - q32.33	69258318	107276012	CN Loss	yes	no	-
1193	14	q24.1 - q32.33	69263470	106208981	CN Loss	yes	yes	G533S
1222	14	q21.2	42969417	43118032	CN Loss	no	no	-
1238	14	q31.3 - q32.12	87944826	93144278	CN Loss	no	no	-
1339	14	q24.2 - q31.3	71875306	89225297	CN Loss	no	no	-
1403	14	q24.3	73885451	74030323	CN Loss	no	no	-
1403	14	q32.12	92484165	92915976	CN Loss	no	no	-
1431	14	q24.1 - q32.33	69244711	106198682	CN Loss	yes	no	-
1446	14	q23.1 - q32.12	58544471	92647239	CN Loss	no	no	-
1484	14	q24.1	68241574	69417627	CN Loss	no	no	-

Supplementary Table S9. Clinical and biological characteristics of CLL patients according to the presence of *TRAF3* alterations (deletion and/or mutations).

		***TRAF3* WT n=43**	***TRAF3* deleted/mutated n=11**	***P***
Age		64 (37-84)	65 (54-89)	0.371
Male, %		30/43 (69.8)	6/11 (54.5)	0.475
White blood cells (10^9/L)		19.3 (6.2-93.8)	10.2 (4.5-37.2)	**0.001**
Lymphocytes (10^9/L)		13.8 (2.7-84)	7.1 (3.5-32.4)	**0.026**
Platelets (10^9/L)		192 (17-376)	147 (84.4-239)	**0.043**
Hemoglobin (g/dL)		14.3 (10-17.1)	12.4 (7.7-14.5)	**0.003**
Binet B/C, %		7/40 (17.5)	5/11 (45.5)	0.102
Hepatomegaly, %		1/37 (2.7)	0/11 (0)	1
Splenomegaly, %		11/38 (28.9)	3/11 (27.3)	1
Lymphadenopathy, %		12/36 (33.3)	5/11 (45.4)	0.493
B Symptoms, %		3/37 (8.1)	1/10 (10)	1
Richter transformation, %		0/43 (0)	2/11 (18.2)	**0.038**
CLL-IPI	Low risk	14/36 (38.9)	2/11 (18.2)	0.287
	Intermediate risk	15/36 (41.7)	6/11(54.5)	0.505
	High risk	7/36 (19.4)	3/11 (27.3)	0.679
IPS-E (Binet A)	Low risk	7/24 (29.2)	3/6 (50)	0.372
	Intermediate risk	10/24 (41.7)	1/6 (16.7)	0.372
	High risk	7/24 (29.2)	2/6 (33.3)	1
CD38+, %		8/29 (27.6)	1/9 (11.1)	0.411
High β2-microglobulin level, %		13/30 (43.3)	4/9 (44.4)	1
High lactate dehydrogenase level, %		8/40 (20)	0/10 (0)	0.184
IGHV-unmutated, %		18/36 (50.0)	6/11 (54.5)	1
del(13q), %		24/43 (55.8)	0/11 (0)	**0.001**
Trisomy 12, %		6/43 (14.0)	6/11 (54.5)	**0.009**
del(11q), %		6/43 (14.0)	0/11 (0)	0.327
del(17p), %		4/43 (9.3)	1/11 (9.8)	1
Need for treatment, %		24/44 (55.8)	11/11 (100)	**0.005**
Death during follow-up, %		7/43 (16.3)	5/11 (45.5)	0.100

Note: Significant values are shown in bold.

SUPPLEMENTARY FIGURES

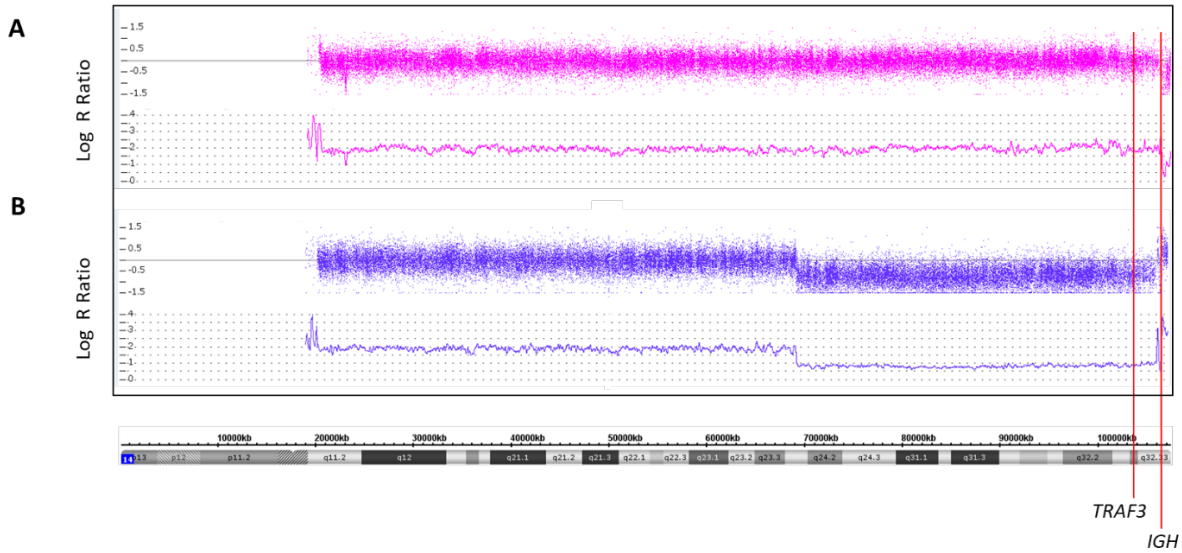

Supplementary Figure S1. 14q losses revealed by SNP6.0 in two CLL cases with del-3'IGH previously detected by FISH. For probes that are normal copy number, the signal intensity ratio of the subject versus controls is expected to be 1, and $\log_2$ R ratio should be approximately 0.0 ($\log_2 1 = 0$). Loss of copy number resulting from deletion in the subject would result in a negative $\log_2$ ratio (mean $\log_2$ ratio ~−0.5). Each dot in the upper histogram represents the $\log_2$ intensity ratio for each SNP locus and curves in the bottom represent copy number inferences based on local mean analysis for 10 consecutive SNPs. Each patient is coded with different color: patient A (ID 23) in pink and patient B (ID 28) in blue. The ratios are mapped horizontally in order of respective chromosomal location, corresponding to the short arm of chromosome 14 (left) through the long arm of the chromosome (right). The deletions detected in both patients are shown in the Table S4. All coordinates listed are based upon the GRCh37 (hg19) reference genome (UCSC Genome Browser). Red lines indicate the localization of *TRAF3* and *IGH* (constant region) genes. Constant region of IGH (*3'IGH*) was deleted in both patients and *TRAF3* was deleted in patient B (ID 28).

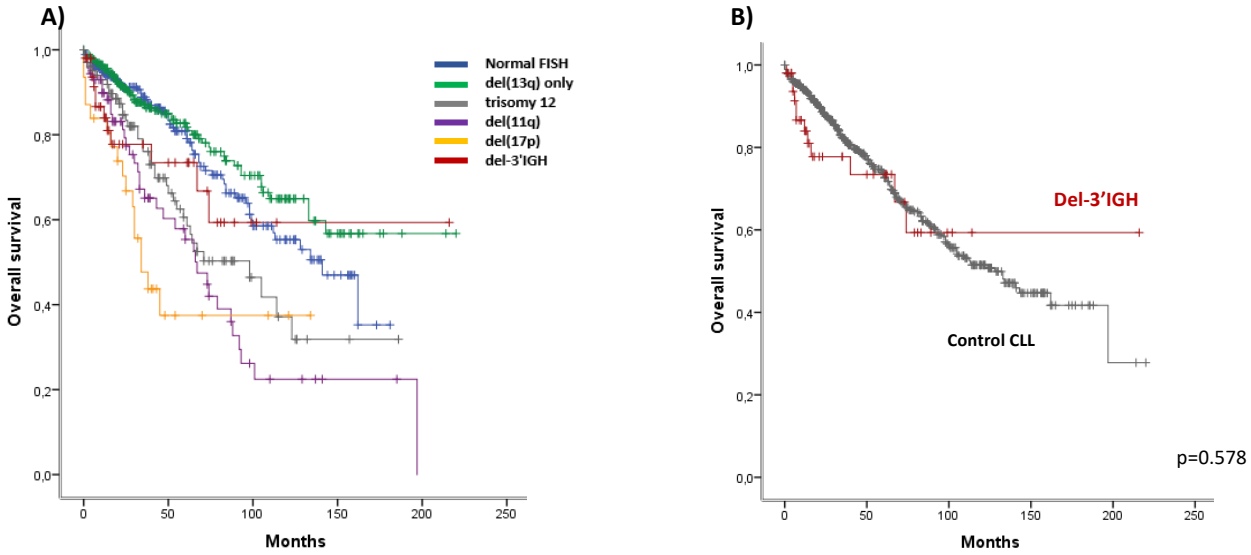

Supplementary Figure S2. Clinical impact of del-3'IGH on the outcome of CLL patients. Kaplan Meier analyses of overall survival according to A) the presence of cytogenetic alterations (del(13q), del(11q), del(17p), del-3'IGH and trisomy 12) and B) the presence of del-3'IGH *vs.* the rest of CLLs (N=871).

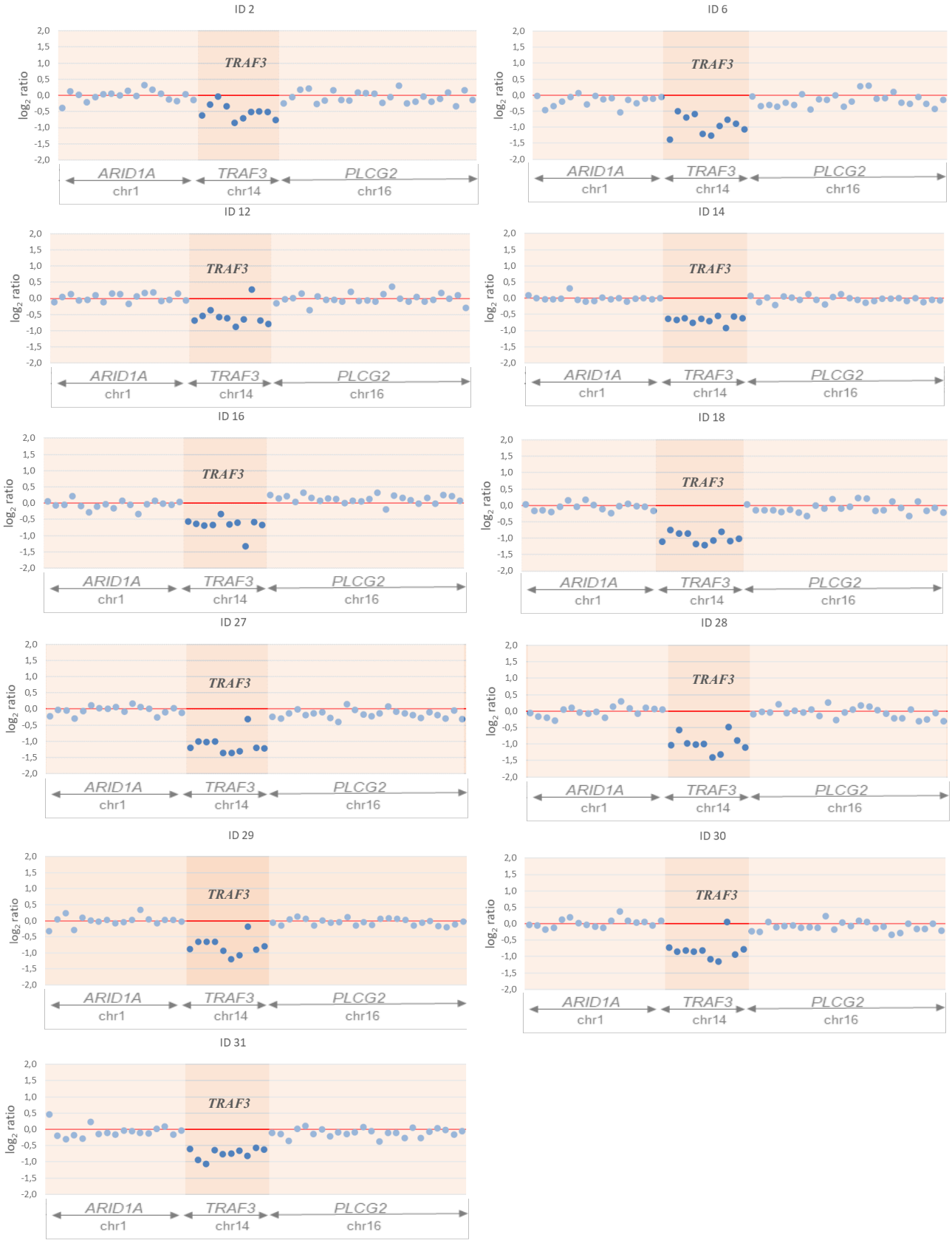
ID 2
ID 6
ID 12
ID 14
ID 16
ID 18
ID 27
ID 28
ID 29
ID 30
ID 31
log2 ratio
2,0
1,5
1,0
0,5
0,0
-0,5
-1,0
-1,5
-2,0
TRAF3
ARID1A
chr1
TRAF3
chr14
PLCG2
chr16

Supplementary Figure S3. ***TRAF3* losses detected using targeted-capture NGS data in CLL patients with del-3'IGH.** Profile of $\log_2$ ratios of normalized mean coverage to that of the reference of individual target exons of *TRAF3* (chr14) and other two genes of the panel (*ARID1A* in chr1 and *PLCG2* in chr16), was plotted against the target. The x-axis shows these targets in the panel plotted by relative genome order. The y-axis corresponds to the $\log_2$ ratio of the mean coverage of testing to that of reference. A $\log_2$ normalized coverage ratio <-0.5 indicates a *TRAF3* loss/deletion. This analysis allowed us to determine whether *TRAF3* is deleted or not in CLL samples with del-3'IGH (Table S7). Copy number analyses by SNP arrays in CLL samples with available material (ID 23, 28) validated these findings (Table S4) (Figure S1).

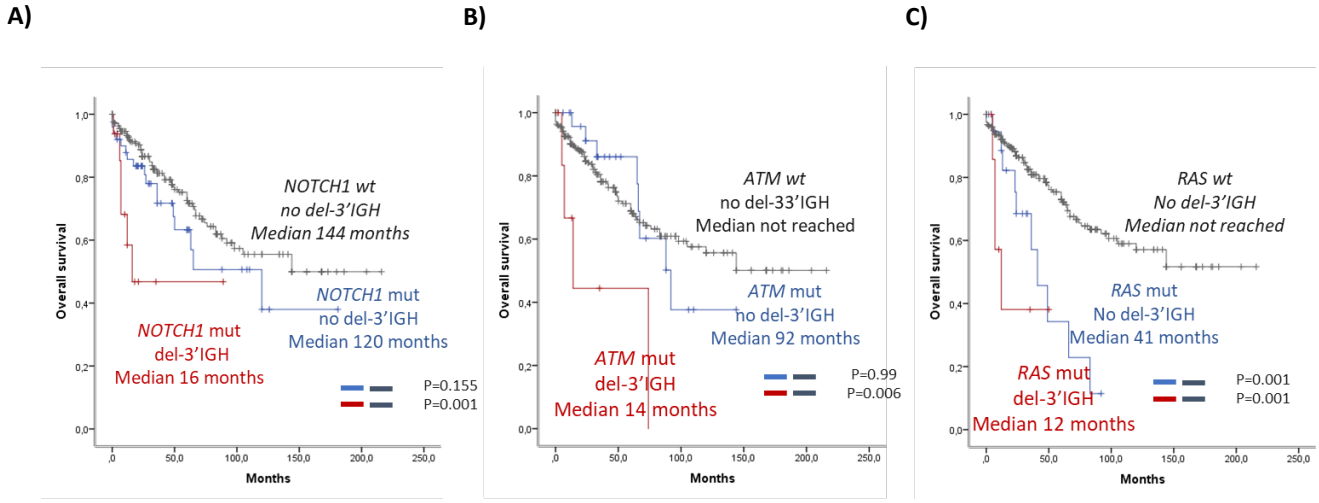

Supplementary Figure S4. Clinical impact of genetic mutations and del-3'IGH on 317 CLLs. Kaplan Meier analyses of OS according to the presence of A) del-3'IGH and/or *NOTCH1* mutations, B) del-3'IGH and/or *ATM* mutations and C) del-3'IGH and/or mutations in the RAS signalling pathway.

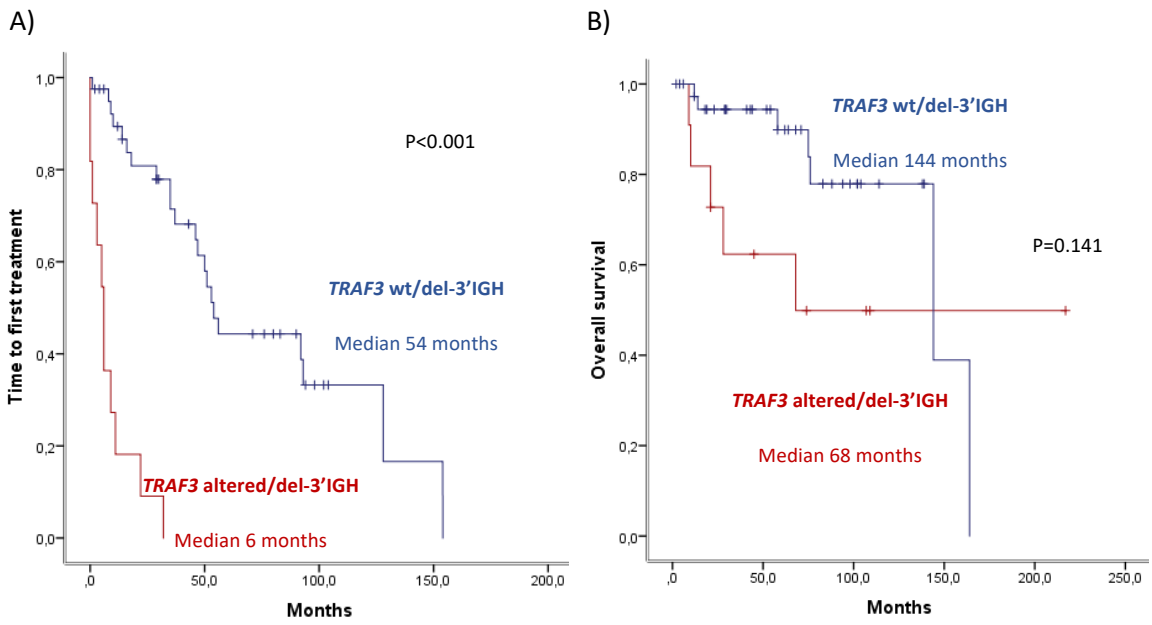

Supplementary Figure S5. Clinical impact of *TRAF3* alterations (deletion/mutations) on del-3'IGH CLLs (n=54). A) TFT and B) OS of CLL patients with del-3'IGH according to the presence of *TRAF3* deletion and/or mutation (N=11).

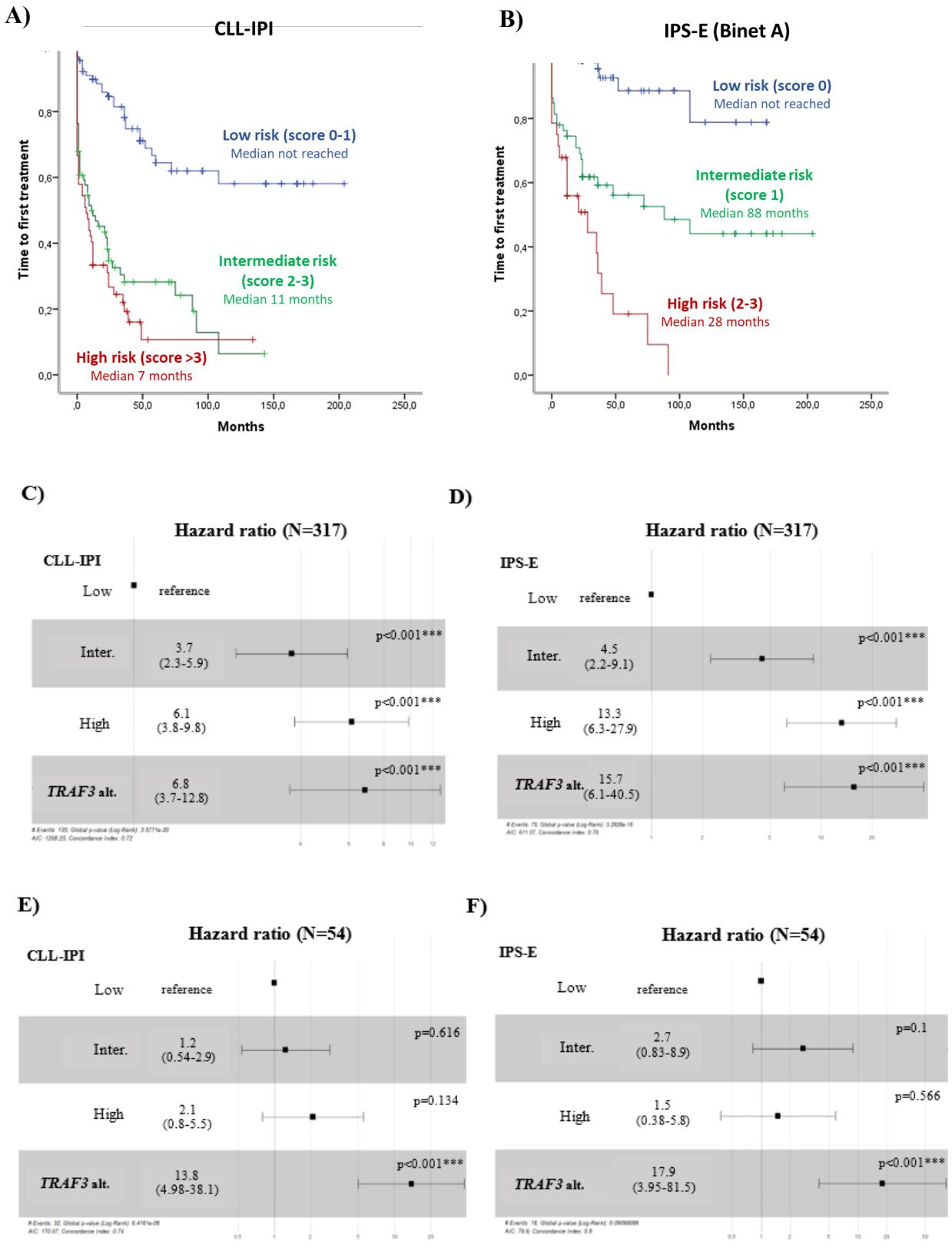
A)
CLL-IPI
Time to first treatment
Months
Low risk (score 0-1)
Median not reached
Intermediate risk
(score 2-3)
Median 11 months
High risk (score >3)
Median 7 months
B)
IPS-E (Binet A)
Low risk (score 0)
Median not reached
Intermediate risk
(score 1)
Median 88 months
High risk (2-3)
Median 28 months
C)
Hazard ratio (N=317)
CLL-IPI
Low reference
Inter. 3.7 (2.3-5.9) p<0.001***
High 6.1 (3.8-9.8) p<0.001***
TRAF3 alt. 6.8 (3.7-12.8) p<0.001***
D)
Hazard ratio (N=317)
IPS-E
Low reference
Inter. 4.5 (2.2-9.1) p<0.001***
High 13.3 (6.3-27.9) p<0.001***
TRAF3 alt. 15.7 (6.1-40.5) p<0.001***
E)
Hazard ratio (N=54)
CLL-IPI
Low reference
Inter. 1.2 (0.54-2.9) p=0.616
High 2.1 (0.8-5.5) p=0.134
TRAF3 alt. 13.8 (4.98-38.1) p<0.001***
F)
Hazard ratio (N=54)
IPS-E
Low reference
Inter. 2.7 (0.83-8.9) p=0.1
High 1.5 (0.38-5.8) p=0.566
TRAF3 alt. 17.9 (3.95-81.5) p<0.001***

Supplementary Figure S6. Stratification of patients according to prognostic indexes CLL-IPI and IPS-E in terms of TFT and multivariate analyses in the entire CLL cohort and del-3'IGH CLLs for *TRAF3* clinical impact assessment. Patients risk stratification in terms of TFT according to A) CLL-IPI (N=235) and B) IPS-E in Binet A cases (N=181). Multivariate analyses of C) CLL-IPI and *TRAF3* alterations (deletion and/or mutation) in patients with both covariables in the entire cohort (235/317), D) IPS-E and *TRAF3* alterations in patients with both covariables in the entire cohort (181/317), E) CLL-IPI and *TRAF3* alterations (deletion and/or mutation) in patients with both covariables in del-3'IGH subgroup (47/54) and F)) IPS-E and *TRAF3* alterations in patients with both covariables in del-3'IGH subgroup (30/54). Boxes indicate the hazard ratio and horizontal lines indicate 95% confident intervals (CIs). P values are shown in the right side of the panel. Hazard ratio of each risk subgroup in the prognostic indexes have been calculated to respect the low-risk subgroup, taking as the reference.

SUPPLEMENTARY APPENDIX: CHAPTER 4

TRAF3 alterations enhance metabolic plasticity through metabolic reprogramming in chronic lymphocytic leukemia

Claudia Pérez Carretero[1,2], Miguel Quijada Álamo[1,2], Mariana Tannoury[3], Léa Dehgane[3], Alberto Rodríguez Sanchez[1,2], David J. Sanz[1,2], Teresa González[1,2], Rocío Benito[1,2], Élise Chapiro[4], Florence Nguyen[4], Ana E. Rodriguez Vicente*[1,2], Santos A. Susin[3], Jesús María Hernández Rivas[1,2]

1.University of Salamanca, IBSAL, IBMCC, CSIC, Cancer Research Center, Salamanca, Spain

2.Department of Hematology, University Hospital of Salamanca, Salamanca, Spain

3.Drug Resistance in Hematological Malignancies, Centre de Recherche des Cordeliers, UMRS 1138, INSERM, Sorbonne Université, Université Paris Cité, F-75006 Paris, France

4.Drug Resistance in Hematological Malignancies, Centre de Recherche des Cordeliers, UMRS 1138, INSERM, Sorbonne Université, Université Paris Cité, F-75006 Paris, France; Groupe Hospitalier Pitié-Salpêtrière, Assistance Publique-Hôpitaux de Paris, F-75013 Paris, France

CPC and MQA contributed equally to this work

Table of contents supplementary appendix Chapter 4

Analysis of mitochondrial respiration (OCR) and glycolytic activity (ECAR) of PGA1-*TRAF3* mutated cells after UK5099 injection

Supplementary Figure S9

Analysis of mitochondrial respiration (OCR) and glycolytic activity (ECAR) of PGA1-*TRAF3* mutated cells after C968 injection.

Supplementary Figure S10

Analysis of mitochondrial respiration (OCR) and glycolytic activity (ECAR) of PGA1-*TRAF3* mutated cells after UK5099 and C968 combined injection.

SUPPLEMENTARY METHODS

Cell lines, culture conditions, drugs and reagents

The human CLL-derived cell lines PGA1 was purchased from DMSZ (Deuthche Sammlung von Mikroorganismen and Zellkulturen). PGA1 cells were cultured in RPMI 1640 medium (Life Technologies) supplemented with 10% Fetal Bovine Serum (FBS), 1% glutaMAX and 1% penicillin/streptomycin (Life Technologies). HS-5 bone marrow stromal cells for *ex vivo* co-cultures were purchased from ATCC and HEK 293T cells for lentiviral production were obtained from DMSZ. Both cell lines were maintained in DMEM (Life Technologies) supplemented with 10% FBS, 1% glutaMAX and 1% penicillin/streptomycin. Cell lines were incubated at 37°C in a 5% CO2 atmosphere. The presence of mycoplasma was tested frequently with MycoAlert kit (Lonza), only using mycoplasma-free cells in all the experiments carried out.

Venetoclax (ABT-199) was obtained from LC Laboratories, ibrutinib, idelalisib, sodium oxamate, UK-5099 were purchased from Selleckchem and Compound C968 was from MERCK. All drugs were resuspended in DMSO (Sigma). In the cell viability experiments, CLL cells were treated with the indicated drug doses on each experiment and viability was measured by CellTiter-Glo Luminescent Assay (Promega) and normalized with cells with no drug treatment.

Ex vivo co-culture conditions

HS-5 stromal cells were seeded 24 h prior to the ex vivo experiments at a concentration of 7.5 × 10^4 cells/well in a 96-well plate. On the following day, primary CLL cells were viably thawed and resuspended in RPMI 1640 medium (Life Technologies) supplemented with 10% FBS, 1% penicillin/streptomycin and 1.5 μg/mL CpG ODN (Sigma-Aldrich) plus 50 ng/mL IL-2

(Peprotech) and subsequently seeded onto the HS-5 cell layer at a co-culture ratio of 100:1 (7.5 × 10^6 CLL cells /well). CLL cells were carefully detached and lysed 24 h after co-culture for protein extraction and luminescence was measured after 48h by applying Cell Titer Glo viability assay.

Subcellular fractionation

Subcellular fractionation was performed using the Subcellular Protein Fractionation Kit (ThermoFisher Scientific) according to the manufacturer's instructions. For whole cell-lysates, cells were washed with PBS and lysed in ice-cold lysis buffer (140 mmol/l NaCl, 50 mmol/l EDTA, 10% glycerol, 1% Nonidet P-40, 20 mmol/l TrisHCl pH 7) containing protease inhibitors (cOmplete™, Roche) and phosphatase inhibitors (PhosSTOP™, Roche).

MitoSOX assay

Mitochondrial reactive oxygen species were measured using MitoSOX Red staining (Thermo Fisher Sientific, #M36008). Cells were incubated with the metabolic dye for 10 minutes at 37C in 5% CO2, at a final concentration of 1 x10^6 cells per mL. Fluorescence was measured with FACS Aria flow cytometer (BD Biosciences). Data was analyzed using FlowJo software (version 10.7.1).

Library preparation for RNA sequencing

The library for RNA-seq analysis was prepared using the TruSeq Stranded mRNA Sample Preparation Kit version 1.0 (Illumina, San Diego, CA, USA), following the manufacturer's instructions. Briefly, mRNAs were purified using poly-T oligo-attached magnetic beads and the RNA was fragmented. The mRNA fragments were used as templates for first-strand cDNA synthesis by reverse transcription with random hexamers. Upon second-strand cDNA synthesis, double-stranded cDNAs were end-repaired and adenylated at the 3′ ends. Universal adapters were ligated to the cDNA fragments, then the sequencing library of DNA fragments that had adapters on both ends was amplified by PCR and used to produce the clusters that were then sequenced in an Illumina Nextseq 500 instrument (Illumina, San Diego, CA, USA). Each sample was sequenced in a separate flow cell lane, producing 26.2–32.4 million paired-end reads, with a final length of 76 bases.

Fluorescence in situ hibrization (FISH)

Interphase FISH was performed in primary CLL cells using commercially available probes for the using 13q14/D13S319, 12p11.1-q11/CEP12, 11q22/ATM, 17p13/P53probes and dual

color break-apart FISH probe for IGH (Vysis, Abbott Laboratories, IL, USA) as previously described[1]. Signal screening was carried out in at least 200 and the cut-off >10% was considered positive, based on the cut-off value used by our laboratory.

Next-generation sequencing

Next-generation sequencing (NGS) approach was applied to analyze the mutational status of 54 CLL-related genes[2,3], including *TRAF3,* in primary samples of CLL patients by using a targeted-capture approach (Agilent, SureSelect) following the manufacturer's instructions. Sequence data generated by the platform NextSeq 500 (Illumina) was analyzed by an in-house bioinformatic pipeline as previously reported[4,5]. **Supplementary Table Sx** shows the list of mutations of CLL patients included in this study.

Multiplex Ligation-Dependent Probe Amplification (MLPA)

MLPA reactions were performed using the SALSA MLPA P425 Multiple Myeloma probemix (MRC-Holland, Amsterdam, Netherlands) according to the manufacturer's instructions, to assess *TRAF3* losses in exon 3 and 11 of primary CLL samples. DNA samples from three healthy donors were used as controls. MLPA amplification products were analyzed on an ABI 3130xl Genetic Analyzer (Applied Biosystems/Hitachi) with GeneMapper software V.3.7, using the Genescan 500LIZ internal size standard (Applied Biosystems), as previously described by our group[6]. The copy number at each locus was estimated according to Schwab *et al.*[7], whereby values above 1.3, between 1.3 and 0.75, between 0.75 and 0.25, and below 0.25 were considered as gain, normal, hemizygous loss, and homozygous loss, respectively.

Western blot analysis

Cells were washed twice in PBS and lysed in ice-cold lysis buffer (50 nM TrisHCl pH 7.4, 150 mM NaCl, 1 mM EDTA, 1% Triton X-100) containing protease inhibitors (Roche) and phosphatase inhibitors (PhosSTOP™, Roche). Protein concentration was measured using the Bradford assay (BioRad). Protein samples were subjected to SDS-PAGE and transferred to a nitrocellulose membrane (GE Healthcare). After blockade, membranes were incubated with the anti-TRAF3 primary antibodies purchased from Cell Signaling Technologies (#4729, Rabbit). Horseradish peroxidase-linked anti-rabbit antibody (#7074, Cell Signaling Technologies) was used as secondary antibody at 1:5.000 dilution. Antibody signal was detected using ECLTM Western Blotting Detection Reagents (RPN2209, GE Healthcare).

ddPCR

RNA was extracted from PGA1-TRAF3 mutated cells using the RNeasy mini kit (Qiagen) according to the manufacturer's protocol. Complementary DNA (cDNA) was synthesized from 500 ng of RNA with the SuperScript™ III First-Strand Synthesis SuperMix (ThermoFisher) using random primers. Droplet Digital polymerase chain reaction (ddPCR) was performed using Bio-Rad QX200 system with ddPCR Supermix for Probes (no dUTP) (Bio-Rad Laboratories), 1 ul of template cDNA and gene specific Taqman probes (FAM/VIC labeled) (ThermoFisher), according to the manufacturer's protocol. The following FAM probes were used: Hs01089753_m1 (MAP3K14), Hs00608023_m1 (BCL2), Hs00236329_m1 (BCL-XL), Hs01050896_m1 (MCL1), Hs00180269_m1 (BAX), Hs00832876_g1 (BAK), Hs03405589_m1 (BCL2A1). ABL1-VIC probe (Hs01104728_m1) was taken as the reference for assessing the gene expression ratio. Droplets were generated with the QX200 Droplet generator and streamed with a QX200 Droplet Reader (Bio-Rad Laboratories). The raw data were analyzed with QuantaSoft™ Software 1.0.596 (Bio-Rad Laboratories), and the results were expressed as the target/reference concentrations (copies/ul) ratio.

REFERENCES

1. González MB, Hernández JM, García JL, Lumbreras E, Castellanos M, Fernández-Calvo J, et al. The value of fluorescence in situ hybridization for the detection of 11q in multiple myeloma. Haematologica. 2004;89(10):1213-8.
2. Landau DA, Tausch E, Taylor-Weiner AN, Stewart C, Reiter JG, Bahlo J, et al. Mutations driving CLL and their evolution in progression and relapse. Nature. 2015;526(7574):525-30.
3. Puente XS, Beà S, Valdés-Mas R, Villamor N, Gutiérrez-Abril J, Martín-Subero JI, et al. Non-coding recurrent mutations in chronic lymphocytic leukaemia. Nature. 2015;526(7574):519-24.
4. Hernández-Sánchez M, Rodríguez-Vicente AE, González-Gascón Y Marín I, Quijada-Álamo M, Hernández-Sánchez JM, Martín-Izquierdo M, et al. DNA damage response-related alterations define the genetic background of patients with chronic lymphocytic leukemia and chromosomal gains. Exp Hematol. 2019. 72:9-13.
5. Quijada-Álamo M, Hernández-Sánchez M, Alonso-Pérez V, Rodríguez-Vicente AE, García-Tuñón I, Martín-Izquierdo M, et al. CRISPR/Cas9-generated models uncover therapeutic vulnerabilities of del(11q) CLL cells to dual BCR and PARP inhibition. Leukemia. 2020. 34(6):1599-1612
6. Forero-Castro M, Montaño A, Robledo C, García de Coca A, Fuster JL, de las Heras N, et al. Integrated Genomic Analysis of Chromosomal Alterations and Mutations in B-Cell Acute

Lymphoblastic Leukemia Reveals Distinct Genetic Profiles at Relapse. Diagnostics [Internet]. 2020; 10(7).
7. Schwab CJ, Jones LR, Morrison H, Ryan SL, Yigittop H, Schouten JP, et al. Evaluation of multiplex ligation-dependent probe amplification as a method for the detection of copy number abnormalities in B-cell precursor acute lymphoblastic leukemia. Genes, Chromosomes and Cancer. 2010;49(12):1104-13.

SUPPLEMENTARY TABLES

Supplementary Table S1. sgRNA sequences and PCR primers of sgRNA target sites.

Target	Forward (5'-3')	Reverse (5'-3')
Control sgRNA1	CACCG**ACGGAGGCTAAGCGTCGCAA**	AAAC**TTGCGACGCTTAGCCTCCGT**C
TRAF3 exon 11 sgRNA1	CACCG**CAGCCAAGCAGAGAAACTGA**	AAAC**TCAGTTTCTCTGCTTGGCTG**C
TRAF3 exon 11 (PCR)	ACAAGCACTTGATCCCAGGG	TCACACCTCTGCGTGTTACC

Supplementary Table S2. Biological features of CLL patients included in *ex vivo* experiments**.**

ID	IGHV status	Cytogenetics (FISH)	*TRAF3* mutations (VAF, %)	*TRAF3* loss (Ratio MLPA: exon 3; exon 11)	Mutated genes
1	NA	+12	c.T262C:p.C88R (81.4%)	Yes (0.53; 0.57)	*ATM, TRAF3*
2	UM	del(13q), del(11q)	c.C565G:p.L189V (36.3%)	No	*TRAF3*
3	M	+12	c.961_965del:p.R321fs (41%), c.G1352A:p.G451D (46%)	No	*TRAF3, KLHL6, IGLL5*
4	M	del(13q)		No	*KLHL6*
5	UM	del(13q), del(11q)		No	*ATM, NFKBIE*
6	UM	+12		No	*FBXW7*
7	UM			No	*ATM, BRAF, MAP2K1*
8	UM			No	*SF3B1, NOTCH1*
9	M			No	-
10	M	del(13q), +12		No	-
11	NA	del(13q), del(17p)		No	-
12	UM	del(13q), del(11q)		No	-
13	NA	+12		No	*SPEN*
14	NA	+12		No	-
15	UM			No	*NOTCH1, ATM, MGA, IKZF3, MED12*
16	M	del(13q)		No	-
17	M	del(13q)		No	*ATM*
18	UM	del(13q)		No	-
19	UM	del(13q), del(11q)		No	*ATM, NXF1*
20	UM	del(13q), del(14q)		No	-
21	NA	del(13q), del(11q), del(14q)		No	*ATM, ARID1A, HIST1H1E*
22	UM	del(14q)		No	-

Supplementary Table S3. List of 56 transcriptionally dysregulated genes analyzed by RNAseq in PGA1-*TRAF3* mutated cells.

GeneID	log2(FC)	Wald-Stats	P-value	P-adj	Gene name
ENSG00000174600.14_8	-1.1804	-6.9479	0.0000	0.0000	*CMKLR1*
ENSG00000102024.18_6	-1.0426	-6.1678	0.0000	0.0000	*PLS3*
ENSG00000131323.16_7	-0.9648	-6.1008	0.0000	0.0000	*TRAF3*
ENSG00000118515.11_8	0.9572	5.3114	0.0000	0.0002	*SGK1*
ENSG00000107249.23_9	0.8857	5.3424	0.0000	0.0002	*GLIS3*
ENSG00000128242.13_8	0.9688	5.3544	0.0000	0.0002	*GAL3ST1*
ENSG00000230438.7_9	0.9021	5.2707	0.0000	0.0003	*SERPINB9P1*
ENSG00000102096.9_6	0.8721	5.2468	0.0000	0.0003	*PIM2*
ENSG00000277734.8_7	0.6054	5.1870	0.0000	0.0003	*TRAC*
ENSG00000006062.17_9	0.5888	5.0291	0.0000	0.0006	*MAP3K14*
ENSG00000100342.21_5	0.7954	5.0210	0.0000	0.0006	*APOL1*
ENSG00000162836.12_9	-0.9027	-4.8944	0.0000	0.0011	*ACP6*
ENSG00000146426.18_11	0.7292	4.8772	0.0000	0.0011	*TIAM2*
ENSG00000103811.18_7	0.5516	4.8243	0.0000	0.0014	*CTSH*
ENSG00000120029.13_9	0.8129	4.6693	0.0000	0.0025	*ARMH3*
ENSG00000140545.15_7	-0.8206	-4.6835	0.0000	0.0025	*MFGE8*
ENSG00000215386.13_8	-0.7998	-4.6591	0.0000	0.0025	*MIR99AHG*
ENSG00000108091.11_6	-0.5024	-4.6306	0.0000	0.0027	*CCDC6*
ENSG00000163346.17_8	0.8155	4.6008	0.0000	0.0030	*PBXIP1*
ENSG00000152689.18_9	0.7669	4.5292	0.0000	0.0040	*RASGRP3*
ENSG00000140092.14_7	-0.8338	-4.5159	0.0000	0.0041	*FBLN5*
ENSG00000180616.9_7	-0.8246	-4.4613	0.0000	0.0050	*SSTR2*
ENSG00000082293.13_9	0.7193	4.4342	0.0000	0.0054	*COL19A1*
ENSG00000115902.11_5	0.6437	4.3576	0.0000	0.0071	*SLC1A4*
ENSG00000156011.17_8	-0.6061	-4.3602	0.0000	0.0071	*PSD3*
ENSG00000163492.15_7	0.7931	4.2926	0.0000	0.0092	*CCDC141*
ENSG00000198502.6_6	0.6227	4.2540	0.0000	0.0105	*HLA-DRB5*
ENSG00000163545.11_7	0.7622	4.2259	0.0000	0.0111	*NUAK2*
ENSG00000168405.17_7	0.7302	4.2251	0.0000	0.0111	*CMAHP*
ENSG00000196126.11_5	0.4546	4.1625	0.0000	0.0142	*HLA-DRB1*
ENSG00000114446.5_10	0.6111	4.0159	0.0001	0.0258	*IFT57*
ENSG00000232783.5_2	0.6839	3.9902	0.0001	0.0278	*FRG2FP*
ENSG00000198133.8_8	-0.7208	-3.9834	0.0001	0.0278	*TMEM229B*
ENSG00000196565.15_8	-0.5049	-3.9759	0.0001	0.0278	*HBG2*
ENSG00000028116.18_7	0.5632	3.9631	0.0001	0.0285	*VRK2*
ENSG00000224220.1_6	0.7064	3.8755	0.0001	0.0399	*DTNB-AS1*
ENSG00000138767.13_8	-0.7021	-3.8399	0.0001	0.0437	*CNOT6L*
ENSG00000120694.20_7	-0.5068	-3.8451	0.0001	0.0437	*HSPH1*
ENSG00000115414.21_10	0.7010	3.8157	0.0001	0.0449	*FN1*
ENSG00000187772.8_8	-0.4807	-3.7972	0.0001	0.0449	*LIN28B*
ENSG00000186193.9_6	-0.4308	-3.8222	0.0001	0.0449	*SAPCD2*
ENSG00000165507.9_10	-0.7025	-3.7995	0.0001	0.0449	*DEPP1*
ENSG00000170579.17_10	0.5176	3.7998	0.0001	0.0449	*DLGAP1*
ENSG00000165168.8_6	0.5958	3.8078	0.0001	0.0449	*CYBB*
ENSG00000132294.15_10	0.5036	3.7859	0.0002	0.0456	*EFR3A*
ENSG00000129353.15_8	0.5500	3.7823	0.0002	0.0456	*SLC44A2*
ENSG00000117016.10_6	0.6809	3.7626	0.0002	0.0478	*RIMS3*
ENSG00000065809.13_10	0.5206	3.7568	0.0002	0.0478	*FAM107B*
ENSG00000169508.7_6	-0.4620	-3.7547	0.0002	0.0478	*GPR183*
ENSG00000187240.16_9	0.6061	3.7417	0.0002	0.0484	*DYNC2H1*
ENSG00000197582.5_4	0.5457	3.7420	0.0002	0.0484	*GPX1P1*
ENSG00000150961.15_7	0.6396	3.7314	0.0002	0.0494	*SEC24D*
ENSG00000117115.13_6	0.6892	3.7108	0.0002	0.0498	*PADI2*
ENSG00000115107.20_7	-0.5190	-3.7229	0.0002	0.0498	*STEAP3*
ENSG00000213931.7_8	-0.4595	-3.7119	0.0002	0.0498	*HBE1*
ENSG00000133985.3_5	0.4611	3.7147	0.0002	0.0498	*TTC9*

S**upplementary Table S4.** List of HALLMARK transcriptionally dysregulated pathways in GSEA enrichment analysis from PGA1-*TRAF3* mutated cells

NAME (MSigDB)	SIZE	ES	NES	NOM p-val	FDR q-val	FWER p-val	RANK AT MAX
HALLMARK_BILE_ACID_METABOLISM	68	0.45	1.64	0.000	0.278	0.190	1149
HALLMARK_MYOGENESIS	85	0.42	1.40	0.000	1.000	0.699	3298
HALLMARK_PI3K_AKT_MTOR_SIGNALING	87	0.36	1.35	0.089	0.900	0.727	4310
HALLMARK_HYPOXIA	133	0.40	1.35	0.054	0.701	0.727	2579
HALLMARK_ALLOGRAFT_REJECTION	135	0.39	1.32	0.035	0.688	0.818	2520
HALLMARK_HEME_METABOLISM	146	0.34	1.32	0.000	0.583	0.818	2733
HALLMARK_ANGIOGENESIS	16	0.59	1.28	0.235	0.606	0.904	2537
HALLMARK_COMPLEMENT	130	0.33	1.25	0.085	0.618	0.923	3128
HALLMARK_PEROXISOME	80	0.28	1.23	0.234	0.586	0.923	1473
HALLMARK_TGF_BETA_SIGNALING	41	0.32	1.21	0.179	0.566	0.923	3375
HALLMARK_SPERMATOGENESIS	65	0.34	1.19	0.241	0.583	0.923	1780
HALLMARK_APOPTOSIS	123	0.30	1.16	0.201	0.624	0.948	2488
HALLMARK_KRAS_SIGNALING_UP	101	0.30	1.11	0.177	0.704	0.972	1848
HALLMARK_WNT_BETA_CATENIN_SIGNALING	31	0.33	1.10	0.233	0.683	0.972	3021
HALLMARK_ESTROGEN_RESPONSE_LATE	116	0.31	1.10	0.373	0.653	0.972	1109
HALLMARK_ESTROGEN_RESPONSE_EARLY	112	0.28	1.06	0.179	0.726	0.972	2291
HALLMARK_GLYCOLYSIS	145	0.29	1.04	0.314	0.745	0.972	2593
HALLMARK_PROTEIN_SECRETION	86	0.31	1.01	0.432	0.790	0.972	3268
HALLMARK_MITOTIC_SPINDLE	184	0.21	1.00	0.433	0.767	0.972	3714
HALLMARK_NOTCH_SIGNALING	24	0.32	1.00	0.524	0.739	0.972	2075
HALLMARK_CHOLESTEROL_HOMEOSTASIS	60	0.34	0.94	0.374	0.849	1.000	2682
HALLMARK_APICAL_SURFACE	25	0.31	0.91	0.716	0.881	1.000	3001
HALLMARK_IL2_STAT5_SIGNALING	141	0.24	0.86	0.686	0.947	1.000	2123
HALLMARK_INTERFERON_GAMMA_RESPONSE	174	0.31	0.82	0.732	0.990	1.000	3300
HALLMARK_INTERFERON_ALPHA_RESPONSE	88	0.37	0.82	0.687	0.958	1.000	3116
HALLMARK_KRAS_SIGNALING_DN	67	0.26	0.78	0.772	0.980	1.000	1530
HALLMARK_FATTY_ACID_METABOLISM	118	0.19	0.75	0.810	0.993	1.000	4685
HALLMARK_ADIPOGENESIS	149	0.16	0.74	0.795	0.982	1.000	3144
HALLMARK_UNFOLDED_PROTEIN_RESPONSE	111	0.21	0.73	0.638	0.968	1.000	1999
HALLMARK_P53_PATHWAY	163	0.23	0.72	0.857	0.945	1.000	3144
HALLMARK_XENOBIOTIC_METABOLISM	114	0.18	0.72	0.863	0.921	1.000	1540
HALLMARK_APICAL_JUNCTION	114	0.20	0.68	0.946	0.927	1.000	3547
HALLMARK_MTORC1_SIGNALING	189	0.21	0.60	0.841	0.952	1.000	1917
HALLMARK_MYC_TARGETS_V1	198	-0.42	-1.45	0.177	0.617	0.414	4734
HALLMARK_MYC_TARGETS_V2	57	-0.65	-1.40	0.058	0.437	0.565	3565
HALLMARK_EPITHELIAL_MESENCHYMAL_TRANSITION	89	-0.33	-1.19	0.086	1.000	0.900	1566
HALLMARK_COAGULATION	55	-0.29	-1.07	0.260	1.000	0.983	1537
HALLMARK_TNFA_SIGNALING_VIA_NFKB	165	-0.33	-1.02	0.563	1.000	1.000	1487
HALLMARK_G2M_CHECKPOINT	194	-0.22	-0.98	0.528	1.000	1.000	4245
HALLMARK_UV_RESPONSE_DN	95	-0.26	-0.95	0.527	1.000	1.000	1059
HALLMARK_UV_RESPONSE_UP	121	-0.23	-0.94	0.346	1.000	1.000	2554
HALLMARK_E2F_TARGETS	200	-0.20	-0.90	0.522	1.000	1.000	4659
HALLMARK_INFLAMMATORY_RESPONSE	131	-0.28	-0.90	0.706	0.952	1.000	1112
HALLMARK_IL6_JAK_STAT3_SIGNALING	60	-0.29	-0.89	0.553	0.896	1.000	1112
HALLMARK_HEDGEHOG_SIGNALING	22	-0.27	-0.79	0.886	1.000	1.000	832
HALLMARK_DNA_REPAIR	142	-0.13	-0.73	0.940	1.000	1.000	4192
HALLMARK_ANDROGEN_RESPONSE	69	-0.20	-0.60	0.847	1.000	1.000	1811
HALLMARK_REACTIVE_OXYGEN_SPECIES_PATHWAY	46	-0.18	-0.59	0.938	1.000	1.000	3287
HALLMARK_OXIDATIVE_PHOSPHORYLATION	194	-0.11	-0.47	0.938	0.988	1.000	4366

SUPPLEMENTARY FIGURES

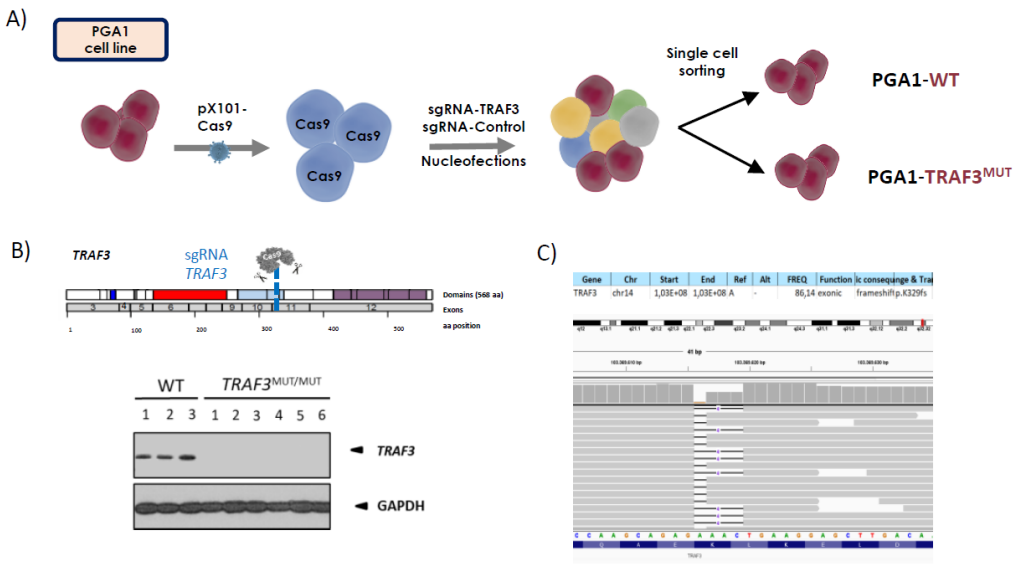

Supplementary Figure S1. CRISPR/Cas9-edited PGA1 cells generation and validation. A) Scheme of CRISPR/Cas9 induction of *TRAF3* mutations in PGA1 cells, showing the lentiviral transduction of Cas9 for its constitutive expression, followed by subsequent nucleofections with the sgRNAs targeting exon 11 of *TRAF3* and non-human genome region as the control. Single-cell sorting was performed in the pool of nucleofected cells. B) Target region of the *TRAF3* sgRNAs in the gene and validation of the absence of protein by Western Blot and C) targeted next generation sequencing.

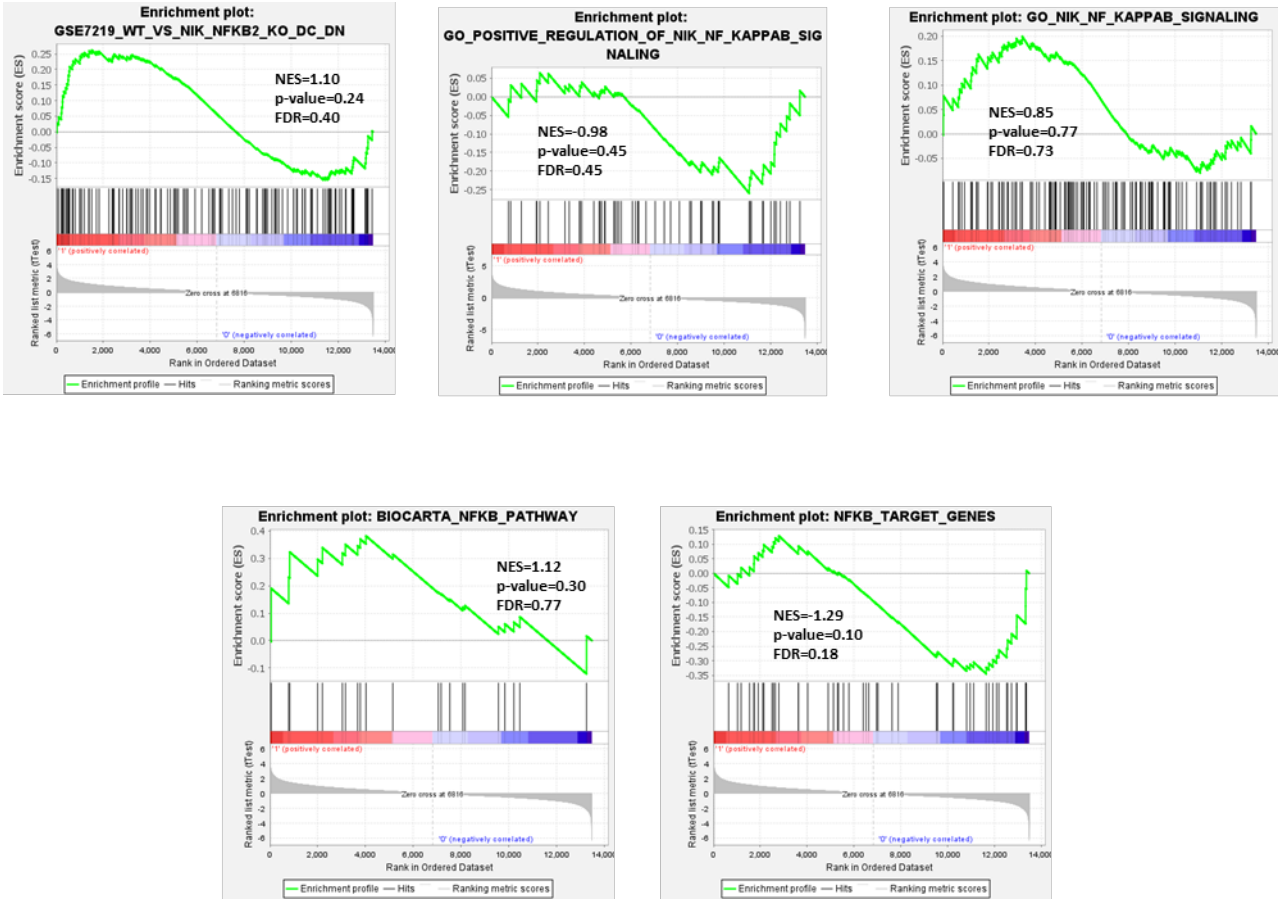

Supplementary Figure S2. Transcriptional analysis of *TRAF3* inactivation in NF-KB signaling. Gene Set Enrichment Analysis (GSEA) of MSigDB gene sets related to NF-kB signaling and their targets for PGA1-*TRAF3* mutated cells vs. PGA1-WT cells.

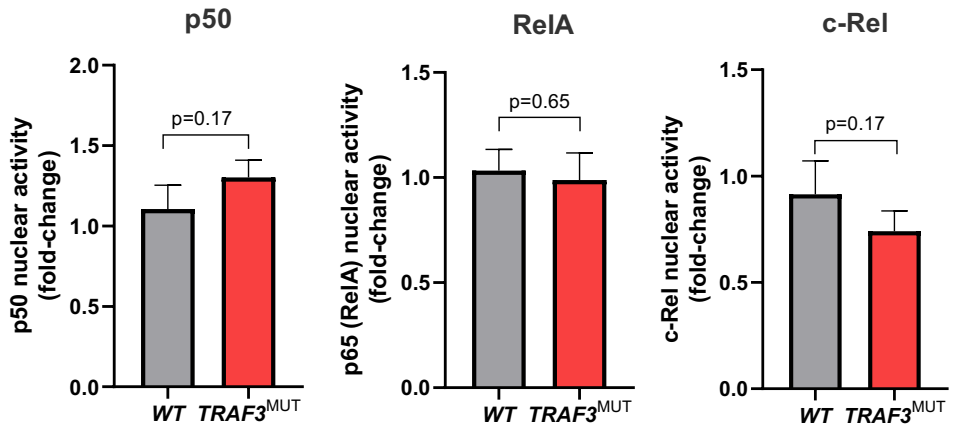

Supplementary figure S3. Impact of *TRAF3* inactivation in canonical NF-kB pathway. Nuclear DNA-binding activity of the canonical NF-κB transcription factors p50, RelA and c-Rel assessed by ELISA in nuclear extracts of PGA1-*TRAF3* mutated cells. Data are represented as the mean ± SD.

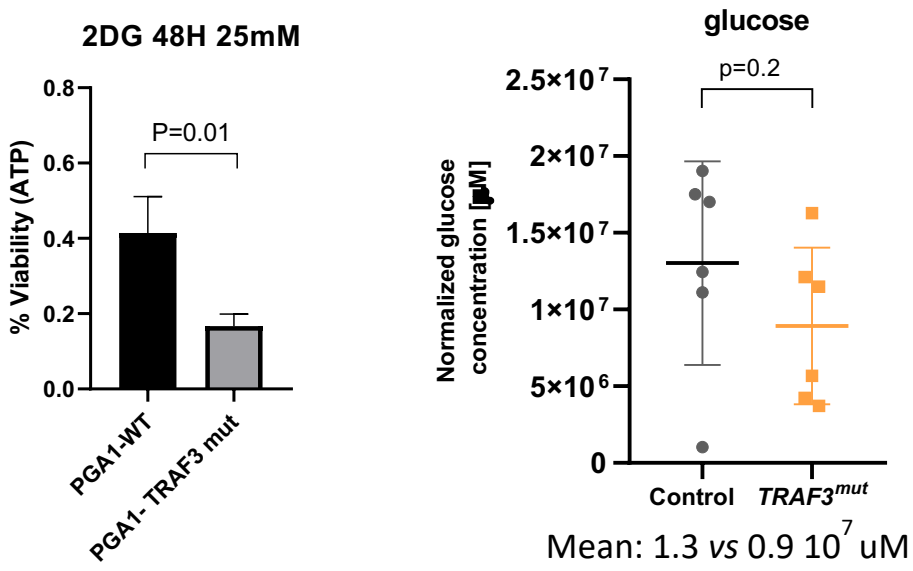

Supplementary Figure S4. Glucose metabolism in PGA1-*TRAF3* mutated cells. Assessment of *TRAF3* implications in A) the response to the glycolytic inhibitor 2-Doxyglucose (2-DG), and B) glucose abundance in the cell by metabolomics. *Cell viability was assessed by CellTiter-Glo luminescent assay. Data are represented as the mean ± SD.*

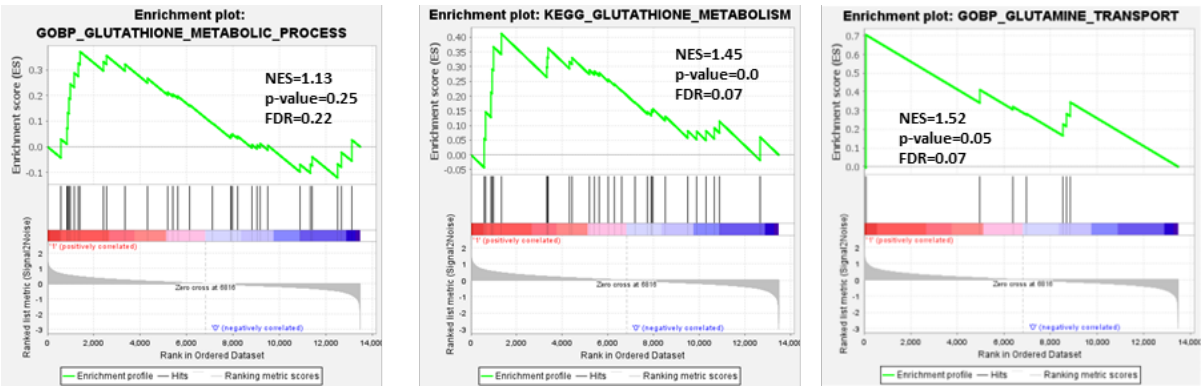

Supplementary figure S5. Transcriptional analysis of *TRAF3* inactivation in glutathione and glutamine metabolism. Gene Set Enrichment Analysis (GSEA) of MSigDB gene sets related to glutathione metabolic processes and glutamine transport for PGA1-*TRAF3* mutated cells vs. PGA1-WT cells.

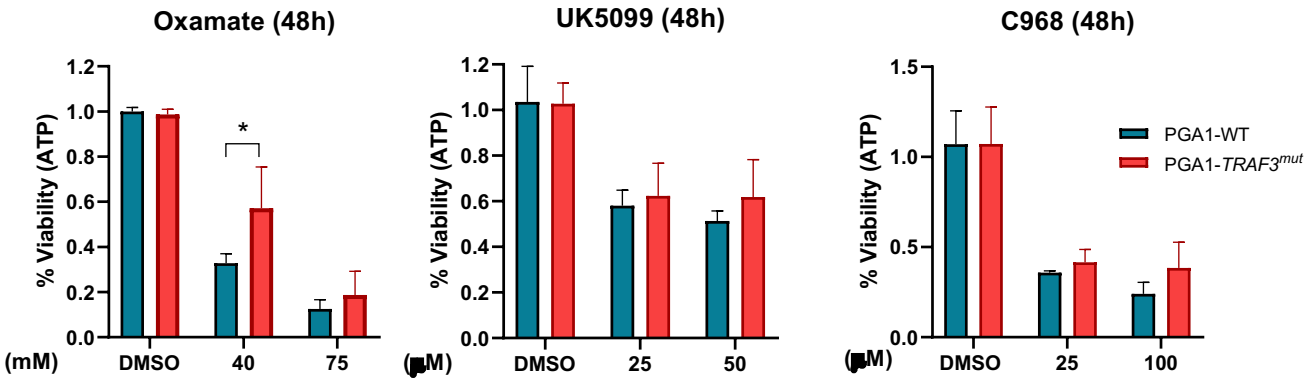

Supplementary Figure S6. Response of PGA1-*TRAF3* mutated and PGA1-WT cells to metabolic inhibitors (oxamate, UK5099 and C968). Cell viability was assessed by CellTiter-Glo luminescent assay. Data are represented as the mean ± SD. Concentrations are shown below the graph. *p<0.05.

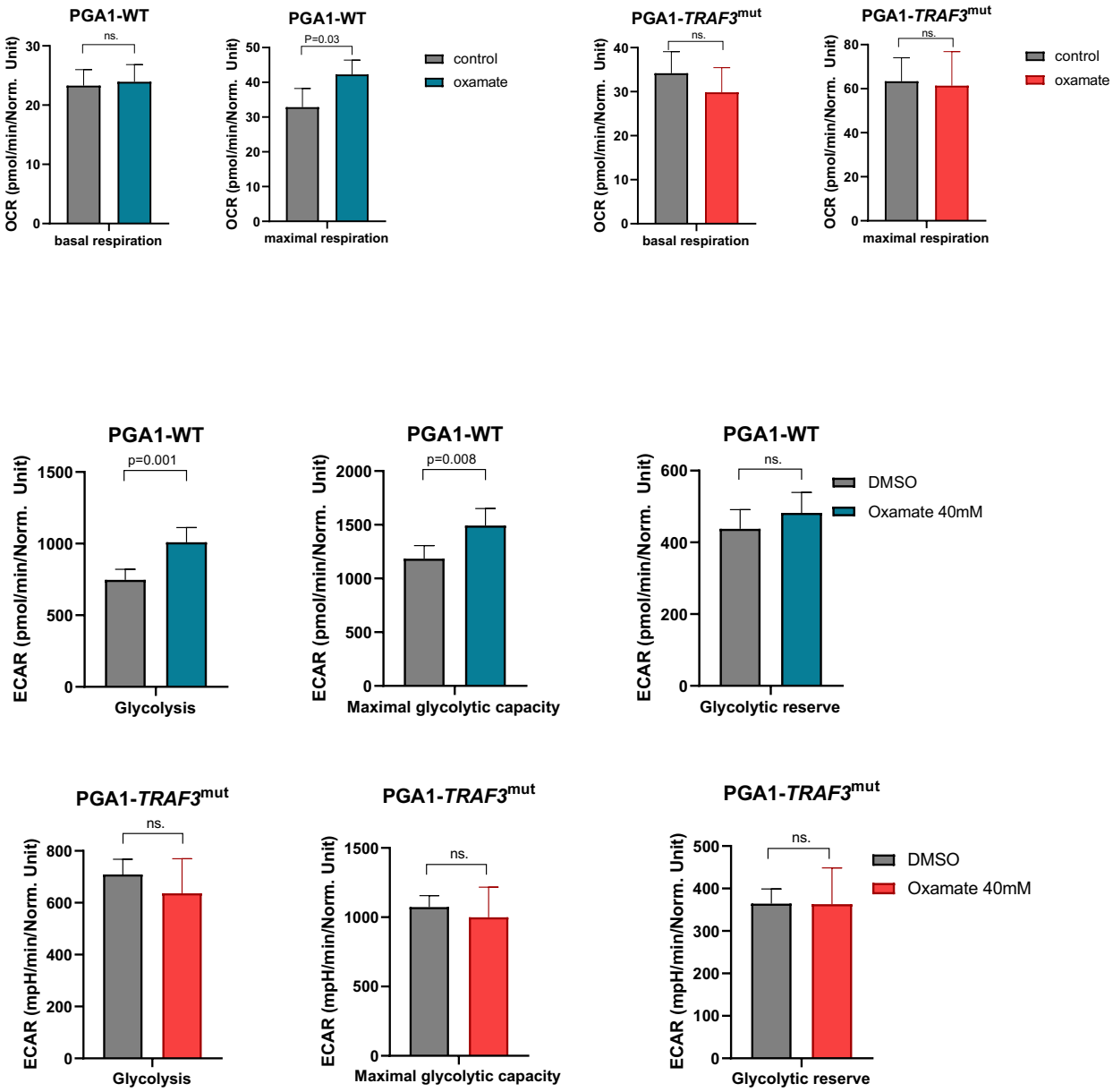

Supplementary Figure S7. Analysis of mitochondrial respiration (OCR) and glycolytic activity (ECAR) of PGA1-*TRAF3* mutated cells after 48h of oxamate treatment (40 mM). Color bars and graphs represent treated PGA1-*TRAF3*^{MUT} (red) and PGA1-WT (blue) cells, and grey bars and graphs represent untreated cells (both WT and *TRAF3* mutated as indicated). Mito stress test of OCR was performed to assess basal and maximal respiration, and gluco stress test of ECAR to assess glycolysis, maximal glycolytic capacity and glycolytic reserve. Data represent the mean ± SD. of five technical replicates from one representative experiment (out of two) in each case.

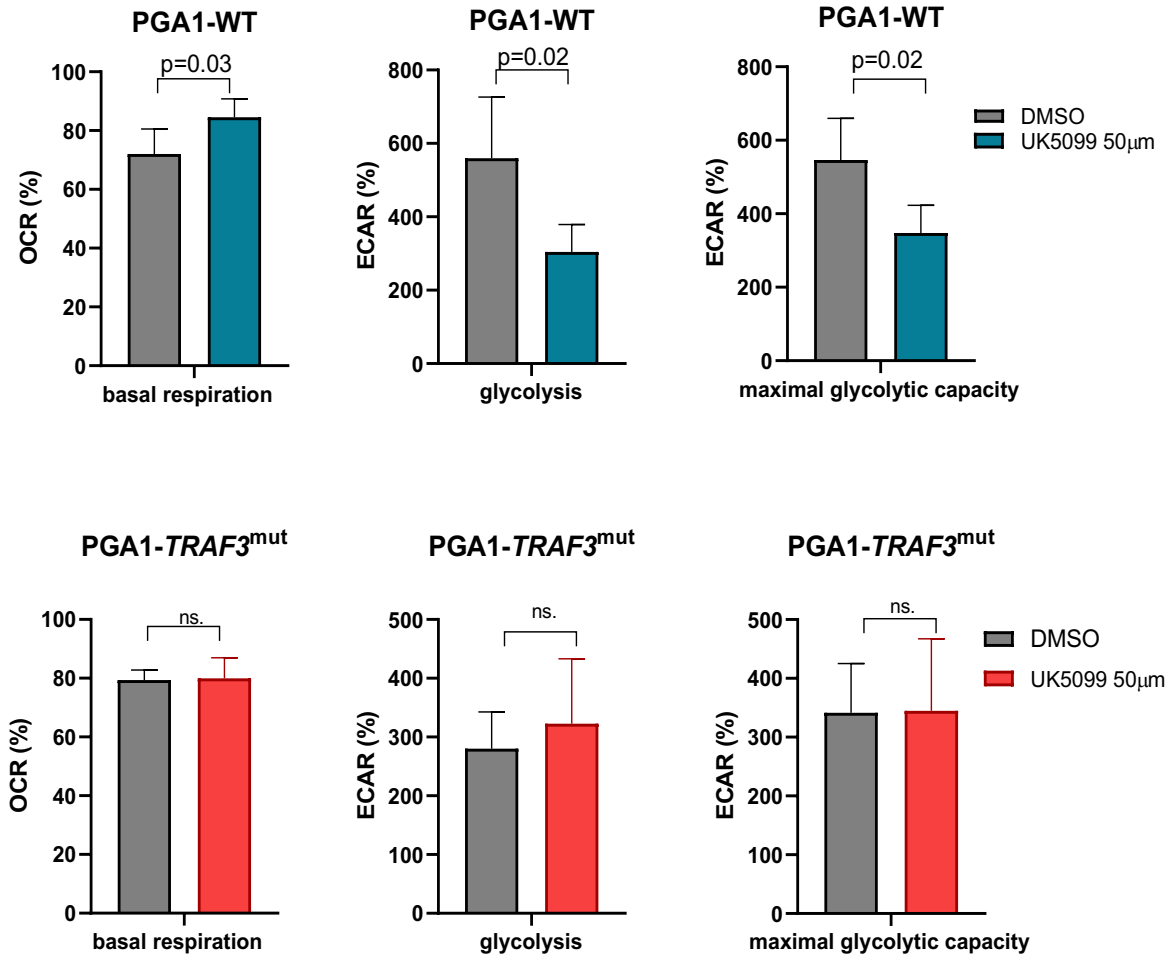

Supplementary Figure S8. Analysis of mitochondrial respiration (OCR) and glycolytic activity (ECAR) of PGA1-*TRAF3* mutated cells after UK5099 injection (50μM). Color bars and graphs represent treated PGA1-TRAF3^{MUT} (red) and PGA1-WT (blue) cells, and grey bars and graphs represent untreated cells (both WT and *TRAF3* mutated as indicated). Mito stress test of OCR was performed to assess basal respiration, and gluco stress test of ECAR to assess glycolysis and maximal glycolytic capacity. Data represent the mean ± SD. of five technical replicates from one representative experiment (out of two) in each case.

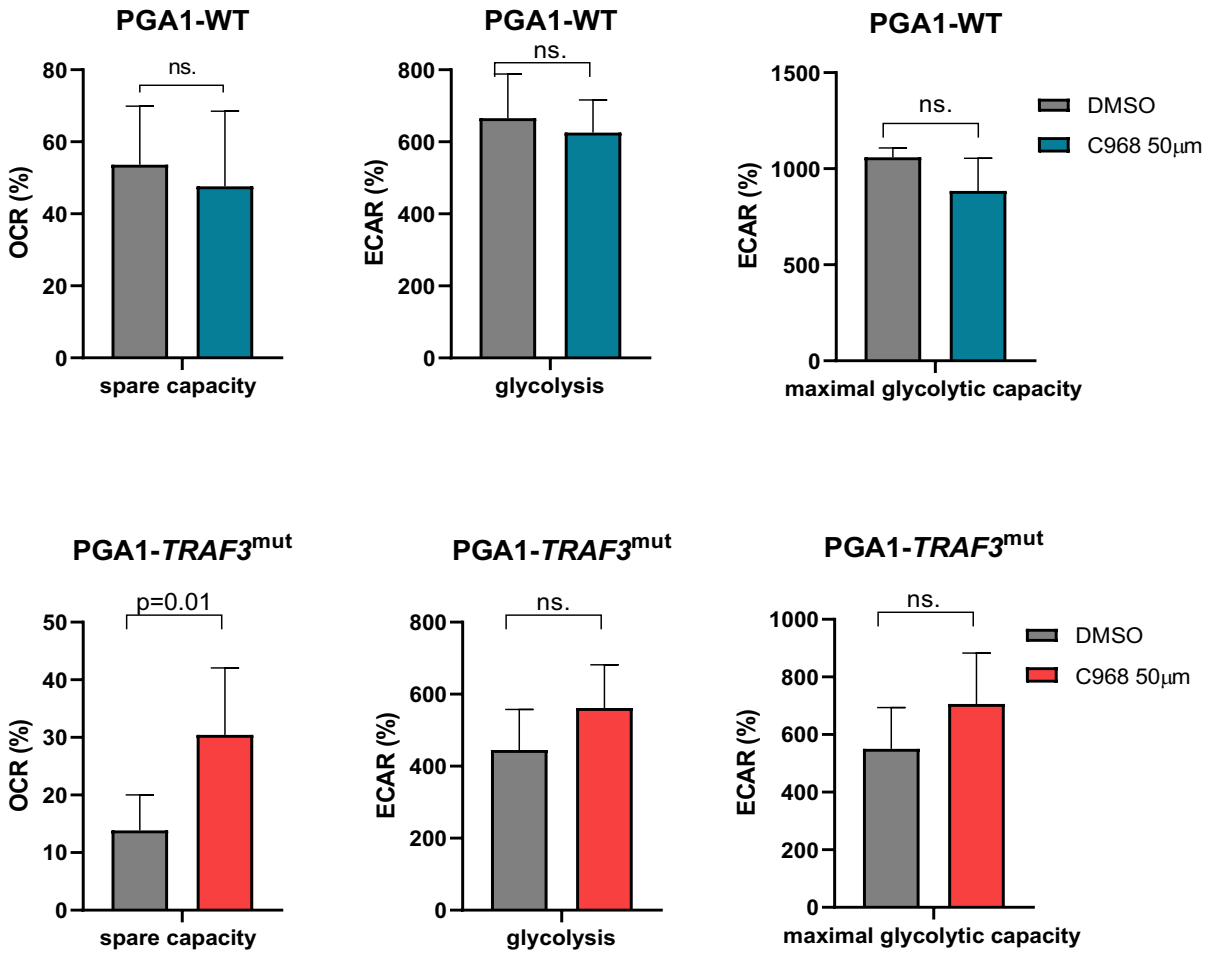

Supplementary Figure S9. Analysis of mitochondrial respiration (OCR) and glycolytic activity (ECAR) of PGA1-*TRAF3* mutated cells after C968 injection (50μM). Color bars and graphs represent treated PGA1-*TRAF3*^{MUT} (red) and PGA1-WT (blue) cells, and grey bars and graphs represent untreated cells (both WT and TRAF3 mutated as indicated). Mito stress test of OCR was performed to assess spare respiration capacity, and gluco stress test of ECAR to assess glycolysis and maximal glycolytic capacity. Data represent the mean ± SD. of five technical replicates from one representative experiment (out of two) in each case.

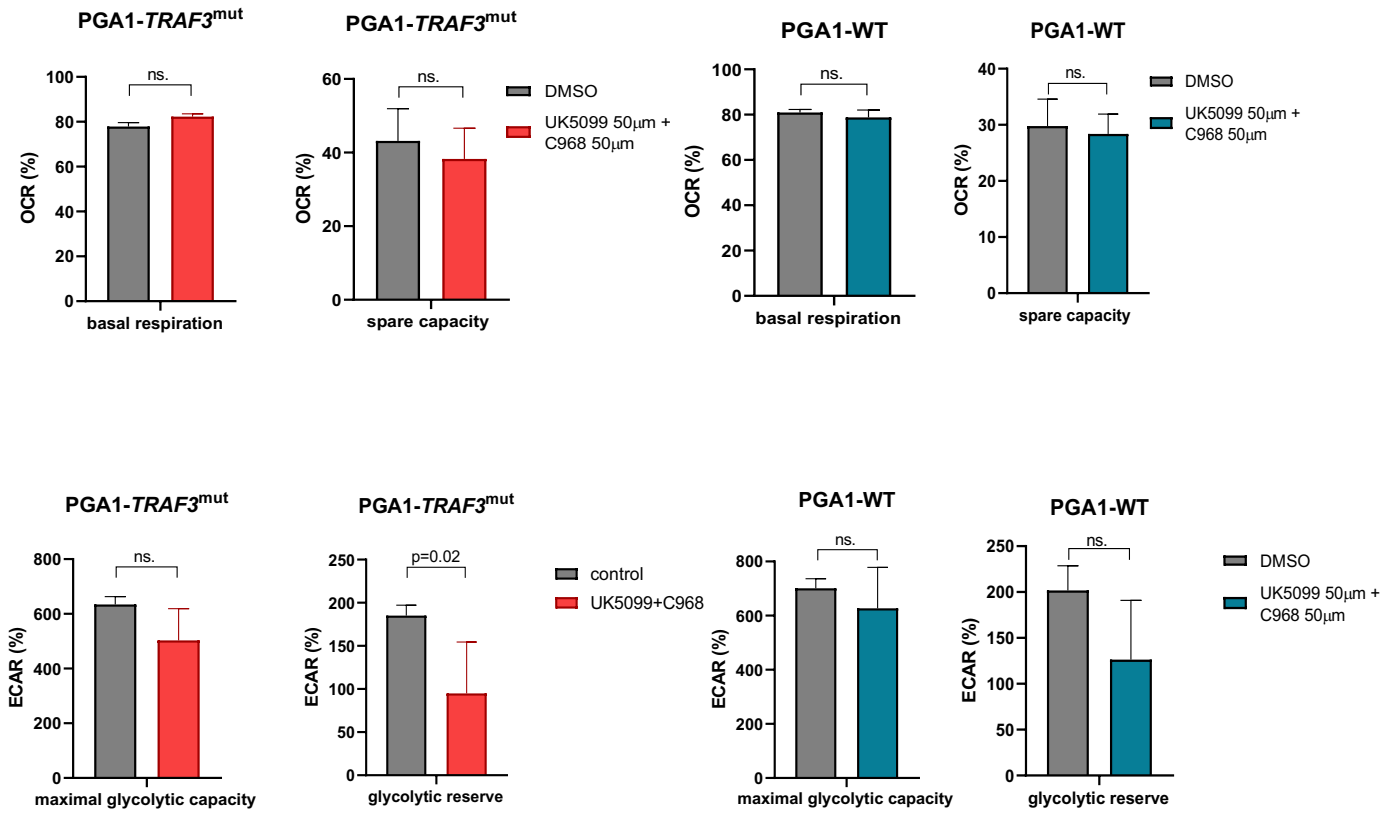

Supplementary Figure S10. Analysis of mitochondrial respiration (OCR) and glycolytic activity (ECAR) of PGA1-*TRAF3* mutated cells after UK5099 and C968 combined injection (50μM: 50μM). Color bars and graphs represent treated PGA1-TRAF3^{MUT} (red) and PGA1-WT (blue) cells, and grey bars and graphs represent untreated cells (both WT and *TRAF3* mutated as indicated). Mito stress test of OCR was performed to assess basal respiration and spare respiration capacity, and gluco stress test of ECAR to assess maximal glycolytic capacity and glycolytic reserve. Data represent the mean ± SD. of five technical replicates from one representative experiment (out of two) in each case.